BEILSTEIN JOURNAL OF ORGANIC CHEMISTRY

Sustainable catalysis

Edited by Nicholas J. Turner

Imprint

Beilstein Journal of Organic Chemistry
www.bjoc.org
ISSN 1860-5397
Email: journals-support@beilstein-institut.de

The *Beilstein Journal of Organic Chemistry* is published by the Beilstein-Institut zur Förderung der Chemischen Wissenschaften.

Beilstein-Institut zur Förderung der Chemischen Wissenschaften
Trakehner Straße 7–9
60487 Frankfurt am Main
Germany
www.beilstein-institut.de

BEILSTEIN JOURNAL OF ORGANIC CHEMISTRY

Sustainable catalysis

Nicholas J. Turner

Editorial

Open Access

Address:
School of Chemistry & Manchester Institute of Biotechnology, The University of Manchester, 131 Princess Street, M1 7DN, Manchester, United Kingdom

Email:
Nicholas J. Turner - nicholas.turner@manchester.ac.uk

Keywords:
green chemistry; sustainable catalysis

Beilstein J. Org. Chem. **2016,** *12,* 1778–1779.
doi:10.3762/bjoc.12.167

Received: 11 July 2016
Accepted: 20 July 2016
Published: 08 August 2016

This article is part of the Thematic Series "Sustainable catalysis".

Guest Editor: N. J. Turner

This focused collection of papers is devoted to recent developments in 'green chemistry', especially the applications of catalytic methods, involving both chemo- and biocatalysis. The development of catalytic processes is an important current theme in organic chemistry, since it aims to reduce the environmental impact of the industrial synthesis of chemicals and polymers by replacing stoichiometric reagents with catalysts and also exchanging harmful organic solvents with less detrimental alternatives. Green processes can also result in lower costs of goods and starting materials as well as in the use of less harmful and toxic reagents, which delivers benefits in terms of safety and disposal of waste byproducts. Recently, many of these aspects of green chemistry have been the focus of the CHEM21 project (http://www.chem21.eu), funded by the Innovative Medicines Initiative, which is supported by the European Federation of Pharmaceutical Industries Association (EFPIA). CHEM21 is a large multi-group consortium organized into six different work-packages spanning various elements of green chemistry including biocatalysis, synthetic biology and non-precious metal catalysis. In addition, there are also work packages devoted to defining current and future targets for green chemistry as well as developing metrics-based assessment protocols and also training packages aimed at embedding the principles of green chemistry within the thinking of future scientists. It is hoped that the outputs from CHEM21, including some of the papers presented here, together with other similar initiatives, will contribute to the overall effort underway globally aimed at transforming the chemical industry into a more sustainable and environmentally operation.

Nicholas Turner

Manchester, July 2016

License and Terms

BEILSTEIN JOURNAL OF ORGANIC CHEMISTRY

Dicarboxylic esters: Useful tools for the biocatalyzed synthesis of hybrid compounds and polymers

Ivan Bassanini[1], Karl Hult[1,2] and Sergio Riva[*1]

Review

Open Access

Address:
[1]Istituto di Chimica del Riconoscimento Molecolare, CNR, via Mario Bianco 9, Milano, Italy and [2]School of Biotechnology, Department of Industrial Biotechnology, Albanova KTH, Royal Institute of Technology, Stockholm, Sweden

Email:
Sergio Riva[*] - Sergo.riva@icrm.cnr.it

* Corresponding author

Keywords:
biocatalysis; dicarboxylic acids; lipase; polyesters; regioselectivity

Beilstein J. Org. Chem. **2015,** *11,* 1583–1595.
doi:10.3762/bjoc.11.174

Received: 29 June 2015
Accepted: 21 August 2015
Published: 09 September 2015

This article is part of the Thematic Series "Sustainable catalysis".

Guest Editor: N. Turner

Abstract

Dicarboxylic acids and their derivatives (esters and anhydrides) have been used as acylating agents in lipase-catalyzed reactions in organic solvents. The synthetic outcomes have been dimeric or hybrid derivatives of bioactive natural compounds as well as functionalized polyesters.

Introduction

The finding that enzymes can work in organic solvents has significantly expanded the scope of preparative scale biocatalyzed transformations [1-4]. An uncountable number of reports have been published on this topic since the eighties of the last century, the vast majority of them dealing with the synthetic exploitation of hydrolases [5,6].

It was found that reactions that are thermodynamically unfavorable in water, like esterifications, transesterifications (transacylations) and amidations, can be efficiently catalyzed by lipases and proteases in organic solvents. Moreover, both substrates and acylating agents' scope could be significantly expanded. Lipases, whose natural substrates are fatty acid triglycerides, and proteases, enzymes acting on peptides and proteins, were found to be able to catalyze, i.e., the esterifications of sugars and steroids, using acylating agents different from simple aliphatic acids [7-9]. Specifically, years ago Dordick and coworkers proposed the so-called 'combinatorial biocatalysis' as an approach to easily produce small libraries of derivatives of bioactive natural compounds using a panel of different acylating agents and hydrolases [10-12].

Among the great number of investigated acyl donors, activated esters of dicarboxylic acids have been found to be particularly versatile for the production of bifunctionalized compounds. As it will be discussed in the following paragraphs, these mole-

cules have allowed the synthesis of dimeric or hybrid derivatives of bioactive natural compounds as well as the biocatalyzed production of functionalized polyesters.

Review

1. Synthetic exploitation of dicarboxylic esters

a) Synthesis of activated esters

In most of the biocatalyzed transesterification reactions, 'activated' esters are usually employed in order to make the reactions irreversible thanks to the release of alcohols that are poor nucleophiles (halogenated derivatives of ethanol, vinyl or isopropenyl alcohol) [13-15]. This has been also the case with several reports on the use of dicarboxylic acid derivatives.

Accordingly, vinyl diesters (**1**) and trifluoroethyl diesters (**2**) have been synthesized following standard procedures [16]. Moreover, succinic (**3**) and glutaric anhydride (**4**) could be used as acylating agents in controlled biocatalyzed reactions (Scheme 1) [17,18].

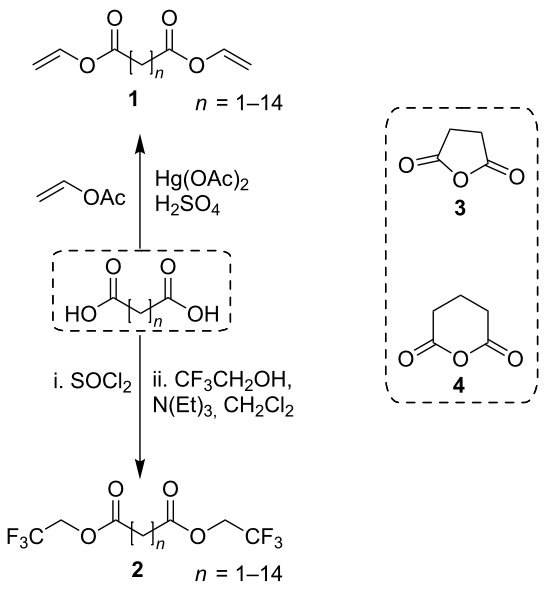

Scheme 1: Activated derivatives of dicarboxylic acids.

b) Regioselective enzymatic acylation of natural products.

Natural products are traditionally classified into groups of substances (terpenes, alkaloids, amino acids, lipids, etc), depending on their biosynthetic origin and on their chemical and structural features [19-21]. The complex structures of most of these molecules along with the presence of multiple functional groups make their chemical manipulation difficult. This inherent "fragility" makes biocatalysis an attractive method for their derivatization. Specifically, glycosides and polyhydroxylated compounds can be selectively acylated at specific hydroxy groups by the action of an activated ester in the presence of a suitable hydrolase in organic solvents [22,23].

Different authors have shown that activated dicarboxylates are also accepted as acyl donors by these enzymes. As an example, Figure 1 shows the products obtained using divinyl adipate in the esterification of the antineoplastic antibiotics mithramycin (**5**) catalyzed by *Candida antarctica* lipase A (CAL-A) and chromomycin A_3 (**6**) catalyzed by *Candida antarctica* lipase B (CAL-B) [24]. In another report a series of mono-substituted troxerutin esters (**7a**) were synthesized by action of the alkaline protease from *Bacillus subtilis* on **7** [25]. The carboxyacetyl (malonyl) derivative of some flavonoid glycosides (i.e., **8b**) and of ginsenoside Rg1 (**9b**) could be obtained with two-step sequences. The preliminary CAL-B catalyzed acylations of **8** with dibenzyl malonate and of **9** with bis(2,2,2-trichloroethyl)malonate to give the mixed malonyl derivatives **8a** and **9a**, respectively, were followed either by a palladium-catalyzed hydrogenolysis of the benzyl moiety to give **8b** [26], or by a selective chemical removal of 2,2,2-trichloroethanol with Zn/AcOH to give **9b** [27].

c) Enzymatic synthesis of symmetric diesters

More recently, symmetric diesters have been synthetized exploiting both the activated extremities of divinyl carboxylates.

C_6-dicarboxylic acid diesters derivatives of the thiazoline of *N*-acetylglucosamine (NAG-thiazoline, **10a**,**b**, Figure 2) were prepared and their inhibitor activities towards fungal β-*N*-acetylhexosaminidase evaluated [28].

Similarly, dimers of sylibin (**11a**,**b**, Figure 3) and dehydrosylibin, obtained by Novozyme 435-catalyzed acylation with the divinyl esters of dodecanedioc acid, were evaluated in terms of antioxidant activity and cytotoxicity [29].

The obvious hypothesis related to the synthesis of these compounds was that a dimer should be more bioactive than a monomer, but this was not always the case [28,29].

d) Enzymatic synthesis of hybrid dimers

According to a pioneering paper Dordick linked glucose to paclitaxel with divinyl adipate in a two-step biocatalyzed acylation [30]. As shown in Scheme 2, the protease thermolysin catalyzed the regioselective acylation of the side chain of paclitaxel (**12**) to give the 2'-vinyl adipate **12a** in 60% isolated yields. Novozyme 435-catalyzed elaboration of this intermediate allowed either to hydrolyze the residual vinyl ester to give the carboxyl derivative **12b** (reaction performed in acetonitrile

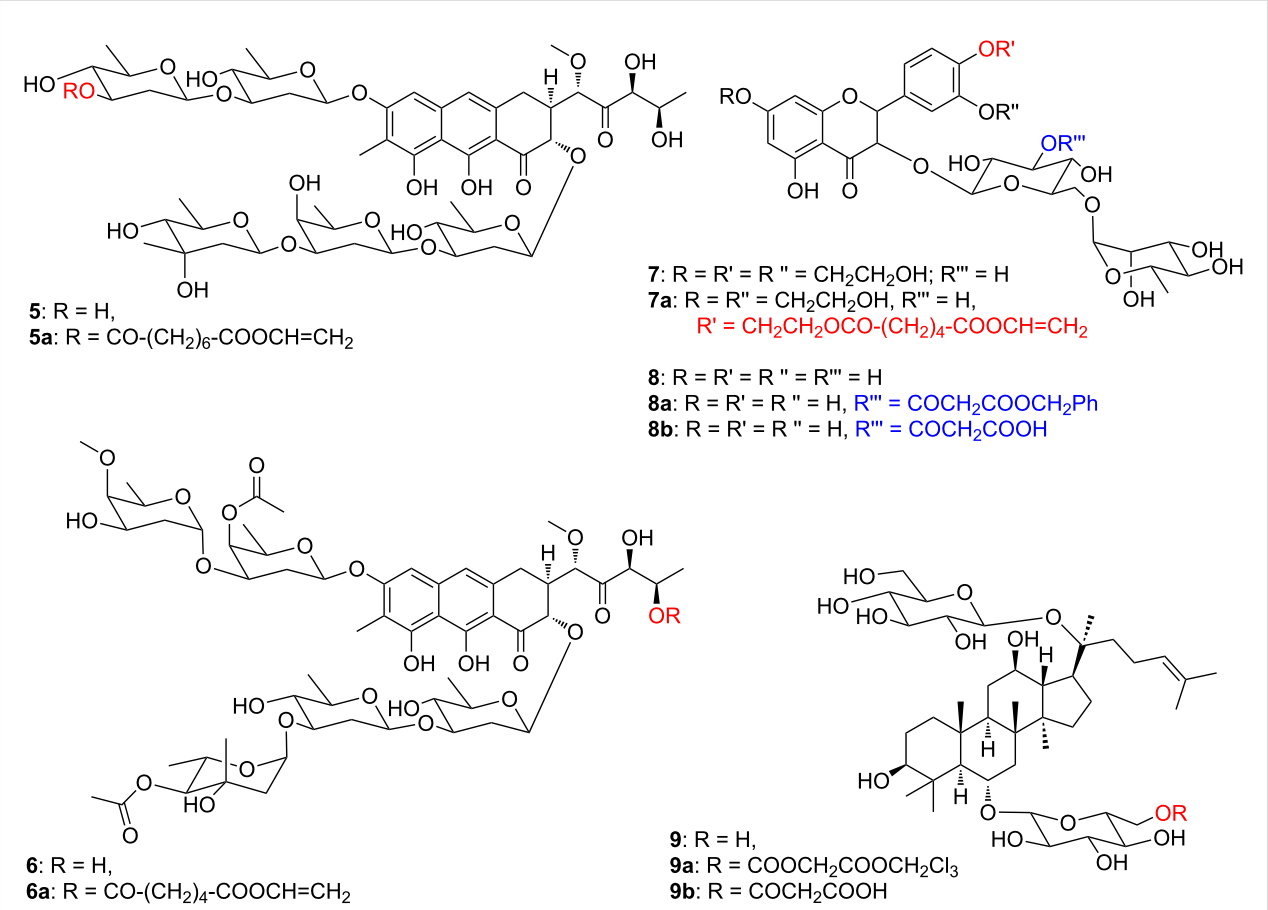

Figure 1: Example of natural compounds selectively acylated with dicarboxylic esters.

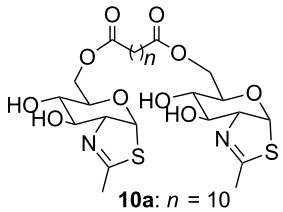

Figure 2: C_6-dicarboxylic acid diesters derivatives of NAG-thiazoline.

containing 1% H_2O v/v) or to link it to a sugar, like glucose to give the hybrid compound **12c** (reaction performed in dry acetonitrile containing glucose). Both derivatives were significantly more soluble in aqueous solutions than the parent compound **12**.

A similar approach was followed later on by Lin and coworkers, who described the enzymatic esterification of the nucleoside 5-fluorouridine (**13**) and of other polyhydroxylated bioactive molecules with divinyl esters of dicarboxylic acids [31-35]. The monovinyl esters obtained (i.e., **13a**) were then used either to acylate monosaccharides (i.e., galactose to give **13b**) in order to increase the solubility of the parent compounds in aqueous solutions (Figure 4) or as co-monomers in radical (AIBN)-catalyzed polymerizations (see next paragraph).

In recent years linking different bioactive molecules with suitable dicarboxylic acids to prepare hybrid compounds has been receiving more and more attention. The interest is due to the fact that these new substances might show additive activities [36], having improved properties or efficacies compared to the combined use of the respective two parent compounds. This is the so-called 'dual drug' strategy [37-41]. For instance [40,41], an increased capacity of inhibiting endothelial cell differentiation and migration (key steps of the angiogenic process) was observed as well as a marked ability to inhibit the polymerization of tubulin in vitro. The same methodology might be applied to direct a drug by conjugation to a molecule binding to a specific receptor on cancer cells. Moreover, by using dicarboxylated linkers with a disulfide bridge, it was possible to generate dynamic libraries of dimeric hybrids based on disulfide exchange reactions in vivo [42,43].

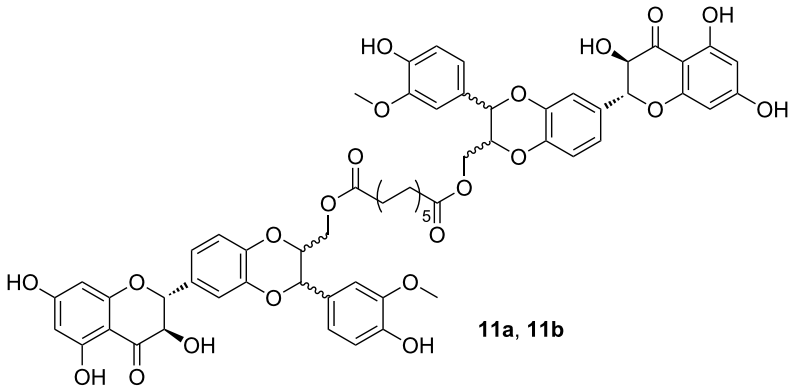

Figure 3: Sylibin dimers obtained by CAL-B catalyzed trans-acylation reactions.

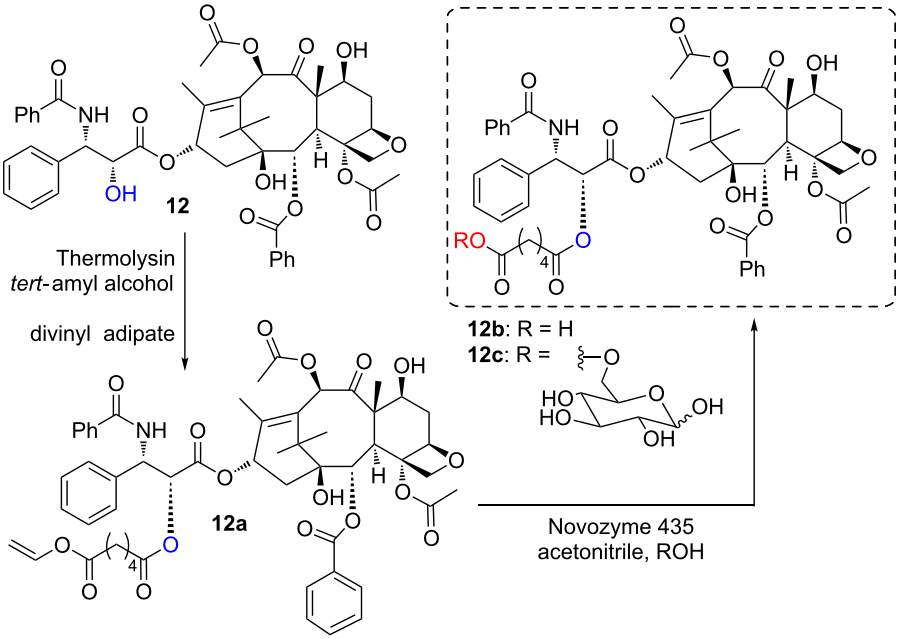

Scheme 2: Biocatalyzed synthesis of paclitaxel derivatives.

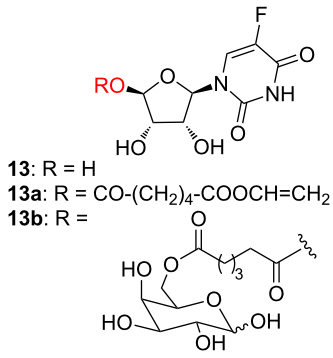

Figure 4: 5-Fluorouridine derivatives obtained by CAL-B catalysis.

All of these compounds were synthesized by (sometimes troublesome) chemical protocols requiring accurate control of the reaction conditions and several protection/deprotection steps. This is avoided using a biocatalyzed approach, as it has been shown exploiting once again the well-known efficiency, selectivity and versatility of CAL-B (Novozyme 435) [16]. As in the previous examples, the mixed esters from the first esterification step can be used as acylating agents in the second esterification step. Scheme 3 shows the synthesis of the hybrid compounds **17** and **18**, obtained by linking together a steroid (cortisone, **14**) and an alkaloid (colchicoside, **15**; thiocolchicoside, **16**). Worth of notice the use, among others, of activated esters of dithiodicarboxylic acids, in **18**.

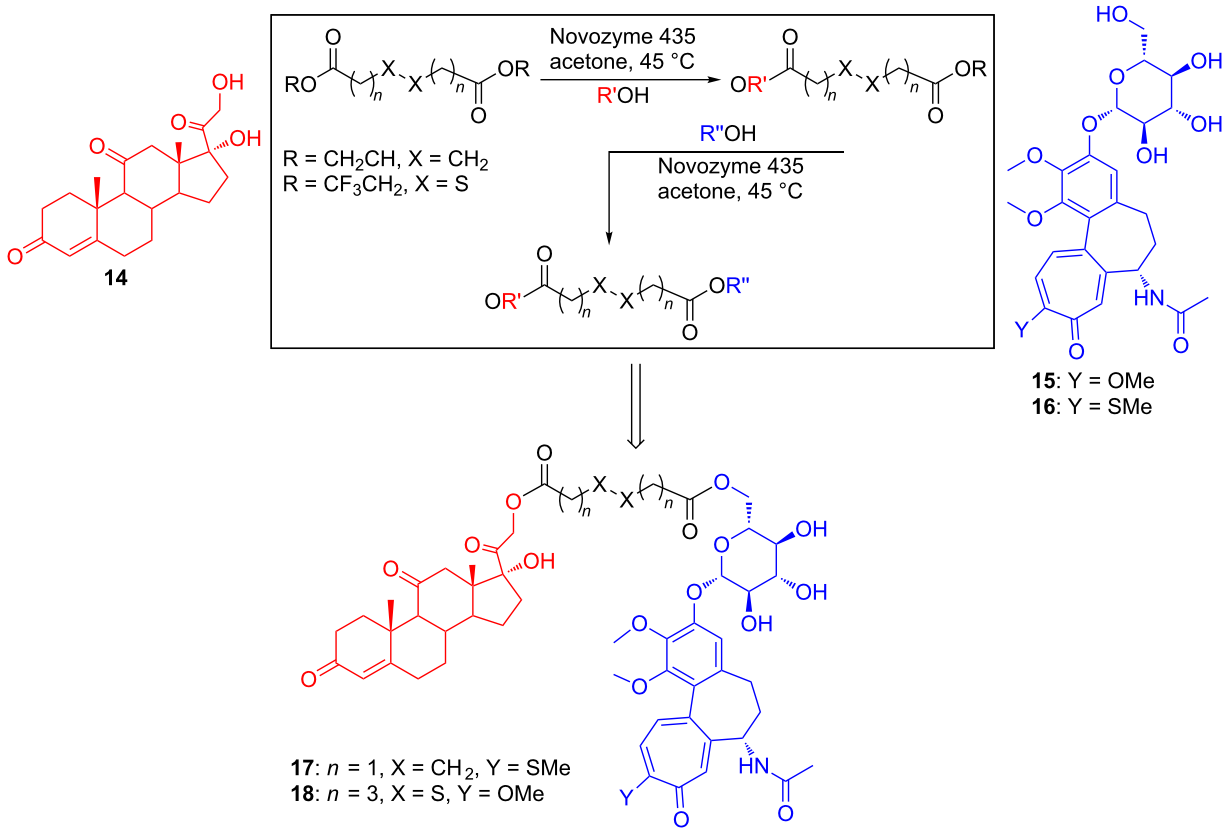

Scheme 3: Biocatalyzed synthesis of hybrid diesters **17** and **18**.

More recently Kren and coworkers have synthesized hybrid dimeric antioxidants **23**–**25** based on the conjugation of an acylated sylibin derivative (**19**) with *L*-ascorbic acid (**20**), tyrosol (**21**) and trolox alcohol (**22**) (Scheme 4) [44]. These compounds proved to have excellent electron donor, antiradical, antioxidant as well as cytoprotective abilities.

Moreover, in a different research area, studying the supramolecular behavior of bolaamphiphile molecules, it has been reported that polyhydroxylated compounds linked via a dicarboxylic chain (like the symmetric vitamin C-based bolaamphiphile **26**, L,L) give origin to regular structures [45]. The previously described biocatalyzed approach allowed the synthesis of an asymmetric dimer combining L-ascorbic acid and D-isoascorbic acid (**27**, L,D), which behaved significantly differently in terms of supramolecular structure when compared to the symmetric dimers **26** (L,L) and **28** (D,D) (Figure 5) [46].

More recently, Gross and coworkers have described the synthesis of "sweet silicones" by Novozyme 435-catalyzed formation of ester bonds between organosilicon carboxylic diacids and the primary OH's of 1-*O*-alkyl glucopyranosides [47].

2. Enzymatic synthesis of polyesters

The interest in the biocatalyzed synthesis of polyester started at the very beginning of the use of lipases in organic solvents. In 1984 Okumura et al. [48] produced oligomers of several dicarboxylic acids (C_6 to C_{14}) in combination with several diols (C_2 and C_3). Since then the use of lipase-catalyzed preparation of polymers has grow very much and has been reviewed many times (see for example Zang et al. [49], Kobayashi and Makino [50], Gross et al. [51]). Nowadays lipases are not only used to achieve simple polycondensation reactions, but are exploited due to their chemo-, stereo- and enantioselectivity. In addition, they are seen as environmentally friendly alternative to traditional polymerization methods [52].

Binns et al. summarized the attempts to scale up synthesis of polyesters by enzyme catalyzed polycondensation of adipic acid and hexane-1,6-diol in a very well-worth reading article [53]. They discussed the very slow progress in achieving high molecular weight polymers and concluded that removal of the leaving group, water, to draw the equilibrium towards polymerization, and the reversal nature of lipase catalysis are two main obstacles. Others have pointed out the latter also [54]. Often a two-

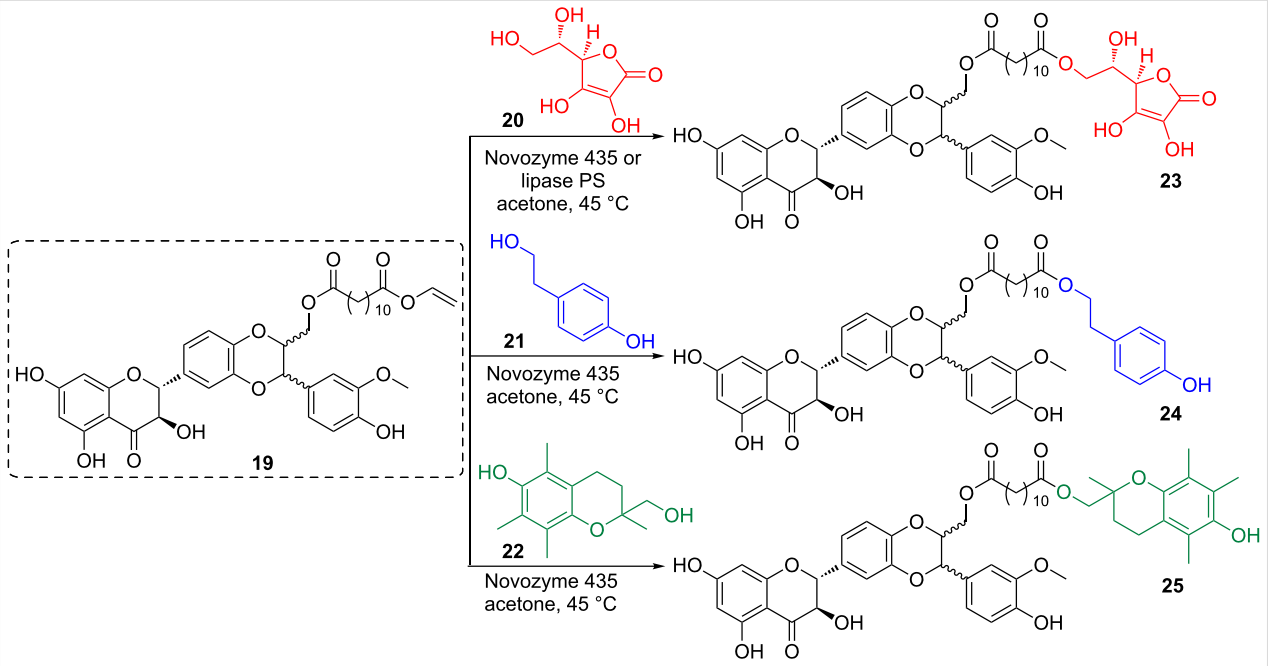

Scheme 4: Hybrid derivatives of sylibin.

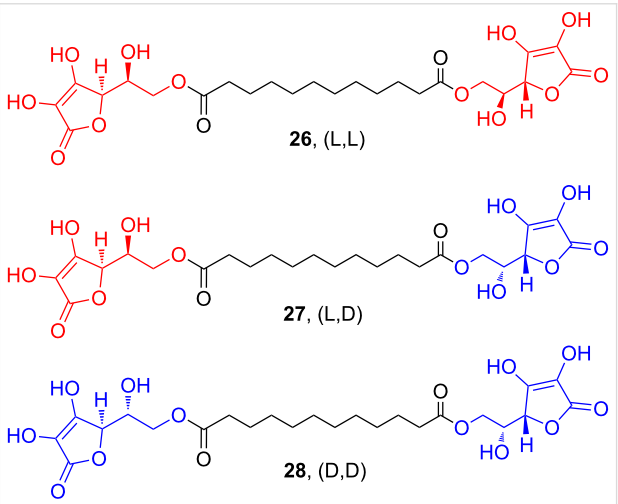

Figure 5: Bolaamphiphilic molecules containing (L)- and/or (D)-isoascorbic acid moieties.

step procedure has been used, an initial polymerization to achieve oligomers followed by a second step at higher temperature and/or lower pressure. The synthesis of oligomers and short telechelics (oligomers with functionalized ends) avoids much of the problems and afford better reaction rates.

Yang et al. polymerized ethyl glycolate with diethyl sebacate and 1,4-butandiol. For this, they used CAL-B in a two step synthesis, started at a low vacuum and then increased the vacuum to drive the reaction to completion [55]. The dicarboxylic acid and the diol were employed in equal molar amounts, while the amount of ethyl glycolate was varied. Polymers with a high molecular weight (12–18000 Dalton) were obtained (Figure 6). Nano particles of the polymer were used for a controlled slow release of the drug doxorubicin (**29**) trapped in this material.

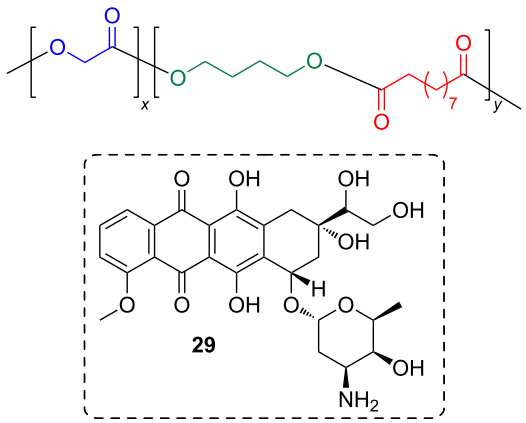

Figure 6: Doxorubicin (29) trapped in a polyester made of glycolate, sebacate and 1,4-butandiol units.

Bhatia et al. used Novozyme 435 to make polymers from functionalized pentofuranose derivatives (i.e, **30**) and PEG-600 dicarboxylic acid dimethyl ester [56]. The obtained polymers formed supramolecular aggregates with diameters between 120 and 250 nm, which were able to encapsulate Nile red (**31**) that was used as a model of a drug compound (Figure 7).

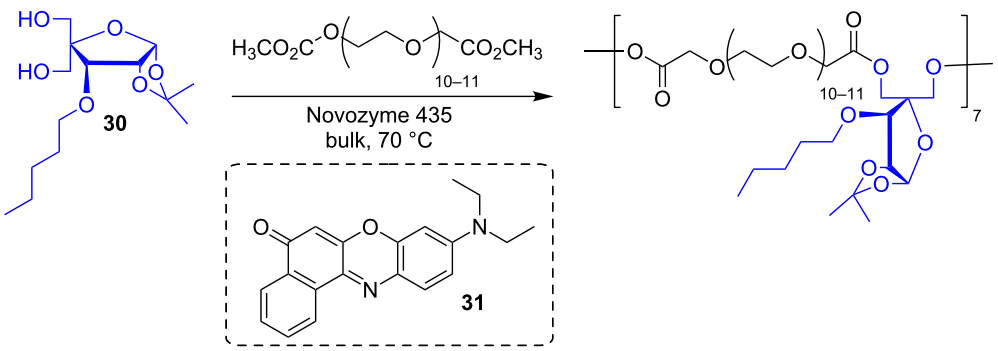

Figure 7: Polyesters containing functionalized pentofuranose derivatives.

Copolymers containing disulfide groups in the main chain were synthesized from 3,3′-dithiodipropionic acid dimethyl ester in combination with pentadecalactone and 1,4-butandiol (Figure 8) [57]. When MeO-PEG-OH was used as chain terminator amphiphilic copolymers were formed. The hydrophobicity of the polymer could easily be changed by the content of the lactone. The copolymers had low toxicity and formed aggregates that could be used as nano-containers of drugs. Reduction of the disulfides caused swelling of the aggregates and fast release of incorporated drugs.

An early attempt to use dicarboxylic acids with an additional functional group was done by Wallace and Morrow [58]. They used the activated 2,2,2-trichloroethyl diester of (±)-3,4-epoxyadipic acid. The stereoselectivity of porcine pancreatic lipase discriminated between the two enantiomers and afforded the chiral (−)-polyester with molecular weight of 7900 Dalton (Figure 9).

Yang et al. compared the polymerization of glycerol and a diacid derivative of oleic acid catalyzed by dibutyltin oxide and Novozyme 435 (Figure 10) [59]. Dibutyltin oxide catalysis resulted in cross-linking and gel formation. This was not observed by enzyme catalysis, presumably due to steric hindrance which may be imposed by the active site of the enzyme.

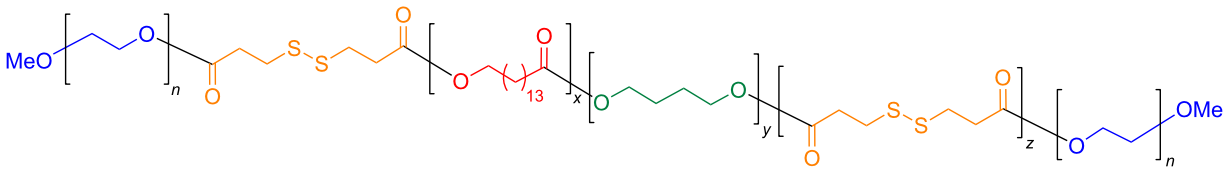

Figure 8: Polyesters containing disulfide moieties.

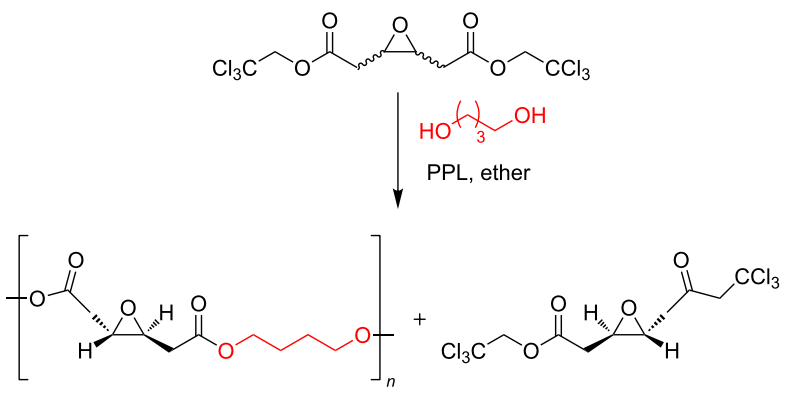

Figure 9: Polyesters containing epoxy moieties.

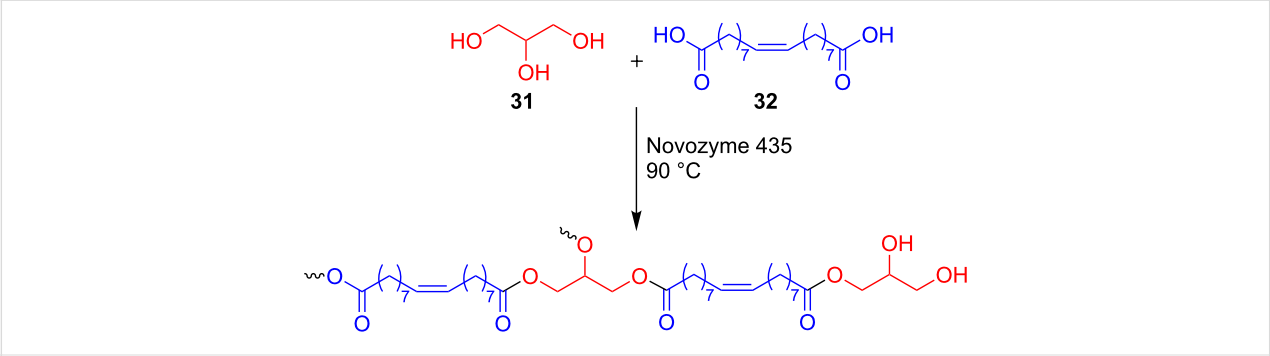

Figure 10: Biocatalyzed synthesis of polyesters containing glycerol.

Symmetrical long-chain (C_{18}, C_{20} and C_{26}) unsaturated or epoxidized dicarboxylic acids were polycondensated with 1,3-propanediol or 1,4-butanediol using CAL-B [60]. At high temperature (70 °C) a number of polyester combinations could be synthesized. Propandiol afforded polymers with rather moderate molecular weights (2000–3000 Dalton), while with butandiol polyesters with higher molecular weights (8000–12000 Dalton) were obtained. Interestingly, the polymers carried functional groups in the chain that could be used for further modifications.

For polymer synthesis involving environmentally benign chemicals the building blocks succinic acid, itaconic acid (**34**, Figure 11) and butanediol are very attractive. The methylene group in itaconic acid is interesting as a handle for second polymerization or derivatization, but causes steric and reactivity problems in lipase catalysis. Anyhow, Jiang et al. were able to synthesize polyesters with a mix of the two acids used as dimethyl esters. The yield was acceptable if the reaction was run in diphenyl ether and the ratio of itaconate did not exceed 30% [61]. The authors discussed the consequences of the low reactivity of itaconic acid in relation to polymer growth. Another dicarboxylic acid carrying an additional functional group is malic acid (**35**, Figure 11). Yao et al. used (L)-malic acid and adipic acid in different ratios to be polymerized with 1,8-octanediol in a reaction catalyzed by CAL-B [62]. The yield depended on the choice of organic solvent, with isooctane being the best one. Using 10% of enzyme by weight compared to total amount of monomers, molecular sieves to trap the produced water and working at 70 °C, high molecular weight polymers were isolated after 48 h. This was a good example, showing that the selectivity of the lipase-driven polymerization using only the primary alcohols of the diol, and not the secondary hydroxy group of malic acid.

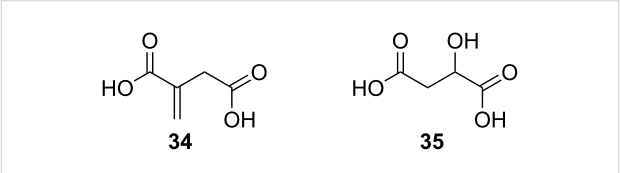

Figure 11: Iataconic (**34**) and malic (**35**) acid.

A few years earlier Kato et al. showed that both enantiomers of dimethyl 2-mercaptosuccinate and 1,6-hexanediol were polymerized by CAL-B, while other lipases failed to give long polymers [63]. In the same article the authors showed that only the (L)-enantiomer of dimethyl malate afforded polymers. A racemate of malate esters gave only short polymers; showing nicely that efficient polymerization of diacids can only be achieved with carboxylic groups of similar reactivity. The poly(hexanediol-2-mercaptosuccinate) could be oxidized by air in DMSO to form a cross-linked insoluble material (Figure 12). In a subsequent paper, the same laboratory prepared different mercaptosuccinate polymers with several diols. In addition they showed that the material cross-linked by air oxidation could be reversibly reduced by tributylphosphine to recover the reduced soluble polymer [64].

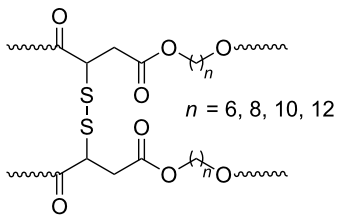

Figure 12: Oxidized poly(hexanediol-2-mercaptosuccinate) polymer.

In a recent review, Khan et al. summarized the synthesis of polymers based on C-5-substituted isophthalates (**36**, Figure 13) and diols [65]. Using hydroxy or amine groups at C-5 afforded polymers, which could be further modified by chemical means. The synthesized products can find a wide range of applications such as drug/gene delivery systems, flame retardant materials, conducting polymers, controlled release systems, diagnostic

agents, and polymeric electrolytes for nano-crystalline solar cells.

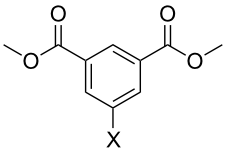

36 X = OH, NH_2

Figure 13: C-5-substituted isophthalates.

Curcumin (**37**) was converted to a diester using ethyl α-bromoacetate. The formed diester was copolymerized with PEG using CAL-B (Figure 14). The final product was an effective activator of nuclear factor (erythroid-derived 2)-like 2 (Nrf2) several times better than the free curcumin [66]. The curcumin diester was used in a second polymer synthesis with carbinol (hydroxy) terminated polydimethylsiloxane catalyzed by CAL-B [67]. The curcumin moiety retained its fluorescence properties without quenching in thin films prepared from the polymer. Films exposed to low concentrations of vapors of the explosives DNT and TNT absorbed the explosives and the fluorescence was quenched. Therefore, it was proposed that the films can be used as sensors for these explosives.

Frampton et al. synthesised a polyester from the dimethyl ester of 1,3-bis(3-carboxypropyl)-1,1,3,3-tetramethyldisiloxane and 1,3-bis(3-hydroxypropyl)-1,1,3,3-tetramethyldisiloxane (Figure 15) using CAL-B. They obtained the polymers as colorless viscous liquids after evaporation of ether used to extract the polymer from the enzyme beads [68].

a) Dicarboxylic esters in combination with functionalized alcohols

The use of diols with additional reactive groups opens up the possibility to synthesize a number of functionalized polymers. For instance, Müller and Frey used 3,3-bis(hydroxymethyl)-oxetane in different blends with 1,8-octanediol and sebacic acid to get polymers with a varied content of oxetane groups (Figure 16). Oxetane is a very acid sensitive moiety, but the mild conditions for enzyme catalysis afforded nice polymers. The obtained polymers could be cross-linked by UV light in the presence of the solid photoinitiator Iracure 270 to form hard films [69].

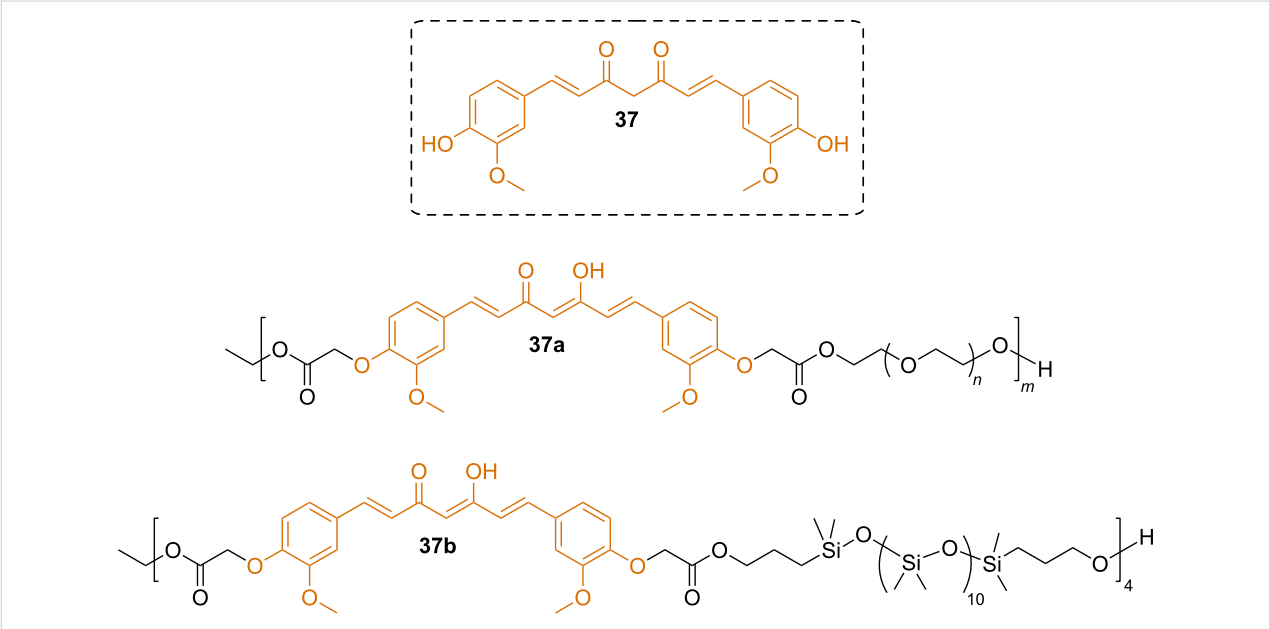

Figure 14: Curcumin-based polyesters.

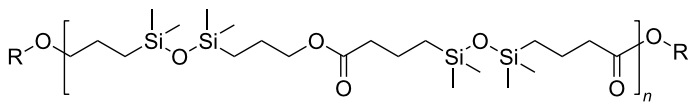

Figure 15: Silylated polyesters.

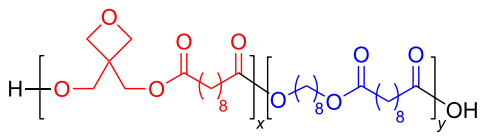

Figure 16: Polyesters containing reactive ether moieties.

Several poly(amine-*co*-ester)s were synthesized directly from dicarboxylic acid diesters and *N*-alkyl- or *N*-phenyldiethanolamines. High molecular weights polymers were obtained in a two step procedure catalyzed by CAL-B [70]. Specifically, the obtained polymers from sebacic acid (Figure 17, x = 7) and *N*-methyl- or *N*-ethyldiethanolamine proved to form good nanometer-sized complexes with DNA, useful for efficient DNA delivery in gene therapy.

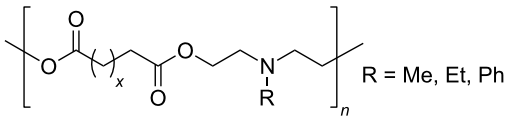

Figure 17: Polyesters obtained by CAL-B-catalyzed condensation of dicarboxylic esters and *N*-substituted diethanolamine.

Mexiletine (**38**) was incorporated into amphiphilic poly(amine-*co*-ester)s through a two-step lipase catalyzed procedure. Firstly, racemic mexiletine was used in a biocatalyzed kinetic resolution to form the amide with pure (*R*)-amide with methyl 3-(bis(2-hydroxyethyl)amino)propanoate. The formed diol was mixed with an equal molar amount of divinyl sebacate and lipase as a catalyst, after some time methoxypoly(ethylene glycol) was added to react with the remaining vinyl carboxylates to give an amphiphilic polymer. This product self-assembled into nanometer-scale-sized particles in water and could be used for drug delivery (Figure 18) [71].

A few years earlier the same authors used the same principle to synthesize amphiphilic mPEG-block-poly(profenamide-co-ester) copolymers that self-assembled in water and could be used for drug release [72]. As a follow up the same laboratory used triethanolamine and different dimethyl esters of linear dicarboxylic acids to synthesize hyperbranched polymers. With a very high load of CAL-B (20% weight compared to

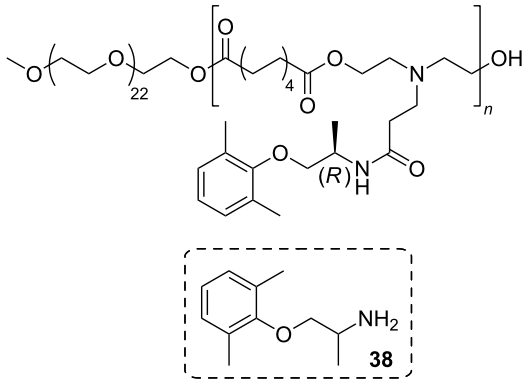

Figure 18: Polyesters comprising mexiletine (**38**) moieties.

triethanolamine), a long incubation time at 85 °C, and 1–2 mmHg pressure the hyperbranched polymers were isolated [73].

b) Amines in combination with dicarboxylic acids

Several high molecular weight poly(amide-*co*-ester)s were prepared in a three-step procedure. Significantly high molecular weights were achieved by first reacting pentadecalactone with equal molar amounts of linear diamines. The formed amides, containing one terminal hydroxy and one terminal amino moiety, were further reacted with diethyl sebacate to form high molecular weight poly(amide-*co*-ester)s with a repetitive pattern of amide and ester bonds (Figure 19) [74].

The problem of high molecular weights in lipase-catalyzed polyamide synthesis using dicarboxylic acids and diamines has been discussed in several articles. The slow catalytic rate and the insolubility of the formed polymers are two main obstacles. The rate problem was addressed by Poulhès et al. who used an α-oxy diacid derivative (Figure 20), obtaining higher reaction rates, but, unfortunately, lower molecular weights [75]. The

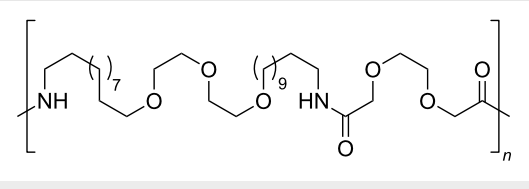

Figure 20: Polymer comprising α-oxydiacid moieties.

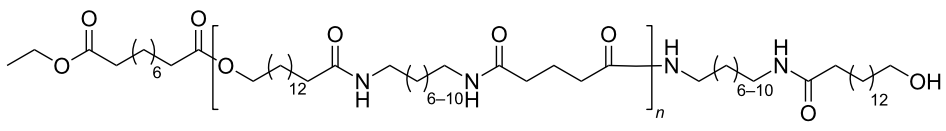

Figure 19: Poly(amide-*co*-ester)s comprising a terminal hydroxy moiety.

observed rate enhancement was presumably an effect of transition state stabilization for the nitrogen inversion in the presence of an oxygen atom in the proximity of the forming amide bond [76].

c) Telechelics

Several authors have discussed the difficulty of obtaining high molecular weight polyesters by lipase catalysis. This problem can be circumvented by the synthesis of telechelics, oligomers with functional ends. The synthesis of oligomers avoids the precipitation of polymers during the synthesis. The functional ends of the telechelics can be used in a second step for polymerisation or crosslinking without the lipase. By exploiting the substrate selectivity of lipases it is possible to obtain well-defined telechelics in a one-pot, or even one-step reaction.

In 1997 Uyama et al. were the first to produce telechelic polyesters from the monomers divinyl sebacate and 12-dodecanolide by lipase PF catalysis. By using 2–3% of the divinyl ester a mixture of telechelic polyesters carrying carboxylic acid ends was achieved [77]. The mixture was probably a result of uncontrolled water content in the incubation. Eriksson et al. used CAL-B to obtain well-defined telechelics in a one-pot polycondensation. The backbone of the telechelics was built from ethylene glycol and divinyl adipate. Specific degrees of polymerisation (4, 8 and 13) were reached by terminating the process with the addition of 2-hydroxyethyl methacrylate. Well-defined telechelics with more than 90% methacrylate ends were used directly in film formation, without any other purification than filtering off the immobilized lipase (Figure 21). The telechelics were either homopolymerized or polymerized in combination with a tetrathiol cross-linker to form strong films under UV irradiation [78].

In a similar approach the same research group synthesized the telechelic tetraallyl ether-poly(butylene adipate) (Figure 22). Each telechelic molecule carried four allyl ether groups, which allowed extensive crosslinking using thiolene chemistry with dithiols or tetrathiols [79].

Through a combination of lipase-catalyzed condensation and ring-opening polymerisation oligomers of pentadecalactone and adipic acid were terminated by glycidol (Figure 23). By changing the stoichiometry of the building blocks, telechelics of different controlled molecular weights could be obtained, which readily polymerized to form films after filtering off the enzyme. The properties of the films depended on the fraction of pentadecalactone and crosslinking density [80].

Conclusion

In this short review it has been discussed the synthetic potential of dicarboxylic esters in biocatalyzed reactions. Literature examples related to polyesters are significantly more numerous. Nevertheless, as it has been shown in the initial paragraphs, this

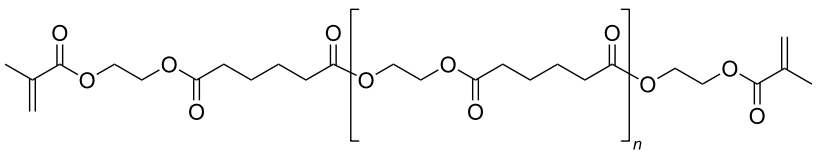

Figure 21: Telechelics with methacrylate ends.

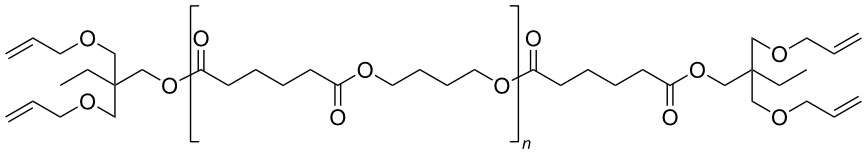

Figure 22: Telechelics with allyl-ether ends.

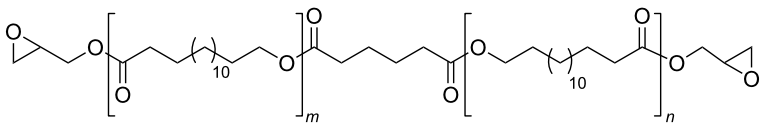

Figure 23: Telechelics with ends functionalized as epoxides.

methodology allows also the facile synthesis of hybrid derivatives of natural compounds with modified physical–chemical properties (i.e., increased water solubility, different supramolecular behavior) and with possible synergic biological activities.

Acknowledgements

The authors acknowledge Fondazione Cariplo and Regione Lombardia for financial support (Progetto BIOREFILL – BIOREFinery Integrated Lombardy Labs, 2013 – 2015).

References

1. Carrea, G.; Riva, S. *Organic Synthesis with Enzymes in Non-Aqueous Media;* Wiley-VCH: Weinheim, Germany, 2008. doi:10.1002/9783527621729
2. Koskinen, A. M. P.; Klibanov, A. M. *Enzymatic Reations in Organic Media;* Chapman & Hall: Glasgow, U.K., 1996.
3. Klibanov, A. M. *Nature* **2001,** *409,* 241–246. doi:10.1038/35051719
4. Klibanov, A. M. *Trends Biochem. Sci.* **1989,** *14,* 141–144. doi:10.1016/0968-0004(89)90146-1
5. Park, S.; Kazlauskas, R. J. *Curr. Opin. Biotechnol.* **2003,** *14,* 432–437.
6. Carrea, G.; Riva, S. *Angew. Chem., Int. Ed.* **2000,** *39,* 2226–2254. doi:10.1002/1521-3773(20000703)39:13<2226::AID-ANIE2226>3.0.CO;2-L
7. Plou, F. J.; Cruces, M. A.; Ferrer, M.; Fuentes, G.; Pastor, E.; Bernabè, M.; Christensen, M.; Comelles, F.; Parra, J. L.; Ballesteros, A. *J. Biotechnol.* **2002,** *96,* 55–66. doi:10.1016/S0168-1656(02)00037-8
8. Therisod, M.; Klibanov, A. M. *J. Am. Chem. Soc.* **1986,** *108,* 5638–5640. doi:10.1021/ja00278a053
9. Cruz Silva, M. M.; Carvalho, J. F.; Riva, S.; Sà e Melo, M. L. *Curr. Org. Chem.* **2011,** *15,* 928–941. doi:10.2174/138527211794518871
10. Michels, P. C.; Khmelnitsky, Y. L.; Dordick, J. S.; Clark, D. S. *Trends Biotechnol.* **1998,** *16,* 210–215. doi:10.1016/S0167-7799(98)01190-1
11. Akbar, U.; Shin, D.-S.; Schneider, E.; Dordick, J. S.; Clark, D. S. *Tetrahedron Lett.* **2010,** *51,* 1220–1225. doi:10.1016/j.tetlet.2009.12.119
12. Secundo, F.; Carrea, G.; De Amici, M.; Joppolo di Ventimiglia, S.; Dordick, J. S. *Biotechnol. Bioeng.* **2003,** *81,* 391–394. doi:10.1002/bit.10486
13. Kirchner, G.; Scollar, M. P.; Klibanov, A. M. *J. Am. Chem. Soc.* **1985,** *107,* 1012–1016. doi:10.1021/ja00310a052
14. Riva, S.; Chopineau, J.; Kieboom, A. P. G.; Klibanov, A. M. *J. Am. Chem. Soc.* **1988,** *110,* 584–589. doi:10.1021/ja00210a045
15. Faber, K.; Riva, S. *Synthesis* **1992,** 895–910. doi:10.1055/s-1992-26255
16. Magrone, P.; Cavallo, F.; Panzeri, W.; Passarella, D.; Riva, S. *Org. Biomol. Chem.* **2010,** *8,* 5583–5590. doi:10.1039/c0ob00304b
17. Bianchi, D.; Cesti, P.; Battistel, E. *J. Org. Chem.* **1988,** *53,* 5531–5534. doi:10.1021/jo00258a024
18. Ottolina, G.; Carrea, G.; Riva, S. *Biocatalysis* **1991,** *5,* 131–136. doi:10.3109/10242429109014861
19. Schrittwieser, J. H.; Resch, V. *RSC Adv.* **2013,** *3,* 17602–17632. doi:10.1039/c3ra42123f
20. Serra, S.; Fuganti, C.; Brenna, E. *Trends Biotechnol.* **2005,** *23,* 193–198. doi:10.1016/j.tibtech.2005.02.003
21. Sima Sariaslani, F.; Rosazza, J. P. N. *Enzyme Microb. Technol.* **1984,** *6,* 242–253.
22. González-Sabín, J.; Morán-Ramallal, R.; Rebolledo, F. *Chem. Soc. Rev.* **2011,** *40,* 5321–5335. doi:10.1039/C1CS15081B
23. Riva, S. *J. Mol. Catal. B: Enzym.* **2001,** *19,* 43–54.
24. Nunez, L. E.; Menendez, N.; Gonzalez-Sabin, J.; Moris-Varas, F.; Garcia-Fernandez, B.; Perez, M.; Brana, V.; Salas, J. A. WO Patent 009987, 2011.
25. Xiao, Y. M.; Mao, P.; Zhao, Z.; Yang, L. R.; Lin, X. F. *Chin. Chem. Lett.* **2010,** *21,* 59–62. doi:10.1016/j.cclet.2009.08.017
26. Danieli, B.; Luisetti, M.; Riva, S.; Bertinotti, A.; Ragg, E.; Scaglioni, L.; Bombardelli, E. *J. Org. Chem.* **1995,** *60,* 3637–3642. doi:10.1021/jo00117a012
27. Riva, S.; Danieli, B.; Luisetti, M. *J. Nat. Prod.* **1996,** *59,* 618–621. doi:10.1021/np960239m
28. Krejzová, J.; Šimon, P.; Vavříková, E.; Slámová, K.; Pelantová, H.; Riva, S.; Spiwok, V.; Křen, V. *J. Mol. Catal. B: Enzym.* **2013,** *87,* 128–134. doi:10.1016/j.molcatb.2012.10.016
29. Vavrivoka, E.; Vack, J.; Valentova, K.; Marhol, P.; Ulrichova, J.; Kuzma, M.; Kren, V. *Molecules* **2014,** *19,* 4115–4134.
30. Khmelnitsky, Y. L.; Budde, C.; Arnold, J. M.; Usyatinsky, A.; Clark, D. S.; Dordick, J. S. *J. Am. Chem. Soc.* **1997,** *119,* 11554–11555. doi:10.1021/ja973103z
31. Wu, Q.; Xia, A.; Lin, X. *J. Mol. Catal. B: Enzym.* **2008,** *54,* 76–82. doi:10.1016/j.molcatb.2007.12.023
32. Xia, A.; Wu, Q.; Liu, B.; Lin, X. *Enzyme Microb. Technol.* **2008,** *42,* 414–420. doi:10.1016/j.enzmictec.2007.12.001
33. Quian, X.; Liu, B.; Wu, Q.; Lv, D.; Lin, X.-F. *Bioorg. Med. Chem.* **2008,** *16,* 5181–5188. doi:10.1016/j.bmc.2008.03.012
34. Quan, J.; Chen, Z.; Han, C.; Lin, X. *Bioorg. Med. Chem.* **2007,** *15,* 1741–1748. doi:10.1016/j.bmc.2006.11.039
35. Wu, Q.; Wang, M.; Chen, Z. C.; Lu, D. S.; Lin, X. F. *Enzyme Microb. Technol.* **2006,** *39,* 1258–1263. doi:10.1016/j.enzmictec.2006.03.012
36. Romeo, S.; Parapini, S.; Dell'Agli, M.; Vaiana, N.; Magrone, P.; Galli, G.; Sparatore, A.; Taramelli, D.; Bosisio, E. *ChemMedChem* **2008,** *3,* 418–420. doi:10.1002/cmdc.200700166
37. Passarella, D.; Giardini, A.; Peretto, B.; Fontana, G.; Sacchetti, A.; Silvani, A.; Ronchi, C.; Cappelletti, G.; Cartelli, D.; Borlak, J.; Danieli, B. *Bioorg. Med. Chem.* **2008,** *16,* 6269–6285. doi:10.1016/j.bmc.2008.04.025
38. Ayral-Kaloustian, S.; Gu, J.; Lucas, J.; Cinque, M.; Gaydos, C.; Zask, A.; Chaudhary, I.; Wang, J.; Di, L.; Young, M.; Ruppen, M.; Mansour, T. S.; Gibbons, J. J.; Yu, K. *J. Med. Chem.* **2010,** *53,* 452–459. doi:10.1021/jm901427g
39. Riva, E.; Comi, D.; Borrelli, S.; Colombo, F.; Danieli, D.; Borlak, J.; Evensen, L.; Lorens, J. B.; Fontana, G.; Gia, O. M.; Via, L. D.; Passarella, D. *Bioorg. Med. Chem.* **2010,** *18,* 8660–8668. doi:10.1016/j.bmc.2010.09.069
40. Passarella, D.; Peretto, B.; Blasco y Yepes, R.; Cappelletti, G.; Cartelli, D.; Ronchi, C.; Snaith, J.; Fontana, G.; Danieli, B.; Borlak, J. *Eur. J. Med. Chem.* **2010,** *45,* 219–226. doi:10.1016/j.ejmech.2009.09.047
41. Passarella, D.; Comi, D.; Cappelletti, G.; Cartelli, D.; Gertsch, J.; Quesada, A. R.; Borlak, J.; Altmann, K.-H. *Bioorg. Med. Chem.* **2009,** *17,* 7435–7440. doi:10.1016/j.bmc.2009.09.032
42. Danieli, B.; Giardini, A.; Lesma, G.; Passarella, D.; Peretto, B.; Sacchetti, A.; Silvani, A.; Pratesi, G.; Zunino, F. *J. Org. Chem.* **2006,** *71,* 2848–2853. doi:10.1021/jo052677g

43. Passarella, D.; Comi, D.; Vanossi, A.; Paganini, G.; Colombo, F.; Ferrante, L.; Zuco, V.; Danieli, B.; Zunino, F. *Bioorg. Med. Chem. Lett.* **2009,** *19,* 6358–6363. doi:10.1016/j.bmcl.2009.09.075
44. Vavrikova, E.; Kalachova, L.; Pyszkova, M.; Riva, S.; Kuzma, M.; Kren, V.; Valentova, K.; Ulrichova, J.; Vrba, J.; Vacek, J. *Chem. – Eur. J.*, submitted.
45. Ambrosi, M.; Fratini, E.; Alfredsson, V.; Ninham, B. W.; Giorgi, R.; Lo Nostro, P.; Baglioni, P. *J. Am. Chem. Soc.* **2006,** *128,* 7209–7214. doi:10.1021/ja057730x
46. Dolle, C.; Magrone, P.; Riva, S.; Ambrosi, M.; Fratini, E.; Peruzzi, N.; Lo Nostro, P. *J. Phys. Chem. B* **2011,** *115,* 11638–11649. doi:10.1021/jp204920y
47. Sahoo, B.; Brandstat, K. F.; Lane, T. H.; Gross, R. A. *Org. Lett.* **2005,** *7,* 3857–3860. doi:10.1021/ol050942e
48. Okumura, S.; Iwai, M.; Tominaga, Y. *Agric. Biol. Chem.* **1984,** *48,* 2805–2808. doi:10.1271/bbb1961.48.2805
49. Zhang, J.; Shi, H.; Di Wu, D.; Xing, Z.; Zhang, A.; Yang, Y.; Li, Q. *Process Biochem.* **2014,** *49,* 797–806. doi:10.1016/j.procbio.2014.02.006
50. Kobayashi, S.; Makino, A. *Chem. Rev.* **2009,** *109,* 5288–5353. doi:10.1021/cr900165z
51. Gross, R. A.; Ganesh, M.; Lu, W. *Trends Biotechnol.* **2010,** *28,* 435–443. doi:10.1016/j.tibtech.2010.05.004
52. Vouyiouka, S. N.; Topakas, E.; Katsini, A.; Papaspyrides, C. D.; Christakopoulos, P. *Macromol. Mater. Eng.* **2013,** *298,* 679–689. doi:10.1002/mame.201200188
53. Binns, F.; Harffey, P.; Roberts, S. M.; Taylor, A. *J. Chem. Soc., Perkin Trans. 1* **1999,** *1,* 2671–2676. doi:10.1039/a904889h
54. Kulshrestha, A. S.; Gao, W.; Gross, R. A. *Macromolecules* **2005,** *38,* 3193–3204. doi:10.1021/ma0480190
55. Yang, Z.; Zhang, X.; Luo, X.; Jiang, Q.; Liu, J.; Jiang, Z. *Macromolecules* **2013,** *46,* 1743–1753. doi:10.1021/ma302433x
56. Bhatia, S.; Mohr, A.; Mathur, D.; Parmar, V. S.; Haag, R.; Prasad, A. K. *Biomacromolecules* **2011,** *12,* 3487–3498. doi:10.1021/bm200647a
57. Liu, B.; Zhang, X.; Chen, Y.; Yao, Z.; Yang, Z.; Gao, D.; Jiang, Q.; Liu, J.; Jiang, Z. *Polym. Chem.* **2015,** *6,* 1997–2010. doi:10.1039/C4PY01321B
58. Wallace, J. S.; Morrow, C. J. *J. Polym. Sci., Part A-1: Polym. Chem.* **1989,** *27,* 2553–2567. doi:10.1002/pola.1989.080270807
59. Yang, Y.; Lu, W.; Cai, J.; Hou, Y.; Ouyang, S.; Xie, W.; Gross, R. A. *Macromolecules* **2011,** *44,* 1977–1985. doi:10.1021/ma102939k
60. Warwel, S.; Demes, C.; Steinke, G. *J. Polym. Sci., Part A-1: Polym. Chem.* **2001,** *39,* 1601–1609. doi:10.1002/pola.1137
61. Jiang, Y.; Woortman, A. J. J.; van Ekenstein, G. O. R. A.; Loos, K. *Biomolecules* **2013,** *3,* 461–480. doi:10.3390/biom3030461
62. Yao, D.; Li, G.; Kuila, T.; Li, P.; Kim, N. H.; Kim, S.-I.; Lee, J. H. *J. Appl. Polym. Sci.* **2011,** *120,* 1114–1120. doi:10.1002/app.33257
63. Kato, M.; Toshima, K.; Matsumura, S. *Biomacromolecules* **2009,** *10,* 366–373. doi:10.1021/bm801132d
64. Tanaka, A.; Kohri, M.; Takiguchi, T.; Kato, M.; Matsumura, S. *Polym. Degrad. Stab.* **2012,** *97,* 1415–1422. doi:10.1016/j.polymdegradstab.2012.05.016
65. Khan, A.; Sharma, S. K.; Kumar, A.; Watterson, A. C.; Kumar, J.; Parmar, V. S. *ChemSusChem* **2014,** *7,* 379–390. doi:10.1002/cssc.201300343
66. Pandey, M. K.; Kumar, S.; Thimmulappa, R. K.; Parmar, V. S.; Biswal, S.; Watterson, A. C. *Eur. J. Pharm. Sci.* **2011,** *43,* 16–24. doi:10.1016/j.ejps.2011.03.003
67. Pandey, M. K.; Kumar, A.; Ravichandran, S.; Parmar, V. S.; Watterson, A. C.; Kumar, J. *J. Macromol. Sci., Part A: Pure Appl. Chem.* **2014,** *51,* 399–404. doi:10.1080/10601325.2014.893131
68. Frampton, M. B.; Séguin, J. P.; Marquardt, D.; Harroun, T. A.; Zelisko, P. M. J. *J. Mol. Catal. B: Enzym.* **2013,** *85–86,* 149–155. doi:10.1016/j.molcatb.2012.09.010
69. Müller, S. S.; Frey, H. *Macromol. Chem. Phys.* **2012,** *213,* 1783–1790. doi:10.1002/macp.201200269
70. Liu, J.; Jiang, Z.; Zhou, J.; Zhang, S.; Saltzman, W. M. *J. Biomed. Mater. Res., Part A* **2011,** *96,* 456–465. doi:10.1002/jbm.a.32994
71. Qian, X.; Jiang, Z.; Lin, X.; Wu, Q. *J. Polym. Sci., Part A-1: Polym. Chem.* **2013,** *51,* 2049–2057. doi:10.1002/pola.26594
72. Qian, X.; Wu, Q.; Xu, F.; Lin, X. *Polymer* **2011,** *52,* 5479–5485. doi:10.1016/j.polymer.2011.10.003
73. Xu, F.; Zhong, J.; Qian, X.; Li, Y.; Lin, X.; Wu, Q. *Polym. Chem.* **2013,** *4,* 3480–3490. doi:10.1039/c3py00156c
74. Ragupathy, L.; Ziener, U.; Dyllick-Brenzinger, R.; von Vacano, B.; Landfester, K. *J. Mol. Catal. B: Enzym.* **2012,** *76,* 94–105. doi:10.1016/j.molcatb.2011.11.019
75. Poulhès, F.; Mouysset, D.; Gil, G.; Bertrand, M. P.; Gastaldi, S. *Polymer* **2013,** *54,* 3467–3471. doi:10.1016/j.polymer.2013.05.011
76. Syrén, P.-O. *FEBS J.* **2013,** *280,* 3069–3083.
77. Uyama, H.; Kikuchi, H.; Kobayashi, S. *Bull. Chem. Soc. Jpn.* **1997,** *70,* 1691–1695. doi:10.1246/bcsj.70.1691
78. Eriksson, M.; Hult, K.; Malmström, E.; Johansson, M.; Trey, S. M.; Martinelle, M. *Polym. Chem.* **2011,** *2,* 714–719. doi:10.1039/C0PY00340A
79. Eriksson, M.; Boyer, A.; Sinigoi, L.; Johansson, M.; Malmström, E.; Hult, K.; Trey, S.; Martinelle, M. *J. Polym. Sci., Part A-1: Polym. Chem.* **2010,** *48,* 5289–5297. doi:10.1002/pola.24328
80. Eriksson, M.; Fogelström, L.; Hult, K.; Malmström, E.; Johansson, M.; Trey, S.; Martinelle, M. *Biomacromolecules* **2009,** *10,* 3108–3113. doi:10.1021/bm9007925

License and Terms

BEILSTEIN JOURNAL OF ORGANIC CHEMISTRY

Robust bifunctional aluminium–salen catalysts for the preparation of cyclic carbonates from carbon dioxide and epoxides

Yuri A. Rulev[1], Zalina Gugkaeva[1], Victor I. Maleev[1], Michael North*[2] and Yuri N. Belokon*[1]

Full Research Paper

Open Access

Address:
[1]Nesmeyanov Institute of Organoelement Compounds, Moscow 19991, Russia and [2]Green Chemistry Centre of Excellence, Department of Chemistry, University of York, Heslington, York, YO10 5DD, UK

Email:
Michael North* - Michael.North@york.ac.uk;
Yuri N. Belokon* - yubel@ineos.ac.ru

* Corresponding author

Keywords:
aluminium; carbon dioxide; cyclic carbonate; epoxide; salen

Beilstein J. Org. Chem. **2015,** *11,* 1614–1623.
doi:10.3762/bjoc.11.176

Received: 25 June 2015
Accepted: 26 August 2015
Published: 11 September 2015

This article is part of the Thematic Series "Sustainable catalysis".

Guest Editor: N. Turner

Abstract

Two new one-component aluminium-based catalysts for the reaction between epoxides and carbon dioxide have been prepared. The catalysts are composed of aluminium–salen chloride complexes with trialkylammonium groups directly attached to the aromatic rings of the salen ligand. With terminal epoxides, the catalysts induced the formation of cyclic carbonates under mild reaction conditions (25–35 °C; 1–10 bar carbon dioxide pressure). However, with cyclohexene oxide under the same reaction conditions, the same catalysts induced the formation of polycarbonate. The catalysts could be recovered from the reaction mixture and reused.

Introduction

Carbon dioxide is a renewable and inexpensive carbon source, so great efforts have been directed at developing novel methods for the valorization of this abundant raw material [1]. One way of achieving this goal is to produce cyclic carbonates or polycarbonates from carbon dioxide and the corresponding epoxides (Scheme 1). Cyclic carbonates are an important class of solvents [2] and starting materials in organic synthesis [3-6].

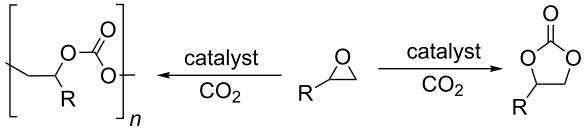

Scheme 1: Synthesis of cyclic and polycarbonates.

Although a significant array of catalysts have been developed for the production of cyclic carbonates [7-9] and polycarbonates [10,11] from carbon dioxide and epoxides, the most developed and privileged set of catalysts are based on Lewis acidic metal–salen complexes. In particular, cobalt(III) and

chromium(III) complexes were found to be highly efficient for polycarbonate production [12]. Further modification of the salen moiety by the introduction of basic or ammonium salts through alkyl spacers attached to the salen aromatic rings led to the formation of a family of bifunctional catalysts possessing both Lewis acid and nucleophilic catalysis capability (via the anion in the case of catalysts containing ammonium salts), with a concomitant increase in their activity [12,13]. Recently, more environmentally benign aluminium-based complexes, including salen complexes, have been introduced to catalyse cyclic carbonate production [14]. The performance of these catalysts was also greatly improved by the introduction of bifunctional versions of the catalyst system, combining an electrophilic aluminium centre with an ammonium cation/nucleophilic-counteranion combination within the framework of a single catalytic species as reported by North [15], Liu and Darensbourg [14], and Lu [16] (Figure 1).

Unfortunately, the bifunctional derivatives with an alkyl spacer are not very stable at higher temperatures because of the well-known ammonium salt decomposition pathways including: Zaitsev and Hoffman type eliminations [17-19] and retro-Menschutkin reactions [20-23]. We reasoned that the direct introduction of ammonium moieties onto the aromatic rings of the salen ligands (as in structures **1** and **2**) would greatly stabilize the whole structure by reducing the number of sp^3-hybridized carbon atoms attached to the nitrogen atoms of the ammonium salts and increasing the steric hindrance around the ammonium salts. Herein, we report the synthesis of two aluminium–salen complexes incorporating quaternary ammonium salts directly attached to the salen ligand and their catalytic activities for the coupling of epoxides and carbon dioxide under solvent free conditions. Catalyst recycling experiments are also reported and show the robustness of this system.

Results and Discussion

The preparation of salen ligands **8a** and **8b** was conducted according to Scheme 2, starting from *tert*-butylphenol, which was formylated and then nitrated to produce 5-nitro-3-(*tert*-butyl)salicylaldehyde (**5**) [24-27]. 5-*N,N*-Dimethylamino-3-(*tert*-butyl)salicylaldehyde (**6**) was prepared directly from **5**, using a literature procedure [28,29]. The salen ligand **7** was then obtained in high yield by condensation with (*R,R*)-cyclohexanediamine, according to a known technique [30]. Ligand **7** was efficiently alkylated under mild reaction conditions using either methyl iodide or benzyl bromide, giving the corresponding

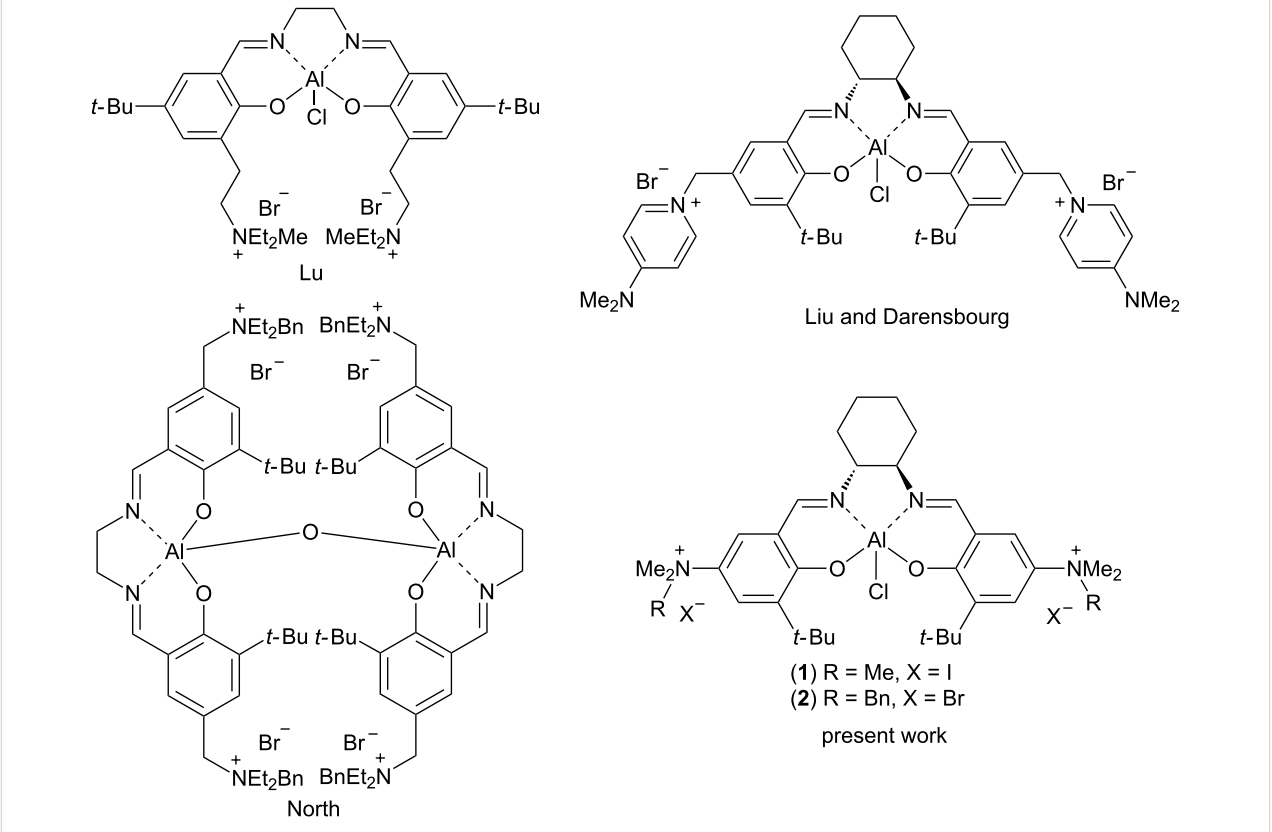

Figure 1: Bifunctional aluminium–salen complexes, including those studied in this work.

positively charged salen ligands **8a** and **8b** in 95 and 78% yields respectively. The aluminium–salen complexes were prepared by treating **8a** and **8b** with diethylaluminium chloride (Scheme 3), affording complexes **1** and **2** in 96% and 91% yields respectively. These complexes could be used without any additional purification.

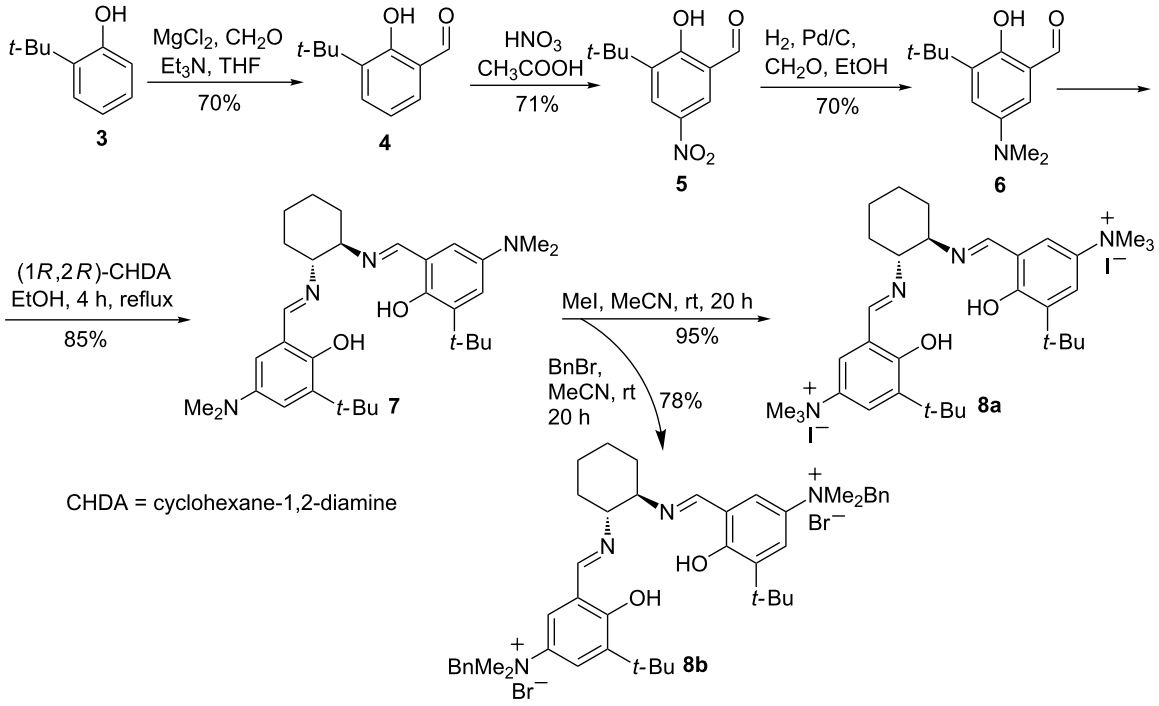

Scheme 2: Synthesis of salen ligands **8a** and **8b**.

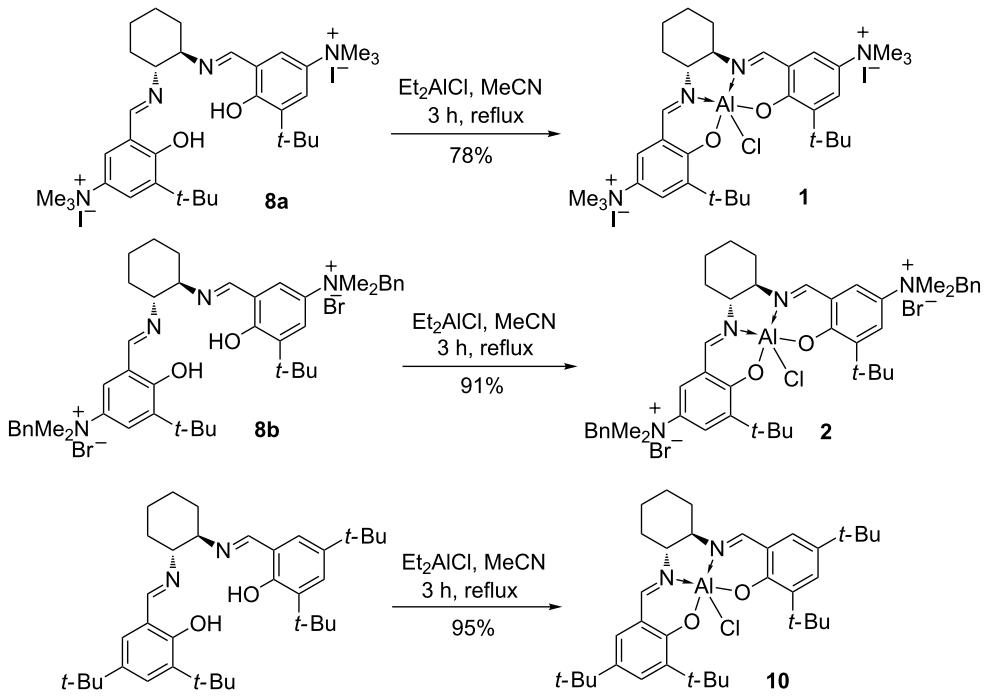

Scheme 3: The preparation of aluminum complexes **1**, **2** and **10**.

Styrene oxide was used as a model substrate to test the catalytic efficiency of complexes **1** and **2** in the coupling reaction with carbon dioxide. Table 1 summarizes the experimental results. It is apparent from the data that both catalysts are effective at promoting the coupling reaction even at room temperature and 1 bar of carbon dioxide pressure (Table 1, entries 1–4 and 10–12). However, complex **2** was a better catalyst, affording 83% conversion of styrene oxide to the corresponding cyclic carbonate after 24 hours, whereas complex **1** gave only 47% conversion under the same conditions (Table 1, entries 4 and 12). Increasing either the temperature of the reaction or the carbon dioxide pressure had positive effects on the catalytic performance (Table 1, entries 8, 9 and 13).

Furthermore, the performance of catalyst **1** could be improved by adding one equivalent of water and triethylamine relative to the catalyst loading (Table 1, entries 5–7). Presumably, some of complex **1** was converted into a highly active oxygen-bridged aluminium complex in situ, as shown in Scheme 4. High activities for this type of dinuclear complexes have been reported before [31].

In order to prove the bifunctional nature of our catalysts, aluminium complex **10** was prepared (Scheme 3) using 3,5-di-(*tert*-butyl)salicylaldehyde as a starting material. It was found that this catalyst was almost inactive in the reaction of styrene oxide with carbon dioxide (Table 1, entry 14). After addition of tetrabutylammonium iodide (5 mol %) as a cocatalyst, the conversion was increased to 80% (Table 1, entry 15), which was close to the performance of catalyst **2** (Table 1, entry 12). This supports the hypothesis that complexes **1** and **2** are bifunctional catalysts in which both the

Table 1: Coupling of CO_2 and styrene oxide promoted by complexes **1**, **2** and **10**.[a]

Entry	Catalyst	Catalyst loading (mol %)	Time (h)	Pressure (bar)	Temperature (°C)	Conversion (%)
1	**1**	0.2	24	1	25	8
2	**1**	1	24	1	25	16
3	**1**	2	24	1	25	40
4	**1**	2.5	24	1	25	47
5[b]	**1**	2.5	3	1	25	8
6[b]	**1**	2.5	6	1	25	17
7[b]	**1**	2.5	24	1	25	72
8	**1**	2.5	24	10	25	70
9	**1**	2.5	24	10	35	100
10	**2**	2.5	3	1	25	14
11	**2**	2.5	6	1	25	43
12	**2**	2.5	24	1	25	83
13	**2**	2.5	24	10	25	100
14	**10**	2.5	24	1	25	5
15[c]	**10**	2.5	24	1	25	80

[a]In neat styrene oxide. [b]One equivalent of H_2O and Et_3N were added to the catalyst. [c]With 5 mol % tetrabutylammonium iodide as cocatalyst.

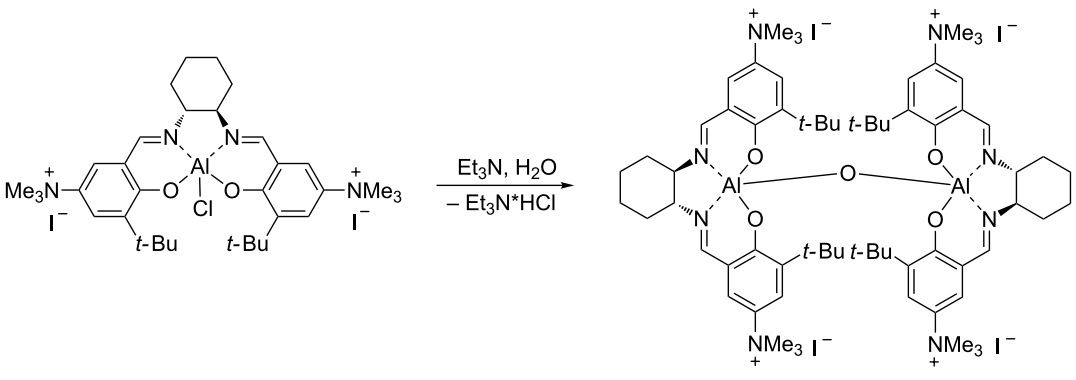

Scheme 4: Possible formation of a dinuclear complex from **1** by treatment with H_2O and Et_3N.

aluminium centre and the ammonium halide play important catalytic roles.

After finding the optimal reaction conditions for each catalyst, both complexes **1** and **2** were tested with a range of epoxides. These experiments were carried out without added water to allow direct comparison of the two catalysts and to avoid complicating the reaction system. The results are summarized in Table 2. Both catalysts proved to be efficient for coupling both aromatic and aliphatic substrates. In all cases reported in Table 2, cyclic carbonate, catalyst and unreacted epoxide (for entries 10 and 11) were the only species detected by ^{1}H NMR spectroscopy of the crude reaction product prior to purification by column chromatography. The moderate yield for propylene oxide (Table 2, entry 6) can be explained by volatility of the starting material under the reaction conditions.

Table 2: Coupling of CO_2 and various epoxides promoted by complexes **1** and **2**.[a]

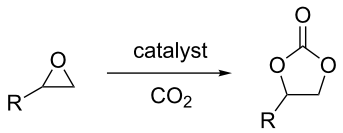

Entry	Catalyst	R	Conversion[b] (%)	Yield[c] (%)
1	**1**	Ph	100	62
2	**1**	CH_2OPh	100	78
3	**1**	*p*-ClPh	100	95
4	**1**	Bu	100	80
5	**1**	Et	100	78
6	**1**	Me	100	52
7	**1**	CH_2Cl	100	82
8	**1**	CH_2OH	100	85
9	**2**	Ph	100	80
10	**2**	CH_2OPh	64	56
11	**2**	*p*-ClPh	99	84
12	**2**	Bu	100	60
13	**2**	Et	100	71
14	**2**	Me	100	88
15	**2**	CH_2Cl	100	80
16	**2**	CH_2OH	100	76

[a]Reaction conditions for catalyst **1**: solvent free, 10 bar pressure of CO_2, 35 °C, 24 h; for catalyst **2**: solvent free, 10 bar pressure of CO_2, 25 °C, 24 h. [b]Determined by ^{1}H NMR spectroscopy of the unpurified product. [c]After purification by column chromatography.

No cyclic carbonate was detected when cyclohexene oxide was used as substrate (Table 3, entries 1–5) and almost no conversion at all was detected in the reaction promoted by complex **1** (Table 3, entries 1 and 2). Catalyst **2** was more active and catalysed the synthesis of the corresponding polycarbonate with 64% conversion at 10 bar (Table 3, entry 4) and 92% at 35 bar carbon dioxide pressure (Table 3, entry 5). Previous reports have indicated that in the presence of a cocatalyst, aluminium–salen complexes can catalyse the formation of either cyclic [32] or polycarbonate [33,34] from cyclohexene oxide, depending on the exact structure of the catalyst and cocatalyst. However, this is the first report of a one-component aluminium–salen-based catalyst for polycyclohexene carbonate synthesis.

MALDI–TOF mass-spectra data (Figure 2) showed that the polycarbonate consisted of a mixture of oligomers with a range of monomer units (*n* from 4 to 10) with the maximum intensity at $n = 6$. Both ends of the polymer chain are capped with alcohol groups, suggesting that chain-transfer to adventitious moisture occurred during the polymerisation. GPC data (Figure 3) was consistent with the MALDI–TOF data, showing that most of the polymer has a molecular weight between 300

Table 3: Addition CO_2 to cyclohexene oxide.[a]

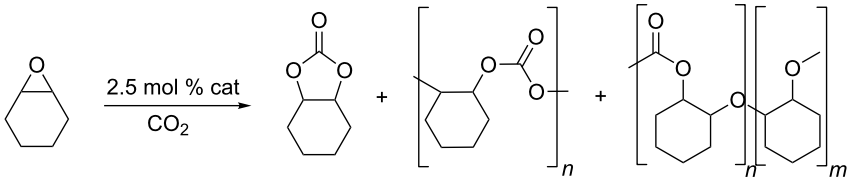

Entry	Catalyst	Pressure (bar)	Time (h)	Conversion (%)	Polycarbonate (%)	Polyether linkages (%)
1	**1**	10	24	6	6	–
2	**1**	10	111	11	11	–
3	**2**	10	24	8	8	–
4[b]	**2**	10	96	64	57	5
5[b]	**2**	35	96	92	85	7

[a]Neat cyclohexene oxide, temperature: for catalyst **1**, 35 °C; for catalyst **2**, 25 °C, only traces of cyclic carbonates were detected. [b]The ratio of polycarbonate/polyether was determined from the ^{1}H NMR spectrum [11].

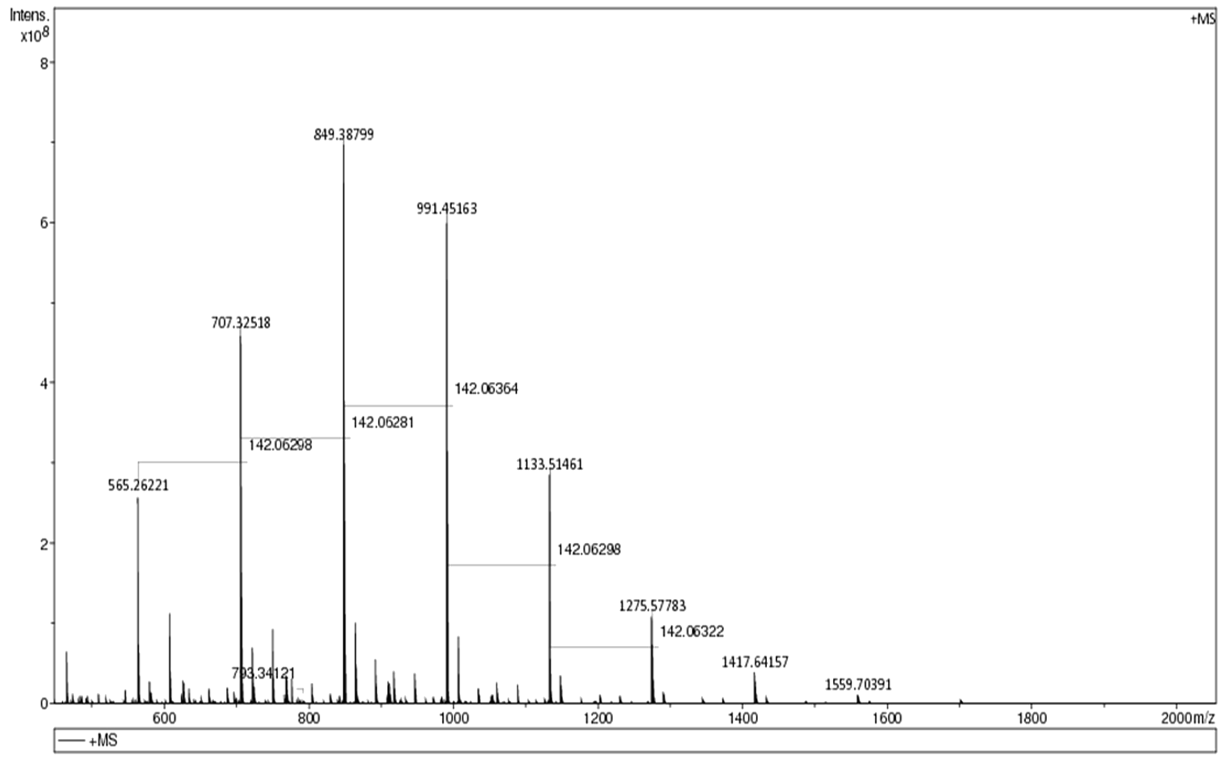

Figure 2: MALDI–TOF spectrum of poly(hexene carbonate) prepared using catalyst **2**. The peak at 565 Daltons corresponds to four ring-opened cyclohexene oxide units, three CO_2 units, 2 hydrogens (to cap the two terminal oxygens) and a sodium ion. The other peaks are then separated by 142 Daltons corresponding to an additional ring-opened cyclohexene oxide and carbon dioxide.

and 1000 Daltons. This type of low molecular weight polycarbonate–polyol is currently attracting much interest associated with its use in sustainable polyurethanes [35].

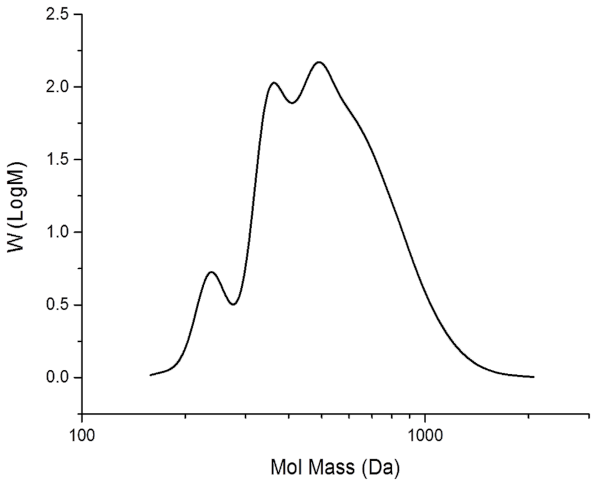

Figure 3: GPC trace of poly(cyclohexene carbonate) prepared using catalyst **2.** The chromatogram was obtained in THF and is referenced to polystyrene standards.

To show the stability of our catalytic system, catalyst **1** was reused three times. For this purpose the catalyst was precipitated from the reaction mixture by the addition of ether followed by filtration. The catalyst was then dried in vacuo and then reused. The results are summarized in Table 4. As can be seen, there were no significant losses of catalytic activity observed after three catalytic cycles.

Table 4: The catalytic activity of recovered catalyst **1**.

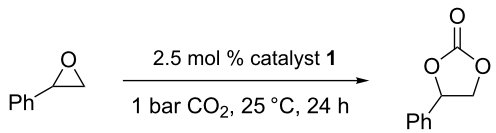

Cycle	Conversion
1	47
2	45
3	43

Conclusion

In conclusion, we have developed two new, bifunctional aluminium(salen) catalysts with quaternary ammonium groups directly attached to the aromatic rings. The catalytic system showed high activity in cyclic carbonate formation with a range of substrates. The bifunctional nature of our catalysts was demonstrated by comparing their performance with similar non-modified aluminium complex **10**. In contrast to previously reported aluminium–salen complexes, catalysts **1** and **2** produce polycarbonate rather than cyclic carbonate from cyclohexene oxide.

Experimental

Materials

Commercial reagents were used as received unless stated otherwise. Column chromatography was performed using Silica Gel Kieselgel 60 (Merck).

Instrumentation

^{1}H NMR and ^{13}C NMR spectra were recorded on Bruker Avance 300 and Bruker Avance III–400 (operating at 300 and 400 MHz for protons, respectively) spectrometers. Optical rotations were measured on a Perkin–Elmer 341 polarimeter in a 5-cm cell. Melting points were determined in open capillary tubes and are uncorrected. Mass spectra were recorded at the University of York Mass Spectrometry Service Unit using ESI and MALDI ionization methods. GPC was carried out using a set (PSS SDV High) of 3 analytical columns (300 × 8 mm, particle diameter 5 μm) of 1000, 10^5 and 10^6 Å pore sizes, plus guard column, supplied by Polymer Standards Service GmbH (PSS) installed in a PSS SECcurity GPCsystem. Elution was with tetrahydrofuran at 1 mL/min with a column temperature of 23 °C and detection by refractive index. 20 μL of a 1 mg/mL sample in THF was injected for each measurement and eluted for 40 minutes. Calibration was carried out in the molecular weight range 400–2 × 10^6 Da using ReadyCal polystyrene standards supplied by Sigma-Aldrich.

General procedures for compounds (**4–10**)

3-(*tert*-Butyl)-2-hydroxybenzaldehyde (**4**)

Prepared as described in previous work [24]. ^{1}H NMR (400 MHz, $CDCl_3$) δ 11.77 (s, 1H), 9.85 (s, 1H), 7.52 (d, J = 7.7 Hz, 1H), 7.39 (d, J = 7.7 Hz, 1H), 7.00–6.95 (m, 1H), 1.45 (s, 9H).

3-(*tert*-Butyl)-2-hydroxy-5-nitrobenzaldehyde (**5**)

Prepared by a modified literature procedure [25]. To a stirred solution of 3-(*tert*-butyl)-2-hydroxybenzaldehyde (1.0 g, 4.5 mmol) in glacial acetic acid (20 mL) was added 3.3 M nitric acid (4.0 mL). The solution was heated to reflux for 30 minutes. After cooling to room temperature, the solution was poured onto ice. The resulting precipitate was filtered and washed with water, giving 3-(*tert*-butyl)-2-hydroxy-5-nitrobenzaldehyde (0.9 g, 71%) as a yellow powder. ^{1}H NMR (400 MHz, $CDCl_3$) δ 12.43 (s, 1H), 9.96 (s, 1H), 8.43–8.35 (m, 2H), 1.45 (s, 9H).

3-(*tert*-Butyl)-5-(dimethylamino)-2-hydroxybenzaldehyde (**6**)

Prepared by a modified literature procedure [28]. Pd/C (10%, 100 mg) was added to a solution of 3-(*tert*-butyl)-2-hydroxy-5-nitrobenzaldehyde **5** (200 mg, 0.9 mmol) and 40% aqueous formaldehyde (4.5 mL) in ethanol (20 mL). The reaction mixture was stirred under 1 bar of hydrogen at room temperature for 24 hours. Then, the Pd/C was removed by filtration on celite, the volume of the filtrate was reduced by half under reduced pressure. Distilled water was added to the solution, resulting in formation of an orange precipitate (140 mg, 70%), which was filtered and washed with water (10 mL) and cold ethanol. ^{1}H NMR (400 MHz, $CDCl_3$) δ 11.27 (s, 1H), 9.83 (s, 1H), 7.14 (s, 1H), 6.71 (s, 1H), 2.88 (s, 6H), 1.41 (s, 9H); ^{13}C NMR (101 MHz, $CDCl_3$) δ 197.28, 154.37, 144.05, 138.97, 122.84, 120.34, 114.90, 42.07, 35.14, 29.22; mp 130–131 °C (lit. [28] 134 °C).

6,6'-((1*E*,1'*E*)-((1*R*,2*R*)-Cyclohexane-1,2-diylbis(azanylylidene))bis(methanylylidene))bis(2-(*tert*-butyl)-4-(dimethylamino)phenol) (**7**)

Prepared by a modified literature procedure [30]. A solution of (1*R*,2*R*)-diaminocyclohexane (64 mg, 0.57 mmol) in ethanol (5 mL) was added dropwise to a solution of **6** (250 mg, 1.13 mmol) in ethanol (15 mL). The resulting mixture was refluxed for 4 hours. After cooling to room temperature, distilled water (30 mL) was added. The resulting precipitate was filtered, washed with water and a small amount of cold ethanol to give a yellow powder (250 mg, 85%). ^{1}H NMR (400 MHz, $CDCl_3$) δ 8.23 (s, 2H), 6.88 (d, J = 3.0 Hz, 2H), 6.41 (d, J = 3.0 Hz, 2H), 3.35–3.18 (m, 2H), 2.74 (s, 12H), 2.00–1.90 (m, 4H), 1.79–1.72 (m, 2H), 1.47–1.43 (m, 2H), 1.38 (s, 18H); mp 106–110 °C; [α_D] −225 (c 0.01, MeOH); ESIMS m/z: $[M + H]^+$ calcd for $C_{32}H_{48}N_4O_2$, 521.38; found, 521.39.

5,5'-((1*E*,1'*E*)-((1*R*,2*R*)-Cyclohexane-1,2-diylbis(azanylylidene))bis(methanylylidene))bis(3-(*tert*-butyl)-4-hydroxy-*N,N,N*-trimethylbenzenaminium iodide) (**8a**)

To a solution of **7** (100 mg, 0.192 mmol) in dry acetonitrile (5 mL) was added methyl iodide (271 mg, 1.92 mmol). The solution was stirred at room temperature for 24 hours. Diethyl ether (10 mL) was then added to the solution resulting in formation of a precipitate which was filtered and washed with ether to leave a bright yellow powder (146 mg, 95%). ^{1}H NMR (400 MHz, DMSO-d_6) δ 8.59 (s, 1H), 7.85 (d, J = 3.2 Hz, 1H),

7.54 (d, J = 3.2 Hz, 1H), 3.58 (s, 1H), 3,49 (s, 9H), 1.88 (d, J = 11.3 Hz, 1H), 1.78 (s, 1H), 1.64 (s, 1H), 1.46 (s, 1H), 1.32 (s, 9H); ^{13}C NMR (75 MHz, CD_3OD) δ 164.76, 161.55, 139.89, 137.05, 121.25, 120.27, 118.11, 71.57, 56.59, 35.20, 32.47, 28.07, 23.83; mp 206–208 °C; [α_D] −175 (*c* 0.01, MeOH); ESIMS *m*/*z*: $[M]^{2+}$ calcd for $C_{34}H_{54}N_4O_2^{2+}$, 275.21; found, 275.21.

5,5'-((1*E*,1'*E*)-((1*R*,2*R*)-Cyclohexane-1,2-diylbis(azanylylidene))bis(methanylylidene))bis(*N*-benzyl-3-(*tert*-butyl)-4-hydroxy-*N*,*N*-dimethylbenzenaminium bromide) (**8b**)

To a solution of **7** (120 mg, 0.231 mmol) in dry acetonitrile (5 mL) was added benzyl bromide (79 mg, 0.46 mmol). The solution was stirred at room temperature for 24 hours. Diethyl ether (10 mL) was then added to the solution resulting in formation of a precipitate which was filtered and washed with ether to leave a bright yellow powder (165 mg, 78%). ^{1}H NMR (400 MHz, $CDCl_3$) δ 9.00 (s, 1H), 8.80 (d, J = 3.1 Hz, 1H), 7.33–7.27 (m, 1H), 7.19–6.98 (m, 4H), 6.76 (d, J = 3.2 Hz, 1H), 5.51–5.37 (s, 2H), 3.98–3.90 (m, 1H), 3.85 (d, J = 8.0 Hz, 6H), 2.2–2.1 (m, 1H), 2.0–1.9 (m, 1H), 1.6–1.4 (m, 2H), 1.25 (s, 9H); ^{13}C NMR (101 MHz, DMSO-d_6) δ 165.63, 162.37, 139.22, 134.33, 133.01, 130.73, 129.06, 128.87, 123.76, 122.83, 117.57, 72.26, 69.97, 53.21, 35.55, 32.51, 29.37, 29.04, 24.05; mp 140–144 °C; [α_D] 107 (*c* 0.05, MeOH); ESIMS *m*/*z*: $[M]^{2+}$ calcd for $C_{46}H_{62}N_4O_2^{2+}$, 351.24; found, 351.24.

Aluminium–salen complex (**1**)

To a solution of **8a** (113 mg, 0.14 mmol) in dry acetonitrile (5 mL) under argon was added diethylaluminum chloride (0.14 mL, 1 M solution in hexane). The reaction mixture was heated at reflux for 3 hours. The solvent was evaporated under reduced pressure to give a dark yellow powder (95 mg, 78%) which was used without any additional purification. ^{1}H NMR (400 MHz, DMSO-d_6) δ 8.46 (s, 1H), 8.10 (s, 1H), 7.66 (s, 1H), 3.55 (s, 9H), 3.38 (s, 1H), 2.55 (s, 1H), 1.94 (s, 1H), 1.50 (s, 9H), 1.44 (s, 1H), 1.33 (s, 1H); mp >300 °C; [α_D] −109.5 (*c* 0.05, MeOH); ESIMS *m*/*z*: $[M]^{2+}$ calcd for $C_{34}H_{52}AlClN_4O_2^{2+}$, 305.18; found, 296.19 (substitution of Cl by OH); 303.20 (substitution of Cl by OMe).

Aluminium–salen complex (**2**)

To a solution of **8b** (140 mg, 0.163 mmol) in dry acetonitrile (5 mL) under argon was added diethylaluminum chloride (0.17 mL, 1 M solution in hexane). The reaction mixture was refluxed for 3 hours. Then, the solvent was evaporated under reduced pressure to give a dark yellow powder (136 mg, 91%) which was used without any additional purification. ^{1}H NMR (400 MHz, DMSO-d_6) δ 8.33 (s, 1H), 7.83 (d, J = 3.0 Hz, 1H), 7.47 (t, J = 8.6 Hz, 1H), 7.40 (s, 1H), 7.28 (t, J = 7.7 Hz, 2H), 7.02 (d, J = 7.3 Hz, 2H), 4.99 (d, J = 7.5 Hz, 2H), 3.55 (d, J = 7.3 Hz, 6H), 3.35 (s, 1H) 1.89 (s, 2H), 1.48 (d, J = 4.5 Hz, 11H); mp >300 °C; [α_D] −83.4 (*c* 0.01, MeOH); ESIMS *m*/*z*: $[M]^{2+}$ calcd for $C_{46}H_{60}AlClN_4O_2^{2+}$, 381.21; found, 372.22 (substitution of Cl by OH); 379.20 (substitution of Cl by OMe).

Aluminium–salen complex (**10**)

Prepared as described in previous work [29]. ^{1}H NMR (400 MHz, DMSO-d_6) δ 8.35 (s, 1H), 7.41 (d, J = 2.4 Hz, 1H), 7.36 (d, J = 2.4 Hz, 1H), 2.60 (d, J = 10.7 Hz, 1H), 1.99–1.90 (s, 1H), 1.53 (s, 9H), 1.40–1.20 (m, 3H), 1.29 (s, 9H).

Synthesis of cyclic carbonates

All cyclic carbonate formations were carried out in autoclaves or, in case of 1 bar CO_2 reactions, in sample vials with a balloon of CO_2 attached to them. In both cases the reactions were magnetically stirred. After completion of the experiment, the reaction mixture was analysed by ^{1}H NMR spectroscopy and passed through a pad of silica to separate the catalyst. In the case of a 100% conversion, CH_2Cl_2 was used as the eluent, if the conversion was incomplete then column chromatography was used to purify the compounds (SiO_2, EtOAc/hexane, 1:3).

Styrene carbonate: ^{1}H NMR (400 MHz, $CDCl_3$) δ 7.44–7.32 (m, 5H), 5.66 (t, J = 8.0 Hz, 1H), 4.82–4.73 (m, 1H), 4.37–4.26 (m, 1H); ^{13}C NMR (101 MHz, $CDCl_3$) δ 155.00, 135.88, 129.80, 129.31, 126.00, 78.11, 71.28.

4-Chlorostyrene carbonate: ^{1}H NMR (400 MHz, $CDCl_3$) δ 7.48–7.25 (m, 4H), 5.65 (t, J = 8.0 Hz, 1H), 4.79 (t, J = 8.2 Hz, 1H), 4.29 (dd, J = 8.6, 7.9 Hz, 1H); ^{13}C NMR (101 MHz, $CDCl_3$) δ 154.65, 135.85, 134.35, 129.59, 127.37, 77.34, 71.10.

3-Chloropropylene carbonate: ^{1}H NMR (400 MHz, $CDCl_3$) δ 5.02–4.93 (m, 1H), 4.60–4.53 (m, 1H), 4.37 (dd, J = 8.9, 5.7 Hz, 1H), 3.82–3.67 (m, 2H); ^{13}C NMR (101 MHz, $CDCl_3$) δ 154.49, 74.48, 67.06, 44.03.

3-Phenoxypropylene carbonate: ^{1}H NMR (400 MHz, $CDCl_3$) δ 7.37–6.84 (m, 5H), 5.08–4.94 (m, 1H), 4.63–4.46 (m, 2H), 4.30–4.06 (m, 2H); ^{13}C NMR (101 MHz, $CDCl_3$) δ 157.83, 154.76, 129.78, 122.08, 114.69, 74.20, 66.95, 66.32.

Propylene carbonate: ^{1}H NMR (400 MHz, $CDCl_3$) δ 4.92–4.67 (m, 1H), 4.64–4.38 (m, 1H), 4.07–3.89 (m, 1H), 1.47–1.36 (m, 3H); ^{13}C NMR (101 MHz, $CDCl_3$) δ 155.22, 73.74, 70.78, 19.45.

1,2-Hexylene carbonate: ^{1}H NMR (400 MHz, $CDCl_3$) δ 4.74–4.59 (m, 1H), 4.53–4.43 (m, 1H), 4.02 (dt, J = 9.9, 4.9 Hz,

1H), 1.82–1.57 (m, 2H), 1.46–1.20 (m, 4H), 0.92–0.81 (m, 3H); ^{13}C NMR (101 MHz, $CDCl_3$) δ 155.24, 77.20, 69.51, 33.59, 26.49, 22.31, 13.86.

3-Hydroxypropylene carbonate: ^{1}H NMR (400 MHz, $CDCl_3$) δ 4.90–4.73 (m, 1H), 4.59–4.39 (m, 2H), 3.96 (dt, *J* = 20.4, 10.2 Hz, 1H), 3.68 (td, *J* =13.1, 5.5 Hz, 1H), 2.84–2.56 (m, 1H); ^{13}C NMR (101 MHz, $CDCl_3$) δ 155.38, 76.64, 65.85, 61.73.

1,2-Butylene carbonate: ^{1}H NMR (400 MHz, $CDCl_3$) δ 4.71–4.55 (m, 1H), 4.48 (t, *J* = 8.1 Hz, 1H), 4.04 (dd, *J* = 8.4, 7.0 Hz, 1H), 1.85–1.63 (m, 2H), 1.03–0.89 (m, 3H); ^{13}C NMR (101 MHz, $CDCl_3$) δ 155.27, 78.16, 69.13, 26.95, 8.52.

Synthesis of polycyclohexene carbonate

Prepared as reported above for the synthesis of cyclic carbonates at 10–35 bar CO_2, but without any additional purification of the reaction product. ^{1}H NMR (400 MHz, $CDCl_3$) δ 4.71–4.56 (broad, 2H), 2.21–2.04 (broad, 4H), 1.79–1.62 (broad, 4H).

Acknowledgements

The authors thank the Royal Society for an Anglo–Russian collaboration grant under the international exchange scheme.

References

1. Aresta, M.; Dibenedetto, A.; Angelini, A. *Chem. Rev.* **2014,** *114,* 1709–1742. doi:10.1021/cr4002758
2. Schäffner, B.; Schäffner, F.; Verevkin, S. P.; Börner, A. *Chem. Rev.* **2010,** *110,* 4554–4581. doi:10.1021/cr900393d
3. Sakakura, T.; Kohno, K. *Chem. Commun.* **2009,** 1312–1330. doi:10.1039/b819997c
4. Takata, T.; Furusho, Y.; Murakawa, K.-i.; Endo, T.; Matsuoka, H.; Hirasa, T.; Matsuo, J.; Sisido, M. *J. Am. Chem. Soc.* **1998,** *120,* 4530–4531. doi:10.1021/ja974337l
5. Nicolaou, K. C.; Yang, Z.; Liu, J. J.; Ueno, H.; Nantermet, P. G.; Guy, R. K.; Claiborne, C. F.; Renaud, J.; Couladouros, E. A.; Paulvannan, K.; Soresen, E. J. *Nature* **1994,** *367,* 630–634. doi:10.1038/367630a0
6. Chang, H.-T.; Sharpless, K. B. *Tetrahedron Lett.* **1996,** *37,* 3219–3222. doi:10.1016/0040-4039(96)00534-5
7. He, Q.; O'Brien, J. W.; Kitselman, K. A.; Tompkins, L. E.; Curtis, G. C. T.; Kerton, F. M. *Catal. Sci. Technol.* **2014,** *4,* 1513–1528. doi:10.1039/c3cy00998j
8. Martín, C.; Fiorani, G.; Kleij, A. W. *ACS Catal.* **2015,** *5,* 1353–1370. doi:10.1021/cs5018997
9. Comerford, J. W.; Ingram, I. D. V.; North, M.; Wu, X. *Green Chem.* **2015,** *17,* 1966–1987. doi:10.1039/C4GC01719F
10. Ikpo, N.; Flogeras, J. C.; Kerton, F. M. *Dalton Trans.* **2013,** *42,* 8998–9006. doi:10.1039/c3dt00049d
11. Taherimehr, M.; Pescarmona, P. P. *J. Appl. Polym. Sci.* **2014,** *131,* 41141. doi:10.1002/app.41141
12. Decortes, A.; Castilla, A. M.; Kleij, A. W. *Angew. Chem., Int. Ed.* **2010,** *49,* 9822–9837. doi:10.1002/anie.201002087
13. North, M.; Pasquale, R.; Young, C. *Green Chem.* **2010,** *12,* 1514–1539. doi:10.1039/c0gc00065e
14. Tian, D.; Liu, B.; Gan, Q.; Li, H.; Darensbourg, D. J. *ACS Catal.* **2012,** *2,* 2029–2035. doi:10.1021/cs300462r
15. Meléndez, J.; North, M.; Villuendas, P. *Chem. Commun.* **2009,** 2577–2579. doi:10.1039/b900180h
16. Ren, W.-M.; Liu, Y.; Lu, X.-B. *J. Org. Chem.* **2014,** *79,* 9771–9777. doi:10.1021/jo501926p
17. Hanhart, W.; Ingold, C. K. *J. Chem. Soc.* **1927,** 997–1020. doi:10.1039/jr9270000997
18. Hughes, E. D.; Ingold, C. K.; Patel, C. S. *J. Chem. Soc.* **1933,** 526–530. doi:10.1039/jr9330000526
19. de la Zerda, J.; Neumann, R.; Sasson, Y. *J. Chem. Soc., Perkin Trans. 2* **1986,** 823–826. doi:10.1039/p29860000823
20. Hofman, A. W. *Proc. R. Soc. London* **1859,** *10,* 594–596. doi:10.1098/rspl.1859.0121
21. Collie, N.; Schryver, S. B. *J. Chem. Soc., Trans.* **1890,** *57,* 767–782. doi:10.1039/ct8905700767
22. Zaki, A.; Fahim, H. *J. Chem. Soc.* **1942,** 270–272. doi:10.1039/jr9420000270
23. Gordon, J. E. *J. Org. Chem.* **1965,** *30,* 2760–2763. doi:10.1021/jo01019a060
24. Gisch, N.; Balzarini, J.; Meier, C. *J. Med. Chem.* **2007,** *50,* 1658–1667. doi:10.1021/jm0613267
25. Braun, M.; Fleischer, R.; Mai, B.; Schneider, M.-A.; Lachenicht, S. *Adv. Synth. Catal.* **2004,** *346,* 474–482. doi:10.1002/adsc.200303178
26. Chen, C.-T.; Kao, J.-Q.; Salunke, S. B.; Lin, Y.-H. *Org. Lett.* **2011,** *13,* 26–29. doi:10.1021/ol1024053
27. Sun, M.; Mu, Y.; Wu, Q.; Gao, W.; Ye, L. *New J. Chem.* **2010,** *34,* 2979–2987. doi:10.1039/c0nj00439a
28. Waibel, M.; Hasserodt, J. *Tetrahedron Lett.* **2009,** *50,* 2767–2769. doi:10.1016/j.tetlet.2009.03.139
29. Sigman, M. S.; Jacobsen, E. N. *J. Am. Chem. Soc.* **1998,** *120,* 5315–5316. doi:10.1021/ja980299+
30. Chiang, L.; Kochem, A.; Jarjayes, O.; Dunn, T. J.; Vezin, H.; Sakaguchi, M.; Ogura, T.; Orio, M.; Shimazaki, Y.; Thomas, F.; Storr, T. *Chem. – Eur. J.* **2012,** *18,* 14117–14127. doi:10.1002/chem.201201410
31. North, M. *ARKIVOC* **2012,** *(i),* 610–628.
32. Beattie, C.; North, M.; Villuendas, P.; Young, C. *J. Org. Chem.* **2013,** *78,* 419–426. doi:10.1021/jo302317w
33. Darensbourg, D. J.; Billodeaux, D. R. *Inorg. Chem.* **2005,** *44,* 1433–1442. doi:10.1021/ic048508g
34. Sugimoto, H.; H. Ohtsuka, H.; Inoue, S. *J. Polym. Sci., Part A: Polym. Chem.* **2005,** *43,* 4172–4186. doi:10.1002/pola.20894
35. Chapman, A. M.; Keyworth, C.; Kember, M. R.; Lennox, A. J. J.; Williams, C. K. *ACS Catal.* **2015,** *5,* 1581–1588. doi:10.1021/cs501798s

BEILSTEIN JOURNAL OF ORGANIC CHEMISTRY

Active site diversification of P450cam with indole generates catalysts for benzylic oxidation reactions

Paul P. Kelly‡, Anja Eichler‡, Susanne Herter, David C. Kranz, Nicholas J. Turner and Sabine L. Flitsch*

Full Research Paper

Open Access

Address:
School of Chemistry & Manchester Institute of Biotechnology, The University of Manchester, 131 Princess Street, M1 7DN, Manchester, United Kingdom

Email:
Sabine L. Flitsch* - sabine.flitsch@manchester.ac.uk

* Corresponding author ‡ Equal contributors

Keywords:
active site mutagenesis; biotransformation; C–H activation; cytochrome P450cam monooxygenase; hydroxylation

Beilstein J. Org. Chem. **2015,** *11,* 1713–1720.
doi:10.3762/bjoc.11.186

Received: 17 June 2015
Accepted: 03 September 2015
Published: 22 September 2015

This article is part of the Thematic Series "Sustainable catalysis".

Associate Editor: A. Kirschning

Abstract

Cytochrome P450 monooxygenases are useful biocatalysts for C–H activation, and there is a need to expand the range of these enzymes beyond what is naturally available. A panel of 93 variants of active self-sufficient P450cam[Tyr96Phe]-RhFRed fusion enzymes with a broad diversity in active site amino acids was developed by screening a large mutant library of 16,500 clones using a simple, highly sensitive colony-based colorimetric screen against indole. These mutants showed distinct fingerprints of activity not only when screened in oxidations of substituted indoles but also for unrelated oxidations such as benzylic hydroxylations.

Introduction

Selective C–H activation and oxyfunctionalisation of hydrocarbons offers a route to chiral alcohols and other industrially important synthetic building blocks from low cost starting materials [1]. One of the most attractive reagents in terms of cost and environmental impact for hydrocarbon oxidation is oxygen in the presence of a catalyst. In this context enzymatic oxidations are attractive, in particular cytochrome P450 monooxygenases (P450s or CYPs) due to their ability to catalyse selective C–H bond oxidations under mild conditions [2].

The soluble bacterial camphor monooxygenase P450cam (CYP101A1, EC 1.14.15.1) from *Pseudomonas putida* is one of the most studied P450s and has been engineered to accept a variety of non-natural substrates including aryl–alkyl compounds [3], olefins [4], polycyclic aromatic hydrocarbons [5], terpenes [6-8] and alkanes as small as ethane [9]. Over the years a number of active site mutants of P450cam have been generated by rational re-design, but the active site has not been explored in a comprehensive and systematic manner. Given that P450cam is a robust biocatalyst with good activity for this class of enzymes, a library of active site mutants with diversity in amino acid side chains lining up the substrate pocket would demonstrate a valuable resource for the development of useful P450cam based biocatalysts.

The generation of libraries of active enzyme mutants requires efficient screening protocols, which is a particular challenge for P450s given that (i) a diverse range of oxidations are catalysed by the enzymes, generally without intrinsic change in chromophore; (ii) the potential substrate range and diversity is high; (iii) each substrate might result in many different oxidation products. Here, we describe how such issues can be overcome by (i) using surrogate high-throughput screening (HTS) protocols that can deal with a large number of mutants; (ii) identification of active mutant libraries; (iii) fingerprinting of these libraries against substrates for a broad substrate panel, activity and chemo-, regio- and stereoselectivity.

The production of indigo from indole derivatives **1**–**4** by P450s can be considered as an effective visual screen for identifying interesting new mutants from diverse libraries. Indole hydroxylation by P450cam [10,11] and various other P450s, including the bacterial P450 BM3 [12,13] and human CYPs 2A6, 2C19 and 2E1 [14,15] has been previously identified to translate well to mutants activities toward structurally distinct and more demanding substrates such as diphenylmethane [10], phenacetin, ethoxyresofurin and chlorzoxazone to only name a few [16].

For the current investigation we sought to develop P450cam further to expand their substrate range in biocatalysis. Our starting point was a catalytically self-sufficient form of the enzyme, previously created by fusion with the reductase domain of P450-RhF (RhFRed) [17-19]. This chimera, named P450cam-RhFRed, operates without the need for additional reductase partners and retains the native activity of non-fused P450cam in the selective oxidation of camphor to 5-*exo*-hydroxycamphor. When generated as a whole-cell biocatalyst in *Escherichia coli* (*E. coli*), variants of the fusion enzyme catalysed the efficient, highly selective hydroxylation of ionones without the need to supply expensive nicotinamide cofactors [20]. Given the previously demonstrated affinity of P450cam for hydrophobic substrates, we were interested to see if P450cam-RhFRed could be used as a template for engineering variants for the stereoselective benzylic hydroxylation of substituted aromatics **5**–**8**.

Results and Discussion

Introducing structural and functional diversity into P450cam

The P450cam-RhFRed libraries were generated by targeting 12 active site residues earlier specified by Loida and Sligar [21], which have been recently identified as universal selectivity determining positions within the P450 enzyme family [22]. In addition, Phe98 and Met184 mutant libraries were generated since Phe98 is thought to contribute to substrate orientation via hydrophobic interactions [23], whereas Met184 is part of the P450cam substrate recognition site 2 (SRS 2) [24]. Accordingly, the entire P450cam active site was partitioned into seven residue pairs which were targeted in site-directed mutagenesis experiments in the manner of CASTing (Figure 1) [25]. NDT codon degeneracy was introduced for each pair in turn, thus generating seven libraries I–VII as shown in the grid of Figure 1: Phe87/Phe96 (I), Phe98/Thr101 (II), Met184/Thr185 (III), Leu244/Val247 (IV), Gly248/Thr252 (V), Val295/Asp297 (VI) and Ile395/Val396 (VII).

Pairing of adjacent residues and the use of NDT codons helped to restrict the library size while still ensuring structural and functional diversity among the substituted residues. It was also hoped that favourable pairings would produce synergistic effects that might not otherwise have been discovered by substituting individual amino acids separately. Based on previous studies [10,11], the Tyr96Phe variant of P450cam was chosen as the template for screen development and subsequent mutagenesis. Thus, ≈16,500 colonies containing P450cam[Tyr96Phe]-RhFRed variants were rapidly screened for indigo formation (Figure 1, right), from which 93 new variants were identified in seven sub-libraries (Figure 1, bottom). Among this new population, structural and functional diversity was evident as can be seen from the grid structure (Figure 1, bottom) representing all active variant combinations identified across libraries I–VII. Cysteine, asparagine and histidine were not among the active site residues of the parent (or wild type) enzyme but appeared in several of the new variants, thus introducing a thiol, polar or basic group where previously none existed. More bulky aromatic side chains in libraries I and II were often substituted for smaller side chains, including that of Gly, introducing space in the upper part of the active site and substrate entrance channel. The small glycine side chain was substituted at seven different positions including former Phe, Thr, Met, Leu and Asp residues. Library II also included a Gly–Gly double substitution. Threonines in libraries II and III were often substituted for Phe, Gly or aliphatic side chains. The OH group was also frequently preserved by substitution with Ser, which in library V was always the case. Thr252 (library V) is involved in a proton relay network that promotes O–O bond scission during catalysis [21,27-29]. The retention of an OH group at position 252 is consistent with this important catalytic function. Indigo positive variants in library III substituted Met184 for Cys but also six of the other eleven NDT residues. Aliphatic residues Val, Leu and Ile in libraries IV, VI and VII were often interchanged with each other or Phe, but also Cys, Asn and Ser. Of all the sub-libraries, the fewest variants (just 4) were identified in library VII (I395–V396), possibly indicating an important role in indole binding and orientation for this amino acid pair. The acidic Asp residue was not identified except where it had

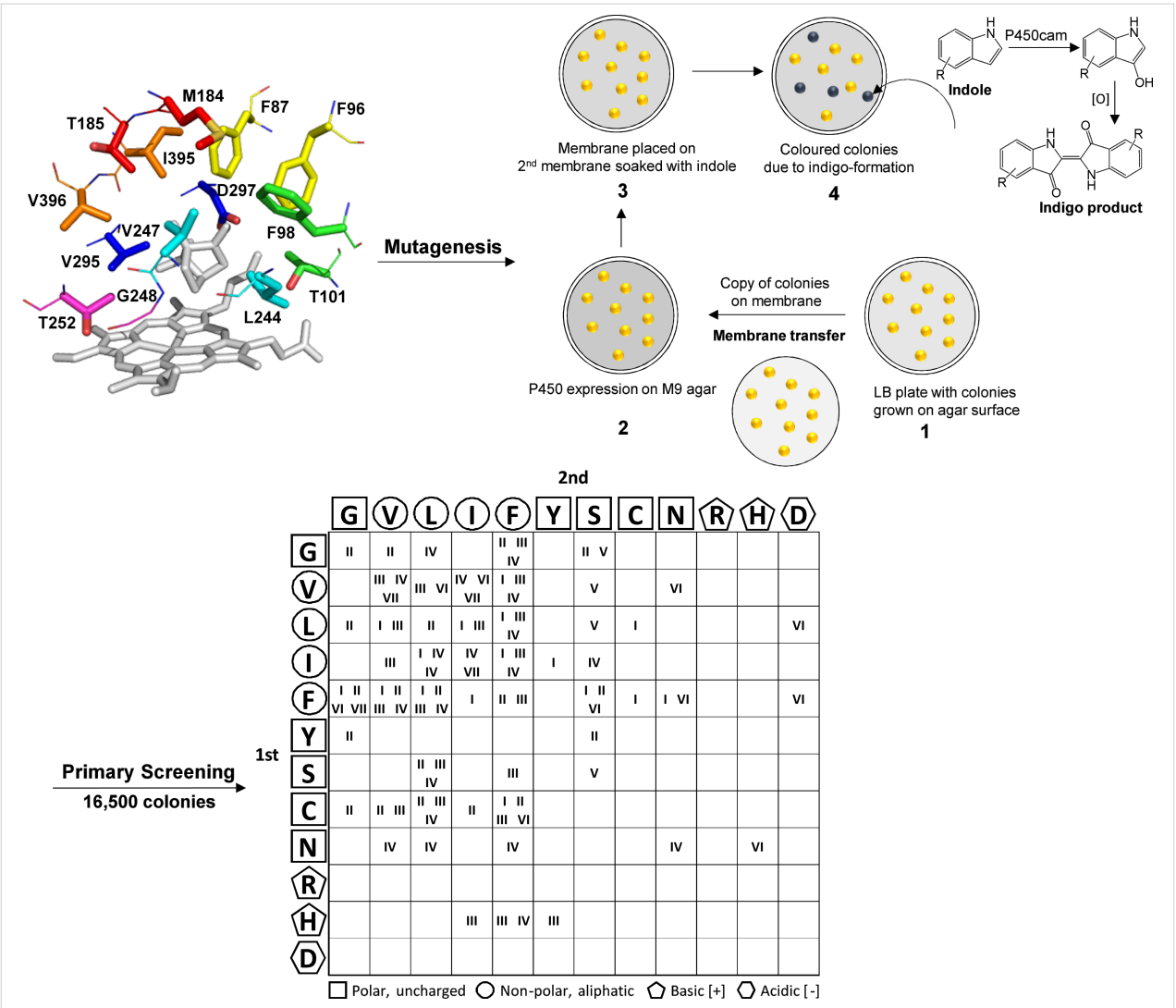

Figure 1: Library generation of P450cam[Tyr96Phe]-RhFRed. Active site of the P450cam-RhFRed variant Tyr96Phe (PDB ID: 1PHG) [26] with the 7 amino acid residue pairs representing the libraries Phe87/Phe96 I (yellow), Phe98/Thr101 II (green), Met184/Thr185 III (red), Leu244/Val247 IV (cyan), Gly248/Thr252 V (magenta), Val295/Asp297 VI (blue), Ile395/Val396 VII (orange). Following pairwise mutagenesis and solid-phase screening (using indole (**1**) as substrate), 93 new indigo positive variants were identified as represented in the grid. The grid represents all variant combinations identified across libraries I–VII. Rows in position 1 and columns in position 2 show the NDT amino acids classified according to their symbols in structure and chemical properties. The roman letters I–VII confirm that a member of that library with the amino acid configuration in position 1 and 2 has been found as an active enzyme – for example the mutant 98Gly/101Gly in library II (Phe98/Thr101) was found to be active as indicated in the top left box of the grid.

previously existed at Asp297. Although this residue forms a hydrogen bond with the heme-7-propionate [30-32] several other residues, including His, were evident at this position, indicating that this interaction was not crucial for activity. Adding the P450cam-RhFRed library parent Tyr96Phe to the pool of 93 new variants gave a total of 94 for further screening.

Investigation of P450cam activity toward a panel of substituted indoles

To begin exploring the substrate range of this new population, library I (Phe87/Phe96) variants were tested with a small panel of substituted indoles **1**–**4**.

Using a solid-phase screen as before, the level of colour formation in colonies was assessed visually, generating 'fingerprints' of activity as summarised in Figure 2 (also see Figure S1, Supporting Information File 1). The fingerprints show that variations in the configuration of the active site corresponded to variations in substrate acceptance. Variations in colour intensity might also be attributed to altered levels of active P450 or altered enzyme stability due to the substitutions made. If used in the context of an initial screen for activity following a diversification process, the use of indoles with P450s has a number of potential applications for enzyme optimisation studies and for developing protocols for neutral evolution. Selection for P450

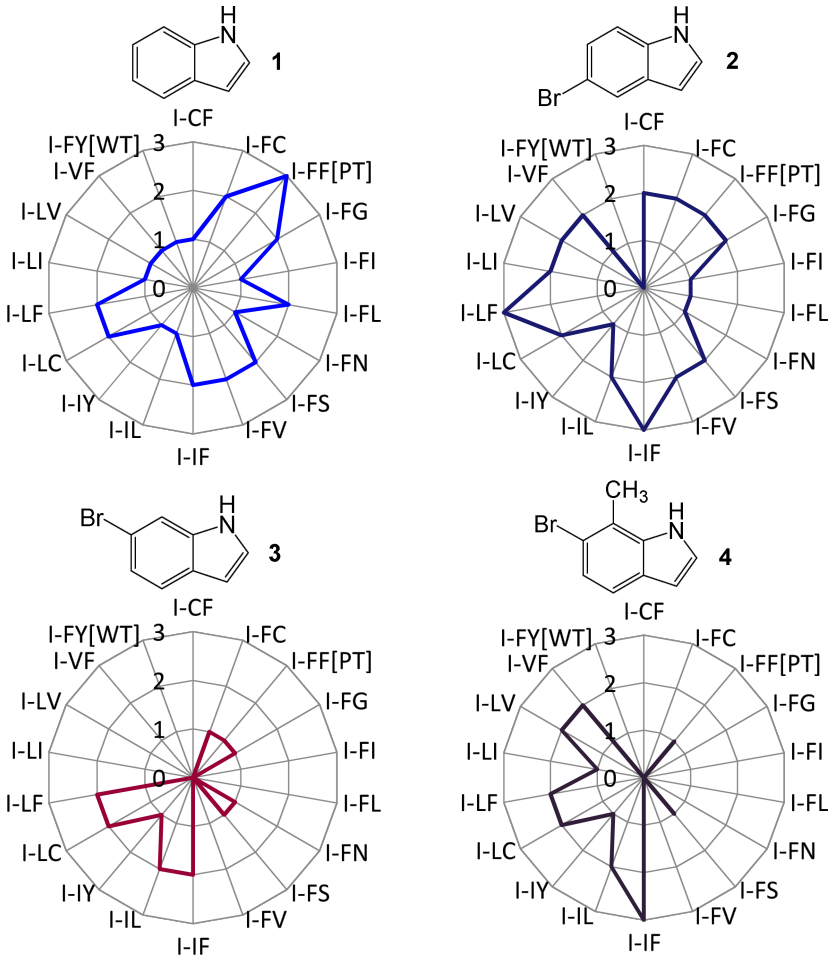

Figure 2: Radar plots illustrating the substrate acceptance of P450cam-RhFRed variants from library I. Colour formation in colonies was scored visually from 0–3, where 0 = no colour, 1 = low-level, 2 = mid-level and 3 = high-level colour. PT = parental type (P450cam[Tyr96Phe]-RhFRed), WT = wild type (P450cam-RhFRed).

variants that retain a threshold level of activity towards indole (**1**), such as the manner described herein, provides a diversified panel of variants with novel activities and increased capacity for improvement in subsequent rounds of directed evolution.

Investigation of the P450cam libraries toward ethylbenzenes

To further explore the scope of variant libraries, the test substrate ethylbenzene (**5**), the *para*-methylated derivative **6** and the *para*-brominated derivative **7** were screened in liquid whole cell biotransformations (Tables S15–S21, Supporting Information File 1). Initially, indigo positive variants were combined from each library, with a roughly equal size of 5–8 variants per pool [33]. This pooling strategy allowed us to quickly identify active mutants without the need to screen all 93 variants separately. In addition, levels in P450 expression in library pools were assessed through CO difference spectroscopy [34] in order to distinguish between differences in activity due either to changes in specific activity or enzyme expression levels in the respective sub-pools (Tables S2–S8, Supporting Information File 1).

Screening for P450 expression

The levels in P450 expression were determined using CO difference spectroscopy in whole cells. The assay could be significantly improved both in terms of speed and safety by using carbon monoxide releasing molecules (CORMs) [35-37] as a source of CO rather than the gas CO itself. P450 concentrations determined in whole cells (1.1–5.9 μM) incubated with CORMs were similar or slightly higher when compared to concentrations determined in cell-free extracts (1.1–4.9 μM) treated with gaseous CO (Tables S2–S8, Supporting Information File 1). Based on this P450 quantification, very similar levels of expression were observed for all cells expressing the different P450 mutant pools (Table S9, Supporting Information File 1). Given the small differences in P450 expression observed, it was decided not to normalise enzyme activity to expression levels in subsequent activity studies.

Biotransformation reactions with library pools

Biotransformations with pooled libraries and ethylbenzene (**5**) provided the average yield of alcohols (*R*,*S*)-**9** up to 10%, which is comparable to previously published data with isolated P450cam enzymes (Figure 3A) [21,27,38]. Highest concentrations of (*R*,*S*)-**9** were achieved in sub-pools of libraries III and IV revealing a 25–150% improvement in product formation as compared to the parent. With the *para*-methylated derivative **6** a

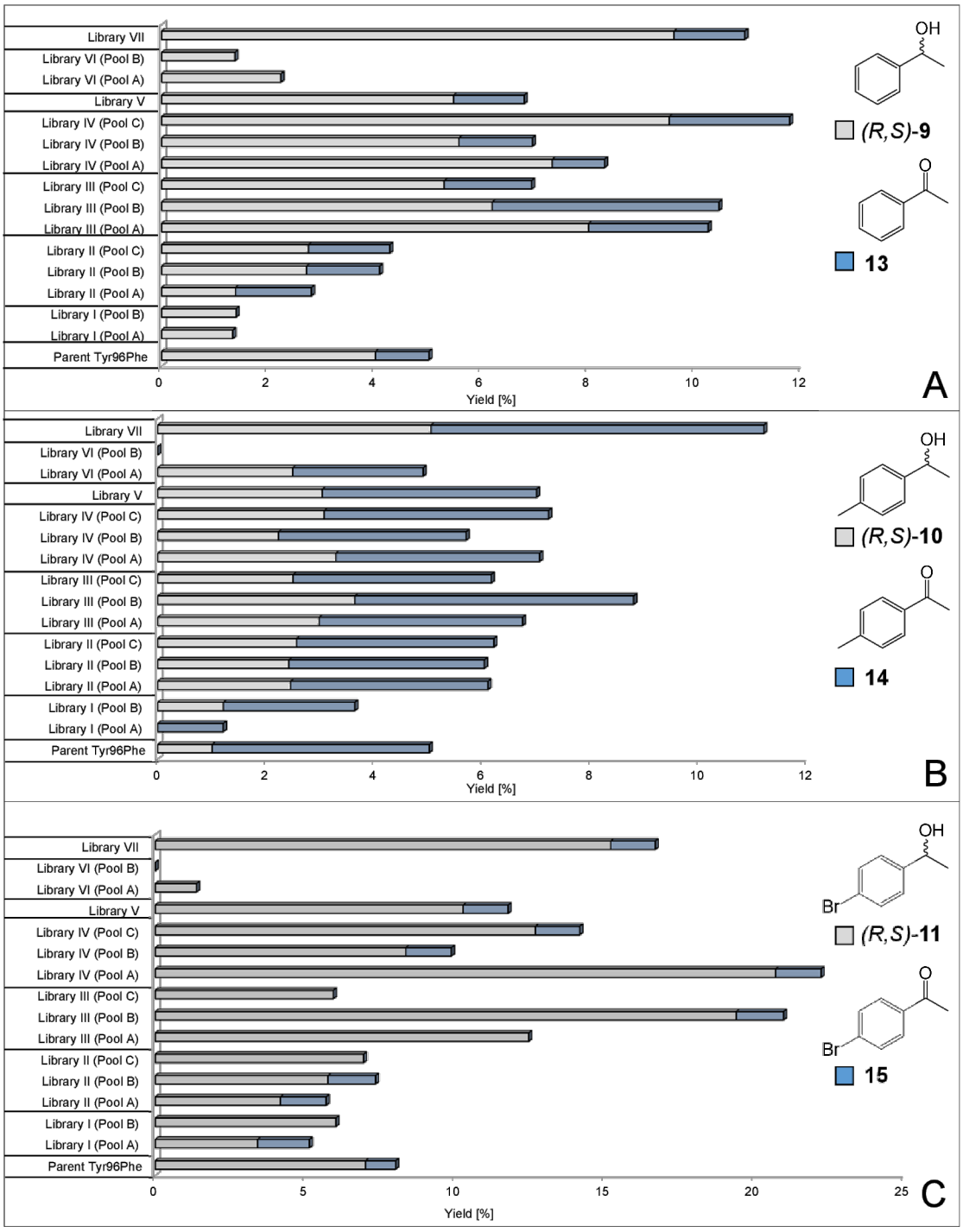

Figure 3: Yields of alcohols (*R*,*S*)-**9**-**11** (grey bars) and ketone products **13**–**15** (blue bars) in sub-pools of libraries I–VII and the Tyr96Phe parent with A) ethylbenzene (**5**), B) the *para*-methylated derivative **6** and C) the *para*-brominated derivative **7**. Reaction conditions: 180 mg/mL cells, 1 mM substrates, 50 mM sodium phosphate buffer (pH 7.2, 100 mM KCl, 0.4% glycerol (v/v)), 20 °C, 250 rpm, 48 h.

Table 1: Product yields and ee's obtained in biotransformation experiments with substrates **5**–**8** with the parent P450cam[Tyr96Phe]-RhFRed and indigo positive variants from library III (Met184/Thr185).[a]

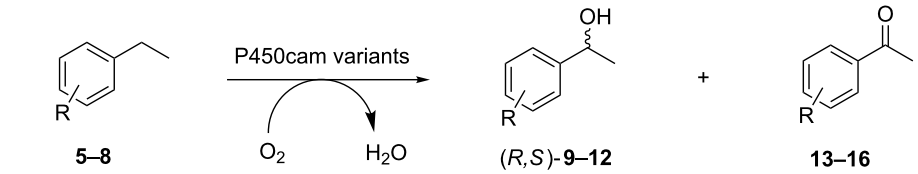

5–8 | (*R,S*)-**9–12** | **13–16**

5 R = H, **6** R = 4-CH_3, **7** R = 4-Br, **8** R = 2-Br

9 R = H, **10** R = 4-CH_3, **11** R = 4-Br, **12** R = 2-Br

13 R = H, **14** R = 4-CH_3, **15** R = 4-Br, **16** R = 2-Br

Substrate	Variant	Overall yield [%] (*R,S*)-**9–12, 13–16**[b]	Yield [%] (*R,S*)-**9–12**	ee [%][c]
5	Tyr96Phe	5	4	32 *(R)*
5	184Cys/185Phe	16	13	17 *(R)*
6	Tyr96Phe	5	4	35 *(S)*
6	184Cys/185Phe	6	5	9 *(S)*
7	Tyr96Phe	8	7	37 *(S)*
7	184Cys/185Phe	20	20	22 *(S)*
8	Tyr96Phe	16	11	6 *(S)*
8	184His/185Phe	46	37	15 *(S)*

[a]Reaction conditions: 2 mL scale, 180 mg/mL cells, 50 mM NaPi (pH 7.2, 0.4% glycerol (v/v), 100 mM KCl), 1 mM substrates **5**–**8**, 0.4% DMSO, 20 °C, 250 rpm, 48 h. [b]Product yields determined by GC/FID. [c]Enantioselectivities determined via chiral normal phase HPLC. All assays were accomplished in three replicates (Table S23, Supporting Information File 1).

pronounced over-oxidation to the ketone **14** occurred averagely yielding alcohols (*R*,*S*)-**10** in up to 5% with libraries I–VII showing distinct improvements in product yields when compared to the parental enzyme (Figure 3B). Library pools incubated with the *para*-brominated derivative **7** produced alcohols (*R*,*S*)-**11** in up to 21% as a significant improvement over the parent (Figure 3C). Overall yields were hampered by the volatility of starting materials, as shown by control experiments using dead cells, where 13% of starting material **5**, 17% of **6** and 19% of **7** were recovered (Table S22, Supporting Information File 1). Generally, the highest concentrations of (*R*,*S*)-alcohol products from compounds **5**–**7** were identified in subpools of libraries III (Met184/Thr185) and IV (Leu244/Val247) (Tables S17 and S18, Supporting Information File 1), which also seemed to contain the greatest diversity of variants.

Substrate specificity of individual library III variants toward ethylbenzene derivatives 5–8

Following on from the results with pools of libraries I–VII, individual variants from library III (Met184/Thr185) were further investigated towards ethylbenzene derivatives **5**–**8** to see if chiral alcohols could be generated with improved rates compared to the parent variant Tyr96Phe (Table 1). Mutants harbouring the 185Phe mutation were specifically targeted since it was previously described that additional steric bulk at position 185 can lead to improved oxidation rates of ethylbenzene (**5**) [21,27].

The 184Cys/185Phe mutation produced a 2.5-fold improved formation of alcohols (*R*,*S*)-**9** with ethylbenzene (**5**) as compared to the parent Tyr96Phe albeit a decrease in ee from 32% (Tyr96Phe) to 17% (184Cys/185Phe) was evident. Interestingly, the *para*-methylated derivative **6** produced alcohol **10** with opposite (*S*)-selectivity both in the parent and mutant. Similar to substrate **6**, the *para*-brominated derivative **7** also produced (*S*)-selectivity with 2.4-fold improved yields of alcohol products (*R*,*S*)-**11** (20%) with the 184Cys/185Phe variant. In comparison to the *para*-bromo derivative **7**, the regioisomer **8** produced with the 184His/185Phe mutant significantly improved yields of (*R*,*S*)-**12** alcohols (37%) albeit with a slight decrease in selectivity (15%).

Conclusion

A colony-based solid-phase screen for P450 indole activity was developed and used to generate a population of 93 indole active enzyme variants from screening a large library (16,500) of variants. The application of CORMs in place of the commonly used gaseous CO was found to be an attractive alternative for assessing P450 concentrations in whole cells. In a comprehensive pooling approach, P450cam mutants were shown to exhibit improved activities in the benzylic oxidation of ethylbenzene derivatives. The configuration of the newly generated chiral centre was highly dependent on substitution and subtle changes in substrate structure resulting in significant changes in both conversion and enantioselectivity. The active site library of

93 P450cam variants promises to be a useful tool for the discovery of new P450 activities and can be used as a starting point for further mutagenic studies.

Supporting Information

Supporting Information File 1

General experimental information and procedures.
[http://www.beilstein-journals.org/bjoc/content/supplementary/1860-5397-11-186-S1.pdf]

Acknowledgements

We acknowledge support from the Centre of Excellence for Biocatalysis, Biotransformations and Biocatalytic Manufacture (CoEBio3, to PPK), the FP7-PEOPLE-2011-ITN under grant agreement no. 289217 (P4fifty, to AE), the Innovative Medicines Initiative Joint Undertaking under the grant agreement no. 115360 (Chemical manufacturing methods for the 21st century pharmaceutical industries, CHEM21, to SH) and the Royal Society Wolfson Merit Awards (to NJT and SLF).

References

1. Breuer, M.; Ditrich, T.; Habicher, T.; Hauer, B.; Keßeler, M.; Stürmer, R.; Zelinski, T. *Angew. Chem., Int. Ed.* **2004,** *43,* 788–824. doi:10.1002/anie.200300599
2. Schulz, S.; Girhard, M.; Urlacher, V. B. *ChemCatChem* **2012,** *4,* 1889–1895. doi:10.1002/cctc.201200533
3. Filipovic, D.; Paulsen, M. D.; Loida, P. J.; Sligar, S. G.; Ornstein, R. L. *Biochem. Biophys. Res. Commun.* **1992,** *189,* 488–495. doi:10.1016/0006-291X(92)91584-D
4. Jin, S.; Makris, T. M.; Bryson, T. A.; Sligar, S. G.; Dawson, J. H. *J. Am. Chem. Soc.* **2003,** *125,* 3406–3407. doi:10.1021/ja029272n
5. Harford-Cross, C. F.; Carmichael, A. B.; Allan, F. K.; England, P. A.; Rouch, D. A.; Wong, L.-L. *Protein Eng., Des. Sel.* **2000,** *13,* 121–128. doi:10.1093/protein/13.2.121
6. Bell, S. G.; Sowden, R. J.; Wong, L.-L. *Chem. Commun.* **2001,** 635–636. doi:10.1039/b100290m
7. Bell, S. G.; Chen, X. H.; Sowden, R. J.; Xu, F.; Williams, J. N.; Wong, L.-L.; Rao, Z. H. *J. Am. Chem. Soc.* **2003,** *125,* 705–714. doi:10.1021/ja028460a
8. Sowden, R. J.; Yasmin, S.; Rees, N. H.; Bell, S. G.; Wong, L.-L. *Org. Biomol. Chem.* **2005,** *3,* 57–64. doi:10.1039/b413068e
9. Xu, F.; Bell, S. G.; Lednik, J.; Insley, A.; Rao, Z. H.; Wong, L.-L. *Angew. Chem., Int. Ed.* **2005,** *44,* 4029–4032. doi:10.1002/anie.200462630
10. Çelik, A.; Speight, R. E.; Turner, N. J. *Chem. Commun.* **2005,** 3652–3654. doi:10.1039/B506156C
11. Manna, S. K.; Mazumadar, S. *Dalton Trans.* **2010,** *39,* 3115–3123. doi:10.1039/b922885c
12. Li, Q.-S.; Schwaneberg, U.; Fischer, P.; Schmid, R. D. *Chemistry* **2000,** *6,* 1531–1536. doi:10.1002/(SICI)1521-3765(20000502)6:9<1531::AID-CHEM1531>3.3.CO;2-4
13. Li, H.-m.; Mei, L.-h.; Urlacher, V. B.; Schmid, R. D. *Appl. Biochem. Biotechnol.* **2008,** *144,* 27–36. doi:10.1007/s12010-007-8002-5
14. Gillam, E. M. J.; Aguinaldo, A. M. A.; Notley, L. M.; Kim, D.; Mundkowski, R. G.; Volkov, A. A.; Arnold, F. H.; Souček, P.; De Voss, J. J.; Guengerich, F. P. *Biochem. Biophys. Res. Commun.* **1999,** *265,* 469–472. doi:10.1006/bbrc.1999.1702
15. Gillam, E. M. J.; Notley, L. M.; Chai, H.; De Voss, J. J.; Guengerich, F. P. *Biochemistry* **2000,** *39,* 13817–13824. doi:10.1021/bi001229u
16. Park, S.-H.; Kim, D.-H.; Kim, D.; Kim, D.-H.; Jung, H.-C.; Pan, J.-G.; Ahn, T.; Kim, D.; Yun, C.-H. *Drug Metab. Dispos.* **2010,** *38,* 732–739. doi:10.1124/dmd.109.030759
17. Nodate, M.; Kubota, M.; Misawa, N. *Appl. Microbiol. Biotechnol.* **2006,** *71,* 455–462. doi:10.1007/s00253-005-0147-y
18. Robin, A.; Roberts, G. A.; Kisch, J. A.; Sabbadin, F.; Grogan, G.; Bruce, N.; Turner, N. J.; Flitsch, S. L. *Chem. Commun.* **2009,** 2478–2480. doi:10.1039/b901716j
19. Sabbadin, F.; Hyde, R.; Robin, A.; Hilgarth, E.-M.; Deleune, M.; Flitsch, S.; Turner, N.; Grogan, G.; Bruce, N. C. *ChemBioChem* **2010,** *11,* 987–994. doi:10.1002/cbic.201000104
20. Robin, A.; Köhler, V.; Jones, A.; Ali, A.; Kelly, P. P.; O'Reilly, E.; Turner, N. J.; Flitsch, S. L. *Beilstein J. Org. Chem.* **2011,** *7,* 1494–1498. doi:10.3762/bjoc.7.173
21. Loida, P. J.; Sligar, S. G. *Biochemistry* **1993,** *32,* 11530–11538. doi:10.1021/bi00094a009
22. Gricman, Ł.; Vogel, C.; Pleiss, J. *Proteins: Struct., Funct., Bioinf.* **2015,** *83,* 1593–1603. doi:10.1002/prot.24840
23. Poulos, T. L.; Finzel, B. C.; Howard, A. J. *J. Mol. Biol.* **1987,** *195,* 687–700. doi:10.1016/0022-2836(87)90190-2
24. Gotoh, O. *J. Biol. Chem.* **1992,** *267,* 83–90.
25. Reetz, M. T.; Bocola, M.; Carballeira, J. D.; Zha, D.; Vogel, A. *Angew. Chem., Int. Ed.* **2005,** *44,* 4192–4196. doi:10.1002/anie.200500767
26. Poulos, T. L.; Howard, A. J. *Biochemistry* **1987,** *26,* 8165–8174. doi:10.1021/bi00399a022
27. Loida, P. J.; Sligar, S. G. *Protein Eng., Des. Sel.* **1993,** *6,* 207–212. doi:10.1093/protein/6.2.207
28. Lee, Y.-T.; Glazer, E. C.; Wilson, R. F.; Stout, C. D.; Goodin, D. B. *Biochemistry* **2010,** *50,* 693–703. doi:10.1021/bi101726d
29. Schlichtling, I.; Berendzen, J.; Chu, K.; Stock, A. M.; Maves, S. A.; Benson, D. E.; Sweet, R. M.; Ringe, D.; Petsko, G. A.; Sligar, S. G. *Science* **2000,** *287,* 1615–1622. doi:10.1126/science.287.5458.1615
30. Poulos, T. L.; Finzel, B. C.; Gunsalus, I. C.; Wagner, G. C.; Kraut, J. *J. Biol. Chem.* **1985,** *260,* 16122–16130.
31. Pochapsky, T. C.; Kazanis, S.; Dang, D. *Antioxid. Redox Signaling* **2010,** *13,* 1273–1296. doi:10.1089/ars.2010.3109
32. Hayashi, T.; Harada, K.; Sakurai, K.; Shimada, H.; Hirota, S. *J. Am. Chem. Soc.* **2009,** *131,* 1398–4000. doi:10.1021/ja807420k
33. Hoffmann, G.; Bönsch, K.; Greiner-Stöffele, T.; Ballschmiter, M. *Protein Eng., Des. Sel.* **2011,** *24,* 439–446. doi:10.1093/protein/gzq119
34. Omura, T.; Sato, R. *J. Biol. Chem.* **1964,** *293,* 2370–2378.
35. Geier, M.; Braun, A.; Emmerstorfer, A.; Pichler, H.; Glieder, A. *Biotechnol. J.* **2012,** *7,* 1346–1358. doi:10.1002/biot.201200187
36. Gudiminchi, R. K.; Geier, M.; Glieder, A.; Camattari, A. *Biotechnol. J.* **2013,** *8,* 146–152. doi:10.1002/biot.201200185
37. García-Gallego, S.; Bernardes, G. J. L. *Angew. Chem., Int. Ed.* **2014,** *53,* 9712–9721. doi:10.1002/anie.201311225
38. Bell, S. G.; Harford-Cross, C. F.; Wong, L.-L. *Protein Eng., Des. Sel.* **2001,** *14,* 797–802. doi:10.1093/protein/14.10.797

BEILSTEIN JOURNAL OF ORGANIC CHEMISTRY

Engineering *Pichia pastoris* for improved NADH regeneration: A novel chassis strain for whole-cell catalysis

Martina Geier[1], Christoph Brandner[1], Gernot A. Strohmeier[1,2], Mélanie Hall[3], Franz S. Hartner[4,5] and Anton Glieder[*5]

Full Research Paper

Open Access

Address:
[1]Austrian Centre of Industrial Biotechnology (ACIB GmbH), Petersgasse 14, Graz, 8010, Austria, [2]Institute of Organic Chemistry, Graz University of Technology, Stremayrgasse 9, Graz, 8010, Austria, [3]Department of Chemistry, University of Graz, Heinrichstrasse 28, Graz, 8010, Austria, [4]Sandoz GmbH, Biochemiestrasse 10, 6250, Kundl, Austria and [5]Institute of Molecular Biotechnology, Graz University of Technology, Petersgasse 14, Graz, 8010, Austria

Email:
Anton Glieder[*] - a.glieder@tugraz.at

* Corresponding author

Keywords:
bioreduction; cofactor regeneration; dihydroxyacetone synthase; methanol utilization pathway; whole-cell biotransformation

Beilstein J. Org. Chem. **2015,** *11,* 1741–1748.
doi:10.3762/bjoc.11.190

Received: 03 June 2015
Accepted: 26 August 2015
Published: 25 September 2015

This article is part of the Thematic Series "Sustainable catalysis".

Guest Editor: N. Turner

Abstract

Many synthetically useful reactions are catalyzed by cofactor-dependent enzymes. As cofactors represent a major cost factor, methods for efficient cofactor regeneration are required especially for large-scale synthetic applications. In order to generate a novel and efficient host chassis for bioreductions, we engineered the methanol utilization pathway of *Pichia pastoris* for improved NADH regeneration. By deleting the genes coding for dihydroxyacetone synthase isoform 1 and 2 (*DAS1* and *DAS2*), NADH regeneration via methanol oxidation (dissimilation) was increased significantly. The resulting *Δdas1 Δdas2* strain performed better in butanediol dehydrogenase (BDH1) based whole-cell conversions. While the BDH1 catalyzed acetoin reduction stopped after 2 h reaching ~50% substrate conversion when performed in the wild type strain, full conversion after 6 h was obtained by employing the knock-out strain. These results suggest that the *P. pastoris Δdas1 Δdas2* strain is capable of supplying the actual biocatalyst with the cofactor over a longer reaction period without the over-expression of an additional cofactor regeneration system. Thus, focusing the intrinsic carbon flux of this methylotrophic yeast on methanol oxidation to CO_2 represents an efficient and easy-to-use strategy for NADH-dependent whole-cell conversions. At the same time methanol serves as co-solvent, inductor for catalyst and cofactor regeneration pathway expression and source of energy.

Introduction

Bioreductions represent a sustainable strategy to obtain enantiopure molecules which serve as chiral building blocks for fine chemicals and drugs [1,2]. Such reactions are catalyzed by oxidoreductases, which mainly depend on nicotinamide cofactors as electron donors and acceptors. As these cofactors are required in stoichiometric amounts to drive the reaction to

completion and the simple addition of these compounds is not acceptable from an economical point of view, efficient in situ regeneration of the consumed cofactor is required. During the recent years, a broad range of cofactor regeneration systems based on enzymatic, chemical, photochemical or electrochemical processes have been developed [3].

In living (growing) cells, NAD(P)H can be recycled via the cellular metabolism of a co-substrate such as glucose. Alternatively, cofactor regeneration enzymes such as D-glucose-6-phosphate dehydrogenase, formaldehyde dehydrogenase and formate reductase can be co-expressed ensuring cofactor supply also in non-growing, resting cells. In addition to the cofactor supply, the application of whole cells circumvents time-consuming enzyme isolation and purification steps and improves enzyme stabilities during a process [4]. Nowadays, efforts are made to further increase the cofactor availability within cells and to allow the use of alternative and cheaper co-substrates by strain engineering [1,5-7].

Here, we present a novel, engineered platform strain for the use in whole-cell bioreductions and NADH-dependent biosynthetic pathways based on the methylotrophic yeast *Pichia pastoris* (*Komagataella phaffi*). *P. pastoris* is well known as an excellent host for recombinant protein production [8,9]. More recently it also attracted attention as a suitable whole-cell catalyst [10-15]. The target of the presented engineering approach is the methanol utilization (MUT) pathway, which is schematically depicted in Figure 1. This pathway enables methylotrophic yeasts to use methanol as sole carbon source [16]. In the initial step, methanol is oxidized by alcohol oxidase (AOX) to formaldehyde, which is further metabolized either in the assimilatory or in the dissimilatory pathway. In the latter one, formaldehyde spontaneously reacts with glutathione to *S*-hydroxymethylglutathione which is oxidized in a first step by the glutathione- and NAD^+-dependent enzyme formaldehyde dehydrogenase (FLD) to *S*-formylglutathione. *S*-Formylglutathione hydrolase (FGH) then hydrolyses this compound to formate and glutathione. In a second NAD^+-dependent step,

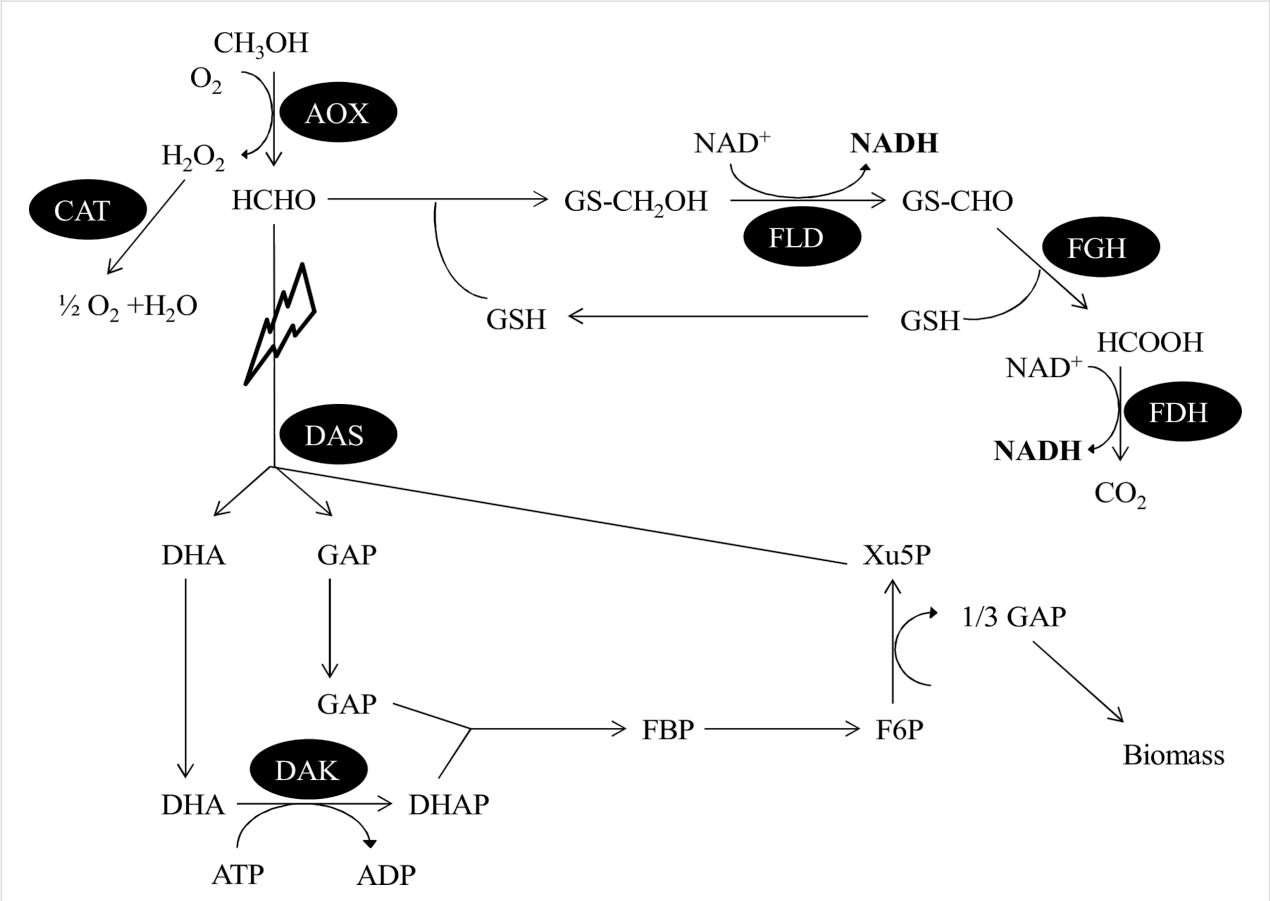

Figure 1: Simplified schematic representation of the methanol utilization pathway in *Pichia pastoris*. The main pathways and the respective enzymes are shown. AOX: alcohol oxidase; FLD: glutathione-dependent formaldehyde dehydrogenase; FGH: *S*-formylglutathione hydrolase; FDH: formate dehydrogenase; CAT: catalase; DAS: dihydroxyacetone synthase; DAK: dihydroxyacetone kinase; DHA: dihydroxyacetone; GAP: D-glyceraldehyde-3-phosphate; DHAP: dihydroxyacetone phosphate; FBP: D-fructose 1,6-bisphosphate; F6P: D-fructose 6-phosphate; Xu5P: D-xylulose 5-phosphate. By deleting dihydroxyacetone synthase the dissimilatory pathway leading to the formation of NADH is strengthened.

formate is oxidized to CO_2 by formate dehydrogenase (FDH). Thus, 2 equivalents of the cofactor NADH are generated via the dissimilatory pathway and full oxidation of the single carbon molecule methanol. Alternatively, in a simplified model formaldehyde is condensed with D-xylulose-5-phosphate and subsequently converted into dihydroxyacetone and D-glyceraldehyde-3-phosphate by dihydroxyacetone synthase (DAS), thereby contributing to biomass production on methanol.

Modifying the dissimilatory part of the MUT pathway has already been shown to improve the substrate conversion by NADH-dependent enzymes in *P. pastoris* [7]. Over-expression of the formaldehyde dehydrogenase, which was identified as the main bottleneck for an efficient cofactor recycling via the dissimilatory pathway, significantly improved the production rates of NADH-dependent whole-cell biotransformations. In contrast, the present study focuses on redirecting the flux in the MUT pathway by disrupting the assimilation pathway. Thus, the co-substrate methanol should be exclusively redirected to cofactor regeneration in theory, increasing the available NADH concentration in whole-cell biotransformations, while cells should not be able to grow any more if methanol is the sole carbon source.

Results and Discussion

Construction of knock-out strains

The assimilatory pathway was disrupted by the knock-out of dihydroxyacetone synthase. In contrast to other methylotrophic yeasts, *P. pastoris* has two genes encoding two isoforms of this enzyme (*DAS1* and *DAS2*) [17,18]. Therefore, three knock-out strains were generated to investigate their impact on cofactor regeneration: the single knock-outs *Δdas1* and *Δdas2* as well as the double knock-out *Δdas1 Δdas2*.

The targeted gene disruption was accomplished with knock-out cassettes as described earlier [19,20]. The cassettes were harboring a Zeocin™ resistance marker for the selection of integrative transformants and the FLP recombinase system [21] to enable marker recycling. Thereby, marker-free knock-out strains were obtained which only have one 34 bp FLP recombination target sequence (FRT) left in the targeted locus. The cassettes were designed such that the complete coding sequence including the start and stop codons of the corresponding *DAS* gene was deleted as schematically depicted in Figure 2. In the case of *Δdas1 Δdas2*, the coding sequences of both genes were deleted in one step, thereby also removing *HOB3*, coding for a hypothetical guanosine nucleotide exchange factor.

Characterization of knock-out strains

In a first step, the generated *das* knock-out strains were characterized by determining their specific growth rate on different carbon sources. As expected, the growth of the single and double knock-out strains on D-glucose and glycerol was not significantly impaired, showing growth rates in the same order of magnitude as the wild type strain (Table 1). A distinct phenotype was observed when methanol was used as the sole carbon source for growth. A slight, but residual growth was observed for the double knock-out strain, although both dihydroxyacetone synthase genes, that are linking methanol to biomass production, were deleted. In the course of 38 h, the optical density

Table 1: Specific growth rates of *P. pastoris* CBS7435 and generated *das* knock-out strains on different carbon sources. Values represent mean values ± standard deviations of the growth rate during the exponential growth phase determined in biological triplicates.

Strain	Growth rate [h^{-1}]		
	D-Glucose	Glycerol	Methanol
P. pastoris CBS7435	0.25 ± 0.03	0.19 ± 0.05	0.15 ± 0.03
P. pastoris CBS7435 *Δdas1*	0.23 ± 0.06	0.21 ± 0.04	0.12 ± 0.03
P. pastoris CBS7435 *Δdas2*	0.23 ± 0.03	0.20 ± 0.02	0.09 ± 0.01
P. pastoris CBS7435 *Δdas1 Δdas2*	0.26 ± 0.03	0.20 ± 0.04	0.01 ± 4 × 10^{-3}

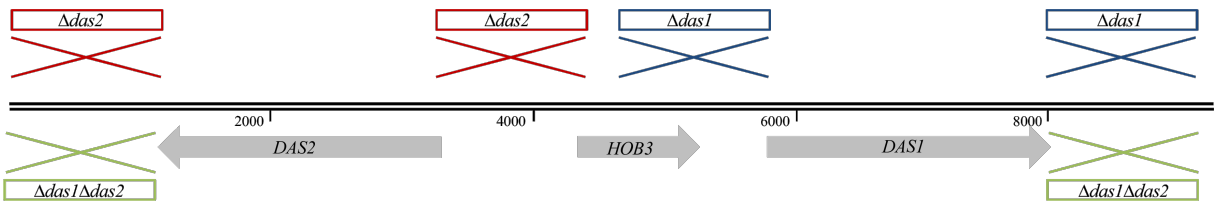

Figure 2: Representation of the genomic region coding for dihydroxyacetone synthases. The *DAS1* and *DAS2* coding sequences are located in close proximity on chromosome 3 in opposite direction. The two genes are separated by a short sequence encoding a hypothetical guanosine nucleotide exchange factor (*HOB3*). The target sites for the respective *das* knock-out cassettes are indicated schematically.

of the *P. pastoris Δdas1 Δdas2* cultures on methanol doubled. This remaining carbon flux into cellular metabolism might also enable the continuation of protein expression and thus biocatalyst production, while still maintaining a strong methanol flux towards oxidation to CO_2 and NADH regeneration.

Deleting only one isoform of the dihydroxyacetone synthase did not have such a severe impact on the methanol depending growth of *P. pastoris*. The growth rates were reduced by ~20% and by ~40% for the *Δdas1* and *Δdas2* single knock-out strains, respectively.

The behavior of the *das* knock-out strains in heterologous protein production was tested by expressing green fluorescent protein (GFP) under the control of the *AOX1* promoter (P_{AOX1}), which is the most prominent, methanol inducible promoter for *P. pastoris*.

A possible negative effect on P_{AOX1} driven protein expression might arise from changes in the energy metabolism due to the interrupted input into the pentose phosphate cycle. In addition, a possible accumulation of methanol oxidation products due to the lack of the two key metabolizing enzymes might be unfavorable for recombinant protein production. However, as shown in Figure 3, the P_{AOX1} driven expression of GFP was not negatively affected by deleting the *DAS* gene(s). In fact, the obtained expression levels in the generated single knock-out strains were increased up to ~30% in comparison to the wild type *P. pastoris* strain. These findings are of importance for the use of the knock-out strains in whole-cell processes, as impairments in recombinant protein production, i.e., the production of the actual biocatalyst, would reduce its applicability.

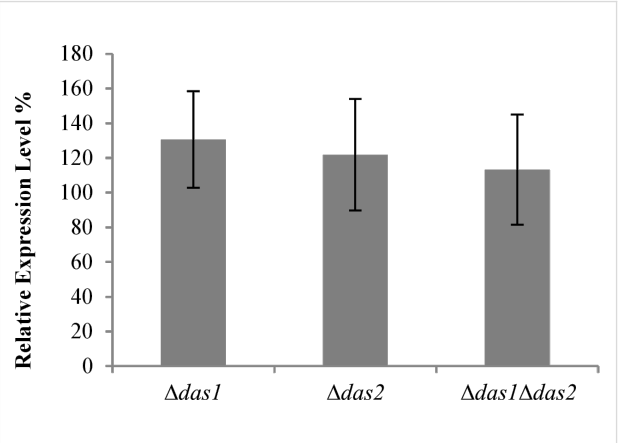

Figure 3: Relative expression levels of the green fluorescent protein (GFP) in the *das* knock-out strains. GFP expression obtained in the wild type *P. pastoris* strain indicated as relative fluorescence units per OD_{600} unit was set as 100%. GFP fluorescence was measured after 70 h of methanol induction. The shown values represent mean values ± standard deviations of 40 individual transformants.

NADH-dependent biotransformations performed in knock-out strains

To evaluate the NADH regeneration potential of the generated knock-out strains, they were employed as hosts in whole-cell bioreductions based on the 2,3-butanediol dehydrogenase from *S. cerevisiae* YAL060W (BDH1). This enzyme was shown to specifically use NADH as cofactor, displaying high turnover numbers in the reduction of racemic acetoin (k_{cat} = 98,000 min^{-1}) [22].

In an initial screening step, BDH1 transformants in the respective wild type and knock-out backgrounds were evaluated by performing acetoin conversions in the 96 well deep-well format. After biomass production on a D-glucose containing medium, methanol was fed as the sole carbon source to induce the production of the BDH1 enzyme and to induce the dissimilatory pathway. After 12 hours of induction acetoin was added to the growing cells as substrate in addition to the co-substrate methanol. The substrate conversions into the two products (2*R*,3*R*)-butane-2,3-diol and *meso*-butane-2,3-diol obtained after 16 h reaction time are shown in Figure 4A. Performing the BDH1-catalyzed acetoin reduction with the wild type strain *P. pastoris* CBS7435 resulted in an average conversion of ~5% (40 individual clones tested). Employing the single knock-out strains *Δdas1* and *Δdas2* in the same reaction did not yield substantially higher conversions. The average conversions were in the same order of magnitude as for the wild type strain (~6% and ~7% for the *Δdas1* and *Δdas2* strain, respectively), indicating that the NADH regeneration was not significantly improved in these strains. In contrast to the single knock-out strains, the acetoin conversion was 5.5-fold higher when using the double knock-out strain in comparison to the wild type (average conversion ~29%), indicating a more efficient cofactor supply. The higher conversions with the double-knock out strain were even obtained with fewer cells per reaction as it grew much slower on methanol than the wild type and the single knock-out strains. These first findings confirm the assumption that the NADH formation via methanol oxidation is increased when the assimilatory pathway is disrupted, if there is a NADH requirement in the cells due to, e.g., a biocatalytic reaction. The latter is only efficiently realized when both genes coding for the dihydroxyacetone synthase proteins are deleted.

The time course of acetoin conversions with representing BDH1 transformants in the wild type and *Δdas1 Δdas2* background were investigated under optimized conditions in shake flasks. To avoid differences in the amount of cells employed in the biotransformation and to obtain higher product yields, cells corresponding to 3000 OD_{600} units were harvested 12 h after the first methanol induction and resuspended in 50 mL of buffered minimal medium before the conversions were started

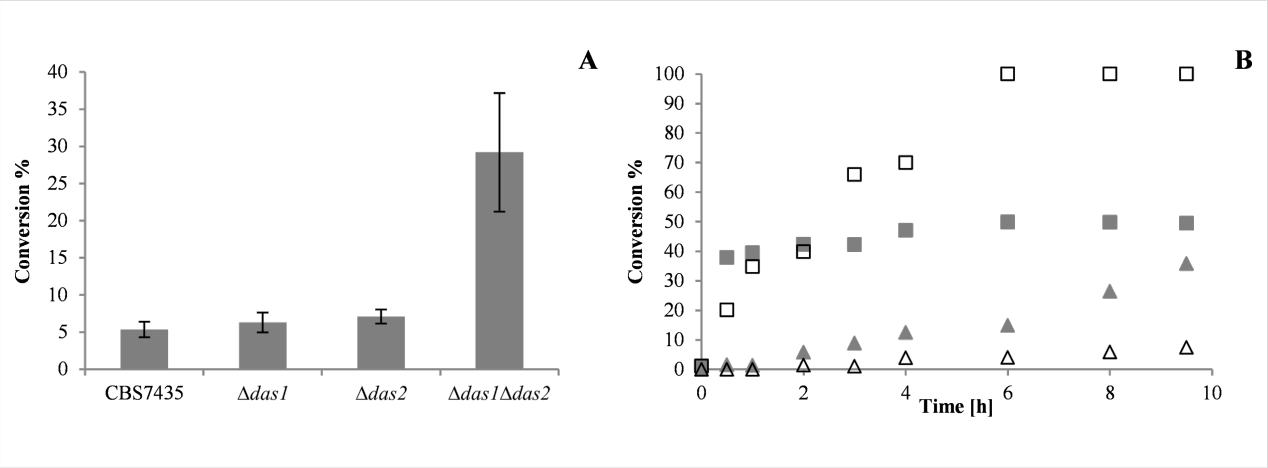

Figure 4: BDH1-based whole-cell conversions of *rac*-acetoin. (A) Conversions of 25 mM *rac*-acetoin in the different knock-out strains were performed in 96 well deep-well plates for 16 h. The shown conversions represent mean values ± standard deviations derived from reactions using whole cells from 40 individual BDH1 transformants. (B) Time-resolved biotransformations of 50 mM substrate were conducted in the wild type (grey squares) and in the *Δdas1 Δdas2* strain background (white squares). Background activity by endogenous acetoin reducing enzymes of *P. pastoris* was observed (grey triangles: *P. pastoris* CSB7435 wild type, white triangles: *P. pastoris Δdas1 Δdas2*).

by the addition of substrate. During the first two hours of the whole-cell biotransformation, the conversions obtained with each of the strains were in the same order of magnitude (see Figure 4B). After longer reaction times, hardly any residual BDH1 activity was observed with the wild type strain (final conversion of ~50%), while the reaction reached 100% conversion after 6 h in the engineered strain. These findings clearly indicate that the NADH supply for the oxidoreductase can be attained over a prolonged reaction time in the *P. pastoris Δdas1 Δdas2* strain, which directly translates into increased yields in the whole-cell reactions.

It has to be noted, that an additional acetoin reduction by endogenous *Pichia* dehydrogenases was also observed for the wild type and the double knock-out strain without the *BDH1* expression cassette, reaching ~35% and ~8% substrate conversion, respectively. As for the recombinant strains, two products were detected, namely (2*R*,3*R*)-butane-2,3-diol and *meso*-butane-2,3-diol.

Conclusion

Efficient cofactor recycling is not only required for an optimal enzyme performance, but is also crucial to render the resulting process economical and sustainable. For this purpose, biotransformations based on whole cells represent an elegant strategy as the cell metabolism can be exploited for cofactor supply. We have generated a novel platform strain for whole-cell catalysis based on the methylotrophic yeast *P. pastoris* by engineering its methanol utilization pathway. By deleting the pathway for methanol assimilation, we forced flux through the dissimilatory pathway in which theoretically two molecules of NADH can be formed per molecule of methanol. The resulting double knock-out strain *P. pastoris* CBS7435 *Δdas1Δdas2* displayed better performance in dehydrogenase based whole-cell biotransformations without the need of an external electron source. Higher conversions were achieved in comparison to reactions carried out with the wild type *Pichia* strain due to an extended NADH supply by the oxidation of methanol.

Methanol, which is a cheap carbon source, fulfills several roles in the presented biotransformations: It acts as an inducer of the P_{AOX1} regulated production of the redox enzyme as well as of the endogenous NADH regeneration system at the same time. The cofactor regeneration itself is based on methanol as co-substrate: the oxidation of methanol is irreversible and represents a strong thermodynamic driving force while only CO_2 is produced as side product. Furthermore, methanol can serve as solvent for the substrate and methylotrophic yeasts are already naturally adapted to elevated concentrations of methanol.

The redesigned *Pichia* strain, thus, represents a valuable host for whole-cell applications where NADH regeneration is an issue. No additional over-expression of cofactor regenerating enzymes such as formate dehydrogenase, which only yields one molecule of NADH per carbon atom, is required. Due to its simplicity it might further boost the use of recombinant whole-cell catalysts in chemical and pharmaceutical industry.

Experimental

General

Unless stated otherwise, all chemicals were obtained from Sigma-Aldrich (Steinheim, Germany) or Carl-Roth (Karlsruhe, Germany) with the highest purity available. Zeocin™ was obtained from InvivoGen (San Diego, CA, USA). Phusion®

High Fidelity Polymerase for DNA amplification and further DNA modifying enzymes were purchased from Thermo Fisher Scientific Inc. (Waltham, MA, USA). *E. coli* Top10 (Invitrogen, Carlsbad, USA) was used for all cloning steps and plasmid propagation. The *P. pastoris* strain CBS7435 as well as the plasmid pPp_T4_S were obtained from the *Pichia* pool of TU Graz [20].

Generation of *das* knock-out strains

The generation of knock-out strains was based on linear excision cassettes harboring a FLP recombinase system for inducible marker recycling. A schematic representation of such a knock-out cassette is provided in Supporting Information File 1, Figure S1. Knock-out cassettes were essentially constructed as described in [20]. Locus specific integration sequences, i.e., DNA fragments of approximately 1.5 kb directly located up- and downstream of the corresponding coding sequences, were amplified from genomic DNA. The corresponding primers were designed based on the genome sequence of *P. pastoris* CBS7435 and are summarized in Supporting Information File 1, Table S1. The resulting knock-out cassettes were employed for the transformation of *P. pastoris* CBS7435 wild type cells according to the condensed protocol by Lin-Cereghino et al. [23]. Transformants were selected on YPD agar plates containing 100 mg/L Zeocin™. The correct integration of the knock-out cassette was confirmed by PCR using genomic DNA as template and primer pairs binding within the cassette and either up- or downstream of the targeted locus (see Supporting Information File 1, Table S2). In a next step, the marker was recycled by inducing the FLP recombinase. Therefore, a single colony from a correct knock-out strain was used to inoculate 50 mL of YPD media (250 mL baffled shake flask) and grown for 24 h at 28 °C. After 24 h of growth, methanol was added to a final concentration of 0.5% to start recombinant protein production, which was maintained by daily methanol addition for 96 h. An aliquot of these cultures was plated on YPD agar plates to obtain single colonies. These were subsequently streaked out on YPD agar plates supplemented with 100 mg/L Zeocin™ to identify clones that had excised the cassette and, thus, were Zeocin™-sensitive. The marker recycling was further validated by PCR using primers that bind in the genomic region directly up- and downstream of the deleted locus (see Supporting Information File 1, Table S3) and Sanger sequencing of the resulting PCR product.

Growth rate studies

Liquid *Pichia* cultures were grown in buffered minimal medium containing 200 mM KP_i (pH 6.0), 13.4 g/L yeast nitrogen base and 0.4 mg/L biotin supplemented either with 2% (w/v) D-glucose (BMD), 1% (w/v) glycerol (BMG) or 0.5% (v/v) methanol (BMM). Growth rates of the generated *das* knock-out strains were determined by measuring the optical density (OD_{600}) of cultures in biological triplicate during the exponential growth phase.

GFP expression in knock-out strains

The plasmid pPp_T4_S_GFP was linearized with *Smi*I and used to transform the wild-type as well as the *das* knock-out *P. pastoris* strains. Single colonies were transferred to 96 well deep-well plates for standard cultivation and protein production as described previously [24]. For comparison of the expression levels, the GFP fluorescence (488 nm excitation, 507 nm emission) and the optical density (OD_{600}) of the cell suspension were measured with a Synergy MX Microplate Reader.

Cloning of model enzyme

To evaluate the cofactor regeneration of the generated knock-out strains, the 2,3-butanediol dehydrogenase of *S. cerevisiae* YAL060W (BDH1) [22] was employed as NADH-dependent model enzyme. The corresponding gene was ligated with the *P. pastoris* expression vector pPp_T4_S_after digestion with *EcoR*I/*Not*I. The thus resulting construct, pPp_T4_S_BDH1, was linearized with *Smi*I for the subsequent transformation of the *Pichia* wild-type as well as *das* knock-out strains.

Screening of BDH1 transformants

Strains harboring the expression cassette for *BDH1* were grown for 60 h in 250 µL of BMD medium in 96 well deep-well plates. Protein expression was started by the addition of 250 µL BMM2 (1% (v/v) in methanol) approximately 12 h prior to the start of the bioreduction reaction. The BDH1-mediated bioreduction was started by adding BMM10 (5% (v/v) methanol) containing 250 mM *rac*-acetoin. After a reaction time of 16 h, 300 µL of the reaction supernatant were extracted twice with 400 µL ethyl acetate containing 50 mM *n*-butanol as internal standard for the determination of acetoin conversions. The combined organic phases were dried over Na_2SO_4 and subjected to GC-FID analyses as described below.

Kinetic studies of biotransformations

Biotransformations in shake flasks were conducted with strains harboring one copy of the *BDH1* expression cassette as determined by quantitative real-time PCR [25]. The corresponding strains were grown for 60 h in 200 mL BMD medium (2 L baffled shake flasks) and protein expression was started by the addition of 20 mL BMM10 approximately 12 h prior to the start of the bioreduction reaction. For BDH1 catalyzed acetoin conversion, cells corresponding to 3000 OD_{600} units were harvested by centrifugation (3000*g*, 10 min, rt) and resuspended in 50 mL of buffered minimal medium. The reaction was started by adding 10 mL of the substrate solution (300 mM *rac*-acetoin, 50% (v/v) methanol, 200 mM KP_i, pH 6.0).

GC-FID analysis of biotransformations

Acetoin conversions were determined using an Agilent Technologies 6890N gas chromatograph equipped with an FID detector and a CTC Analytics CombiPAL autosampler. A Chirasil-DEX CB column (25 m × 0.32 mm, 0.25 µm film) was applied using H_2 as carrier gas. The samples were injected without split. The following temperature program was used: 65 °C for 6.5 min; 50 °C/min to 80 °C; 80 °C for 0.7 min; 2 °C/min to 85 °C; 85 °C for 3 min.

Retention times: *n*-butanol: 1.71 min, (*S*)-acetoin: 2.04 min, (*R*)-acetoin: 2.32 min, (2*R*,3*R*)-butane-2,3-diol: 8.27 min, *meso*-butane-2,3-diol: 8.90 min.

Supporting Information

Supporting Information File 1

Schematic representation of knock-out cassette architecture and sequences of primers used.
[http://www.beilstein-journals.org/bjoc/content/supplementary/1860-5397-11-190-S1.pdf]

Acknowledgements

We gratefully acknowledge the help of Mudassar Ahmad in designing the employed knock-out cassettes. We further want to thank Thomas Vogl (TU Graz, Austria) for providing the plasmid harboring the coding sequence of GFP under the control of the *AOX1* promoter.

The research leading to these results has received funding from the Innovative Medicines Initiative Joint Undertaking project CHEM21 under grant agreement n°115360, resources of which are composed of financial contribution from the European Union's Seventh Framework Programme (FP7/2007-2013) and EFPIA companies' in kind contribution. In addition, the work has been supported by the Federal Ministry of Science, Research and Economy (BMWFW), the Federal Ministry of Traffic, Innovation and Technology (bmvit), the Styrian Business Promotion Agency SFG, the Standortagentur Tirol, the Government of Lower Austria and ZIT - Technology Agency of the City of Vienna through the COMET-Funding Program managed by the Austrian Research Promotion Agency FFG.

References

1. Johanson, T.; Katz, M.; Gorwa-Grauslund, M. F. *FEMS Yeast Res.* **2005,** *5,* 513–525. doi:10.1016/j.femsyr.2004.12.006
2. Winkler, C.; Tasnádi, G.; Clay, D.; Hall, M.; Faber, K. *J. Biotechnol.* **2012,** *162,* 381–389. doi:10.1016/j.jbiotec.2012.03.023
3. Weckbecker, A.; Gröger, H.; Hummel, W. Regeneration of Nicotinamide Coenzymes: Principles and Applications for the Synthesis of Chiral Compounds. In *Biosystems Engineering I;* Wittmann, C.; Krull, R., Eds.; Advances in Biochemical Engineering / Biotechnology, Vol. 120; Springer: Berlin, Germany, 2010; pp 195–242. doi:10.1007/10_2009_55
4. Duetz, W. A.; Beilen, J. B.; Van Witholt, B. *Curr. Opin. Biotechnol.* **2001,** *12,* 419–425. doi:10.1016/S0958-1669(00)00237-8
5. Katz, M.; Sarvary, I.; Frejd, T.; Hahn-Hägerdal, B.; Gorwa-Grauslund, M. F. *Appl. Microbiol. Biotechnol.* **2002,** *59,* 641–648. doi:10.1007/s00253-002-1079-4
6. Baerends, R. J. S.; De Hulster, E.; Geertman, J.-M. A.; Daran, J.-M.; van Maris, A. J. A.; Veenhuis, M.; van der Klei, I. J.; Pronk, J. T. *Appl. Environ. Microbiol.* **2008,** *74,* 3182–3188. doi:10.1128/AEM.02858-07
7. Schroer, K.; Luef, K. P.; Hartner, S. F.; Glieder, A.; Pscheidt, B. *Metab. Eng.* **2010,** *12,* 8–17. doi:10.1016/j.ymben.2009.08.006
8. Cregg, J. M.; Cereghino, J. L.; Shi, J.; Higgins, D. R. *Mol. Biotechnol.* **2000,** *16,* 23–52. doi:10.1385/MB:16:1:23
9. Ahmad, M.; Hirz, M.; Pichler, H.; Schwab, H. *Appl. Microbiol. Biotechnol.* **2014,** *98,* 5301–5317. doi:10.1007/s00253-014-5732-5
10. Engelking, H.; Pfaller, R.; Wich, G.; Weuster-Botz, D. *Tetrahedron: Asymmetry* **2004,** *15,* 3591–3593. doi:10.1016/j.tetasy.2004.09.021
11. Das, S.; Glenn, J. H., IV; Subramanian, M. *Biotechnol. Prog.* **2010,** *26,* 607–615. doi:10.1002/btpr.363
12. Abad, S.; Nahalka, J.; Bergler, G.; Arnold, S. A.; Speight, R.; Fotheringham, I.; Nidetzky, B.; Glieder, A. *Microb. Cell Fact.* **2010,** *9,* 24. doi:10.1186/1475-2859-9-24
13. Geier, M.; Braun, A.; Emmerstorfer, A.; Pichler, H.; Glieder, A. *Biotechnol. J.* **2012,** *7,* 1346–1358. doi:10.1002/biot.201200187
14. Yan, J.; Zheng, X.; Li, S. *Bioresour. Technol.* **2014,** *151,* 43–48. doi:10.1016/j.biortech.2013.10.037
15. Wriessnegger, T.; Augustin, P.; Engleder, M.; Leitner, E.; Müller, M.; Kaluzna, I.; Schürmann, M.; Mink, D.; Zellnig, G.; Schwab, H.; Pichler, H. *Metab. Eng.* **2014,** *24,* 18–29. doi:10.1016/j.ymben.2014.04.001
16. Hartner, F. S.; Glieder, A. *Microb. Cell Fact.* **2006,** *5,* 39. doi:10.1186/1475-2859-5-39
17. De Schutter, K.; Lin, Y.-C.; Tiels, P.; Van Hecke, A.; Glinka, S.; Weber-Lehmann, J.; Rouzé, P.; Van de Peer, Y.; Callewaert, N. *Nat. Biotechnol.* **2009,** *27,* 561–566. doi:10.1038/nbt.1544
18. Krainer, F. W.; Dietzsch, C.; Hajek, T.; Herwig, C.; Spadiut, O.; Glieder, A. *Microb. Cell Fact.* **2012,** *11,* 22. doi:10.1186/1475-2859-11-22
19. Reuß, O.; Vik, A.; Kolter, R.; Morschhäuser, J. *Gene* **2004,** *341,* 119–127. doi:10.1016/j.gene.2004.06.021
20. Näätsaari, L.; Mistlberger, B.; Ruth, C.; Hajek, T.; Hartner, F.; Glieder, A. *PLoS One* **2012,** *7,* e39720. doi:10.1371/journal.pone.0039720
21. Broach, J. R.; Guarascio, V. R.; Jayaram, M. *Cell* **1982,** *29,* 227–234. doi:10.1016/0092-8674(82)90107-6
22. González, E.; Fernández, M. R.; Larroy, C.; Solà, L.; Pericàs, M. A.; Parés, X.; Biosca, J. A. *J. Biol. Chem.* **2000,** *275,* 35876–35885. doi:10.1074/jbc.M003035200
23. Lin-Cereghino, J.; Wong, W. W.; Xiong, S.; Giang, W.; Luong, L. T.; Vu, J.; Johnson, S. D.; Lin-Cereghino, G. P. *BioTechniques* **2005,** *38,* 44–48. doi:10.2144/05381BM04

24. Weis, R.; Luiten, R.; Skranc, W.; Schwab, H.; Wubbolts, M.; Glieder, A. *FEMS Yeast Res.* **2004,** *5,* 179–189. doi:10.1016/j.femsyr.2004.06.016
25. Abad, S.; Kitz, K.; Hörmann, A.; Schreiner, U.; Hartner, F. S.; Glieder, A. *Biotechnol. J.* **2010,** *5,* 413–420. doi:10.1002/biot.200900233

License and Terms

BEILSTEIN JOURNAL OF ORGANIC CHEMISTRY

Synthesis of α,β-unsaturated esters via a chemo-enzymatic chain elongation approach by combining carboxylic acid reduction and Wittig reaction

Yitao Duan, Peiyuan Yao, Yuncheng Du, Jinhui Feng, Qiaqing Wu* and Dunming Zhu*

Full Research Paper

Open Access

Address:
National Engineering Laboratory for Industrial Enzymes and Tianjin Engineering Center for Biocatalytic Technology, Tianjin Institute of Industrial Biotechnology, Chinese Academy of Sciences, Tianjin 300308, P. R. China

Email:
Qiaqing Wu* - wu_qq@tib.cas.cn; Dunming Zhu* - zhu_dm@tib.cas.cn

* Corresponding author

Keywords:
α,β-unsaturated esters; carboxylic acid reductase; chemoenzymatic synthesis; reduction; Wittig reaction

Beilstein J. Org. Chem. **2015,** *11,* 2245–2251.
doi:10.3762/bjoc.11.243

Received: 20 August 2015
Accepted: 28 October 2015
Published: 19 November 2015

This article is part of the Thematic Series "Sustainable catalysis".

Guest Editor: N. Turner

Abstract

α,β-Unsaturated esters are versatile building blocks for organic synthesis and of significant importance for industrial applications. A great variety of synthetic methods have been developed, and quite a number of them use aldehydes as precursors. Herein we report a chemo-enzymatic chain elongation approach to access α,β-unsaturated esters by combining an enzymatic carboxylic acid reduction and Wittig reaction. Recently, we have found that *Mycobacterium* sp. was able to reduce phenylacetic acid (**1a**) to 2-phenyl-1-ethanol (**1c**) and two sequences in the *Mycobacterium* sp. genome had high identity with the carboxylic acid reductase (CAR) gene from *Nocardia iowensis*. These two putative CAR genes were cloned, overexpressed in *E. coli* and one of two proteins could reduce **1a**. The recombinant CAR was purified and characterized. The enzyme exhibited high activity toward a variety of aromatic and aliphatic carboxylic acids, including ibuprofen. The *Mycobacterium* CAR catalyzed carboxylic acid reduction to give aldehydes, followed by a Wittig reaction to afford the products α,β-unsaturated esters with extension of two carbon atoms, demonstrating a new chemo-enzymatic method for the synthesis of these important compounds.

Introduction

α,β-Unsaturated esters are versatile building blocks for organic synthesis and of significant importance for industrial applications [1-13]. A great variety of synthetic methods have been developed to access α,β-unsaturated esters [14-24]. One popular approach is the Wittig reaction which produces α,β-unsaturated esters with two more carbon atoms [25]. While fatty acids are abundant from natural resources, aromatic carboxylic acids could be prepared by the degradation of lignin, an unused and

abundant component of biomass, although the effective methods for the degradation of lignin need to be developed. These carboxylic acids could be reduced to their corresponding aldehydes, which can be used as starting materials for Wittig reaction. The combination of carboxylic acid reduction and Wittig reaction would offer a new approach for the production of bio-based α,β-unsaturated esters. However, the conventional chemical methods for the carboxylic acid reduction require strong reducing reagents such as metal hydrides, posting operational danger and low selectivity. In addition, the conversion of COOH into CHO requires particular hydride reagents, to avoid the further reduction to primary alcohols [26]. On the contrary, enzymatic reduction of carboxylic acids proceeds under mild reaction conditions with high selectivity and tolerance of other functional groups [27,28]. Currently, only a few members of this interesting type of enzymes (CAR, E.C.1.2.1.30) have been biochemically characterized (Table 1). They possess similar consensus sequence characteristics and reaction mechanism (post-translational phosphopantetheinylation, ATP, Mg^{2+}, and NADPH as cofactors) [27-30]. As such, we initiated the search for new carboxylic acid reductases and the exploration of their potential as biocatalysts for the efficient bioreduction of carboxylic acids. Herein we report a new CAR from *Mycobacterium* sp. (*Mycobacterium* CAR) and its application in a chemo-enzymatic chain elongation method for the preparation of α,β-unsaturated esters by combining an enzymatic carboxylic acid reduction and Wittig reaction.

Results and Discussion

Nineteen actinomycete strains available in our laboratory were screened for the carboxylic acid reductase activity using phenylacetic acid (**1a**) as the substrate by GC analysis of the products. Among them, *Mycobacterium* sp. was found to catalyse the reduction of **1a** to 2-phenyl-1-ethanol (**1c**) with low conversion (Supporting Information File 1, Figure S1). The genome of *Mycobacterium* sp. strain was sequenced, and two gene sequences having 58% and 47% protein sequence identity with the NiCAR [30] (accession number AAR91681.1) were found by local BLAST search (tblastn) (Supporting Information File 1, Figure S2). These two genes were also found to have identical sequences with those (Gene ID 17912504 and Gene ID 17917114), respectively, in the genomic sequence of *Mycobacterium neoaurum* VKM Ac-1815D (accession no. CP006936) [34] by NCBI BLAST search (http://www.ncbi.nlm.nih.gov/BLAST/).

Since PPTase from *Mycobacterium* sp. has not been identified, a known *Nocardia* PPTase (accession number ABI83656.1) was selected for the post-translational phosphopantetheinylation in the current study [27,28]. The gene (Gene ID 17912504) was cloned into pET30b(+) and expressed in *E. coli*. The recombinant enzyme (*Mycobacterium* CAR) showed carboxylic acid reductase activity toward **1a**. The other gene (Gene ID 17917114) was cloned into pET28a(+) and expressed in *E. coli*. The gene was well expressed, but less fraction of soluble protein was obtained. The recombinant enzyme showed no carboxylic acid reductase activity toward **1a** when it was tested under same conditions as the gene 17912504 after having been treated with the PPTase enzyme.

The His-tagged *Mycobacterium* CAR and His-PPTase were produced as soluble protein as described in Supporting Information File 1 and purified in one chromatographic step each using a HisTrap^{TM} FF crude column (Supporting Information File 1, Figure S3). The molecular mass of His-CAR was estimated to be about 133 kDa by gel filtration chromatography. Since its theoretical value is 125 kDa, this enzyme is a monomeric protein. This is consistent with NiCAR [31] and SrCAR [28]. The carboxylic acid reductase activity was hardly detected when apo-CAR was used in the reaction system (**1a** as substrate) or the reaction system did not contain Mg^{2+} (Supporting Information File 1, Table S2), indicating that post-translational phosphopantetheinylation and Mg^{2+} were necessary for this enzymatic reduction, similar to the observations for the reaction with the carboxylic acid reductases from *Nocardia* [29,35] and *Segniliparus* [28]. The optimal pH and temperature for the enzymatic reduction of **1a** with *Mycobacterium* CAR were pH 9 and 25 °C, respectively. The apparent K_m and catalytic efficien-

Table 1: Identified CARs (EC 1.2.1.30).

Identified CAR	Accession number	Origin	References
NiCAR[a,b]	AAR91681.1	*Nocardia iowensis*	[30,31]
MsCAR	WP_011855500.1	*Mycobacterium* sp. JLS	[32]
SgCAR	WP_012382217.1	*Streptomyces griseus* subsp. *griseus* NBRC 13350	[32]
MmCAR[a]	WP_012393886.1	*Mycobacterium marinum* M	[33]
SrCAR[a]	WP_013138593.1	*Segniliparus rotundus* DSM 44985	[28]
Mycobacterium CAR[a]	WP_019510583.1	*Mycobacterium* sp.	This work

[a]The protein was biochemically characterized and determined as a monomeric protein. [b]The protein was also purified from natural strain.

cies (k_{cat}/K_m) of *Mycobacterium* CAR toward benzoic acid (**2a**) (Supporting Information File 1, Table S1) were 1.75 ± 0.16 mM and 0.93 $mM^{-1}·s^{-1}$, respectively. They were lower than those for NiCAR [31], SrCAR [28] and MnCAR [33].

In order to explore the application potential of *Mycobacterium* CAR, its substrate specificity was examined with the purified enzyme. The results in Table 2 showed that a series of aromatic and aliphatic carboxylic acids were reduced to their corresponding aldehydes. For the aliphatic acids, the reduction of nonanoic acid (**3a**) and lauric acid (**4a**) resulted in higher yields than those of hexanoic acid (**5a**) and pentadecanoic acid (**6a**), indicating that *Mycobacterium* CAR prefers the mid-chain fatty acids over the short-chain and long-chain ones. *Mycobacterium* CAR also showed activity toward different carboxylic acids with aromatic ring at the end carbon atom. For example, **1a** (75% yield), **2a** (94% yield), 3-phenylpropanoic acid (**7a**, 48% yield), and 4-phenylbutyric acid (**8a**) (64% yield) were reduced to the corresponding aldehydes. In contrast to *ortho*- and *meta*-methylbenzoic acid (**9a** and **10a**), *ortho*-hydroxylbenzoic acid (**11a**) was obviously the poorer substrate than *meta*-counterpart (**12a**), suggesting that in this case the activity of *Mycobacterium* CAR might be strongly influenced by the electronic properties other than the steric factor of the *ortho*-group on the benzene ring. This enzyme was less active toward 2-methylhexanoic acid (**13a**) and 2-phenylpropionic acid (**14a**) than **5a**

Table 2: Substrate specificity of *Mycobacterium* CAR[a].

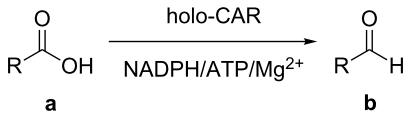

a **b**

Substrate		Analytic yield (%) of aldehyde
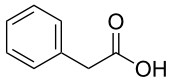	**1a**	75
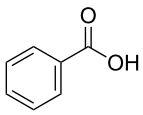	**2a**	94
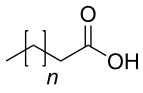	**3a** (*n* = 6) **4a** (*n* = 9) **5a** (*n* = 3) **6a** (*n* = 12)	100 100 68 3
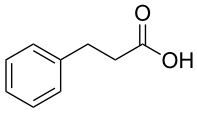	**7a**	48
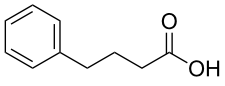	**8a**	64
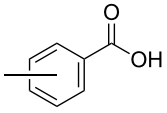	**9a** (*ortho*) **10a** (*meta*)	57 62
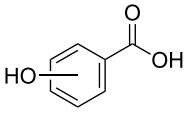	**11a** (*ortho*) **12a** (*meta*)	7 41

Table 2: Substrate specificity of *Mycobacterium* CAR[a]. (continued)

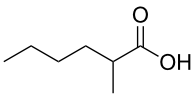	**13a**	62; 100[b]
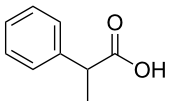	**14a** (*R*/*S*)	47; 100[b]
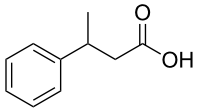	**15a**	44; 95[b]
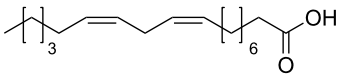	**16a**[c]	14
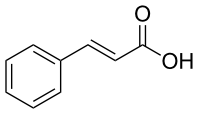	**17a**	36
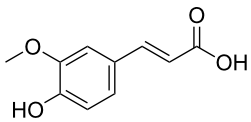	**18a**[d]	40
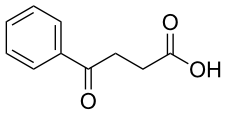	**19a**	68
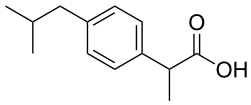	**20a** (*R*/*S*)	98
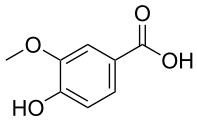	**21a**	76
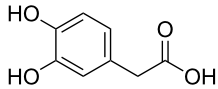	**22a**[c, d]	18

[a]Reaction conditions: Tris-HCl buffer (1 mL, 100 mM, pH 9) contained $NADP^+$ (0.9 mM), GDH (1 U), glucose (60 mM), $MgCl_2$ (10 mM), ATP (15 mM), substrate concentration (10 mM) and enzyme mixture (holo-CAR, 50 ug), 16 h, 25 °C, 200 rpm. [b]Same as [a], but 5 mM of substrate and 100 µg of *Mycobacterium* CAR were used. [c]Same as [a], but the reaction was performed in sodium phosphate buffer (100 mM, pH 7.5). [d]Silylation was performed before the GC analysis.

and **1a**, respectively. This may be due to the sterically hindered effect of the α-methyl substitution, which is consistent with the results for *Pyrococcus furiosus* (whole-cell) [36] and NiCAR [31]. However, no significant difference was noted between 3-phenylbutyric acid (**15a**) and **7a**. *Mycobacterium* CAR showed good chemoselectivity for the reduction of some

carboxylic acids containing C=C or C=O double bonds, such as linoleic acid (1**6a**), cinnamic acid (**17a**), ferulic acid (**18a**), and 3-benzoylpropionic acid (**19a**). These acids were reduced, with C=C or C=O double bonds remaining unaffected. However, this enzyme was less active toward **17a** than its saturated counterpart (**7a**). Interestingly, *Mycobacterium* CAR could effectively reduce ibuprofen (**20a**) more effectively than NiCAR and SrCAR, but it was not enantioselective. Rac-**13a**, rac-**14a** and rac-**15a** (5 mM) were almost completely transformed by *Mycobacterium* CAR (100 μg), suggesting it had no or low enantioselectivity toward these compounds.

The *Mycobacterium* CAR-catalysed carboxylic acid reduction was combined with Wittig reaction to establish a new chemo-enzymatic approach to the synthesis of α,β-unsaturated esters. As described in the Experimental section, the holo-CAR enzyme mixture was prepared and mixed with $NADP^+$, GDH, glucose, ATP and carboxylic acid in Tris-HCl buffer. The reaction mixture was incubated at 25 °C for 16 h and extracted with ethyl acetate. The organic extract was concentrated to about 20 mL, and mixed with ethyl (triphenylphosphoranylidene)acetate and Na_2CO_3. After 24 h at room temperature, the organic solvent was removed under reduced pressure and the residue was purified by silica gel column chromatography to give the product (α,β-unsaturated ester). As shown in Table 3, α,β-unsaturated esters were obtained in moderate to high yields with *trans*-isomer as the major product. The corresponding α,β-unsaturated esters from aromatic carboxylic acids (**1a**, **2a**, **10a**, **12a** and **17a**) had higher yields than those from aliphatic ones (**3a**, **4a** and **5a**), and this might be due to lower yields of aliphatic aldehydes and higher loss in the product separation.

Conclusion

A new CAR from *Mycobacterium* sp. was successfully cloned, overexpressed and identified. It exhibited a broad substrate spectrum and was active toward both aliphatic and aromatic carboxylic acids, including ibuprofen. Other functional groups such as keto groups and C=C double bonds remained unaffected. *Mycobacterium* CAR catalysed carboxylic acid reduction to give aldehydes, followed by a Wittig reaction to afford α,β-unsaturated esters with extension of two carbon atoms. This study demonstrates a new chemo-enzymatic chain elongation method for the synthesis of these important compounds from bio-based fatty and aromatic acids of natural resources. However, the enzymatic reduction of carboxylic acids requires CoA, ATP and NADPH, and this still presents challenge for its application at large scale, which may be overcome by using the whole cell catalyst of the engineered enzyme production strain with efficient amount of CoA, ATP and NADPH or effective regeneration systems of them.

Experimental

Cloning of *Mycobacterium* CAR gene

Mycobacterium sp. chromosomal DNA (gDNA) was extracted and purified using a TIANamp Bacteria DNA Kit. The *Mycobacterium* CAR gene (Gene ID 17912504) was amplified

Table 3: Synthesis of α,β-unsaturated esters via enzymatic reduction and Wittig reaction[a].

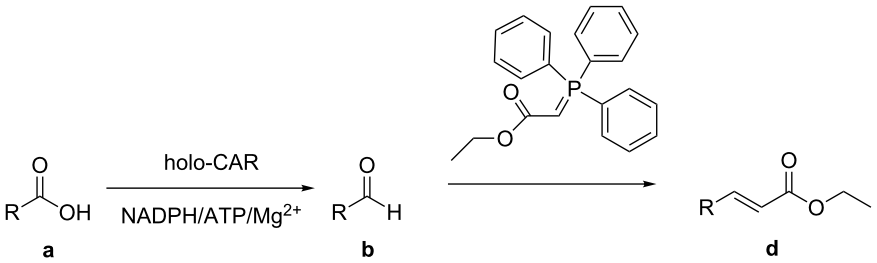

a **b** **d**

Substrate (**a**)	Analytic yield (%) of aldehydes (**b**)[b]	Isolated yield (%) of α,β-unsaturated esters (**d**)	Ratio *E*/*Z*[c]
1a	72	60	68:32
2a	100	70	92:8
3a	65	41	87:13
4a	70	46	89:11
5a	67	38	96:4
10a	100	81	92:8
12a	79	59	90:10
17a	78	65	94:6

[a]The carboxylic acid was first reduced to aldehyde, after being extracted with ethyl acetate, ethyl (triphenylphosphoranylidene)acetate was added for the Wittig reaction. [b]Determined by GC analysis of the reaction mixture. [c]Determined by GC analysis of isolated products.

by PCR using *Mycobacterium* gDNA as template and primers containing the restriction sites *Nde*I and *Xho*I, respectively, CAR-F 5′-CATGCATATGTTCGCCGAAAATCTTGATGACCAG-3′ and CAR-R 5′-CATCTCGA GCAGCAGGCCGAGCAATTGCAGGT-3′. The PCR fragment was purified and then ligated with cloning vector pJET1.2/blunt, which was confirmed by DNA sequencing. A CAR DNA fragment was acquired from the vector pJET1.2-CAR by digesting at the restriction sites *Nde*I and *Xho*I, and then ligated by T4 DNA ligase into pET30b(+) at the same restriction sites to generate the expression vector pET30b(+)-CAR. The confirmed recombinant vector was transformed into *E. coli* BL21(DE3).

Expression and purification of *Mycobacterium* CAR and *Nocardia* PPTase

A culture of *E. coli* BL21 (DE3) cells harboring pET30b(+)-CAR or pET32a(+)-PPTase was grown overnight in LB-ampicillin (100 μg/mL) medium (5 mL) at 37 °C, and then inoculated into 1 L of LB-ampicillin (100 μg/mL) medium. The resulting culture was incubated continually at 200 rpm in a rotary shaker at 37 °C until cells reached mid-log growth (OD_{600} of 0.5–1.0), which was followed by the addition of 0.5 mM IPTG and further incubation for 12 h at 25 °C. Cells were harvested by centrifugation at 12 000*g* for 10 min at 4 °C, and disrupted by high pressure homogenizer after re-suspension in binding buffer (20 mM sodium phosphate buffer, 0.5 M NaCl, 20 mM imidazole, pH 7.4). His-CAR or His-PPTase protein in the supernatant fraction was collected from the crude cell lysate by centrifugation at 12 000*g* for 20 min. Protein purification was performed on a HisTrap™ FF crude column (GE Healthcare, Piscataway, USA), and the protein was desorbed with an elution buffer (20 mM sodium phosphate, 0.5 M NaCl, 0.5 M imidazole, pH 7.4). The purified proteins His-CAR or His-PPTase were dialyzed in a sodium phosphate buffer (50 mM, pH 7.5) and then stored at −20 °C for further use.

Standard reduction procedure

The His-CAR (1.3 mg) was incubated with His-PPTase (256 μg) in the presence of CoA (1 mM) as a cofactor for 1 h at 28 °C in a final volume of 520 μL of sodium phosphate buffer (100 mM, pH 7.5) containing 10 mM of $MgCl_2$. The resulting enzyme mixture (holo-CAR, 50 or 100 μg) was mixed with $NADP^+$ (0.9 mM), GDH (1 U, one unit corresponds to the amout of enzyme which could convert 1 μmol $NADP^+$ to NADPH per minute using D-glucose as the substrate), glucose (60 mM), $MgCl_2$ (10 mM), carboxylic acid (5 or 10 mM, from 1 M stock solution in DMSO), and ATP (15 mM) in Tris-HCl buffer (100 mM, pH 9) with a final volume of 1 mL. The reaction mixture was incubated at 200 rpm in a rotary shaker at 25 °C for 16 h, and extracted with 1 mL of ethyl acetate after the pH was adjusted to 2–3 with 1 M HCl solution. The organic extracts were dried over anhydrous sodium sulfate and analysed by gas chromatography (GC) to determine the amount of substrate (**a**) and products (aldehyde **b**) in the mixture. All experiments were conducted in triplicate.

Substrate specificity

The reduction of a series of carboxylic acids was carried out by following the standard reduction procedure. The yields were determined by GC analysis.

Experimental procedures for the synthesis of compounds **1d**, **2d**, **3d**, **4d**, **5d**, **10d**, **12d** and **17d**

A typical procedure was as follows using ethyl 4-phenylbut-2-enoate (**1d**) as the example. The enzyme mixture (holo-CAR, 0.5 mg/mL) was prepared as described above, and was mixed with $NADP^+$ (0.45 mM), GDH (1 U), glucose (60 mM), ATP (13 mM) and phenylacetic acid (**1a**, 10 mM) in Tris-HCl buffer (total volume 25 mL, 100 mM, pH 9). The reaction mixture was incubated at 100 rpm in a rotary shaker at 25 °C for 16 h, and extracted 3 times with 25 mL of ethyl acetate. The organic extract was concentrated to about 20 mL under reduced pressure, and then ethyl (triphenylphosphoranylidene)acetate (100 mM) and Na_2CO_3 (about 0.5 g) were added, and the reaction mixture was stirred for 24 h at room temperature. The organic solvent was removed under reduced pressure and the residue was purified by silica gel column chromatography to give the product, **1d** (30.1 mg, 60%) was obtained.

Supporting Information

Supporting Information File 1

Materials, bacterial screening, analytical procedures, NMR data and spectra of **1d**, **2d**, **3d**, **4d**, **5d**, **10d**, **12d** and **17d**.
[http://www.beilstein-journals.org/bjoc/content/supplementary/1860-5397-11-243-S1.pdf]

Acknowledgements

This work was financially supported by National Basic Research Program of China (973 Program, No. 2011CB710800) and the Chinese Academy of Sciences (KSZD-EW-Z-015).

References

1. Shibata, K.; Chatani, N. *Org. Lett.* **2014,** *16,* 5148–5151. doi:10.1021/ol502500c
2. Cheng, J.; Huang, Z.; Chi, Y. R. *Angew. Chem., Int. Ed.* **2013,** *52,* 8592–8596. doi:10.1002/anie.201303247
3. Wang, P.; Ling, L.; Liao, S.-H.; Zhu, J.-B.; Wang, S. R.; Li, Y.-X.; Tang, Y. *Chem. – Eur. J.* **2013,** *19,* 6766–6773. doi:10.1002/chem.201204182

4. Hashimoto, T.; Maruoka, K. *Chem. Rev.* **2015,** *115,* 5366–5412. doi:10.1021/cr5007182
5. Zhu, Y.; Wang, Q.; Cornwall, R. G.; Shi, Y. *Chem. Rev.* **2014,** *114,* 8199–8256. doi:10.1021/cr500064w
6. He, J.; Ling, J.; Chiu, P. *Chem. Rev.* **2014,** *114,* 8037–8128. doi:10.1021/cr400709j
7. Yasukawa, T.; Suzuki, A.; Miyamura, H.; Nishino, K.; Kobayashi, S. *J. Am. Chem. Soc.* **2015,** *137,* 6616–6623. doi:10.1021/jacs.5b02213
8. Weber, F.; Brueckner, R. *Eur. J. Org. Chem.* **2015,** 2428–2449. doi:10.1002/ejoc.201403622
9. Peacock, L. R.; Chapman, R. S. L.; Sedgwick, A. C.; Mahon, M. F.; Amans, D.; Bull, S. D. *Org. Lett.* **2015,** *17,* 994–997. doi:10.1021/acs.orglett.5b00103
10. Niu, Z.; Chen, J.; Chen, Z.; Ma, M.; Song, C.; Ma, Y. *J. Org. Chem.* **2015,** *80,* 602–608. doi:10.1021/jo5021135
11. Parveen, S.; Hussain, S.; Qin, X.; Hao, X.; Zhu, S.; Rui, M.; Zhang, S.; Fu, F.; Ma, B.; Yu, Q.; Zhu, C. *J. Org. Chem.* **2014,** *79,* 4963–4972. doi:10.1021/jo500338c
12. Hatano, M.; Horibe, T.; Ishihara, K. *Angew. Chem., Int. Ed.* **2013,** *52,* 4549–4553. doi:10.1002/anie.201300938
13. Časar, Z.; Steinbücher, M.; Košmrlj, J. *J. Org. Chem.* **2010,** *75,* 6681–6684. doi:10.1021/jo101050z
14. Oliveira, M. E. R.; da Silva Filho, E. C.; Filho, J. M.; Ferreira, S. S.; Oliveira, A. C.; Campos, A. F. *Chem. Eng. J.* **2015,** *263,* 257–267. doi:10.1016/j.cej.2014.11.016
15. Nakagiri, T.; Murai, M.; Takai, K. *Org. Lett.* **2015,** *17,* 3346–3349. doi:10.1021/acs.orglett.5b01583
16. Liu, J.; Liu, Q.; Franke, R.; Jackstell, R.; Beller, M. *J. Am. Chem. Soc.* **2015,** *137,* 8556–8563. doi:10.1021/jacs.5b04052
17. El-Batta, A.; Jiang, C.; Zhao, W.; Anness, R.; Cooksy, A. L.; Bergdahl, M. *J. Org. Chem.* **2007,** *72,* 5244–5259. doi:10.1021/jo070665k
18. Chen, Y.; Romaire, J. P.; Newhouse, T. R. *J. Am. Chem. Soc.* **2015,** *137,* 5875–5878. doi:10.1021/jacs.5b02243
19. Kona, J. R.; King'ondu, C. K.; Howell, A. R.; Suib, S. L. *ChemCatChem* **2014,** *6,* 749–752. doi:10.1002/cctc.201300942
20. Shearouse, W. C.; Korte, C. M.; Mack, J. *Green Chem.* **2011,** *13,* 598–601. doi:10.1039/c0gc00671h
21. Zeitler, K. *Org. Lett.* **2006,** *8,* 637–640. doi:10.1021/ol052826h
22. Kantam, M. L.; Kumar, K. B. S.; Balasubramanyam, V.; Venkanna, G. T.; Figueras, F. *J. Mol. Catal. A: Chem.* **2010,** *321,* 10–14. doi:10.1016/j.molcata.2010.01.012
23. List, B.; Doehring, A.; Hechavarria Fonseca, M. T.; Job, A.; Rios Torres, R. *Tetrahedron* **2006,** *62,* 476–482. doi:10.1016/j.tet.2005.09.081
24. Barma, D. K.; Kundu, A.; Bandyopadhyay, A.; Kundu, A.; Sangras, B.; Briot, A.; Mioskowski, C.; Falck, J. R. *Tetrahedron Lett.* **2004,** *45,* 5917–5920. doi:10.1016/j.tetlet.2004.05.113
25. Maryanoff, B. E.; Reitz, A. B. *Chem. Rev.* **1989,** *89,* 863–927. doi:10.1021/cr00094a007
26. Seyden-Penne, J. *Reductions by the Alumino-and Borohydrides in Organic Synthesis;* Wiley-VCH: Weinheim, Germany, 1997.
27. Napora-Wijata, K.; Strohmeier, G. A.; Winkler, M. *Biotechnol. J.* **2014,** *9,* 822–843. doi:10.1002/biot.201400012
28. Duan, Y.; Yao, P.; Chen, X.; Liu, X.; Zhang, R.; Feng, J.; Wu, Q.; Zhu, D. *J. Mol. Catal. B: Enzym.* **2015,** *115,* 1–7. doi:10.1016/j.molcatb.2015.01.014
29. Venkitasubramanian, P.; Daniels, L.; Rosazza, J. P. N. *J. Biol. Chem.* **2007,** *282,* 478–485. doi:10.1074/jbc.M607980200
30. He, A. M.; Li, T.; Daniels, L.; Fotheringham, I.; Rosazza, J. P. N. *Appl. Environ. Microbiol.* **2004,** *70,* 1874–1881. doi:10.1128/Aem.70.3.1874-1881.2004
31. Li, T.; Rosazza, J. P. *J. Bacteriol.* **1997,** *179,* 3482–3487.
32. Behrouzian, B.; McDaniel, R.; Zhang, X.; Clark, L. Engineered Biosynthesis of Fatty Alcohols. WO Patent WO2,010,135,624, Nov 25, 2010.
33. Akhtar, M. K.; Turner, N. J.; Jones, P. R. *Proc. Natl. Acad. Sci. U. S. A.* **2013,** *110,* 87–92. doi:10.1073/pnas.1216516110
34. Shtratnikova, V. Y.; Bragin, E. Y.; Dovbnya, D. V.; Pekov, Y. A.; Schelkunov, M. I.; Strizhov, N.; Ivashina, T. V.; Ashapkin, V. V.; Donova, M. V. *Genome Announce.* **2014,** *2,* No. 1e01177-13. doi:10.1128/genomeA.01177-13
35. Li, T.; Rosazza, J. P. *J. Biol. Chem.* **1998,** *273,* 34230–34233. doi:10.1074/jbc.273.51.34230
36. van den Ban, E. C. D.; Willemen, H. M.; Wassink, H.; Laane, C.; Haaker, H. *Enzyme Microb. Technol.* **1999,** *25,* 251–257. doi:10.1016/s0141-0229(99)00036-8

License and Terms

The definitive version of this article is the electronic one which can be found at:
doi:10.3762/bjoc.11.243

BEILSTEIN JOURNAL OF ORGANIC CHEMISTRY

Biocatalysis for the application of CO_2 as a chemical feedstock

Apostolos Alissandratos* and Christopher J. Easton

Review

Open Access

Address:
Research School of Chemistry, Australian National University, Canberra ACT 2601, Australia

Email:
Apostolos Alissandratos* - Apostolos.Alissandratos@anu.edu.au

* Corresponding author

Keywords:
biocatalysis; carboxylase; CO_2 transformation; formate dehydrogenase; RuBisCO

Beilstein J. Org. Chem. **2015,** *11,* 2370–2387.
doi:10.3762/bjoc.11.259

Received: 09 September 2015
Accepted: 20 November 2015
Published: 01 December 2015

This article is part of the Thematic Series "Sustainable catalysis".

Guest Editor: N. Turner

Abstract

Biocatalysts, capable of efficiently transforming CO_2 into other more reduced forms of carbon, offer sustainable alternatives to current oxidative technologies that rely on diminishing natural fossil-fuel deposits. Enzymes that catalyse CO_2 fixation steps in carbon assimilation pathways are promising catalysts for the sustainable transformation of this safe and renewable feedstock into central metabolites. These may be further converted into a wide range of fuels and commodity chemicals, through the multitude of known enzymatic reactions. The required reducing equivalents for the net carbon reductions may be drawn from solar energy, electricity or chemical oxidation, and delivered in vitro or through cellular mechanisms, while enzyme catalysis lowers the activation barriers of the CO_2 transformations to make them more energy efficient. The development of technologies that treat CO_2-transforming enzymes and other cellular components as modules that may be assembled into synthetic reaction circuits will facilitate the use of CO_2 as a renewable chemical feedstock, greatly enabling a sustainable carbon bio-economy.

Introduction

Depletion of fossil-fuel feedstocks and pollution resulting from their unsustainable processing and use constitute challenging global issues [1,2]. Catalysis has an important role to play in addressing these challenges through the generation of fuels and commodity chemicals from renewable sources in a sustainable manner [3]. In this context, CO_2 has become a compound of key interest as it is one of the main contributors to fossil-fuel pollution [4,5]. As a result, decreasing CO_2 emissions and CO_2 sequestration technologies are subjects of intense research. In addition, CO_2 may hold an even more important role in a sustainable future, as a readily available and renewable material that may be utilised as an alternative feedstock for the production of many of the chemicals we have come to rely on [6-11]. Chemical processes that employ CO_2 as a synthon for the production of commodity chemicals may form the basis of a sustainable carbon economy.

The benefits notwhithstanding, chemical conversion of CO_2 into other forms of carbon remains challenging because the transformations typically have high activation barriers and are therefore very energy intensive [12]. Catalysis will therefore play a critical role in the development of viable solutions for the transformation of CO_2. Biocatalysts are very likely to contribute towards this end due to their ability to efficiently catalyse processes under mild conditions with limited byproduct formation [13,14]. These catalysts have been developed by nature to utilise diverse substrates including simple compounds such as CO_2. Indeed, life itself depends on the ability of autotrophic organisms to convert CO_2 into other materials, and these are therefore a valuable source of the required biocatalysts.

The development of methodologies for expression, characterisation, engineering and optimisation of CO_2-transforming enzymes will form the basis of any future biotechnology that aims to use CO_2 as a feedstock for the generation of other materials. Here we provide an overview of the biocatalysts that have already been applied to relevant technologies and are set to play an important role in future bioprocesses for the transformation of CO_2 into fuels and commodity chemicals. As well as reviewing applications of these biocatalysts, we highlight the chemical, biochemical and biological contexts in which they operate, the understanding of which is critical for effective application. As commodity chemicals contain carbon at lower oxidation states than CO_2, only enzymes that involve CO_2 reduction will be covered here and not carbonic anhydrase for the conversion to HCO_3^-, which is extensively covered in other reviews on carbon-capture technology [15].

Review

Biotechnological transformation of CO_2

Synthesis of commercial materials through the biological transformation of CO_2 is the basis of all agriculture. Through the cultivation of crops, CO_2 is converted into more useful forms of carbon, such as starch and lignocellulosic materials. In turn, these materials have been employed as carbon sources for fermentative processes, and more recently in first and second generation biofuel production processes. In this way, the carbon fixed by plants (biomass) is further transformed into a wide array of products through microbial processing [16]. Genetically engineered plants and algae have been employed to divert carbon flux in planta towards other metabolic products of interest, as an alternative to microbial processes [17,18]. Yet another alternative approach is to directly fix the CO_2 with microorganisms, circumventing the intermediacy of crop derived biomass [19,20]. This can be done with autotrophic microbes, though these are generally poorly understood, and the genetic tools required to divert carbon flux towards useful products are still under-developed with these species. Alternatively, as discussed in detail below, well understood microbes for which genetic modification methodologies are widely available, such as *E. coli*, have been used as hosts for heterologous CO_2 fixation reactions [21], that may then be coupled to an extensive array of metabolic pathways for the delivery of target compounds.

Biological strategies to increase CO_2 reactivity

Energetic demand of CO_2 transformation

Most of the carbon associated with fossil-fuel based technologies will eventually be converted to CO_2 through combustion or oxidative degradation [12,19,22], because this is the most oxidised and stable state of carbon (+4). Converting CO_2 into other more reduced forms of carbon, as found in organic commodity chemicals, requires large energy inputs. As a result, there are only a limited number of examples of industrial chemical processes which use CO_2 as feedstock, and those that do, such as the Bosch–Meiser process [7], are very energy intensive.

Associated with the dependence of autotrophic organisms on CO_2 as a carbon source, biological systems have developed various strategies to avoid energy constraints, and as a result there are several metabolic pathways for reductive transformation of CO_2 (Figure 1) [23,24]. Generally, such processes are driven by coupling the CO_2 transformations with oxidations that generate reducing equivalents, sometimes in conjunction with the hydrolysis of phosphoanhydride bonds [25-27]. For reductases or dehydrogenases operating in reverse, the electrons required to reduce CO_2 are provided through oxidation of reduced forms of redox cofactors, either directly or through electron driving protein mediation (NAD(P)H or equivalents). For a number of carboxylases, phosphoanhydride bonds in ATP are hydrolysed to drive CO_2 transformation through various molecular mechanisms. For example, biotin carboxylase catalysed reactions proceed through electrophilic activation of CO_2 to carboxyphosphate to facilitate an attack by a nucleophile [28].

In all known natural CO_2 fixation pathways, ATP and NADH or their equivalents are consumed in order to generate the intermediates that may feed into central metabolism [23]. This consumption is used as a measure of pathway efficiency for CO_2-fixation, and pathways are considered most efficient when it is minimised [25,27]. By balancing thermodynamic feasibililty and a low requirement in NADH and ATP or equivalents, Milo and coworkers [25] were able to computationally predict the most efficient synthetic CO_2 fixation pathways, using all known natural enzymes.

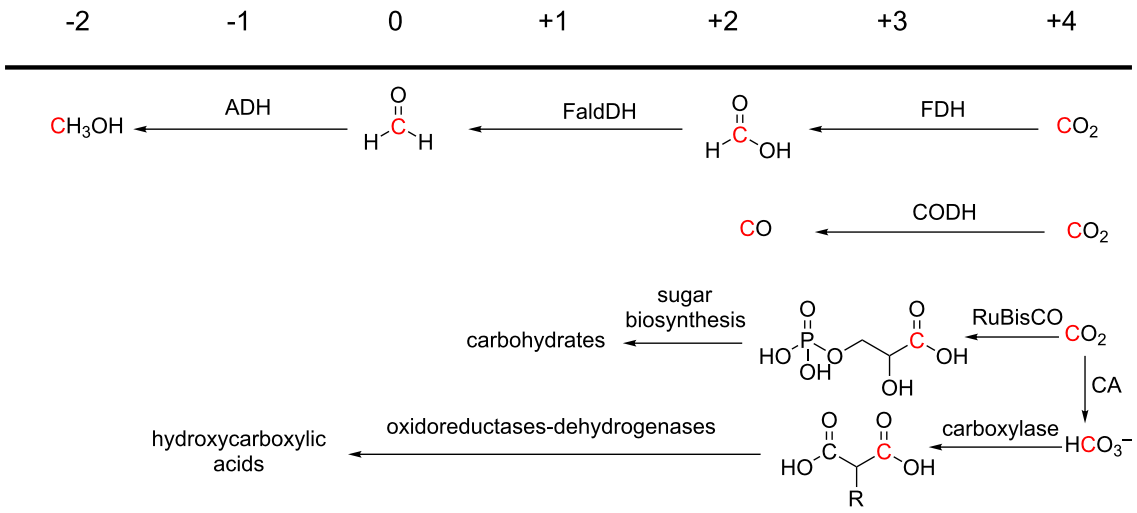

Figure 1: Biocatalytic routes for conversion of CO_2 into compounds with carbon in the reduced oxidation states indicated at the top. FDH: formate dehydrogenase, FaldDH: formaldehyde dehydrogenase, ADH: alcohol dehydrogenase, CODH: carbon monoxide dehydrogenase, RuBisCO: ribulose-1,5-bisphosphate carboxylase oxygenase, CA: carbonic anhydrase, R: H, CH_3.

Aqueous solubility and hydration of CO_2

A particular limitation for aqueous CO_2 transformations stems from the low concentration of dissolved CO_2 at saturation. At physiological pH, CO_2 is hydrated and exists predominantly as the bicarbonate anion (HCO_3^-) [29]. Within cells, CO_2 and HCO_3^- rapidly interconvert through catalysis by carbonic anhydrase, the archetypal super-enzyme for which catalytic rates reach the limits of diffusion [30,31]. CO_2 consumed by enzymes is therefore efficiently replenished through rapid HCO_3^- dehydration (Figure 2). Living organisms have developed various mechanisms to increase the effective concentration of CO_2, ranging from the use of carboxylated cofactors [28,32] to complex extended metabolic pathways in C_4 and CAM plants [17,33,34] and substrate channelling. In addition, a number of enzymes accept HCO_3^- as a substrate, which is converted to CO_2 close to the active site before the reductive step [26,28].

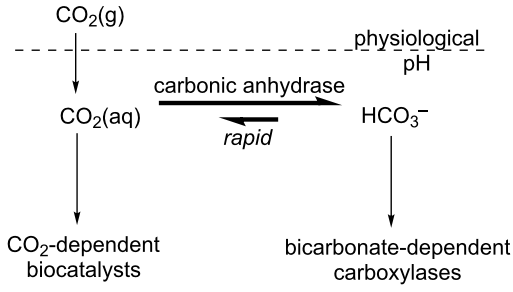

Figure 2: Carbonic anhydrase-catalysed rapid interconversion of CO_2 and HCO_3^- in living systems.

In photoautotrophic bacteria (cyanobacteria) micro-compartmentalisation of the CO_2-fixing reactions increases reaction rates [35,36]. The bacterial micro-compartments, called carboxysomes, are highly elaborate proteinic structures that usually also incorporate carbonic anhydrase [36,37]. Carboxysomes have been the subject of studies on increasing the efficiency of C_3 carbon fixation in plants [38-40]. The recent production of a transgenic tobacco plant, expressing bacterial carboxysome proteins and able to photosynthesise at an increased rate, was a significant breakthrough in this field [39]. Carboxysomal proteins have also been expressed in *E. coli* yielding a highly organised structure [41]. Use of carboxysomes for micro-compartmentalisation of CO_2 biotransformation may therefore become a viable strategy in a range of synthetic biology applications, because not only CO_2-transforming enzymes, but also the cohort of supporting cellular equipment and mechanisms that living systems employ, may be used to drive these processes.

Sources of CO_2 transforming enzymes

Emergence of CO_2 transforming enzymes

Autotrophic enzymes have evolved to promote and control CO_2 fixation and are an obvious starting point for the biotechnological transformation of CO_2 [42].

To understand the properties and distribution of these CO_2-assimilating enzymes, it is important to consider the geochemical context in which they have evolved as there appears to be a strong link with atmospheric concentrations of CO_2. The environment from which life emerged is thought to have been anoxic with high concentrations of CO_2 [43]. In this environ-

ment, the first CO_2-fixing enzymes evolved to take advantage of the most readily available carbon source. Through the action of these enzymes and geological processes for CO_2 sequestration, CO_2 concentrations steadily decreased, leading to average atmospheric concentrations of 200 ppm over the last 400,000 years [44]. During this time, oxygen levels steadily increased through the action of photosynthetic organisms that oxidise water to produce molecular oxygen [43]. Consequently many CO_2-assimiliating enzymes evolved to be strictly anaerobic, and are limited to specific environments, while others tolerate O_2 [45]. As a result, the environmental $[CO_2]/[O_2]$ ratio is an important effector of enzymatic properties.

RuBisCO and the Calvin cycle

For many years, the Calvin cycle for C_3 carbon fixation was thought to be the only important biological process for CO_2 assimilation, as a result of its prevalence in our immediate environment. It is found in photosynthetic organisms, predominantly in plants on land and algae in water, and photosynthetic prokaryotes (cyanobacteria). This carbon fixation pathway forms part of photosynthesis and the required reducing equivalents are generated through electron gradients initiated by photons and generated through the splitting of water [46]. However, a number of autotrophic bacteria fix carbon through the Calvin cycle with electrons generated through oxidation of inorganic chemicals (chemoautotrophs) [47]. As detailed in Scheme 1, the carbon fixation step entails the carboxylation of ribulose-1,5-bisphosphate (**1**), generating two equivalents of 3-phosphoglycerate (**2**) and is catalysed by ribulose-1,5-bisphosphate carboxylase oxygenase (RuBisCO). The glycerate **2** is subsequently phosphorylated with ATP for the production of 1,3-bisphosphoglycerate (**3**), which is in turn reduced with NADPH to 3-phosphoglyceraldehyde (**4**). For every six equivalents of the aldehyde **4**, one is diverted to carbohydrate biosynthesis, while the other five are used to produce the RuBisCO substrate **1**.

A property of RuBisCO with great implications is that it may also accept O_2 instead of CO_2 as an electrophile in the addition step, thus catalysing a counter-productive reaction, which reduces the photosynthetic output of plants using the Calvin cycle by 25% [48]. In the O_2-rich environments in which it operates, this property makes RuBisCO a particularly inefficient biocatalyst and a major bottleneck to C_3 carbon fixation. Through evolution, RuBisCO has adapted to rising oxygen concentrations by developing higher specifities for CO_2 at the expense of catalytic turnover, making it a particularly slow enzyme [49]. As a result, evolutionary bias from limited nutrient availability has driven some plants to develop more elaborate carbon assimilation mechanisms (C_4 and CAM plants) [48]. These involve an initial temporary carbon fixation step with phosphoenolpyruvate carboxylase (PEPC), followed by

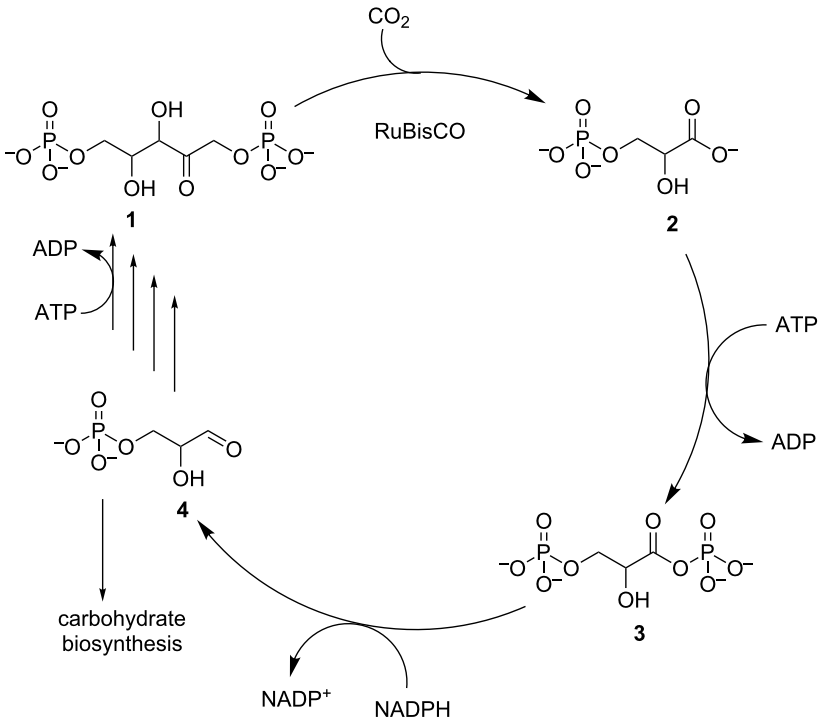

Scheme 1: The Calvin cycle for fixation of CO_2 with RuBisCO.

transport and release as CO_2 in the vicinity of RuBisCO within cellular compartments with low O_2 concentrations [48]. RuBisCO variants from these plants display higher turnover rates, and lower specificities for CO_2 over O_2. This apparent trade-off between CO_2 specificity and catalytic activity greatly influences efforts towards RuBisCO biotechnological applications.

The Calvin cycle is not the only carbon fixation pathway, and at least five alternative pathways have been elucidated in recent years [24]. It is now thought that some of these alternative pathways contribute significantly to the global carbon cycle, particularly with regard to the oceanic section [50,51]. This is due to the extensive global distribution of many oceanic chemolithoautotrophic organisms, and the estimated carbon fixation in deep-sea hydrothermal vents, the meso- and bathy-pelagic ocean, and in oxygen-deficiency zones [50].

Reductive tricarboxylic acid cycle

The tricarboxylic acid (TCA) cycle is used by all aerobic organisms to generate NADH through the oxidation of small organic metabolites. For pyruvate (**11**), isocitrate (**7**) and 2-oxoglutarate (**6**), oxidation occurs together with a decarboxylation. In some autotrophs this pathway is known to operate in the reverse (reductive) direction resulting in CO_2 fixation through carboxylation [52]. Autotrophic fixation through the reductive TCA cycle was first described by Arnon and Buchanan [53], and hence is also referred to as the Arnon–Buchanan cycle. It is considered the most efficient CO_2 fixation pathway as it requires the lowest amount of reducing equivalents per carbon fixed [23,26]. This is mainly due to the fact that CO_2 fixation occurs through three efficient reductive carboxylations, of which two are coupled to oxidation of the low-potential electron donor ferredoxin [26], with a requirement for strict anaerobicity, thus limiting the distribution of the reductive TCA cycle.

As detailed in Scheme 2, the reductive TCA cycle contains three CO_2 fixation steps [24]. Succinyl-CoA (**5**) is carboxylated by ferredoxin-dependent 2-oxoglutarate synthase to produce 2-oxoglutarate (**6**), which is subsequently transformed to isocitrate (**7**) through a second CO_2 fixation catalysed by isocitrate dehydrogenase. Isocitrate (**7**) is concominantly isomerised to

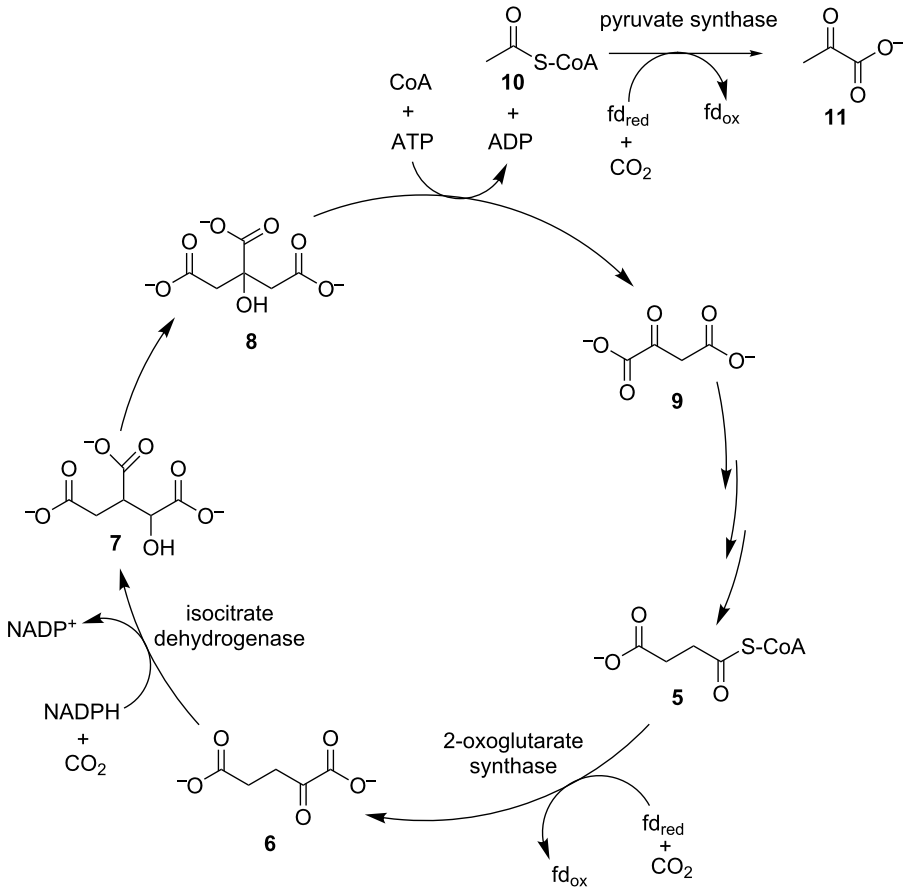

Scheme 2: The reductive TCA cycle with CO_2 fixation enzymes designated.

citrate (**8**) and lysed to oxaloacetate (**9**) which remains in the cycle and regenerates succinyl-CoA through three catalytic steps, and acetyl-CoA (**10**) which enters central metabolism through a third CO_2-fixation step, carried out by ferredoxin-dependent pyruvate synthase to produce pyruvate (**11**). The carboxylating enzymes are mechanistically complex and highly adapted to the cellular conditions in which they operate, and as a result there has been little development of their use in synthetic processes.

Wood–Ljungdahl pathway

The Wood–Ljungdahl pathway, or reductive acetyl-CoA pathway, is used by acetogenic bacteria to reduce CO_2 to either formate with formate dehydrogenase (FDH) or CO with CO dehydrogenase (CODH) [54,55]. As presented in Scheme 3, these initial steps of two separate branches of the pathway meet to produce a unit of acetyl-CoA (**10**) which is then incorporated into central metabolic processes [56-59]. FDHs are widely distributed enzymes, discussed in more detail below. The formate (**12**) produced through FDH activity is incorporated onto a tetrahydrofolate (**14**) and reduced to an activated methyl group (**13**), which is then utilised as a substrate by acetyl-CoA synthase together with the CO produced by CODH. The acetyl-CoA synthase forms a complex with CODH, to channel CO through a molecular tunnel [60]. This enzyme has been the focus of much interest due to its unusual reactivity, however, it remains poorly understood [61].

Formate dehydrogenases are an extremely heterogeneous enzyme family, most commonly found to physiologically catalyse formate oxidation and release of CO_2. Autotrophic acetogen FDHs are usually bound to metallo-pterin cofactors, with either a Mo or W centre [55,62,63], coordinated to a SeCys or Cys ligand. These features are not limited to acetogenic FDHs, and Mo and W FDHs are broadly distributed throughout the bacterial kingdom [63-68]. In addition, various types of Fe–S clusters are observed in FDHs, through which electrons are transported to other protein domains or to other oxidoreductases altogether [63,64,68]. Due to the presence of oxidisable cofactors, metallo-FDHs are most commonly found in anaerobic organisms. Another large family of FDHs do not contain metal cofactors, and catalyse a direct hydride transfer from formate to a nicotinamide cofactor [69]. They are commonly found in aerobic species, are generally robust and amenable to recombinant expression, but have high catalytic preferences for formate oxidation to CO_2.

Acyl-CoA pathways

A number of recently elucidated cyclic pathways that exist primarily in archaea initiate through the fixation of CO_2 onto acetyl-CoA (**10**) [51,70], and end with the generation of two

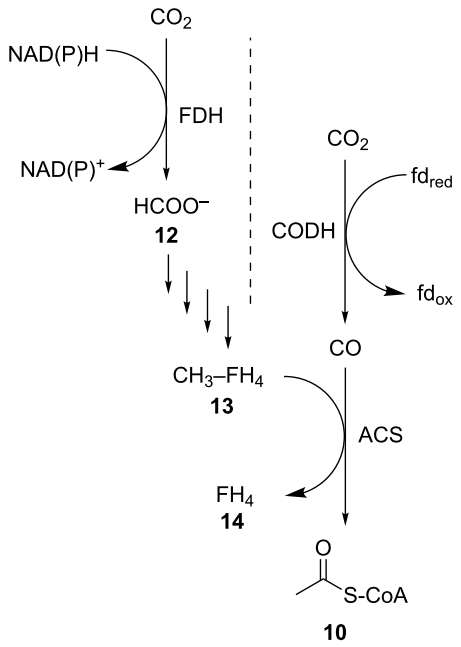

Scheme 3: The Wood–Ljungdahl pathway for generation of acetyl-CoA through reduction of CO_2 to formate and CO. FDH: formate dehydrogenase, CODH: CO dehydrogenase, ACS: acetyl-CoA synthase, FH_4: tetrahydrofolate.

equivalents of the starting substrate **10** (Scheme 4). One equivalent of the CoA thioester **10** is fed to central metabolism while the other is used in a subsequent cycle. As seen in Scheme 4, acetyl-CoA (**10**) is carboxylated by a bifunctional acetyl-CoA/propionyl-CoA carboxylase to malonyl-CoA (**15**) with HCO_3^- and hydrolysis of ATP. The malonate **15** is reduced to 3-hydroxypropionate (**16**), in two steps catalysed by NAD(P)H dependent dehydrogenases. Later in the pathway, propionyl-CoA (**17**) is the substrate for a second carboxylation with HCO_3^- to methylmalonyl-CoA (**18**), performed by the same ATP-dependent bifunctional carboxylase that carries out the first step [71,72]. Succinyl-CoA (**5**) is formed through isomerisation and recycled into two equivalents of acetyl-CoA (**10**). This route is encountered in two separate pathways, namely the 3-hydroxypropionate/4-hydroxybutyrate cycle and the 3-hydroxypropionate bicycle. An alternative CO_2 fixation route is found in the dicarboxylate/4-hydroxybutyrate cycle [73]. Here acetyl-CoA (**10**) is initially reductively carboxylated to pyruvate (**11**), as in the reductive TCA cycle. The pyruvate **11** is phosphorylated with ATP to generate phosphoenolpyruvate (**19**), followed by a second carboxylation with HCO_3^- to oxaloacetate by PEPC.

Non-autotrophic CO_2 fixation

A large number of enzymes use CO_2 (or HCO_3^-) as a substrate without taking part in autotrophic pathways [26]. These are

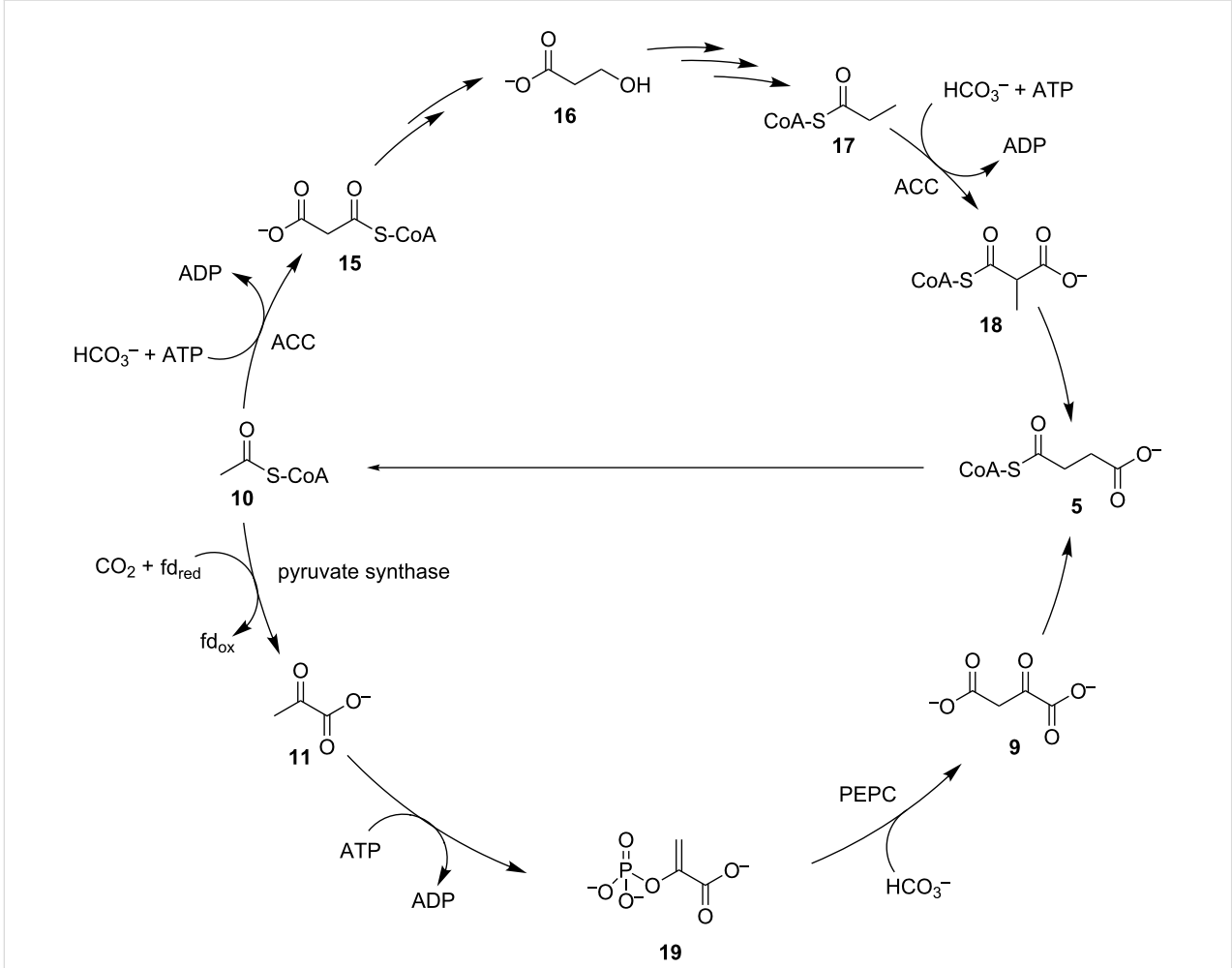

Scheme 4: The acyl-CoA carboxylase pathways for autotrophic CO_2 fixation. ACC: acetyl-CoA/propionyl-CoA carboxylase, PEPC: phosphoenolpyruvate carboxylase.

predominantly found in assimilatory pathways where small organic molecules are used as carbon sources, and anaplerosis through which intermediate metabolites in central pathways (e.g., the TCA cycle) are replenished.

These enzymes also represent interesting targets for use in CO_2 transforming processes, particularly when involved in the production of TCA cycle dicarboxylates that constitute target platform chemicals, as in the cases of pyruvate carboxylase and PEPC. Enzymes that catalyse CO_2 fixation in autotrophic pathways are also found in non-autotrophic pathways operating either in the same direction (PEPC), or in the reverse direction for CO_2 production (FDH). However, these enzymes are still suitable targets and have been used in vitro for CO_2 fixation. Finally degradative pathways contain enzymes capable of working in both carboxylating or decarboxylating direction depending on reaction conditions [12]. These, have also attracted some attention as a source for relevant biocatalysts.

Biotechnological CO_2 transformation

CO_2-transforming enzymes sourced from natural metabolic pathways have been utilised in biotechnological applications for the conversion of CO_2, through either direct reduction of CO_2 or carboxylation of another substrate.

CO_2 transformation with RuBisCO

As the most well studied and best characterised autotrophic CO_2-fixation enyzme, RuBisCO has received much attention for application in biotechnology for CO_2-fixation, particularly using engineered photosynthetic hosts, such as plants and algae. The inefficiency of RuBisCO and promiscuity towards oxygen have directed efforts in protein engineering towards the generation of optimised mutants that overcome these limitations [74,75]. Though these studies have resulted in the recombinant expression of RuBisCO in useful hosts such as *E. coli* [75], development of improved selection systems for directed evolution [74], and further elucidation of RuBisCO properties [76],

little progress has been made toward expression of an enzyme which is more efficient and less promiscuous. A possible explanation for this was provided by Tlusty, Milo and coworkers [77]. By processing kinetic data from various RuBisCO enzymes, it was found that variations in enzyme specificity and velocity are mutually constrained. Within this limited space, it appears that the various wild-type enzymes have been optimised through evolution to operate within their respective environments. Point-mutations in the protein itself are therefore unable to lead to great improvements in enzyme efficiency. A more promising strategy may be to employ outlying natural variants of RuBisCO that display the best properties, such as those from red algae, in combination with other components of the Calvin cycle carbon assimilation mechanism [39]. Long et al. [78] estimated that incorporation of wild-type enzymes, with higher CO_2 specificity or higher catalytic activity, into C_3 plants could potentially raise crop yields by more than 25%. Furthermore, incorporation of cyanobacterial carbon concentration mechanisms such as carboxysomes, combined with RuBisCO variants adapted to higher CO_2 concentrations, could result in a 36% to 60% crop yield increase [79].

The main difficulties of heterologous expression of RuBisCO for CO_2 fixation relate to the poorly understood post-translational steps for production of the fully active enzyme that require the action of specific chaperones as well as a separate enzymatic species, RuBisCO activase. In some cases these have to also be incorporated into the host organism in order to obtain an active enzyme.

Recently there have been two important breakthroughs on carbon assimilation in plants through RuBisCO, relating to alternative components of the RuBisCO catalytic system. Whitney et al. [80] increased the expression levels of a heterologous RuBisCO in tobacco plants, through co-expression of a RuBisCO chaperone that facilitates the assembly of the active multimeric enzyme. This resulted in two-fold increases in CO_2 assimilation rate and plant growth. Hanson, Parry and co-workers [39] were able to prepare tobacco plants that expressed cyanobacterial RuBisCO together with a protein that forms part of the carboxysomal structure, which led to the generation of macromolecular complexes that are observed early in the carboxysomal biogenesis in cyanobacteria. In addition, the engineered plants were photosynthetically active, and the RuBisCO complex showed higher specific activities than the enzyme in the control tobacco line.

Algae that utilise efficient variants of RuBisCO for fixation of CO_2 have been targeted as a biomass source for a third generation of biofuels, due to their lack of requirement for arable land [81]. In addition, microalgae have been employed for the production of chemicals as a metabolic end-product of the fixed carbon, with particular emphasis on oils for use as biodiesel feedstock [82]. Cyanobacteria, mainly *Synechocystis* spp., have proven easier to engineer than their algal and plant counterparts and have also been applied to generate higher titres of oils and alcohols [18].

Despite difficulties related to heterologous expression, recently there have also been reports of succesful use of RuBisCO in non-photosynthetic host organisms (Figure 3). In *E. coli* it was possible to incorporate a CO_2-fixing bypass in central metabolism through expression of phosphoribulosekinase to produce ribulose-1,5-bisphosphate (**1**) (Scheme 1), and a cyanobacterial

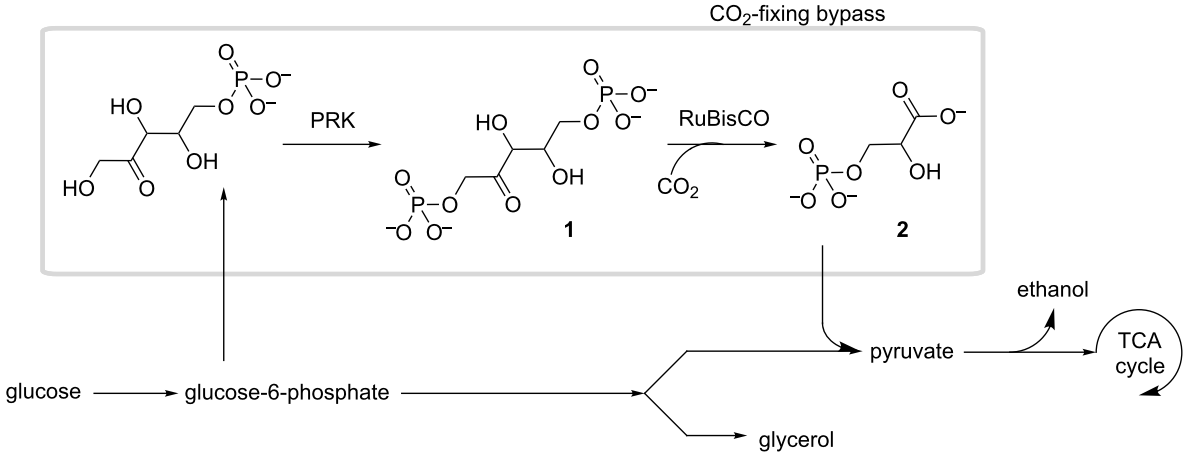

Figure 3: RuBisCO CO_2-fixing bypass installed in *E. coli* and *S. cerevisiae* to increase carbon flux toward products of interest. PRK: phosphoribulosekinase.

RuBisCO along with a RuBisCO-folding chaperone from the same source [21]. It was found that the main limiting factor to carbon fixation was the availability of CO_2 in *E. coli*, and the yield could be increased through incorporation of a cyanobacterial carbonic anhydrase. In the yeast *Saccharomyces cerevisiae*, spinach phosphoribulosekinase was able to provide the bisphosphate **1** to a prokaryotic RuBisCO from *Hydrogenovibrio marinus*, which folded with the aid of *E. coli* protein chaperones (GroEL/GroES) [83]. This resulted in catalysis of CO_2 fixation and increase of carbon flux towards the ethanol product and away from glycerol, a major fermentation byproduct (Figure 3).

Synthesis of dicarboxylates through pyruvate carboxylation

Enzymatic carboxylation of a pyruvate backbone offers an avenue to dicarboxylates, which are important biotechnological targets, through the use of CO_2 as feedstock. As seen, this may be carried out by pyruvate carboxylase or PEPC which acts on phosphoenolpyruvate (**19**). Purified PEPC has been used in an integrated system with carbonic anhydrase for in vitro carbon capture and transformation to oxaloacetate (**9**) (Scheme 5) [84]. This system has been further optimised with engineered variants of PEPC leading to increased rates and yields of CO_2 transformation [85].

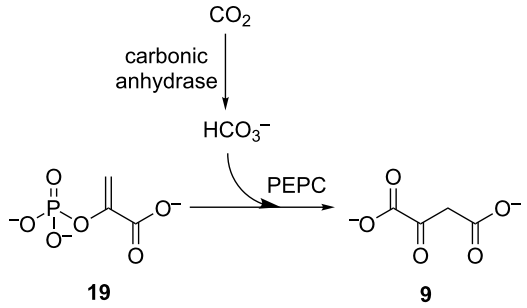

Scheme 5: Integrated biocatalytic system for carboxylation of phosphoenolpyruvate (**19**), using PEPC and carbonic anhydrase.

In *E. coli* fermentative processes, as presented in Scheme 6, PEPC is used to produce oxaloacetate (**9**) directly from phosphoenolpyruvate (**19**) from glycolysis, through carboxylation with HCO_3^-. This may then be further transformed, by reversal of the activity of native oxidative TCA cycle enzymes, to produce malate (**20**), fumarate (**21**) and succinate (**22**), all of which have been listed in the top twelve target platform chemicals from biomass, by the US Department of Energy [86]. In this way, overexpression of *Sorghum vulgare* PEPC in *E. coli* resulted in higher fermentative yields of succinate (**22**) [87]. Recombinant co-expression of cyanobacterial carbonic anhydrase in *E. coli* BL21(DE3) increased available HCO_3^- resulting in a higher than five-fold increase in the observed activity of endogenous PEPC [88]. Similarly, strains with overexpressed PEPC have been engineered for the production of high yields of fumaric acid (**21**) [89].

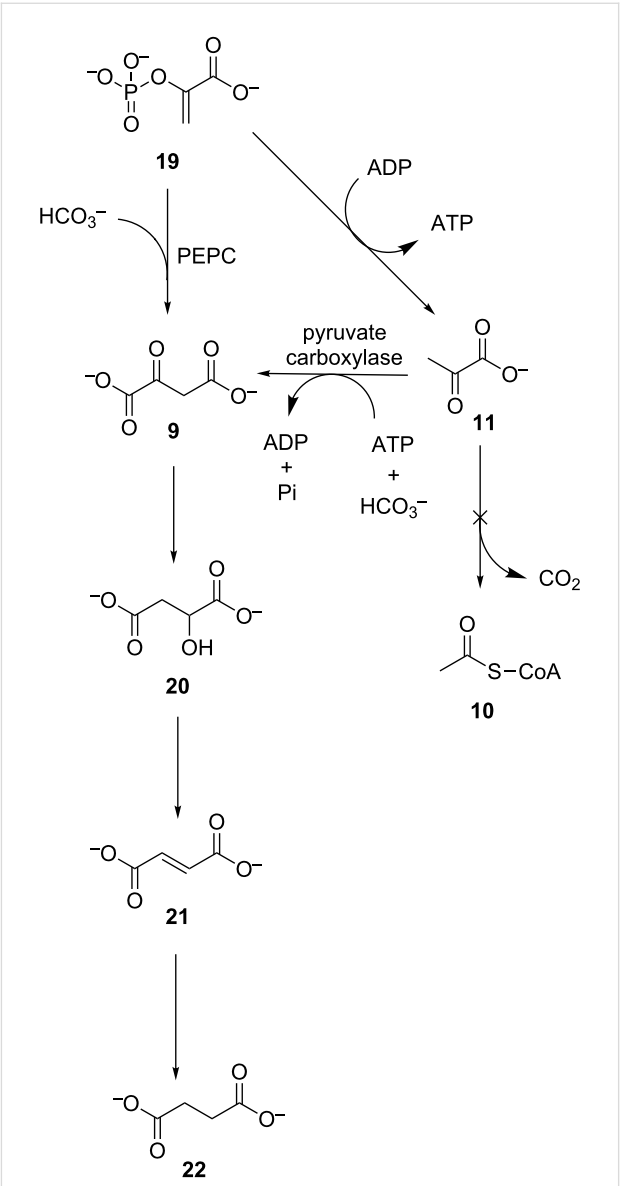

Scheme 6: PEPC and pyruvate carboxylase catalysed carboxylation of pyruvate backbone for the generation of oxaloacetate (**9**) and other dicarboxylates.

As some phosphoenolpyruvate (**19**) is lost to pyruvate (**11**), pyruvate carboxylase, not present naturally in *E. coli*, was used to increase the carbon flux to the desired products, by providing a secondary oxaloacetate (**9**) production route through CO_2-fixation. In this way, *E. coli* strains overexpressing pyruvate carboxylase have been applied to CO_2 fixation with the produc-

tion of equimolar succinate (**22**) [90]. In addition the succinate yields were found to strongly depend on CO_2 availability and increased by up to four-fold under increased CO_2 partial pressures. Such engineered *E. coli* strains were also able to utilise CO_2 generated during ethanol fermentation with *Saccharomyces cerevisiae* as the substrate for succinate production, through an integrated bioprocess [91]. Through gene deletion, other undesirable pyruvate consumption reactions such as lysis to acetyl-CoA (**10**) with liberation of CO_2 could be blocked, allowing improved yields of dicarboxylates [92]. The carbon from CO_2 was also directed to other products through the use of other types of host organisms. Overexpression of *E. coli* PEPC in *Propionibacteria* resulted in increased rates of propionic acid production as well as increased rates of carbon fixation under higher CO_2 partial pressures [93,94].

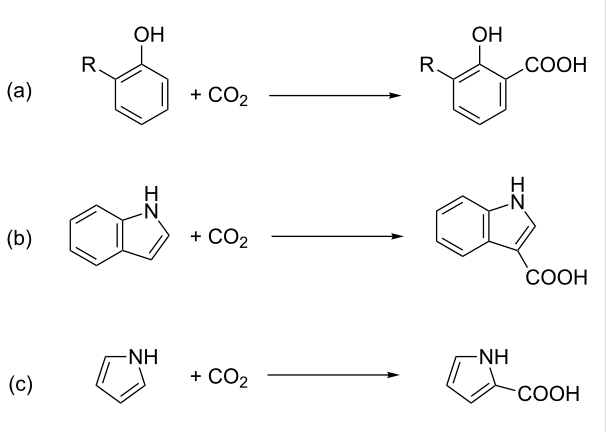

Scheme 7: Decarboxylase catalysed carboxylation of (a) phenol derivatives, (b) indole and (c) pyrrole.

Acyl-CoA carboxylases

Though acetyl-CoA carboxylases are widely distributed in living organisms, the existence of bifunctional variants with a role in autotrophy has attracted further interest for their biotechnological applications in CO_2 transformation technologies. The autotrophic enzymes from *Metallosphaera sedula* and *Acidianus berleyi* have been purified and found to be catalytically active in vitro for the production of malonyl-CoA through acetyl-CoA carboxylation [71,95]. As seen in Scheme 4, two subsequent steps in the 3-hydroxypropionate/4-hydroxybutyrate cycle lead to further reduction of the fixed carbon for the generation of 3-hydroxypropionate (**16**), a platform chemical also in the US Department of Energy top twelve [86,96]. Archaeal thermoacidophilic *Metallosphaera sedula* genes were utilised in the hyperthermophilic archaeon *Pyrococcus furiosus* to express the first three steps of the autotrophic 3-hydroxypropionic/4-hydroxybutyrate cycle for the synthesis of 3-hydroxypropionate (**16**) [97,98]. This was carried out at 70 °C, where the *Metallosphaera* enzymes show optimal activity and background metabolism of *Pyrococcus furiosus* does not interfere.

Decarboxylases

A number of enzymes are capable of catalysing the reversible interconversion of lipophilic aromatics and the more polar respective carboxylates [12]. It is thought these reactions may proceed in the carboxylation direction as a detoxification mechanism under anaerobic conditions, where oxidative degradation is not possible. In work pioneered by Nagasawa and coworkers [99-102], Kirimura and coworkers [103,104], and Faber and coworkers [105-109], these enzymes have been successfully applied in vitro under conditions that drive the equilibrium toward carboxylation, such as high CO_2 concentration. Successful examples include the carboxylation of phenol and hydroxystyrene derivatives including catechol [102], guaiacol [110], indole [101] and pyrrole [100] (Scheme 7).

Isocitrate dehydrogenase

As discussed above, as part of the reductive TCA cycle (Scheme 2) isocitrate dehydrogenase catalyses the carboxylation of 2-oxoglutarate (**6**) to produce isocitrate (**7**). Exploitation in biotechnological applications has been challenging due to the unfavourable thermodynamics of the carboxylation. Recently, the use of purified isocitrate dehydrogenase for CO_2 fixation was reported [111]. Carbon fixation was driven thermodynamically by maintaining a low pH, where CO_2 concentrations are highest, and coupling the reaction to aconitase catalysed removal of isocitrate (**7**) to produce aconitate. Switching the pH allowed for subsequent release of the captured CO_2 and regeneration of the carbon-capture substrate 2-oxoglutarate (**6**). Though this application is aimed at CO_2 sequestration rather than transformation, it shows that the reductive TCA cycle isocitrate dehydrogenase may be used in vitro to fix CO_2 to a species that may be further transformed enzymatically.

FDH catalysed formate production

Due to the direct CO_2 reduction to a C_1 species, as opposed to carboxylation of a secondary substrate catalysed by most other enzymes, FDHs have attracted more widespread attention as catalysts for the transformation of CO_2 with numerous examples in recent literature. Applications span all aspects of enzyme technology including isolated biocatalysts, immobilised biocatalysts, whole-cell catalysts and bioelectrocatalytic systems. Theoretical studies modelling potential formatotrophic organisms showed significant promise for such systems [112].

Isolated FDH. Enzymes from acetogenic sources have been characterised and found to be capable of catalysing CO_2 reduction in vitro under thermodynamically favourable conditions. Acetogenic FDH from *Clostridium thermoaceticum* (now *Moorella thermoacetica*) was reported by Wood and Ljundahl in 1966 [113], where an exchange between $^{14}CO_2$ and formate

was observed, though no net synthesis of formate. Thauer [114] was the first to observe a net CO_2 reduction to formate for the acetogenic FDH by recycling of the reduced cofactor, and prove that this enzyme utilised NADPH for the reduction of CO_2 as the first step in one branch of the Wood–Ljungdahl pathway. Similarly, FDH in cell-free lysate of *Clostridium acidiurici* catalysed CO_2 reduction to formate with reduced ferredoxin and NADH [115]. Earlier, it had been shown that it was possible for an enzyme found in the related non-acetogenic *Clostridium pasteurianum* to carry out direct reduction of CO_2 to formate with reduced ferredoxin alone, rather than through a two-step process involving acetyl-CoA as a CO_2 acceptor, disproving the established view at that time that biological CO_2 reduction may only proceed indirectly [116]. Furthermore, Thauer et al. [117] were able to prove that this FDH utilises CO_2, rather than HCO_3^-, as the active species, through experiments carried out at low temperatures where CO_2 hydration is slow. The enzyme from *Clostridium carboxidivorans* was recombinantly expressed in *E. coli* and shown to display higher CO_2 reducing activity and poorer affinity for formate, as compared to a non-acetogenic *Candida boidinii* FDH prepared in parallel, known to efficiently oxidise formate [62]. This suggests that weak formate binding contributes toward the catalytic preference of the acetogenic enzyme. *Clostridium autoethanogenum* was purified as a complex with an electron bifurcating hydrogenase that is NADPH and ferredoxin dependent, and found to catalyse reduction of CO_2 with NADPH and reduced ferredoxin or H_2 [63]. An FDH was also purified as a complex with hydrogenase from the acetogen *Acetobacterium woodii* and found to directly utilise H_2 as an electron donor for the reduction of CO_2 [118].

Furthermore, there is a growing list of examples of non-acetogenic metallo-FDHs, naturally catalysing formate oxidation, found to also be capable of catalysing CO_2 reduction in vitro. FDH from *Pseudomonas oxalaticus* was the first isolated enzyme reported to catalyse both formate oxidation and CO_2 reduction under appropriate conditions, using substrate amounts of NAD^+/NADH [119]. This enzyme was later used in the seminal work of Parkinson and Weaver [120], where electrons were supplied through a semiconductor photoelectrode using light in the visible spectrum (>1.35 eV) and coupled to FDH activity through a mediator to drive CO_2 reduction. Two W-dependent FDHs, isolated from the syntrophic bacterium *Syntrophobacter fumaroxidans*, showed high catalytic activity for CO_2 reduction, using reduced methyl viologen as the electron donor. Later, one of these was immobilised onto an electrode and shown to reduce CO_2 electrochemically through direct use of the electrons provided [121]. In this way the reaction could be electrochemically driven in either direction. Recently the Mo-dependent FDH from *E. coli* was shown to be capable of catalysing CO_2 reduction employing a similar approach [122]. An oxygen-tolerant Mo-dependent FDH from *Rhodobacter capsulatus* was reported to catalyse the reduction of CO_2 with NADH [123].

FDHs without metal cofactors have also been employed to reduce CO_2 in vitro. Despite interest in application of *Candida boidinii* FDH due to its stability, the observed turnover for this enzyme is generally low. However, application of a bioelectrochemical system allowed production of formate from CO_2 with proton transfer from an electrical source through NAD^+ to this FDH [124]. Choe et al. [125,126] showed that a series of robust acidophilic nonmetallo-FDHs were particularly useful in the catalysis of CO_2 reduction. As these enzymes are stable at the lower pH ranges where the concentration of solvated CO_2 is highest, improved formate yields were obtained.

All this suggests that the ability of FDHs to reversibly catalyse formate and CO_2 interconversion is broadly distributed in nature, irrespective of metabolic directionality, however, catalytic properties vary greatly depending on the source organism. As expected, the enzymes that naturally catalyse CO_2 reduction and highly homologous FDHs from formate oxidation pathways display higher reduction activities than FDHs of lower homology. The possibility of recycling the reduced electron donating cofactor, through the action of a second enzyme such as hydrogenase, or through direct or mediated electron delivery from an electrode, greatly enhance the potential of FDHs for application in large-scale biotechnological processes (Figure 4).

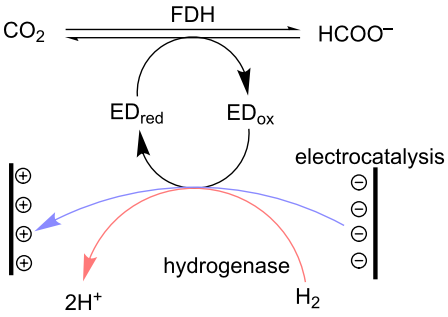

Figure 4: Formate dehydrogenase (FDH) catalysed reversible reduction of CO_2 to formate with electron donor regeneration through hydrogenase-catalysed H_2 oxidation (red arrow) or electrochemical reduction at a cathode (blue arrow).

Whole-cell FDH application. In addition to the examples already mentioned for in vitro enzymatic production of formate, this has also been achieved using resting or immobilised cells as catalysts. Due to the ease of combination of multiple enzymatic activities in whole-cell applications, there has been a particular focus on coupling FDH activity to a hydrogenase, with which it

is commonly found as the formate hydrogen lyase complex in nature. To this effect, immobilised *Alcaligenes eutrophus* (reclassified as *Ralstonia eutropha*) whole-cell catalysts were able to catalyse hydrogenation of CO_2 to similar levels as Pd adsorbed on activated carbon [127]. In the previously mentioned work [118] on the purified acetogenic FDH-hydrogenase complex from *Acetobacterium woodii*, a whole-cell biocatalyst was also reported, generating high yields of formate from CO_2 and H_2. Resting cells from the common biotechnological host *E. coli* have been known to generate modest yields of formate from CO_2 hydrogenation, when grown on formate for induction of the native enzymes [128]. More recently, by overexpressing suitable recombinant FDHs in *E. coli* JM109(DE3), high formate yields were obtained from CO_2 hydrogenation, without need for cellular growth on formate for induction [129]. An alternative whole-cell system was later reported, using an electrochemical cell, where the reducing equivalents are generated by an electrode, rather than H_2 oxidation, as has been done for purified enzymes [130].

Methanol production through formate. Due to the advantages of direct formatogenesis from CO_2, there has been a number of investigations into further biocatalytic conversion of formate into other desirable chemicals. A possibility that has gathered much attention is the consecutive reduction to formaldehyde and methanol, first described by Kuwabata and co-workers [131,132]. This is of particular interest due to the potential use of methanol as a fuel. Methanol production has been achieved in vitro utilising FDH in series with formaldehyde dehydrogenase (FaldDH) and alcohol dehydrogenase (ADH) [133-136]. One of the main hurdles to the utilisation of this process relates to the requirement for the additional two enzymes to work in the reverse to physiological direction, as well as the generally unfavourable thermodynamic equilibria. An attractive approach utilised photocatalysts to generate electrons from solar energy, which in turn were donated for the production of methanol [137]. Though methanol yields and catalyst efficiencies are low, these results are highly promising for the future development of biochemical systems for the solar-driven generation of formate, formaldehyde and methanol from CO_2 (Figure 5).

FDHs for hydrogen storage. The significance of biocatalytic systems for the production of formate with reducing equivalents from H_2 extends beyond the generation of a platform chemical. Formate has also been targeted as a form of chemical storage of hydrogen fuel, due to energetic demands and hazards associated with H_2 liquefaction, transport and storage [138,139]. Effective use of CO_2 to store H_2 would enable a sustainable hydrogen based economy, through carbon neutral technologies. Formate in particular, due to its chemical properties and the atom efficiency in complete stoichiometric retention of hydrogen, has been touted as a very promising reduced form of CO_2 [138,140,141]. Consequently, many catalytic systems working in the reverse direction have also been investigated, for the regeneration of H_2, along with CO_2.

Many organisms, including *E. coli*, naturally produce H_2 as an electron sink for oxidative pathways [142]. As a result, whole-cell systems have been described that work efficiently toward formate oxidation and direct electron delivery to a hydrogenase [143,144]. However, biocatalytic systems are unlikely to become suitable for decentralised H_2 release, as for example will be required in hydrogen fuelled transportation vehicles. Transition metal catalysts have been reported to reach desired turnovers [138], however, in these cases cost and metal availability become hurdles in sustaining a hydrogen economy. Zeolite systems utilising Ge or Si, recently described, were able to efficiently dehydrogenate formic acid. This was guided through computational calculations, allowing the design of a zeolite catalyst displaying over 94% selectivity over the counter-productive formate dehydration reaction [145]. The

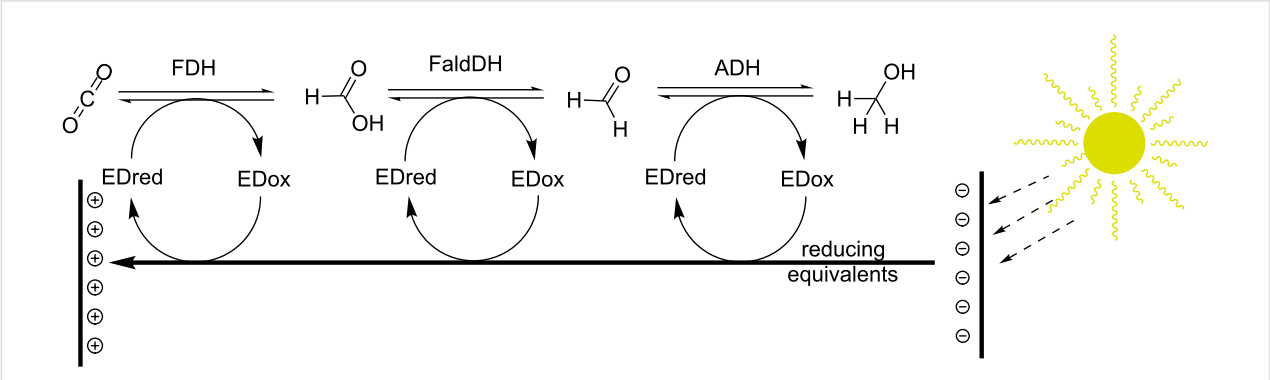

Figure 5: Sequential generation of formate, formaldehyde and methanol from CO_2 using reducing equivalents sourced through electrochemical cells or photocatalysts. ED: electron donor, FDH: formate dehydrogenase, FladDH: formaldehyde dehydrogenase, ADH: alcohol dehydrogenase.

combination of biological systems for centralised hydrogen storage through CO_2 reduction as formate, with cheap zeolite catalysts for decentralised on demand hydrogen regeneration appears a very promising sustainable approach toward a hydrogen economy (Figure 6).

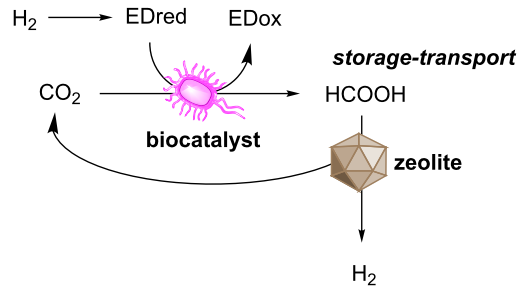

Figure 6: Hydrogen storage as formic acid through biocatalytic hydrogenation of CO_2 and subsequent on-demand release through zeolite catalysed dehydrogenation.

In vitro production of CO with CODH

Reduction of CO_2 to CO through in vitro application of CODH has been of interest as the enzymatic product may be further converted into hydrocarbons through the Fischer–Tropsch process [146]. In work carried out by Armstrong, Ragsdale and coworkers [147,148], metal oxide nanoparticles were functionalised with CODH and photosensitised with a Ru dye to catalyse the reduction of CO_2 using visible light. Further to this, the reported ability of a V-dependent nitrogenase to slowly reduce CO to various small-chain hydrocarbons holds much promise for the development of enzymatic processes to further transform CO into products of interest [149].

Prospects and challenges for future biotechnological applications

In order for CO_2 biotransformation to target a broad range of commodity chemicals, the CO_2-fixing enzymes must be used as part of multi-enzymatic cascades that convert CO_2 through multiple steps [111,150]. Such reactions may be performed in vitro, where the relative amounts of each biocatalyst and the intermediate concentrations during the reaction can be closely monitored and controlled. However, this is accompanied by a requirement in cost related to enzyme purification, proportional to the number of enzymes used. The application of enzymes within whole-cells allows their production and utilisation with minimal processing and circumvents biocatalyst purification, though in this case there are limitations related to substrate/product diffusion and background metabolic activity. The optimal approach in each case, as for any multi-enzymatic synthesis, will depend on a combination of factors such as the number of enzymes to be utilised, the ease of substrate and product diffusion through the cell membrane, and the presence of unwanted background reactions.

Within a well-understood cellular chassis, the heterologous expression of a CO_2 fixing enzyme allows its use as a module that may be matched with other modules of choice, for the assembly of synthetic pathways [150,151]. In a CO_2 transforming modular process, the CO_2 fixing modules will play a central role, much like CO_2 fixing enzymes do in a carbon assimilation pathway. However, the assembly will also include other genes that allow process control or express desirable features such as acid tolerance [152,153]. For these modules to be easily applied, the enzymes must be easy to express in heterologous hosts. This is greatly complicated by requirements for specialised cofactors or maturation and folding processes.

RuBisCO presents significant challenges for use in modular synthetic biology approaches, due to the observed inefficiency and requirement for expression of large amounts of protein. The difficulty of expression in hosts that do not naturally contain RuBisCO, such as *E. coli*, and the complicated nature of the heterologous RuBisCO systems currently developed in transgenic plants [80], means that the Calvin cycle is a challenging target for synthetic biology in non-photosynthetic microorganisms. Efforts focusing on increasing carbon fixation yields through optimisation of RuBisCO expression and activity may lead to optimised plant based synthetic systems [18,40].

In microbial systems carboxylases are promising candidates for modular design, due to their broad distribution in living organisms and lack of particular requirements in cofactors. Also the great variety of carboxylases found in nature represents a very large library from which suitable modules may be sourced that introduce carbon into metabolic pathways [26,154]. On the other hand, in order to generate a synthetic pathway where the only carbon input is CO_2, these enzymes would also require the co-expression of cyclic pathways to recycle the co-substrates that are carboxylated. This may greatly hinder the overall process, as the metabolic pathways that have been developed by nature to carry out these tasks contain many steps and a number of unfavourable reactions. Indeed, attempts to transfer entire autotrophic CO_2 fixation pathways into *E. coli* have been unsuccesful [155].

Dehydrogenases used in the reductive acetyl-CoA pathway, do not present this complication as the CO_2 is reduced directly to another species, either formate or CO, with no other reactant other than a source of electrons. This means that a single enzymatic module is able to catalyse the incorporation of CO_2 as a C_1 species, with no other carbon requirement. In this case, the

difficulties associated with expression of enzymes from niche organisms in heterologous hosts, such as requirement for particular metal cofactors and oxygen stability, complicate use in modular approaches. Also, the metabolic product must be efficiently transformed into other species in order to drive this energetically uphill carbon fixation process. Finally, as formate and CO are not metabolites in central anabolic pathways, it may be challenging to find suitable pathways that allow access to the variety of chemicals that may be produced through metabolism. This will inevitably require heterologous expression of the full reductive pathway, for production of acetyl-CoA, which however is extremely challenging due to the requirement for use of poorly understood enzymes and unusual cofactors. A recent breakthrough came with the production of a computationally designed enzyme, catalysing the carboligation of three formaldehyde units into dihydroxyacetone, thus providing direct access to central carbon metabolism through formate [156].

Sourcing of reducing equivalents. As mentioned above, any process that transforms CO_2 into other chemicals, where the carbon is in a more reduced state, represents a net reduction. Therefore there is a requirement for reductive potential in the form of electrons, and the method used to source these will greatly define the utility of the overall process (Figure 7). The ATP required to drive CO_2 fixation processes within living systems will be mainly produced using reducing equivalents through the complicated mechanism of oxidative phosphorylation.

Ultimately the most sustainable source of reducing equivalents is sunlight [20]. Solar energy may be directly utilised through the application of photosynthetic machinery employed by photoautotrophs to carry out the “light reactions” of photosynthesis. This will require technological advances, such as the development of bioreactors capable of maximising exposure to sunlight [157]. Another limitation to any approach relying on photosynthesis to harvest solar energy is the inherently poor efficiency and sensitivity of photosynthetic pigments and reaction centres, as highlighted by Michel [158]. An alternative approach is to convert solar energy into electricity for use as a source of electrons [20,159]. As seen, a number of enzymes and organisms are indeed capable of directly accepting electrons from electrodes in bioelectrochemical systems [160-162]. The use of electricity generated through photovoltaics allows the mediated application of solar energy for the fixation of CO_2. Finally, electrons can be stored within chemical species that may then be oxidised by organisms to regenerate the electrons on-demand [20]. Hydrogen and formic acid appear most suited for such applications, due to their chemical properties, and the existence of efficient biological tools for electron regeneration through oxidation.

Conclusion

It is evident that the use of biological catalysts for CO_2 fixation and conversion to a variety of chemicals is a promising approach, not limited by the availability of natural enzymes. However, in order for these to be employed in suitable bioprocesses, where they may be assembled into multi-enzymatic synthetic cascades, suitable methodologies for facile recombinant expression need to be developed further. This will extend beyond simple expression of a single gene, and may require simultaneous expression of multiple subunits, expression of seleno-proteins, proteins that deliver particular cofactors, as well as chaperones and maturation proteins that allow the production of the final active biocatalyst. Furthermore, the various biological mechanisms used in nature to improve the activity of these enzymes must be fully understood, in order to be suitably harnessed for application in synthetic processes. Host organisms must be developed with features geared towards the fixation of CO_2 and its transformation through multiple enzymatic steps. Finally the reducing equivalents required for

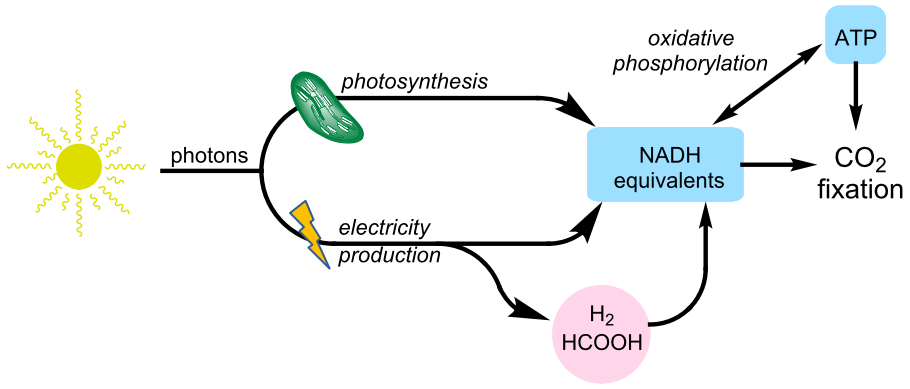

Figure 7: Schematic showing required flow of reducing equivalents for CO_2 fixation through biotechnological applications.

the carbon fixation step, as well as subsequent transformations, must be harnessed efficiently. Suitable technological platforms are yet to be developed.

Though there is much progress to be made before CO_2 fixing enzymes may be readily used as modules in designer synthetic pathways, the rapid progress that is being made in the fields of genetic engineering, bioinformatics and synthetic biology, as well as renewable electricity generation and bioelectrochemical engineering hold much promise for the development of the biotechnological platforms that will support a future carbon bio-economy.

References

1. Capellan-Pérez, I.; Mediavilla, M.; de Castro, C.; Carpintero, Ó.; Javier Miguel, L. *Energy* **2014,** *77,* 641. doi:10.1016/j.energy.2014.09.063
2. Höök, M.; Tang, X. *Energy Policy* **2013,** *52,* 797. doi:10.1016/j.enpol.2012.10.046
3. Christensen, C. H.; Rass-Hansen, J.; Marsden, C. C.; Taarning, E.; Egeblad, K. *ChemSusChem* **2008,** *1,* 283. doi:10.1002/cssc.200700168
4. Stocker, T. F.; Qin, D.; Plattner, G.-K.; Tignor, M.; Allen, S. K.; Boschung, J.; Nauels, A.; Xia, Y.; Bex, V.; Midgley, P. M. Climate change 2013: The Physical Science Basis. Working Group I Contribution to the IPCC 5th Assessment Report of the Intergovernmental Panel on Climate Change. 2013; http://www.ipcc.ch/report/ar5/wg1 (accessed Nov 11, 2015).
5. Wei, T.; Yang, S.; Moore, J. C.; Shi, P.; Cui, X.; Duan, Q.; Xu, B.; Dai, Y.; Yuan, W.; Wei, X.; Yang, Z.; Wen, T.; Teng, F.; Gao, Y.; Chou, J.; Yan, X.; Wei, Z.; Guo, Y.; Jiang, Y.; Gao, X.; Wang, K.; Zheng, X.; Reng, F.; Lv, S.; Yu, Y.; Liu, B.; Luo, Y.; Li, W.; Ji, D.; Feng, J.; Wu, Q.; Cheng, H.; He, J.; Fu, C.; Ye, D.; Xu, G.; Dong, W. *Proc. Natl. Acad. Sci. U. S. A.* **2012,** *109,* 12911. doi:10.1073/pnas.1203282109
6. Aresta, M.; Dibenedetto, A. *Dalton Trans.* **2007,** 2975. doi:10.1039/b700658f
7. Barzagli, F.; Mani, F.; Peruzzini, M. *Green Chem.* **2011,** *13,* 1267. doi:10.1039/c0gc00674b
8. Demirel, Y.; Matzen, M.; Winters, C.; Gao, X. *Int. J. Energy Res.* **2015,** *39,* 1011. doi:10.1002/er.3277
9. Langanke, J.; Wolf, A.; Hofmann, J.; Böhm, K.; Subhani, M. A.; Müller, T. E.; Leitner, W.; Gürtler, C. *Green Chem.* **2014,** *16,* 1865. doi:10.1039/C3GC41788C
10. Lively, R. P.; Sharma, P.; McCool, B. A.; Beaudry-Losique, J.; Luo, D.; Thomas, V. M.; Realff, M.; Chance, R. R. *Biofuels, Bioprod. Biorefin.* **2015,** *9,* 72. doi:10.1002/bbb.1505
11. Yang, Z.-Z.; He, L.-N.; Gao, J.; Liu, A.-H.; Yu, B. *Energy Environ. Sci.* **2012,** *5,* 6602. doi:10.1039/c2ee02774g
12. Glueck, S. M.; Gümüs, S.; Fabian, W. M. F.; Faber, K. *Chem. Soc. Rev.* **2010,** *39,* 313. doi:10.1039/B807875K
13. Bornscheuer, U. T.; Huisman, G. W.; Kazlauskas, R. J.; Lutz, S.; Moore, J. C.; Robins, K. *Nature* **2012,** *485,* 185. doi:10.1038/nature11117
14. Wohlgemuth, R. *Curr. Opin. Biotechnol.* **2010,** *21,* 713. doi:10.1016/j.copbio.2010.09.016
15. Savile, C. K.; Lalonde, J. J. *Curr. Opin. Biotechnol.* **2011,** *22,* 818. doi:10.1016/j.copbio.2011.06.006
16. Philbrook, A.; Alissandratos, A.; Easton, C. J. In *Environmental Biotechnology - New Approaches and Prospective Applications;* Petre, M., Ed.; InTech: Rijeka, 2013; p 39.
17. Ort, D. R.; Merchant, S. S.; Alric, J.; Barkan, A.; Blankenship, R. E.; Bock, R.; Croce, R.; Hanson, M. R.; Hibberd, J. M.; Long, S. P.; Moore, T. A.; Moroney, J.; Niyogi, K. K.; Parry, M. A. J.; Peralta-Yahya, P. P.; Prince, R. C.; Redding, K. E.; Spalding, M. H.; van Wijk, K. J.; Vermaas, W. F. J.; von Caemmerer, S.; Weber, A. P. M.; Yeates, T. O.; Yuan, J. S.; Zhu, X. G. *Proc. Natl. Acad. Sci. U. S. A.* **2015,** *112,* 8529. doi:10.1073/pnas.1424031112
18. Rosgaard, L.; de Porcellinis, A. J.; Jacobsen, J. H.; Frigaard, N.-U.; Sakuragi, Y. *J. Biotechnol.* **2012,** *162,* 134. doi:10.1016/j.jbiotec.2012.05.006
19. Hawkins, A. S.; McTernan, P. M.; Lian, H.; Kelly, R. M.; Adams, M. W. W. *Curr. Opin. Biotechnol.* **2013,** *24,* 376. doi:10.1016/j.copbio.2013.02.017
20. Li, H.; Liao, J. C. *Energy Environ. Sci.* **2013,** *6,* 2892. doi:10.1039/c3ee41847b
21. Gong, F.; Liu, G.; Zhai, X.; Zhou, J.; Cai, Z.; Li, Y. *Biotechnol. Biofuels* **2015,** *8,* 86. doi:10.1186/s13068-015-0268-1
22. Matthessen, R.; Fransaer, J.; Binnemans, K.; De Vos, D. E. *Beilstein J. Org. Chem.* **2014,** *10,* 2484. doi:10.3762/bjoc.10.260
23. Ducat, D. C.; Silver, P. A. *Curr. Opin. Chem. Biol.* **2012,** *16,* 337. doi:10.1016/j.cbpa.2012.05.002
24. Fuchs, G. *Annu. Rev. Microbiol.* **2011,** *65,* 631. doi:10.1146/annurev-micro-090110-102801
25. Bar-Even, A.; Noor, E.; Lewis, N. E.; Milo, R. *Proc. Natl. Acad. Sci. U. S. A.* **2010,** *107,* 8889. doi:10.1073/pnas.0907176107
26. Erb, T. J. *Appl. Environ. Microbiol.* **2011,** *77,* 8466. doi:10.1128/AEM.05702-11
27. Bar-Even, A.; Noor, E.; Milo, R. *J. Exp. Bot.* **2012,** *63,* 2325. doi:10.1093/jxb/err417
28. Knowles, J. R. *Annu. Rev. Biochem.* **1989,** *58,* 195. doi:10.1146/annurev.bi.58.070189.001211
29. Pierre, A. C. *ISRN Chem. Eng.* **2012,** *2012,* 753687. doi:10.5402/2012/753687
30. Moroney, J. V.; Ma, Y.; Frey, W. D.; Fusilier, K. A.; Pham, T. T.; Simms, T. A.; DiMario, R. J.; Yang, J.; Mukherjee, B. *Photosynth. Res.* **2011,** *109,* 133. doi:10.1007/s11120-011-9635-3
31. Khalifah, R. G. *Proc. Natl. Acad. Sci. U. S. A.* **1973,** *70,* 1986. doi:10.1073/pnas.70.7.1986
32. Tong, L. *Cell. Mol. Life Sci.* **2013,** *70,* 863. doi:10.1007/s00018-012-1096-0
33. Christin, P.-A.; Arakaki, M.; Osborne, C. P.; Bräutigam, A.; Sage, R. F.; Hibberd, J. M.; Kelly, S.; Covshoff, S.; Wong, G. K.-S.; Hancock, L.; Edwards, E. J. *J. Exp. Bot.* **2014,** *65,* 3609. doi:10.1093/jxb/eru087
34. Winter, K.; Holtum, J. A. M. *J. Exp. Bot.* **2014,** *65,* 3425. doi:10.1093/jxb/eru063
35. Chen, A. H.; Robinson-Mosher, A.; Savage, D. F.; Silver, P. A.; Polka, J. K. *PLoS One* **2013,** *8,* e76127. doi:10.1371/journal.pone.0076127
36. Long, B. M.; Badger, M. R.; Whitney, S. M.; Price, G. D. *J. Biol. Chem.* **2007,** *282,* 29323. doi:10.1074/jbc.M703896200

37. Chen, A. H.; Robinson-Mosher, A.; Savage, D. F.; Silver, P. A.; Polka, J. K. *PLoS One* **2013,** *8,* e76127. doi:10.1371/journal.pone.0076127
38. Lin, M. T.; Occhialini, A.; Andralojc, P. J.; Devonshire, J.; Hines, K. M.; Parry, M. A. J.; Hanson, M. R. *Plant J.* **2014,** *79,* 1. doi:10.1111/tpj.12536
39. Lin, M. T.; Occhialini, A.; Andralojc, P. J.; Parry, M. A. J.; Hanson, M. R. *Nature* **2014,** *513,* 547. doi:10.1038/nature13776
40. Price, G. D.; Pengelly, J. J. L.; Forster, B.; Du, J.; Whitney, S. M.; von Caemmerer, S.; Badger, M. R.; Howitt, S. M.; Evans, J. R. *J. Exp. Bot.* **2013,** *64,* 753. doi:10.1093/jxb/ers257
41. Bonacci, W.; Teng, P. K.; Afonso, B.; Niederholtmeyer, H.; Grob, P.; Silver, P. A.; Savage, D. F. *Proc. Natl. Acad. Sci. U. S. A.* **2012,** *109,* 478. doi:10.1073/pnas.1108557109
42. Berg, I. A.; Kockelkorn, D.; Ramos-Vera, W. H.; Say, R. F.; Zarzycki, J.; Hügler, M.; Alber, B. E.; Fuchs, G. *Nat. Rev. Microbiol.* **2010,** *8,* 447. doi:10.1038/nrmicro2365
43. Nisbet, E. G.; Grassineau, N. V.; Howe, C. J.; Abell, P. I.; Regelous, M.; Nisbet, R. E. R. *Geobiology* **2007,** *5,* 311. doi:10.1111/j.1472-4669.2007.00127.x
44. Galmés, J.; Kapralov, M. V.; Andralojc, P. J.; Conesa, M. À.; Keys, A. J.; Parry, M. A. J.; Flexas, J. *Plant, Cell Environ.* **2014,** *37,* 1989. doi:10.1111/pce.12335
45. Berg, I. A. *Appl. Environ. Microbiol.* **2011,** *77,* 1925. doi:10.1128/AEM.02473-10
46. Zhu, X.-G.; Long, S. P.; Ort, D. R. *Annu. Rev. Plant Biol.* **2010,** *61,* 235. doi:10.1146/annurev-arplant-042809-112206
47. Shively, J. M.; van Keulen, G.; Meijer, W. G. *Annu. Rev. Microbiol.* **1998,** *52,* 191. doi:10.1146/annurev.micro.52.1.191
48. Singh, J.; Pandey, P.; James, D.; Chandrasekhar, K.; Achary, V. M. M.; Kaul, T.; Tripathy, B. C.; Reddy, M. K. *Plant Biotechnol. J.* **2014,** *12,* 1217. doi:10.1111/pbi.12246
49. Studer, R. A.; Christin, P.-A.; Williams, M. A.; Orengo, C. A. *Proc. Natl. Acad. Sci. U. S. A.* **2014,** *111,* 2223. doi:10.1073/pnas.1310811111
50. Hügler, M.; Sievert, S. M. *Annu. Rev. Mar. Sci.* **2011,** *3,* 261. doi:10.1146/annurev-marine-120709-142712
51. Hugler, M.; Huber, H.; Stetter, K. O.; Fuchs, G. *Arch. Microbiol.* **2003,** *179,* 160.
52. Buchanan, B. B.; Arnon, D. I. *Photosynth. Res.* **1990,** *24,* 47. doi:10.1007/BF00032643
53. Evans, M. C. W.; Buchanan, B. B.; Arnon, D. I. *Proc. Natl. Acad. Sci. U. S. A.* **1966,** *55,* 928. doi:10.1073/pnas.55.4.928
54. Ljungdahl, L.; Wood, H. G. *Annu. Rev. Microbiol.* **1969,** *23,* 515. doi:10.1146/annurev.mi.23.100169.002503
55. Ragsdale, S. W.; Pierce, E. *Biochim. Biophys. Acta, Proteins Proteomics* **2008,** *1784,* 1873. doi:10.1016/j.bbapap.2008.08.012
56. Clark, J. E.; Ragsdale, S. W.; Ljungdahl, L. G.; Wiegel, J. *J. Bacteriol.* **1982,** *151,* 507.
57. Ragsdale, S. W. *Crit. Rev. Biochem. Mol. Biol.* **1991,** *26,* 261. doi:10.3109/10409239109114070
58. Eden, G.; Fuchs, G. *Arch. Microbiol.* **1982,** *133,* 66. doi:10.1007/BF00943772
59. Eden, G.; Fuchs, G. *Arch. Microbiol.* **1983,** *135,* 68. doi:10.1007/BF00419485
60. Maynard, E. L.; Lindahl, P. A. *J. Inorg. Biochem.* **1999,** *74,* 227.
61. Fesseler, J.; Jeoung, J.-H.; Dobbek, H. *Angew. Chem., Int. Ed.* **2015,** *54,* 8560. doi:10.1002/anie.201501778
62. Alissandratos, A.; Kim, H.-K.; Matthews, H.; Hennessy, J. E.; Philbrook, A.; Easton, C. J. *Appl. Environ. Microbiol.* **2013,** *79,* 741. doi:10.1128/AEM.02886-12
63. Wang, S.; Huang, H.; Kahnt, J.; Mueller, A. P.; Köpke, M.; Thauer, R. K. *J. Bacteriol.* **2013,** *195,* 4373. doi:10.1128/JB.00678-13
64. Almendra, M. J.; Brondino, C. D.; Gavel, O.; Pereira, A. S.; Tavares, P.; Bursakov, S.; Duarte, R.; Caldeira, J.; Moura, J. J. G.; Moura, I. *Biochemistry* **1999,** *38,* 16366. doi:10.1021/bi990069n
65. Khangulov, S. V.; Gladyshev, V. N.; Dismukes, G. C.; Stadtman, T. C. *Biochemistry* **1998,** *37,* 3518. doi:10.1021/bi972177k
66. Maia, L. B.; Moura, J. J. G.; Moura, I. *J. Biol. Inorg. Chem.* **2015,** *20,* 287. doi:10.1007/s00775-014-1218-2
67. de Bok, F. A. M.; Hagedoorn, P.-L.; Silva, P. J.; Hagen, W. R.; Schiltz, E.; Fritsche, K.; Stams, A. J. M. *Eur. J. Biochem.* **2003,** *270,* 2476. doi:10.1046/j.1432-1033.2003.03619.x
68. Seol, E.; Jang, Y.; Kim, S.; Oh, Y.-K.; Park, S. *Int. J. Hydrogen Energy* **2012,** *37,* 15045. doi:10.1016/j.ijhydene.2012.07.095
69. Tishkov, V. I.; Popov, V. O. *Biochemistry (Moscow)* **2004,** *69,* 1252. doi:10.1007/s10541-005-0071-x
70. Berg, I. A.; Kockelkorn, D.; Buckel, W.; Fuchs, G. *Science* **2007,** *318,* 1782. doi:10.1126/science.1149976
71. Chuakrut, S.; Arai, H.; Ishii, M.; Igarashi, Y. *J. Bacteriol.* **2003,** *185,* 938. doi:10.1128/JB.185.3.938-947.2003
72. Menendez, C.; Bauer, Z.; Huber, H.; Gad'on, N.; Stetter, K.-O.; Fuchs, G. *J. Bacteriol.* **1999,** *181,* 1088.
73. Ramos-Vera, W. H.; Berg, I. A.; Fuchs, G. *J. Bacteriol.* **2009,** *191,* 4286. doi:10.1128/JB.00145-09
74. Mueller-Cajar, O.; Whitney, S. M. *Photosynth. Res.* **2008,** *98,* 667. doi:10.1007/s11120-008-9324-z
75. Mueller-Cajar, O.; Whitney, S. M. *Biochem. J.* **2008,** *414,* 205. doi:10.1042/BJ20080668
76. Mueller-Cajar, O.; Morell, M.; Whitney, S. M. *Biochemistry* **2007,** *46,* 14067. doi:10.1021/bi700820a
77. Savir, Y.; Noor, E.; Milo, R.; Tlusty, T. *Proc. Natl. Acad. Sci. U. S. A.* **2010,** *107,* 3475. doi:10.1073/pnas.0911663107
78. Long, S. P.; Zhu, X.-G.; Naidu, S. L.; Ort, D. R. *Plant, Cell Environ.* **2006,** *29,* 315. doi:10.1111/j.1365-3040.2005.01493.x
79. McGrath, J. M.; Long, S. P. *Plant Physiol.* **2014,** *164,* 2247. doi:10.1104/pp.113.232611
80. Whitney, S. M.; Birch, R.; Kelso, C.; Beck, J. L.; Kapralov, M. V. *Proc. Natl. Acad. Sci. U. S. A.* **2015,** *112,* 3564. doi:10.1073/pnas.1420536112
81. Singh, A.; Nigam, P. S.; Murphy, J. D. *Bioresour. Technol.* **2011,** *102,* 10. doi:10.1016/j.biortech.2010.06.032
82. Lue, J.; Sheahan, C.; Fu, P. *Energy Environ. Sci.* **2011,** *4,* 2451. doi:10.1039/c0ee00593b
83. Guadalupe-Medina, V.; Wisselink, H. W.; Luttik, M. A. H.; de Hulster, E.; Daran, J.-M.; Pronk, J. T.; van Maris, A. J. A. *Biotechnol. Biofuels* **2013,** *6,* 125. doi:10.1186/1754-6834-6-125
84. Chang, K. S.; Jeon, H.; Gu, M. B.; Pack, S. P.; Jin, E. *Bioprocess Biosyst. Eng.* **2013,** *36,* 1923. doi:10.1007/s00449-013-0968-5
85. Chang, K. S.; Jeon, H.; Seo, S.; Lee, Y.; Jin, E. *Enzyme Microb. Technol.* **2014,** *60,* 64. doi:10.1016/j.enzmictec.2014.04.007
86. Werpy, T.; Peterson, G. *Top value added chemicals from Biomass;* National Renewable Energy Laboratory, US Department of Energy, 2004.
87. Lin, H.; San, K.-Y.; Bennett, G. N. *Appl. Microbiol. Biotechnol.* **2005,** *67,* 515. doi:10.1007/s00253-004-1789-x

88. Wang, D.; Li, Q.; Li, W.; Xing, J.; Su, Z. *Enzyme Microb. Technol.* **2009,** *45,* 491. doi:10.1016/j.enzmictec.2009.08.003
89. Song, C. W.; Kim, D. I.; Choi, S.; Jang, J. W.; Lee, S. Y. *Biotechnol. Bioeng.* **2013,** *110,* 2025. doi:10.1002/bit.24868
90. Liu, R.; Liang, L.; Wu, M.; Chen, K.; Jiang, M.; Ma, J.; Wei, P.; Ouyang, P. *Biochem. Eng. J.* **2013,** *79,* 77. doi:10.1016/j.bej.2013.07.004
91. Wu, H.; Li, Q.; Li, Z.-m.; Ye, Q. *Bioresour. Technol.* **2012,** *107,* 376. doi:10.1016/j.biortech.2011.12.043
92. Liang, L.; Liu, R.; Wang, G.; Gou, D.; Ma, J.; Chen, K.; Jiang, M.; Wei, P.; Ouyang, P. *Enzyme Microb. Technol.* **2012,** *51,* 286. doi:10.1016/j.enzmictec.2012.07.011
93. Wang, Z.; Lin, M.; Wang, L.; Ammar, E. M.; Yang, S.-T. *Process Biochem.* **2015,** *50,* 194. doi:10.1016/j.procbio.2014.11.012
94. Ammar, E. M.; Jin, Y.; Wang, Z.; Yang, S.-T. *Appl. Microbiol. Biotechnol.* **2014,** *98,* 7761. doi:10.1007/s00253-014-5836-y
95. Hügler, M.; Krieger, R. S.; Jahn, M.; Fuchs, G. *Eur. J. Biochem.* **2003,** *270,* 736. doi:10.1046/j.1432-1033.2003.03434.x
96. Ishii, M.; Chuakrut, S.; Arai, H.; Igarashi, Y. *Appl. Microbiol. Biotechnol.* **2004,** *64,* 605. doi:10.1007/s00253-003-1540-z
97. Thorgersen, M. P.; Lipscomb, G. L.; Schut, G. J.; Kelly, R. M.; Adams, M. W. W. *Metab. Eng.* **2014,** *22,* 83. doi:10.1016/j.ymben.2013.12.006
98. Keller, M. W.; Schut, G. J.; Lipscomb, G. L.; Menon, A. L.; Iwuchukwu, I. J.; Leuko, T. T.; Thorgersen, M. P.; Nixon, W. J.; Hawkins, A. S.; Kelly, R. M.; Adams, M. W. W. *Proc. Natl. Acad. Sci. U. S. A.* **2013,** *110,* 5840. doi:10.1073/pnas.1222607110
99. Yoshida, T.; Nagasawa, T. *J. Biosci. Bioeng.* **2000,** *89,* 111. doi:10.1016/S1389-1723(00)88723-X
100. Wieser, M.; Yoshida, T.; Nagasawa, T. *J. Mol. Catal. B: Enzym.* **2001,** *11,* 179. doi:10.1016/S1381-1177(00)00038-2
101. Yoshida, T.; Fujita, K.; Nagasawa, T. *Biosci., Biotechnol., Biochem.* **2002,** *66,* 2388. doi:10.1271/bbb.66.2388
102. Yoshida, T.; Inami, Y.; Matsui, T.; Nagasawa, T. *Biotechnol. Lett.* **2010,** *32,* 701. doi:10.1007/s10529-010-0210-3
103. Kirimura, K.; Gunji, H.; Wakayama, R.; Hattori, T.; Ishii, Y. *Biochem. Biophys. Res. Commun.* **2010,** *394,* 279. doi:10.1016/j.bbrc.2010.02.154
104. Kirimura, K.; Yanaso, S.; Kosaka, S.; Koyama, K.; Hattori, T.; Ishii, Y. *Chem. Lett.* **2011,** *40,* 206. doi:10.1246/cl.2011.206
105. Wuensch, C.; Pavkov-Keller, T.; Steinkellner, G.; Gross, J.; Fuchs, M.; Hromic, A.; Lyskowski, A.; Fauland, K.; Gruber, K.; Glueck, S. M.; Faber, K. *Adv. Synth. Catal.* **2015,** *357,* 1909. doi:10.1002/adsc.201401028
106. Pesci, L.; Glueck, S. M.; Gurikov, P.; Smirnova, I.; Faber, K.; Liese, A. *FEBS J.* **2015,** *282,* 1334. doi:10.1111/febs.13225
107. Wuensch, C.; Gross, J.; Steinkellner, G.; Lyskowski, A.; Gruber, K.; Glueck, S. M.; Faber, K. *RSC Adv.* **2014,** *4,* 9673. doi:10.1039/c3ra47719c
108. Wuensch, C.; Glueck, S. M.; Gross, J.; Koszelewski, D.; Schober, M.; Faber, K. *Org. Lett.* **2012,** *14,* 1974. doi:10.1021/ol300385k
109. Wuensch, C.; Schmidt, N.; Gross, J.; Grischek, B.; Glueck, S. M.; Faber, K. *J. Biotechnol.* **2013,** *168,* 264. doi:10.1016/j.jbiotec.2013.07.017
110. Lupa, B.; Lyon, D.; Shaw, L. N.; Sieprawska-Lupa, M.; Wiegel, J. *Can. J. Microbiol.* **2008,** *54,* 75. doi:10.1139/W07-113
111. Xia, S.; Zhao, X.; Frigo-Vaz, B.; Zheng, W.; Kim, J.; Wang, P. *Bioresour. Technol.* **2015,** *182,* 368. doi:10.1016/j.biortech.2015.01.093
112. Bar-Even, A.; Noor, E.; Flamholz, A.; Milo, R. *Biochim. Biophys. Acta, Bioenerg.* **2013,** *1827,* 1039. doi:10.1016/j.bbabio.2012.10.013
113. Li, L. F.; Ljungdah, L.; Wood, H. G. *J. Bacteriol.* **1966,** *92,* 405.
114. Thauer, R. K. *FEBS Lett.* **1972,** *27,* 111. doi:10.1016/0014-5793(72)80421-6
115. Thauer, R. K. *J. Bacteriol.* **1973,** *114,* 443.
116. Jungermann, K.; Kirchniawy, H.; Thauer, R. K. *Biochem. Biophys. Res. Commun.* **1970,** *41,* 682. doi:10.1016/0006-291X(70)90067-7
117. Thauer, R. K.; Käufer, B.; Fuchs, G. *Eur. J. Biochem.* **1975,** *55,* 111. doi:10.1111/j.1432-1033.1975.tb02143.x
118. Schuchmann, K.; Müller, V. *Science* **2013,** *342,* 1382. doi:10.1126/science.1244758
119. Ruschig, U.; Müller, U.; Willnow, P.; Höpner, T. *Eur. J. Biochem.* **1976,** *70,* 325. doi:10.1111/j.1432-1033.1976.tb11021.x
120. Parkinson, B. A.; Weaver, P. F. *Nature* **1984,** *309,* 148. doi:10.1038/309148a0
121. Reda, T.; Plugge, C. M.; Abram, N. J.; Hirst, J. *Proc. Natl. Acad. Sci. U. S. A.* **2008,** *105,* 10654. doi:10.1073/pnas.0801290105
122. Bassegoda, A.; Madden, C.; Wakerley, D. W.; Reisner, E.; Hirst, J. *J. Am. Chem. Soc.* **2014,** *136,* 15473. doi:10.1021/ja508647u
123. Hartmann, T.; Leimkühler, S. *FEBS J.* **2013,** *280,* 6083. doi:10.1111/febs.12528
124. Srikanth, S.; Maesen, M.; Dominguez-Benetton, X.; Vanbroekhoven, K.; Pant, D. *Bioresour. Technol.* **2014,** *165,* 350. doi:10.1016/j.biortech.2014.01.129
125. Choe, H.; Joo, J. C.; Cho, D. H.; Kim, M. H.; Lee, S. H.; Jung, K. D.; Kim, Y. H. *PLoS One* **2014,** *9,* e103111. doi:10.1371/journal.pone.0103111
126. Choe, H.; Ha, J. M.; Joo, J. C.; Kim, H.; Yoon, H.-J.; Kim, S.; Son, S. H.; Gengan, R. M.; Jeon, S. T.; Chang, R.; Jung, K. D.; Kim, Y. H.; Lee, H. H. *Acta Crystallogr., Sect. D: Biol. Crystallogr.* **2015,** *71,* 313. doi:10.1107/S1399004714025474
127. Klibanov, A. M.; Alberti, B. N.; Zale, S. E. *Biotechnol. Bioeng.* **1982,** *24,* 25. doi:10.1002/bit.260240104
128. Woods, D. D. *Biochem. J.* **1936,** *30,* 515. doi:10.1042/bj0300515
129. Alissandratos, A.; Kim, H.-K.; Easton, C. J. *Bioresour. Technol.* **2014,** *164,* 7. doi:10.1016/j.biortech.2014.04.064
130. Hwang, H.; Yeon, Y. J.; Lee, S.; Choe, H.; Jang, M. G.; Cho, D. H.; Park, S.; Kim, Y. H. *Bioresour. Technol.* **2015,** *185,* 35. doi:10.1016/j.biortech.2015.02.086
131. Kuwabata, S.; Tsuda, R.; Nishida, K.; Yoneyama, H. *Chem. Lett.* **1993,** *22,* 1631. doi:10.1246/cl.1993.1631
132. Kuwabata, S.; Tsuda, R.; Yoneyama, H. *J. Am. Chem. Soc.* **1994,** *116,* 5437. doi:10.1021/ja00091a056
133. Cazelles, R.; Drone, J.; Fajula, F.; Ersen, O.; Moldovan, S.; Galarneau, A. *New J. Chem.* **2013,** *37,* 3721. doi:10.1039/c3nj00688c
134. Luo, J.; Meyer, A. S.; Mateiu, R. V.; Pinelo, M. *New Biotechnol.* **2015,** *32,* 319. doi:10.1016/j.nbt.2015.02.006
135. Amao, Y.; Watanabe, T. *Chem. Lett.* **2004,** *33,* 1544. doi:10.1246/cl.2004.1544
136. Amao, Y.; Watanabe, T. *Appl. Catal., B* **2009,** *86,* 109. doi:10.1016/j.apcatb.2008.08.008

137. Yadav, R. K.; Oh, G. H.; Park, N.-J.; Kumar, A.; Kong, K.-j.; Baeg, J.-O. *J. Am. Chem. Soc.* **2014,** *136,* 16728. doi:10.1021/ja509650r
138. Enthaler, S.; von Langermann, J.; Schmidt, T. *Energy Environ. Sci.* **2010,** *3,* 1207. doi:10.1039/b907569k
139. Joo, F. *ChemSusChem* **2008,** *1,* 805. doi:10.1002/cssc.200800133
140. Boddien, A.; Gärtner, F.; Federsel, C.; Sponholz, P.; Mellmann, D.; Jackstell, R.; Junge, H.; Beller, M. *Angew. Chem., Int. Ed.* **2011,** *50,* 6411. doi:10.1002/anie.201101995
141. Enthaler, S. *ChemSusChem* **2008,** *1,* 801. doi:10.1002/cssc.200800101
142. Sinha, P.; Roy, S.; Das, D. *Int. J. Hydrogen Energy* **2015,** *40,* 8806. doi:10.1016/j.ijhydene.2015.05.076
143. Lipscomb, G. L.; Schut, G. J.; Thorgersen, M. P.; Nixon, W. J.; Kelly, R. M.; Adams, M. W. W. *J. Biol. Chem.* **2014,** *289,* 2873. doi:10.1074/jbc.M113.530725
144. Hu, H.; Wood, T. K. *Biochem. Biophys. Res. Commun.* **2010,** *391,* 1033. doi:10.1016/j.bbrc.2009.12.013
145. Amos, R. I. J.; Heinroth, F.; Chan, B.; Zheng, S.; Haynes, B. S.; Easton, C. J.; Masters, A. F.; Radom, L.; Maschmeyer, T. *Angew. Chem., Int. Ed.* **2014,** *53,* 11275. doi:10.1002/anie.201405360
146. Bezemer, G. L.; Bitter, J. H.; Kuipers, H.; Oosterbeek, H.; Holewijn, J. E.; Xu, X. D.; Kapteijn, F.; van Dillen, A. J.; de Jong, K. P. *J. Am. Chem. Soc.* **2006,** *128,* 3956. doi:10.1021/ja058282w
147. Woolerton, T. W.; Sheard, S.; Reisner, E.; Pierce, E.; Ragsdale, S. W.; Armstrong, F. A. *J. Am. Chem. Soc.* **2010,** *132,* 2132. doi:10.1021/ja910091z
148. Woolerton, T. W.; Sheard, S.; Pierce, E.; Ragsdale, S. W.; Armstrong, F. A. *Energy Environ. Sci.* **2011,** *4,* 2393. doi:10.1039/c0ee00780c
149. Hu, Y.; Lee, C. C.; Ribbe, M. W. *Science* **2011,** *333,* 753. doi:10.1126/science.1206883
150. Muschiol, J.; Peters, C.; Oberleitner, N.; Mihovilovic, M. D.; Bornscheuer, U. T.; Rudroff, F. *Chem. Commun.* **2015,** *51,* 5798. doi:10.1039/C4CC08752F
151. Ford, T. J.; Silver, P. A. *Curr. Opin. Chem. Biol.* **2015,** *28,* 20. doi:10.1016/j.cbpa.2015.05.012
152. Gaida, S. M.; Al-Hinai, M. A.; Indurthi, D. C.; Nicolaou, S. A.; Papoutsakis, E. T. *Nucleic Acids Res.* **2013,** *41,* 8726. doi:10.1093/nar/gkt651
153. Zingaro, K. A.; Nicolaou, S. A.; Papoutsakis, E. T. *Trends Biotechnol.* **2013,** *31,* 643. doi:10.1016/j.tibtech.2013.08.005
154. Fuchs, G.; Berg, I. A. *J. Biotechnol.* **2014,** *192,* 314. doi:10.1016/j.jbiotec.2014.02.015
155. Mattozzi, M. D.; Ziesack, M.; Voges, M. J.; Silver, P. A.; Way, J. C. *Metab. Eng.* **2013,** *16,* 130. doi:10.1016/j.ymben.2013.01.005
156. Siegel, J. B.; Smith, A. L.; Poust, S.; Wargacki, A. J.; Bar-Even, A.; Louw, C.; Shen, B. W.; Eiben, C. B.; Tran, H. M.; Noor, E.; Gallaher, J. L.; Bale, J.; Yoshikuni, Y.; Gelb, M. H.; Keasling, J. D.; Stoddard, B. L.; Lidstrom, M. E.; Baker, D. *Proc. Natl. Acad. Sci. U. S. A.* **2015,** *112,* 3704. doi:10.1073/pnas.1500545112
157. Cuaresma, M.; Janssen, M.; Vilchez, C.; Wijffels, R. H. *Bioresour. Technol.* **2011,** *102,* 5129. doi:10.1016/j.biortech.2011.01.078
158. Michel, H. *Angew. Chem., Int. Ed.* **2012,** *51,* 2516. doi:10.1002/anie.201200218
159. Hawkins, A. S.; Han, Y.; Lian, H.; Loder, A. J.; Menon, A. L.; Iwuchukwu, I. J.; Keller, M.; Leuko, T. T.; Adams, M. W. W.; Kelly, R. M. *ACS Catal.* **2011,** *1,* 1043. doi:10.1021/cs2003017
160. Guo, K.; Prévoteau, A.; Patil, S. A.; Rabaey, K. *Curr. Opin. Biotechnol.* **2015,** *33,* 149. doi:10.1016/j.copbio.2015.02.014
161. Freguia, S.; Teh, E. H.; Boon, N.; Leung, K. M.; Keller, J.; Rabaey, K. *Bioresour. Technol.* **2010,** *101,* 1233. doi:10.1016/j.biortech.2009.09.054
162. Rabaey, K.; Rodríguez, J.; Blackall, L. L.; Keller, J.; Gross, P.; Batstone, D.; Verstraete, W.; Nealson, K. H. *ISME J.* **2007,** *1,* 9. doi:10.1038/ismej.2007.4

License and Terms

BEILSTEIN JOURNAL OF ORGANIC CHEMISTRY

Continuous formation of *N*-chloro-*N*,*N*-dialkylamine solutions in well-mixed meso-scale flow reactors

A. John Blacker* and Katherine E. Jolley

Full Research Paper

Open Access

Address:
Institute of Process Research and Development, School of Chemistry and School of Chemical and Process Engineering, University of Leeds, Woodhouse Lane, Leeds, LS2 9JT, Leeds, UK

Email:
A. John Blacker* - j.blacker@leeds.ac.uk

* Corresponding author

Keywords:
amine; biphasic; chloramine; chlorination; continuous flow chemistry; CSTR; static mixer; sodium hypochlorite; tube reactor

Beilstein J. Org. Chem. **2015,** *11,* 2408–2417.
doi:10.3762/bjoc.11.262

Received: 13 October 2015
Accepted: 19 November 2015
Published: 02 December 2015

This article is part of the Thematic Series "Sustainable catalysis".

Guest Editor: N. Turner

Abstract

The continuous flow synthesis of a range of organic solutions of *N*,*N*-dialkyl-*N*-chloramines is described using either a bespoke meso-scale tubular reactor with static mixers or a continuous stirred tank reactor. Both reactors promote the efficient mixing of a biphasic solution of *N*,*N*-dialkylamine in organic solvent, and aqueous sodium hypochlorite to achieve near quantitative conversions, in 72–100% in situ yields, and useful productivities of around 0.05 mol/h with residence times from 3 to 20 minutes. Initial calorimetric studies have been carried out to inform on reaction exotherms, rates and safe operation. Amines which partition mainly in the organic phase require longer reaction times, provided by the CSTR, to compensate for low mass transfer rates in the biphasic system. The green metrics of the reaction have been assessed and compared to existing procedures and have shown the continuous process is improved over previous procedures. The organic solutions of *N*,*N*-dialkyl-*N*-chloramines produced continuously will enable their use in tandem flow reactions with a range of nucleophilic substrates.

Introduction

N-Chloramines provide a versatile and reactive class of reagents for use in electrophilic amination and other reactions. *N*-Chloro-*N*,*N*-dialkylamines have been shown to offer a broad range of products from reactions with i) unsaturated C–C bonds to give amines [1-3] and heterocycles [1,4]; ii) Grignard and organozinc reagents to give amines [1]; iii) aldehydes to give amides [5-7]; iv) base to give imines [8]; v) alkyl and aryl C–H bonds in the presence of acid and visible light to form heterocycles [9,10]. Furthermore they have also been used for chlorination of aromatics in the presence of acid [11], and as reagents in the syntheses of natural products [12,13].

Despite their versatility as reagents, the exothermicity and instability that occurs in both their formation and reaction, has

reduced the interest in their use for reasons of process safety. Isolation of many *N*-chloramines is unadvisable with reports of unpredictable and rapid decomposition [11,14-16].

N-Chloramines are prepared conventionally by reaction of the amine precursor with an electrophilic chlorine source [14]. Despite its atom efficiency use of chlorine gas is undesirable due to its toxicity and strong oxidising properties, making it highly hazardous and operationally difficult to use. In addition, the hydrochloric acid byproduct requires additional processing to neutralise and separate it. *N*-Chlorosuccinimide is used frequently in the laboratory because it is a relatively stable solid that is easily weighed and added to reactions [3,17], however, it has a low atom economy, poor economics, and requires separation of the succinimide byproduct [18]. The *tert*-butyl hypochlorite (*t*-BuOCl) reagent is also used regularly, but is similarly expensive, wasteful and hazardous [14,19-21]. On the other hand sodium hypochlorite (NaOCl) is an inexpensive byproduct of chlorine manufacture, and offers a safer, greener source of electrophilic chlorine for producing *N*-chloramines [11,14,22]. Reaction times can, however, be long [14,23,24], and yields low [25]. Zhong et al. have reported a process using NaOCl to generate *t*-BuOCl in situ for chloramine formation, applying the methodology to a broad range of substrates in high yields [20].

Published literature on chloramine formation is limited to batch procedures, however, the use of continuous processes could offer significant advantages. Use of continuous flow reactors to achieve steady-state allows precise control over the reaction parameters to improve safety, selectivity, productivity and consistency. Reduced reactor volumes compared to conventional batch reactors limit the quantity of reacting material at any one time; particularly important for the preparation of hazardous or unstable products. Furthermore smaller volumes with higher surface areas enable faster heat removal and better temperature control to limit unwanted side reactions. Further kinetic control is achieved with reactant concentrations, feed rates, mixing regime and residence time resulting in higher product yields.

Herein we report the use of different types of bespoke continuous reactors for preparing different *N*-chloro-*N*,*N*-dialkylamines. The use of these materials in forming a range of different nitrogen containing products via a cascade/tandem procedure will be reported elsewhere. This atom efficient procedure, with sodium hydroxide and water the only byproducts, should have better green metrics than other methods. Using biphasic reaction conditions with the amine dissolved in a water immiscible, organic solvent such as toluene enabled facile separation of the organic soluble product from the water soluble NaOH (Scheme 1). Such separation of biphasic mixtures is known in continuous systems, for example membrane-based separators [26,27].

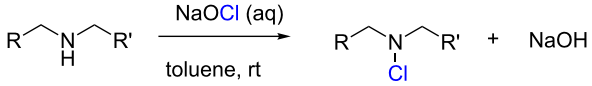

Scheme 1: Two-phase reaction of *N*,*N*-dialkylamine and sodium hypochlorite.

Mixing is a key parameter for reactions in multiphasic systems and characterisation of material flows within different continuous reactors is widely studied by both modelling and experiment [28,29]. The rate of reaction of NaOCl and amines at high pH is very fast with a second order rate constant, k_{obs} of 1.52×10^5 L·mol^{-1}·min^{-1} reported for dimethylamine [30]. In this case it is the rate of mass transfer of the reagents, partitioned between the two liquid phases that limits the rate of product formation, rather than the chemical rate of reaction between the two species. Continuous liquid biphasic reactions are usually poorly mixed within micro-scale reactors, as low fluid velocities and frictional wall effects cause laminar flow and phase separation into alternating organic–aqueous segmented flow; whilst meso-scale reactors are much better suited, and provide more accurate and reliable information for scale-up. Interaction of the reactants occurs only at the phase interface, so efficient mixing increases the surface area and promotes product formation. Within batch or continuous stirred tank reactors an increase in mixing intensity is achieved with optimised impellor design and speed, alongside a reactor designed to disrupt the flow and increase turbulence. Within meso-scale tubular reactors the addition of in-line aids such as split and recombination streams [31,32], or static mixers [32,33], can enhance mixing and mass transfer between phases. Phase-transfer catalysts (PTCs) can also be used to promote reactions across phase boundaries [31], their use would, however, incur additional financial costs for the reaction, and also the need for purification and removal of the catalyst from the reaction solution.

Results and Discussion

Calorimetry

In view of the potential dangers involved in making chloramines we began our studies with calorimetric analysis. The formation *N*-chloromorpholine was studied by feeding 1.1 M NaOCl (aq) into a 1 M morpholine (aq) at a rate of 1 g/min. The calorimeter jacket temperature was set at −15 °C, and power compensation used to maintain the reactor at 5 °C. 20 mL of the NaOCl solution were added to 20 mmol of morpholine over 20 min, and after subtracting the feed solution temperature

(*Q* Dose) from compensatory power (*Q* Comp) the total was 2.76 W. For this calibrated calorimeter this equates to −1.47 kJ which gives a heat of reaction, $\Delta H_r = -73.4$ kJ·mol^{-1} for the formation of *N*-chloromorpholine (Figure 1). Calculation of the heat of reaction by bond forming/bond breaking calculation, according to mechanisms proposed in the literature, give a ΔH_r of −72 kJ·mol^{-1} (Supporting Information File 1) [30].

Figure 1 shows the calorimetric trace for the formation of *N*-chloromorpholine. Following the addition of NaOCl (aq) there is a small delay in the reaction which may be mixing related. A rapid exotherm then occurs with 1.37 kJ energy released continuously over the 20 minute feed. When the NaOCl (aq) addition is stopped there is a further release of 0.09 kJ energy over 2 minutes indicating a small accumulation of heat. Analysis of the crude reaction product shows no side products, and no decomposition of the *N*-chloromorpholine product.

When the same reaction was carried out using a toluene–water biphasic system, the calorimeter trace was more complex with mass transfer effects making interpretation difficult (Supporting Information File 1).

The calorimetric analysis shows chloramine formation to be an energetic process with a significant associated exotherm illustrating the need for efficient temperature control during the reaction to ensure a safe process. In batch it would be necessary to cool the reaction with an ice bath or similar, however, the continuous reactors employed in this work, with increased surface area-to-volume ratio, allows effective heat dissipation under ambient conditions.

Continuous reactor

A nylon/PTFE tubular reactor was constructed that incorporates static mixers for enhanced mixing of the biphasic reaction solution, made of the acetal homopolymer, Delrin® that are solvent and oxidant resistant [34]. The set-up comprised one pump for the organic phase (amine/toluene) and one for the aqueous phase (NaOCl/water). The feeds were connected via a stainless steel T-piece to tubing (1/4 inch OD, 3/16 inch ID) containing static mixer tubes (1/8 inch ID, 3/16 inch OD) along the flow channel (Figure 2). The length of the reactor and number of static mixer inserts were adjusted to vary the residence time, thus maintaining sufficient flow rate to give effective mixing.

Initial experiments using toluene and an aqueous dye were used to assess static mixer performance. Figure 3 shows the solutions being pumped simultaneously into a T-piece with equal flow rates. As the solution progresses into the tube containing the static mixers, it can be seen to be a well-mixed emulsion. Shortly after emanating from the mixed region, the biphase separates into a segmented flow before being collected into a flask.

Initial reactions looked at the effect of increasing the number of static mixers within the reactor and also increasing residence

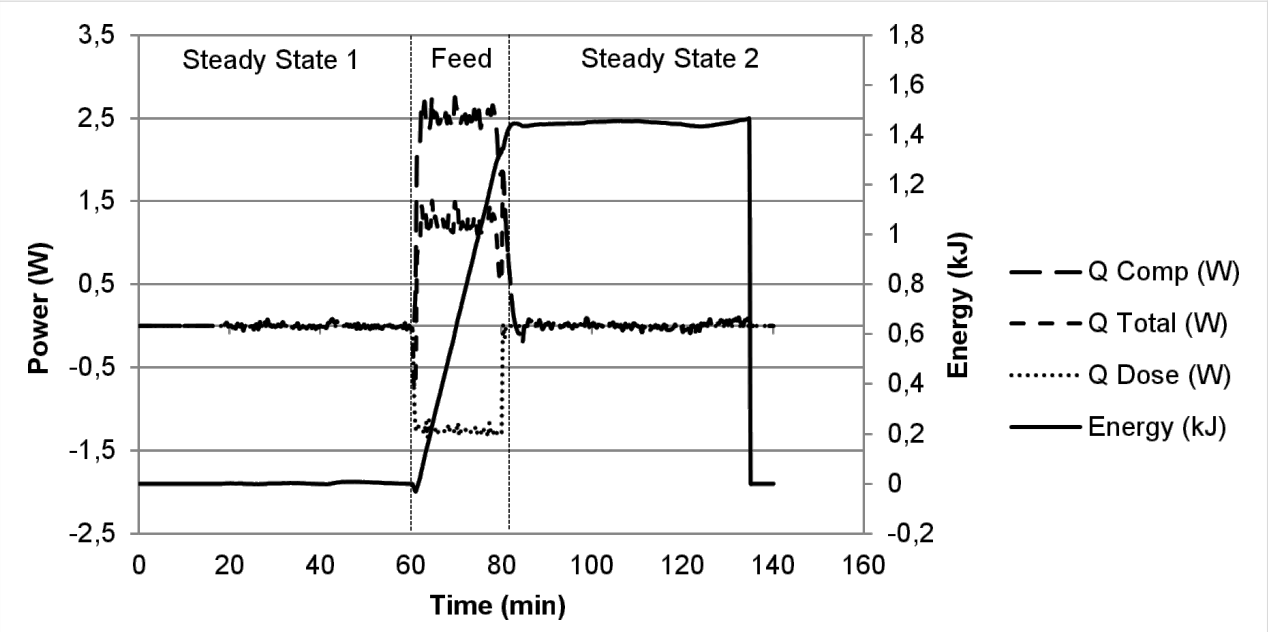

Figure 1: Calorimeter trace for the single phase reaction of morpholine (aq) and NaOCl (aq). *Q* Comp: compensatory power, *Q* Total: total power, *Q* Dose: power delivered by dosing of room temperature NaOCl (aq) to cooled reaction solution. Energy: heat energy.

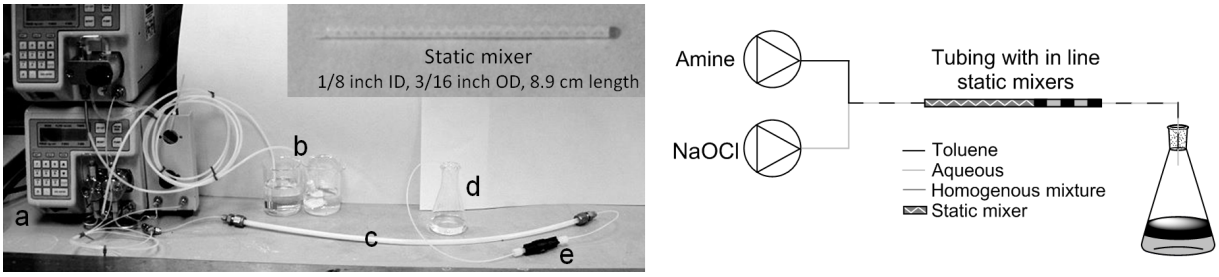

Figure 2: Meso-scale static mixer set-up for continuous *N*-chloramine formation. (a) Pumps, (b) reagent solution reservoirs, (c) reactor tube containing static mixers, (d) collection vessel, (e) back pressure regulator (75 psi).

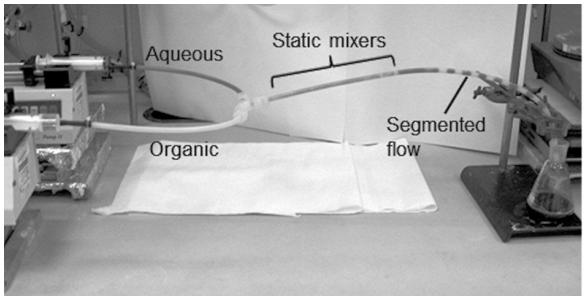

Figure 3: Effect of static mixers on biphasic solution.

time by decreasing the flow rate of reagents. The progress of the reaction was studied to determine the point at which steady state is achieved and to assess the consistency of the reaction over several reactor volumes (Figure 4). The reaction reaches steady state after 6 minutes (2 residence times) with fairly consistent conversion achieved thereafter. The *N*-chloromorpholine yield was measured by direct sampling of the toluene solution and measuring by quantitative ^{1}H NMR.

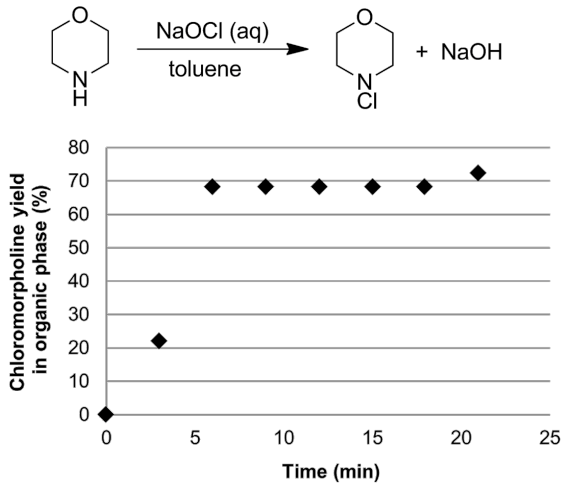

Figure 4: Progress of reaction for continuous formation of *N*-chloromorpholine. Morpholine (toluene) 0.9 M 1 mL/min, NaOCl (aq) 0.9 M, 1.1 mL/min, 6 mL total reactor volume, of which 0.8 mL is static mixers. Residence time = 2.9 min. Conversion refers to composition of organic phase of reaction solution.

Table 1 entry 1 shows the poor conversion observed using the T-piece alone, whilst higher conversions are seen with increased static mixed volume. Table 1 entry 2 shows higher chloramine formation with increased residence time (T_{res}) as a result of lower flow rates, with a maximum 89% conversion at a T_{res} of 20 min. Even at flow rates of 0.15 mL/min there appears to be intimate mixing of the aqueous–organic phases. Both intense mixing and long residence times are required because the *N*-benzylmethanamine partitions mainly in the organic phase with K_D [organic]/[aqueous] = 28.8, causing the reaction to be limited by the mass transfer rate. For example mixing in the T-piece alone gives 11% conversion with *N*-benzylmethanamine, but 46% with 1,4-morpholine; also 65% conversion is seen with 0.8 min of intense mixing of *N*-benzylmethanamine with NaOCl, whilst 68% is seen with 1,4-morpholine mixed for half this time, because it partitions more favourably into the aqueous phase with K_D = 0.01.

Substrates

The formation of a range of *N*-chloro-*N*,*N*-dialkylamines was investigated. Some were found to react relatively slowly, partly for the mass transfer reasons discussed above, and possibly for electronic and steric reasons as well. The tube reactor did not conveniently allow sufficient residence times for full conversion of amine to chloramine to be achieved, and in such cases a continuous stirred tank reactor (CSTR), able to provide longer residence times, was used instead (Figure 5 and Figure 6).

Table 2 shows reaction parameters investigated for the reaction of different amines: residence time, reactor volume, number of static mixers and molar equivalents of NaOCl. Formation of *N*-chloromorpholine and *N*-chloropiperidine (Table 2, entries 1 and 2) proceeded with high yields under short reaction times using the static mixers. *N*-chloro-*N*-methyl-*p*-toluenesulfonamide and *N*-chloro-*N*-benzylmethanamine proceeded with

Table 1: Effect of reactor parameters on chloramine formation.[a]

Entry	Product	NaOCl (equiv)	Mixed volume (mL)	Total RV (mL)	T_{res} (min)	Amine conv. (%)[b]
1	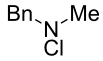	1.1	0[c] 0[c] 0.8 1.6	<0.1 6 6 6	<0.05 3 3 3	11 39 57 65
2	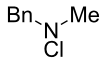	1.1	1.6	6	1.2[d] 3 6[e] 12[f] 20[g]	41 65 69 78 89
3	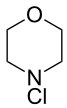	1.1	0[c] 0.8	<0.1 6	<0.05 3	46 68

[a]T_{res} = residence time, RV = reactor volume. Reaction conditions: 1 M amine in toluene and 1.1 M NaOCl (aq) at equal flow rates of 1 mL/min, room temperature. [b]Steady state conversion by NMR vs internal standard. [c]T-piece only. [d]Flow rates = 2.5 mL/min. [e]Flow rates = 0.5 mL/min. [f]Flow rates = 0.25 mL/min. [g]Flow rates = 0.15 mL/min.

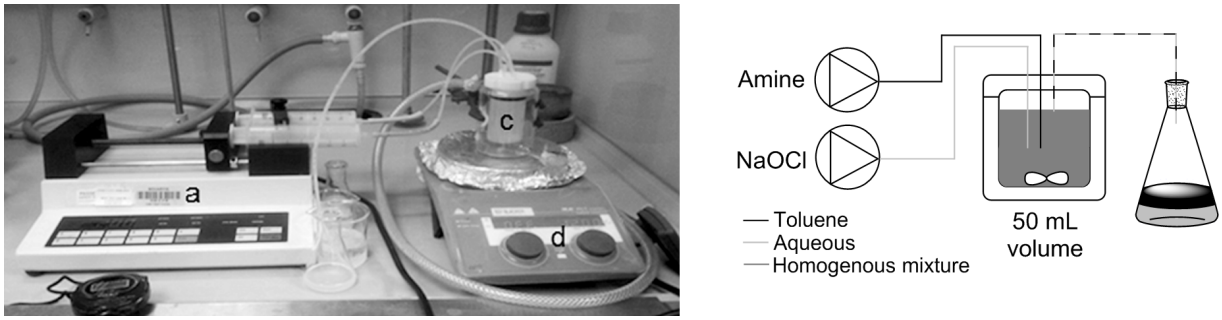

Figure 5: CSTR set-up for *N*-chloramine formation. (a) Syringe pump, (b) collection vessels, (c) reactor (50 mL), (d) stirrer plate: stirring rate 1200 rpm.

Figure 6: Interior of 50 mL CSTR.

good yields in both the tube reactor and CSTR, however, for the tube reactor 1.5 equiv NaOCl were required for complete reaction of *N*-methyl-*p*-toluenesulfonamide, and 20 min residence time was required for high yields of *N*-chloro-*N*-benzylmethylamine. Due to the low solubility of *N*-methyl-*p*-toluenesulfonamide in toluene the tube reactor was susceptible to blockage. This was overcome using EtOAc as the organic phase, and gave more consistent results. Formation of *N*-chlorodibutylamine proceeded slowly within the tube reactor and the longer residence times leant themselves to the CSTR. Table 2 entry 8 shows the need for 2 equiv NaOCl with 20 min residence time to give 35% conversion of the chloramine product with the tubular reactor. However, the conversion was improved markedly using the CSTR and enabled use of only 1.1 equiv of NaOCl to give quantitative formation of the product. The reaction of dibenzylamine with NaOCl proceeds slowly within the CSTR achieving only 40% conversion in 50 min, which may reflect its lower reactivity, since the partition coefficient is

Table 2: Formation of secondary chloramines.[a]

Entry	Product	K_D	Reactor type	Reactor vol. (mL)[b]	T_{res} (min)	Amine conv. (%)[c]	Yield (%)[c]
1[d]	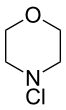	0.01	Static mixers	6 (0.8)	4	100	84
2[e]	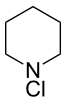	0.84	Static mixers	4 (1.6)	4	100	94
3[f]	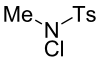	28.9	Static mixers	6 (1.6)	3	97	100
4	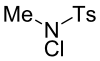	28.9	CSTR	50	50	100	72–98[g]
5	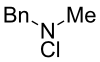	28.8	Static mixers	6 (1.6)	20	89	87
6	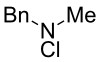	28.8	CSTR	50	25	100	100
7[h]	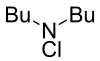	118	Static mixers	4 (1.6)	20	35	Not determined
8	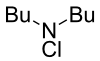	118	CSTR	50	50	100	100
9	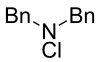	114	CSTR	50	50	40[h]	Not determined

[a]K_D = [amine] in organic/[amine] in aqueous phase. Reaction conditions: Equal flow rates of amine and NaOCl solutions used. 1 M amine in toluene and 1.1 M NaOCl (aq) were used. Reactions conducted at room temperature. [b]Static mixed volume in parentheses. [c]Determined by NMR vs internal standard. [d]NaOCl (aq) 2.2 M, flow rate 0.5 mL/min, amine 1 M in toluene, flow rate 1 mL/min. [e]1.5 M NaOCl (aq). [f]EtOAc solvent instead of toluene used due to solubility of amine. [g]Low solubility of starting material in toluene caused problems with amine feed giving variation in yields. [g]2 M NaOCl (aq) used. [h]40% *N*-chlorodibenzylamine and 60% residual dibenzylamine observed by ^{1}H NMR, no other products observed.

similar to that of dibutylamine. The productivities of *N*-chloramine formation are in the range of 0.04–0.06 mol/h.

Green metrics

A key driver within the chemical industry is the need for greener, more sustainable processes. In order to assess the sustainability of the continuous process for chloramine formation described in this publication, the metrics of the reaction were assessed and compared with existing literature procedures [35]. The results are summarised in Table 3.

The yields of the continuous *N*-chloramine process were high, and comparable to literature batch procedures. The atom economy of our process was increased compared to the use of *N*-chlorosuccinimide [3], or NaOCl/*t*-BuOH, Table 3, entries 2 and 3 [20]. There are also improvements to the total mass intensity of the flow procedure, primarily by avoiding work-up and purification procedures. The mass efficiency remains low, but is comparable to literature procedures. Whilst increasing the reactant concentrations is possible, the safe removal of the heat of reaction must be considered, moreover the flow process is much more productive than batch. Nevertheless the *N*-chloramine solution that is generated should be used directly, so is ideally coupled with a second flow process, and the results of this will be reported elsewhere.

Conclusion

The facile synthesis of *N*,*N*-dialkyl-*N*-chloramines is described using either a tubular reactor with static mixers or a continuous stirred tank reactor; both are able to promote efficient mixing of

Table 3: Comparison of green metrics for different chloramine formation procedures.

Entry	1[a]	2[b]	3[c]	4[d]	5[e]
Amine	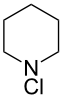	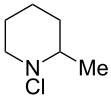	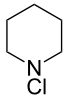	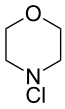	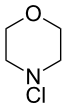
Chlorine source	NaOCl	NaOCl/ *t*-BuOH	*N*-chloro succinimide	NaOCl	NaOCl
Reactor	Flow	Batch	Batch	Batch	Flow
Reaction solvent	toluene, H_2O	TBME, H_2O	Et_2O[f]	H_2O	toluene, H_2O
Work-up solvents	–	H_2O, brine	H_2O	Et_2O	–
Conversion	100	100	100	100	100
Yield	94	100	90	88	84
Reaction mass efficiency	57.73	63.42	46.37	63.44	60.24
Atom economy	74.94	53.94	54.69	75.25	75.25
Mass intensity: total	18.17	37.5	80.3	12.39	15.09
Mass intensity: reaction	18.17	7.56	33.71	8.43	15.09
Mass intensity: reaction chemicals	1.73	2.03	2.16	1.58	1.66
Mass intensity: reaction solvents	16.43	5.54	31.55	6.85	13.43
Mass intensity: work-up	–	29.94	46.58	3.96	–

[a]See Table 2, entry 3. [b]Reference [20]. [c]Reference [36]. [d]Reference [11]. [e]See Table 2, entry 1. [f]DCM has also been used for reactions of other amines with NCS [3].

the biphasic reaction solution. Those amines which partition mainly in the organic phase required longer reaction times to compensate for the reduced mass transfer between the organic and aqueous phases, and good yields with useful productivities were achieved for most. The green metrics of the reaction have been assessed and compared to existing procedures for chloramine formation, and have shown the continuous process is improved over previous procedures. Work to expand the scope of *N*-chloramines, and their subsequent use in flow reactions with alkenes to make amines, aldehydes to make amides, and base to make imines is ongoing.

Experimental

All reagents were used as received from suppliers without purification. Sodium hypochlorite solution 10–15% available chlorine was purchased from Sigma-Aldrich. The accurate NaOCl concentration was determined by titration (Supporting Information File 1) and diluted to the required concentration with distilled water. $CDCl_3$ purchased from Sigma-Aldrich was used for NMR analysis. NMR spectra (^1H and ^{13}C) were obtained on either a Bruker Advance 500 MHz, 400 MHz or a Bruker DPX 300 MHz spectrometer. NMR spectra were referenced to either TMS or $CHCl_3$. The partitioning of the amine reagents in the organic phase of a biphasic organic/aqueous solution was determined by GC analysis using an Agilent HP 6890 with FID (Supporting Information File 1). Calorimetry experiments were carried out using HEL AutoMATE parallel reactors with HEL WinISO 2225 and HEL IQ 1.2.16 software. For the tube reactor, Harvard syringe pumps (model 981074) or JASCO PU-980 HPLC pumps were connected via a syringe and 1.5 inch, 21 guage disposable needle to PTFE tubing with 1/16 inch OD. The 1/16 inch stainless steel T-piece and stainless steel 1/16 inch to 1/4 inch increasing connector were obtained from Swagelok. The reactor tube comprises of PTFE tubing 1/4 inch OD and in-line plastic static mixers supplied by Nordson EFD (3/16 inch OD, mixer element diameter 1/8 inch, 3.5 inch length). For the CSTR, the same Harvard syringe pumps were used along with PTFE tubing with 1/8 inch OD.

General procedure for *N*-chloramine formation using the tube reactor and static mixers

The required number of static mixers (3/16 inch OD, 1/8 inch mixing element diameter 3.5 inch length) was inserted into a length of 1/4 inch PTFE tubing to give the overall required reactor volume. The reactor was connected to 1/16 inch tubing via a 1/4–1/16 inch reducing adapter. The tubing was split with a T-piece to 2 pumps (either piston or syringe pumps). A 1 M solution of amine in toluene was prepared and fed via pump 1 at

the required flow rate. A 1.1 M solution of aqueous NaOCl was fed via pump 2 at the required flow rate. The reaction solution was flowed through the reactor and collected in residence time fractions. The organic phase was separated from each fraction to avoid further interaction with the NaOCl solution. The organic phase was analysed by ^{1}H NMR. For non-volatile products yields were obtained by removal of toluene from the organic phase of each residence time fraction and weighing the resulting product. For volatile products yields were obtained by ^{1}H NMR analysis. 100 μL or the organic phase was weighed and analysed by ^{1}H NMR. The ratio of toluene/starting material/product and mass of 100 μL of the solution was used to determine the *N*-chloramine concentration in the solution. From this the yield of *N*-chloramine in the full organic phase could be determined.

General procedure for *N*-chloramine formation using the CSTR

Through the lid of a 50 mL jacketed glass vessel containing a stirrer bar was inserted 2 lengths of 1/8 inch PTFE tubing connected to syringe pumps. A third length of tubing was inserted so that it ended flush with the base of the lid to act as an overflow tube out of the reactor into a collection vessel. The reactor was secured on a stirrer plate.

A 1 M solution of amine in toluene was prepared and fed via pump 1 at the required flow rate. A 1.1 M solution of aqueous NaOCl was fed via pump 2 at the required flow rate. The reaction solution was flowed into the reactor, and once full was eluted from the reactor via the overflow tube and collected. The solution was collected in residence time fractions. The organic phase was separated from each fraction to avoid further interaction with the NaOCl solution. The organic phase was analysed by ^{1}H NMR. For non-volatile products yields were obtained by removal of toluene from the organic phase of each residence time fraction and weighing the resulting product. For volatile products, yields were obtained by ^{1}H NMR analysis. 100 μL or the organic phase was weighed and analysed by ^{1}H NMR. The ratio of toluene/starting material/product and mass of 100 μL of the solution was used to determine the *N*-chloramine concentration in the organic solution. From this the yield of *N*-chloramine in the full organic phase could be determined.

N-Chloro-1,4-morpholine

Prepared according to the general procedure using the tube reactor with 2 static mixers, a 6 mL reactor volume and a residence time of 4 min, 2.2 M NaOCl (aq) at 0.5 mL/min and 1 M morpholine in toluene at 1 mL/min. Due to the high volatility of *N*-chloromorpholine and its reported instability the product was not isolated and was instead obtained as a solution in toluene (0.84 M, 84%) by separation of the organic phase form the aqueous phase of the reaction solution. The yield of product was determined by NMR analysis as in the typical procedure for volatile products. The toluene solution was analysed by NMR and data matches that reported in the literature [17]. ^{1}H NMR ($CDCl_3$, 500 MHz) δ ppm 3.69 (br s, 4H, CH_2OCH_2), 3.12 (br s, 4H CH_2NClCH_2); ^{13}C NMR ($CDCl_3$, 125 MHz) δ ppm 67.72 (CH_2OCH_2), 63.03 (CH_2NClCH_2).

N-Chloropiperidine

Prepared according to the general procedure using the tube reactor with 4 static mixers, a 4 mL reactor volume and a residence time of 4 min, 1.5 M NaOCl (aq) at 0.5 mL/min and 1 M piperidine in toluene at 0.5 mL/min. Due to the high volatility of *N*-chloropiperidine the product was not isolated and was instead obtained as a solution in toluene (0.94 M, 94%) by separation of the organic phase from the aqueous phase of the reaction solution. The yield of product was determined by NMR analysis as in the typical procedure for volatile products. The toluene solution was analysed by NMR and data matches that reported in the literature [17]. ^{1}H NMR ($CDCl_3$, 300 MHz) δ ppm 3.49–2.63 (br m, 4H, CH_2NClCH_2), 1.84 (quin, J = 5.8 Hz, 4H, 2 x $CH_2CH_2CH_2$), 1.75–1.32 (br m, 2H, $NCH_2CH_2CH_2$); ^{13}C NMR ($CDCl_3$, 125 ppm) δ ppm 64.00 (2 × CH_2NCl), 27.68 (2 × CH_2CH_2NCl), 23.07 ($CH_2(CH_2)_2NCl$).

N-Benzyl-*N*-chloromethanamine

Prepared according to the general procedures. 1) Tube reactor with 4 static mixers, a 6 mL reactor volume and a residence time of 3 min, 1.1 M NaOCl (aq) at 0.15 mL/min and 1 M *N*-benzylmethylamine in toluene at 0.15 mL/min. 2) CSTR with a reactor volume of 50 mL, and residence time of 25 min. 1.1 M NaOCl (aq) at 1 mL/min and 1 M *N*-benzylmethylamine in toluene at 1 mL/min were used. Due to the volatility of *N*-benzyl-*N*-chloromethanamine the product was not isolated and was instead obtained as a solution in toluene (1 M, quantitative yield) by separation of the organic phase from the aqueous phase of the reaction solution. The yield of product was determined by NMR analysis as in the typical procedure or volatile products. The toluene solution was analysed by NMR and data matches that reported in the literature [17]. ^{1}H NMR ($CDCl_3$, 300 MHz) δ ppm 7.32–7.28 (m, 5H, $CHAr$), 3.99 (s, 2H, CH_2), 2.88 (s, 3H, CH_3); ^{13}C NMR ($CDCl_3$, 125 MHz) δ ppm 139.37 (CAr), 128.58 (2 × $CHAr$), 128.49 (2 × $CHAr$), 127.32 ($CHAr$), 55.85 (CH_2), 35.68 (CH_3).

N-Chloro-*N*-methyl-*p*-toluenesulfonamide

Prepared according to the general procedures. 1) Tube reactor with 4 static mixers, a 6 mL reactor volume and a residence time of 3 min, 1.5 M NaOCl (aq) at 1 mL/min and 1 M *N*-benzylmethylamine in EtOAc at 1 mL/min. 2) CSTR with a

reactor volume of 50 mL, and residence time of 25 min. 1.1 M NaOCl (aq) at 1 mL/min and 1 M *N*-benzylmethylamine in toluene at 1 mL/min were used. The product was isolated for each reactor volume by separation of the organic phase for each reactor volume of solution and removal of the solvent by rotary evaporation to give a white solid (1 reactor volume gives 666 mg, 3.0 mmol, quantitative yield). NMR data matches that reported in the literature [37]. ^{1}H NMR ($CDCl_3$, 500 MHz) δ ppm 7.82 (d, J = 8.4 Hz, 2H, C*H*Ar), 7.42 (d, J = 8.4 Hz, 2H, C*H*Ar), 3.09 (s, 3H, NCH_3), 2.48 (s, 3H, Ar-CH_3); ^{13}C NMR ($CDCl_3$, 125 MHz) δ ppm 145.75 (*C*Ar), 129.80 (2*C*HAr), 129.78 (2 *C*HAr), 128.28 (*C*Ar), 45.51 (N*C*H$_3$), 21.70 (Ar*C*H$_3$).

N-Chloro-*N*,*N*-dibutylamine

Prepared according to the general procedures. 1) Tube reactor with 4 static mixers, a 4 mL reactor volume and a residence time of 20 min, 2 M NaOCl (aq) at 0.1 mL/min and 1 M dibutylamine in toluene at 0.1 mL/min. 2) CSTR with a reactor volume of 50 mL, and residence time of 50 min. 1.1 M NaOCl (aq) at 0.5 mL/min and 1 M dibutylamine in toluene 0.5 mL/min were used. The product was isolated for each reactor volume by separation of the organic phase for each reactor volume of solution and removal of the solvent by rotary evaporation to give a colourless oil (1 reactor volume gives 8.17 g, 50 mmol, quantitative yield). NMR data matches that reported in the literature [17]. ^{1}H NMR ($CDCl_3$, 300 MHz) δ ppm 3.07–3.02 (m, 4H, 2 × NClCH_2), 1.85–1.74 (m, 4H, 2 × NCH$_2$CH_2CH$_2$), 1.54–1.45 (m, 4H, 2 × CH_2CH$_3$), 1.11–1.05 (t, J = 7.4 Hz, 6H, 2 × CH_3); ^{13}C NMR ($CDCl_3$, 125 MHz) δ ppm 64.04 (2 × *C*H$_2$NCl), 30.01 (2 × *C*H$_2$CH$_2$NCl), 20.03 (2 × *C*H$_2$(CH$_2$)$_2$NCl), 13.90 (2 × *C*H$_3$).

N-Chloro-*N*,*N*-dibenzylamine

Prepared according to the general procedure using the CSTR with a reactor volume of 50 mL, and residence time of 50 min, 1.1 M NaOCl (aq) at 0.5 mL/min and 1 M dibenzylamine in toluene 0.5 mL/min were used. The product was not isolated and was instead obtained as a solution in toluene (0.4 M, 40% conversion) by separation of the organic phase from the aqueous phase of the reaction solution and removal of the solvent by rotary evaporation. The conversion to product was determined by NMR analysis of dried product (orange oil) and data obtained matches that reported in the literature [38]. ^{1}H NMR ($CDCl_3$, 300 MHz) 40% conversion to chloramine δ ppm 7.56–7.44 (m, 20H, C*H*Ar in amine and chloramine), 4.28 (s, 4H, 2 × NClCH_2 in chloramine), 3.80 (s, 4H 2 × NHCH_2 in amine); ^{13}C NMR ($CDCl_3$, 125 MHz) δ ppm chloramine: 137.17 (2 × *C*Ar), 129.18 (4 × *C*HAr), 128.52 (4 × *C*HAr), 127.95 (2 × *C*HAr), 67.24 (2 × *C*H$_2$NCl); amine: 136.26 (2 × *C*Ar), 128.47 (4 × *C*HAr), 128.39 (4 × *C*HAr), 127.19 (2 × *C*HAr), 52.94 (2 × *C*H$_2$NH).

Supporting Information

Supporting Information File 1

Details of the titration method for determination of NaOCl strength, determination of amine partition coefficients, GC analytical conditions and calorimetry.
[http://www.beilstein-journals.org/bjoc/content/supplementary/1860-5397-11-262-S1.pdf]

Acknowledgements

The research for this work has received funding from the Innovative Medicines Initiative joint undertaking project Chem21 under *grant agreement* no. 115360, resources of which are composed of financial contribution from the European Union's Seventh Framework Programme (FP7/2007-2013) and EFPIA companies in kind contribution.

References

1. Chemler, S. R.; Bovino, M. T. *ACS Catal.* **2013,** *3,* 1076–1091. doi:10.1021/cs400138b
2. Göttlich, R. *Synthesis* **2000,** 1561–1564. doi:10.1055/s-2000-7605
3. Heuger, G.; Kalsow, S.; Göttlich, R. *Eur. J. Org. Chem.* **2002,** 1848–1854. doi:10.1002/1099-0690(200206)2002:11<1848::AID-EJOC1848>3.0.CO;2-V
4. Liu, X.-Y.; Gao, P.; Shen, Y.-W.; Liang, Y.-M. *Adv. Synth. Catal.* **2011,** *353,* 3157–3160. doi:10.1002/adsc.201100382
5. Porcheddu, A.; De Luca, L. *Adv. Synth. Catal.* **2012,** *354,* 2949–2953. doi:10.1002/adsc.201200659
6. Vanjari, R.; Guntreddi, T.; Singh, K. N. *Green Chem.* **2014,** *16,* 351–356. doi:10.1039/C3GC41548A
7. Vanjari, R.; Guntreddi, T.; Singh, K. N. *Org. Lett.* **2013,** *15,* 4908–4911. doi:10.1021/ol4023886
8. Bartsch, R. A.; Cho, B. R. *J. Am. Chem. Soc.* **1979,** *101,* 3587–3591. doi:10.1021/ja00507a025
9. Anderson, P. S.; Lundell, G. F.; Cias, J. L.; Robinson, F. M. *Tetrahedron Lett.* **1971,** *12,* 2787–2790. doi:10.1016/S0040-4039(01)96980-1
10. Qin, Q.; Yu, S. *Org. Lett.* **2015,** *17,* 1894–1897. doi:10.1021/acs.orglett.5b00582
11. Lindsay Smith, J. R.; McKeer, L. C.; Taylor, J. M. *Org. Synth.* **1989,** *67,* 222–228. doi:10.15227/orgsyn.067.0222
12. Cossy, J.; Tresnard, L.; Gomez Pardo, D. *Tetrahedron Lett.* **1999,** *40,* 1125–1128. doi:10.1016/S0040-4039(98)02585-4
13. Leal, R. A.; Beaudry, D. R.; Alzghari, S. K.; Sarpong, R. *Org. Lett.* **2012,** *14,* 5350–5353. doi:10.1021/ol302535r
14. Enders, D.; Schaumann, E., Eds. *Science of Science - Houben-Weyl Methods of Molecular Transformations: Compounds with one saturated carbon-heteroatom bond;* Thieme: Stuuttgart, Germany, 2008; Vol. 40b, pp 901–919.
15. Urben, P. G.; Pitt, M. J., Eds. *Bretherick's Handbook of Reactive Chemical Hazards;* Academic Press: Oxford, UK, 2006; Vol. 2, pp 167–168.
16. Kovacic, P.; Lowery, M. K.; Field, K. W. *Chem. Rev.* **1970,** *70,* 639–665. doi:10.1021/cr60268a002

17. Barker, T. J.; Jarvo, E. R. *J. Am. Chem. Soc.* **2009,** *131,* 15598–15599. doi:10.1021/ja907038b
18. Paquette, L. A., Ed. *Encyclopedia of Reagents for Organic Synthesis;* John Wiley and Sons: New York, 1995; Vol. 2.
19. Zimmer, H.; Audrieth, L. F. *J. Am. Chem. Soc.* **1954,** *76,* 3856–3857. doi:10.1021/ja01643a082
20. Zhong, Y.-L.; Zhou, H.; Gauthier, D. R.; Lee, J.; Askin, D.; Dolling, U. H.; Volante, R. P. *Tetrahedron Lett.* **2005,** *46,* 1099–1101. doi:10.1016/j.tetlet.2004.12.088
21. Paquette, L. A., Ed. *Encyclopedia of Reagents for Organic Synthesis;* John Wiley and Sons: New York, 1995; Vol. 2, pp 889–891.
22. Zhu, R.; Xu, Z.; Ding, W.; Liu, S.; Shi, X.; Lu, X. *Chin. J. Chem.* **2014,** *32,* 1039–1048. doi:10.1002/cjoc.201400471
23. Padegimas, S. J.; Kovacic, P. *J. Org. Chem.* **1972,** *37,* 2672–2676. doi:10.1021/jo00982a008
24. Pedder, D. J.; Fales, H. M.; Jaouni, T.; Blum, M.; MacConnell, J.; Crewe, R. M. *Tetrahedron* **1976,** *32,* 2275–2279. doi:10.1016/0040-4020(76)88001-5
25. Lee, S. J.; Terrazas, M. S.; Pippel, D. J.; Beak, P. *J. Am. Chem. Soc.* **2003,** *125,* 7307–7312. doi:10.1021/ja0300463
26. Adamo, A.; Heider, P. L.; Weeranoppanant, N.; Jensen, K. F. *Ind. Eng. Chem. Res.* **2013,** *52,* 10802–10808. doi:10.1021/ie401180t
27. Hamlin, T. A.; Lazarus, G. M. L.; Kelly, C. B.; Leadbeater, N. E. *Org. Process Res. Dev.* **2014,** *18,* 1253–1258. doi:10.1021/op500190j
28. Nagy, K. D.; Shen, B.; Jamison, T. F.; Jensen, K. F. *Org. Process Res. Dev.* **2012,** *16,* 976–981. doi:10.1021/op200349f
29. Schwolow, S.; Hollmann, J.; Schenkel, B.; Röder, T. *Org. Process Res. Dev.* **2012,** *16,* 1513–1522. doi:10.1021/op300107z
30. Weil, I.; Morris, J. C. *J. Am. Chem. Soc.* **1949,** *71,* 1664–1671. doi:10.1021/ja01173a033
31. Zhang, Y.; Born, S. C.; Jensen, K. F. *Org. Process Res. Dev.* **2014,** *18,* 1476–1481. doi:10.1021/op500158h
32. Darvas, F.; Dorman, G.; Hessel, V. *Flow Chemistry Fundamentals;* Walter De Gruyter and Co KG: Berlin, 2014.
33. Van Waes, F. E. A.; Seghers, S.; Dermaut, W.; Cappuyns, B.; Stevens, C. V. *J. Flow Chem.* **2014,** *4,* 118–124. doi:10.1556/JFC-D-14-00006
34. In-line static mixers obtained from Nordsen EFD. 3/16 inch OD, 1/8 inch ID, 839 cm length.
35. McElroy, C. R.; Constantinou, A.; Jones, L. C.; Summerton, L.; Clark, J. H. *Green Chem.* **2015,** *17,* 3111–3121. doi:10.1039/C5GC00340G
36. Grandl, J.; Sakr, E.; Kotzyba-Hibert, F.; Krieger, F.; Bertrand, S.; Bertrand, D.; Vogel, H.; Goeldner, M.; Hovius, R. *Angew. Chem., Int. Ed.* **2007,** *46,* 3505–3508. doi:10.1002/anie.200604807
37. Pastoriza, C.; Antelo, J. M.; Crugeiras, J. *J. Phys. Org. Chem.* **2013,** *26,* 551–559. doi:10.1002/poc.3127
38. Pandiancherri, S.; Lupton, D. W. *Tetrahedron Lett.* **2011,** *52,* 671–674. doi:10.1016/j.tetlet.2010.11.142

License and Terms

BEILSTEIN JOURNAL OF ORGANIC CHEMISTRY

A convergent, umpoled synthesis of 2-(1-amidoalkyl)pyridines

Tarn C. Johnson and Stephen P. Marsden*

Letter

Open Access

Address:
Institute of Process Research and Development, School of Chemistry, University of Leeds, Woodhouse Lane, Leeds LS2 9JT, UK

Email:
Stephen P. Marsden* - s.p.marsden@leeds.ac.uk

* Corresponding author

Keywords:
azlactones; pyridines; pyridine *N*-oxides; substitution

Beilstein J. Org. Chem. **2016,** *12,* 1–4.
doi:10.3762/bjoc.12.1

Received: 05 October 2015
Accepted: 21 December 2015
Published: 04 January 2016

This article is part of the Thematic Series "Sustainable catalysis".

Guest Editor: N. Turner

Abstract

A convenient, one-pot, two-component synthesis of 2-(1-amidoalkyl)pyridines is reported, based upon the substitution of suitably-activated pyridine *N*-oxides by azlactone nucleophiles, followed by decarboxylative azlactone ring-opening. The synthesis obviates the need for precious metal catalysts to achieve a formal enolate arylation reaction, and constitutes a formally 'umpoled' approach to this valuable class of bioactive structures.

Introduction

Pyridines constitute the most frequently observed class of heterocycles found in pharmaceutical products [1]. As such, there is significant demand for synthetic methods that enable access both to structurally novel and diverse substituted pyridines for new medicines discovery, and for the development of clean, efficient and robust methods for their manufacture on large scale. Pyridines bearing a 1-amidoalkyl substituent at the 2-position are found in numerous biologically active natural products such as the antitumour antibiotic kedarcidin chromophore **1** [2] and the RNA polymerase inhibitor cyclothiazomycin B1 **2** [3] (Figure 1). Additionally, the motif is commonly incorporated into synthetic pharmaceutical candidates, for example in the factor XIa inhibitor **3** [4], the orally-active renin inhibitor **4** [5] and the threonine tyrosine kinase inhibitor CFI-401870 (**5**) [6].

The 2-(1-amidoalkyl)pyridines are almost always synthesised by acylation of the related 2-(1-aminoalkyl)pyridines, which can be prepared by reduction of ketimines derived from 2-acylpyridines [5] or 2-cyanopyridines [6], addition of carbon nucleophiles to aldimines derived from pyridine-2-carboxaldehydes [4,7], or nucleophilic substitution of 2-(1-hydroxyalkyl)pyridines [8]. Alternatively, acyclic precursors bearing the amidoalkyl (or protected aminoalkyl) substituent can be applied in de novo construction of the pyridine ring, exemplified by approaches to the core of the cyclothiazomycins [9,10]. Regardless of the method employed, these are multistep protocols, frequently employing moisture-sensitive organometallic agents or reducing agents. In this paper, we report a new one-pot, two-component synthesis of 2-(1-amidoalkyl)pyridines that arises from a formally 'umpoled' coupling

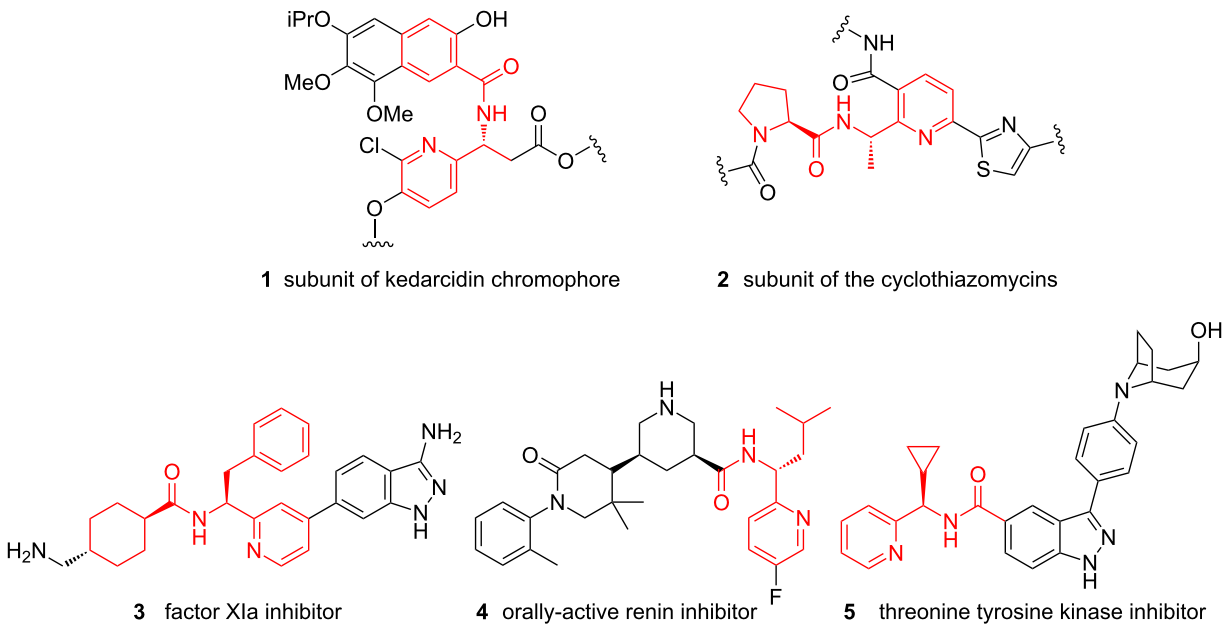

Figure 1: Examples of naturally-occurring and synthetic bioactive (amidoalkyl)pyridines.

of an α-(amidoalkyl) anion equivalent with a pyridyl electrophile.

Results and Discussion

Reaction discovery

Our research group has a longstanding interest in the synthesis of α,α-disubstituted amino acids [11-15], and in particular has developed methods for the preparation of α-aryl variants by palladium-catalysed enolate arylation reactions [13-15]. More recently, we have sought to develop more sustainable methods for the arylation of amino acid enolate equivalents that avoid the use of precious metal salts and expensive bespoke ligands, based upon the electrophilic activation of pyridine *N*-oxides and subsequent reaction with acidic carbon nucleophiles [16-20]. Specifically, we have demonstrated that α-pyridyl,α-alkyl-amino acid derivatives can be prepared in a one-pot three component coupling between readily-available azlactones and pyridine *N*-oxides in the presence of *p*-toluenesulfonyl chloride as an activating agent, followed by opening of the arylated azlactone intermediate with nucleophiles such as alcohols, primary and secondary amines, and *N*,*O*-dialkylhydroxylamines [21] (Scheme 1). However, in the reaction of alanine-derived azlactone **6** with 4-methylpyridine *N*-oxide (**7**) we found that when water (in the form of 1 M HCl) was employed as a nucleophile, the product isolated was in fact the 2-(1-benzamidoethyl)-4-methylpyridine (**8a**), formed by facile decarboxylation of the intermediate pyridylamino acid **9** (Nu = OH) [22,23]. After some minor process optimisation, this product was isolated in 64% yield.

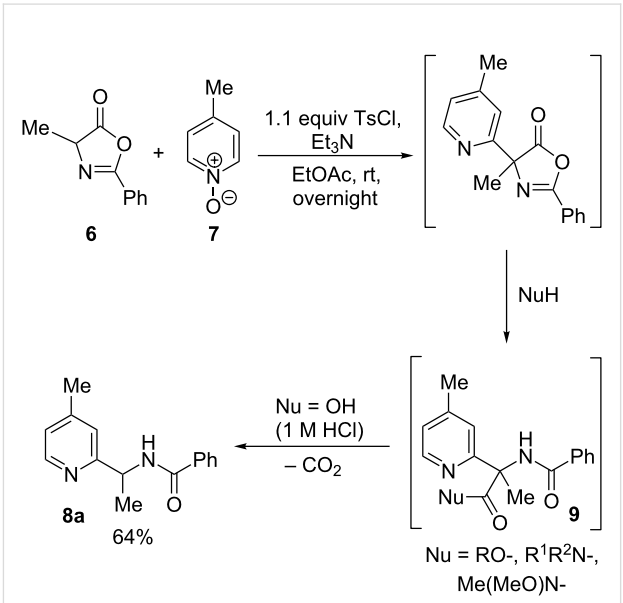

Scheme 1: Discovery of the azlactone arylation/decarboxylative hydrolysis approach to 2-(1-amidoalkyl)pyridines.

We recognised that this constitutes a formally 'umpoled' [24] coupling of an α-amino- or amidoalkyl anion [25-27] with a pyridyl electrophile and hence would complement existing synthetic methods. Given the ready availability of azlactones bearing differential functionality at C2 and C4, a wide range of 2-(1-amidoalkyl)pyridines should become available and we elected to exemplify this process.

Substrate scope

We first examined variation of azlactone substituents in their reaction with 4-methylpyridine *N*-oxide (Scheme 2). Pleasingly, bulkier C4-substituents such as benzyl or isobutyl groups (derived from phenylalanine and leucine, respectively) were well tolerated, with isolated yields for the products **8b** and **8c** of 75% and 69%, respectively. Variation of the C2-azlactone substituent was also evaluated: swapping a phenyl substituent for a *tert*-butyl substituent gave rise to the pivaloyl amide **8d**, albeit in a modest 36% yield.

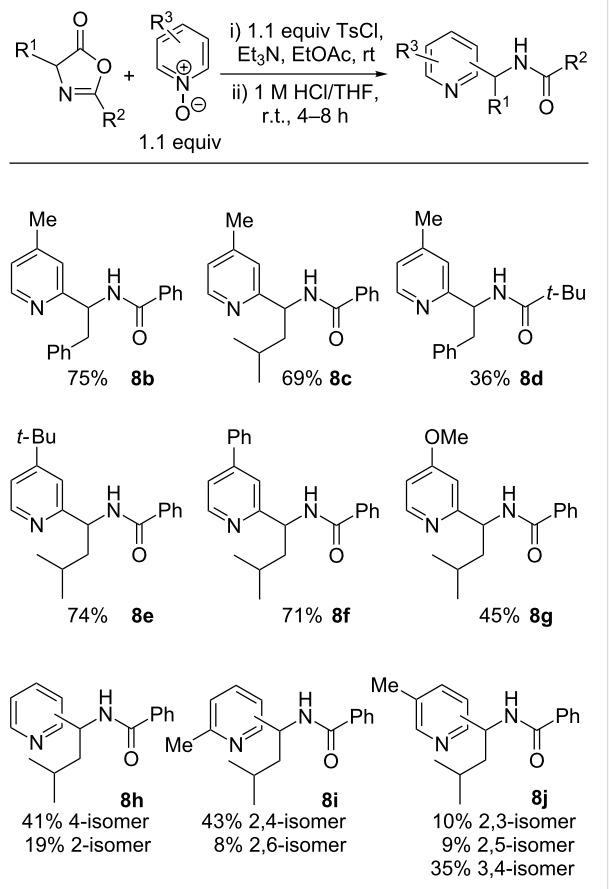

Scheme 2: Substrate scope of the direct amidoalkylation of pyridine *N*-oxides.

Next we examined the behaviour of different 4-substituted pyridine *N*-oxides (either commercially available or prepared by oxidation of the corresponding pyridine with *m*-chloroperbenzoic acid) with a leucine-derived azlactone. The presence of bulkier alkyl or aromatic substituents was well tolerated, giving products **8e** and **8f** in good yield; however, the presence of an electron-donating methoxy group led to a lower yield of **8g** (45%). This may reflect the lower electrophilicity of the activated pyridine *N*-oxide, which may allow non-productive azlactone decomposition pathways to compete with the desired substitution.

Finally, we examined the regiochemical outcome of the reaction of pyridine *N*-oxides with other substitution patterns. Pyridine *N*-oxide itself delivered a ca. 2:1 mixture of the separable 4- and 2-substituted isomers of **8h** in overall 60% yield. Statistically corrected for the available reactive positions, this reflects an inherent 4:1 preference for reaction at the 4-position, which may in part be due to steric hindrance at the C2-positions by the activated *N*-oxide. The high C4-selectivity was also evident in the formation of a >5:1 selectivity for the formation of the 2,4-isomer of **8i** over the 2,6-isomer when 2-methylpyridine *N*-oxide was used as substrate. Finally, the use of 3-methylpyridine *N*-oxide gave a ca. 7:2:2 mixture of 3,4-:2,3-:2,5-isomers of **8j**. Although the regioselectivities are not exceptionally high, the ready chromatographic separation of the various isomers makes this a synthetically tractable approach to 4-substituted (1-amidoalkyl)pyridine derivatives.

Conclusion

In summary, we have demonstrated a new umpoled disconnection for the one-pot, two-component synthesis of 2-(1-amidoalkyl)pyridines using simple, widely-available coupling partners without the requirement for expensive or critically-available reagents and catalysts. The reactions display good generality over 10 examples (36–75% yields, average 60%). Given the medicinal relevance of the (amidoalkyl)pyridine products, and the convergent nature of the reaction, we believe that the method should find ready application in the concise synthesis of bioactive molecules.

Supporting Information

Supporting Information File 1

Experimental procedures and full compound characterisation data for products **8a**–**j**.
[http://www.beilstein-journals.org/bjoc/content/supplementary/1860-5397-12-1-S1.pdf]

Supporting Information File 2

Copies of spectra for products **8a**–**j**.
[http://www.beilstein-journals.org/bjoc/content/supplementary/1860-5397-12-1-S2.pdf]

Acknowledgements

The research for this work has received funding from the Innovative Medicines Institute joint undertaking project CHEM21 under grant agreement no. 115360, resources of which are composed of financial contribution from the Euro-

pean Union's Seventh Framework Programme (FP7/2007-2013) and EFPIA companies in kind contribution.

References

1. Carey, J. S.; Laffan, D.; Thomson, C.; Williams, M. T. *Org. Biomol. Chem.* **2006,** *4,* 2337–2347. doi:10.1039/b602413k
2. Leet, J. E.; Schroeder, D. R.; Langley, D. R.; Colson, K. L.; Huang, S.; Klohr, S. E.; Lee, M. S.; Golik, J.; Hofstead, S. J.; Doyle, T. W.; Matson, J. A. *J. Am. Chem. Soc.* **1993,** *115,* 8432–8443. doi:10.1021/ja00071a062
3. Hashimoto, M.; Murakami, T.; Funahashi, K.; Tokunaga, T.; Nihei, K.-i.; Okuno, T.; Kimura, T.; Naoki, H.; Himeno, H. *Bioorg. Med. Chem.* **2006,** *14,* 8259–8270. doi:10.1016/j.bmc.2006.09.006
4. Corte, J. R.; Fang, T.; Hangeland, J. J.; Friends, T. J.; Rendina, A. R.; Luettgen, J. M.; Bozarth, J. M.; Barbera, F. A.; Rossi, K. A.; Wei, A.; Ramamurthy, V.; Morin, P. E.; Seiffert, D. A.; Wexler, R. R.; Quan, M. L. *Bioorg. Med. Chem. Lett.* **2015,** *25,* 925–930. doi:10.1016/j.bmcl.2014.12.050
5. Mori, Y.; Ogawa, Y.; Mochikuzi, A.; Nakamura, Y.; Fujimoto, T.; Sugita, C.; Miyazaki, S.; Tamaki, K.; Nagayama, T.; Nagai, Y.; Inoue, S.-i.; Chiba, K.; Nishi, T. *Bioorg. Med. Chem.* **2013,** *21,* 5907–5922. doi:10.1016/j.bmc.2013.06.057
6. Liu, Y.; Lang, Y.; Patel, N. K.; Ng, G.; Laufer, R.; Li, S.-W.; Edwards, L.; Forrest, B.; Sampson, P. B.; Feher, M.; Ban, F.; Awrey, D. E.; Beletskaya, I.; Mao, G.; Hodgson, R.; Plotnikova, O.; Qiu, W.; Chirgadze, N. Y.; Mason, J. M.; Wei, X.; Lin, D. C.-C.; Che, Y.; Kiarash, R.; Madeira, B.; Fletcher, G. C.; Mak, T. W.; Bray, M. R.; Pauls, H. W. *J. Med. Chem.* **2015,** *58,* 3366–3392. doi:10.1021/jm501740a
7. Ren, F.; Hogan, P. C.; Anderson, A. J.; Myers, A. G. *J. Am. Chem. Soc.* **2007,** *129,* 5381–5383. doi:10.1021/ja071205b
8. Shin, C.-g.; Okabe, A.; Ito, A.; Ito, A.; Yonezawa, Y. *Bull. Chem. Soc. Jpn.* **2002,** *75,* 1583–1596. doi:10.1246/bcsj.75.1583
9. Zou, Y.; Liu, Q.; Deiters, A. *Org. Lett.* **2011,** *13,* 4352–4355. doi:10.1021/ol201682k
10. Bagley, M. C.; Xiong, X. *Org. Lett.* **2004,** *6,* 3401–3404. doi:10.1021/ol0485870
11. Jones, M. C.; Marsden, S. P.; Muñoz-Subtil, D. M. *Org. Lett.* **2006,** *8,* 5509–5512. doi:10.1021/ol062162r
12. Jones, M. C.; Marsden, S. P. *Org. Lett.* **2008,** *10,* 4125–4128. doi:10.1021/ol801709c
13. Marsden, S. P.; Watson, E. L.; Raw, S. A. *Org. Lett.* **2008,** *10,* 2905–2908. doi:10.1021/ol801028e
14. Ja, Y.-X.; Hillgren, J. M.; Watson, E. L.; Marsden, S. P.; Kündig, E. P. *Chem. Commun.* **2008,** 4040–4042. doi:10.1039/b810858g
15. Watson, E. L.; Marsden, S. P.; Raw, S. A. *Tetrahedron Lett.* **2009,** *50,* 3318–3320. doi:10.1016/j.tetlet.2009.02.076
16. Yousif, M. M.; Saeki, S.; Hamana, M. *Chem. Pharm. Bull.* **1982,** *30,* 1680–1691. doi:10.1248/cpb.30.1680
17. Jones, G.; Pitman, M. A.; Lunt, E.; Lythgoe, D. J.; Abarca, B.; Ballesteros, R.; Elmasnaouy, M. *Tetrahedron* **1997,** *53,* 8257–8268. doi:10.1016/S0040-4020(97)00491-2
18. Londregan, A. T.; Jennings, S.; Wei, L. *Org. Lett.* **2011,** *13,* 1840–1843. doi:10.1021/ol200352g
19. Londregan, A. T.; Burford, K.; Conn, E. L.; Hesp, K. D. *Org. Lett.* **2014,** *16,* 3336–3339. doi:10.1021/ol501359r
20. Lecointre, B.; Azzouz, R.; Bischoff, L. *Tetrahedron Lett.* **2014,** *55,* 1913–1915. doi:10.1016/j.tetlet.2014.01.134
21. Johnson, T. C.; Marsden, S. P. *unpublished observations.*
22. Edgar, M. T.; Pettit, G. R.; Krupa, T. S. *J. Org. Chem.* **1979,** *44,* 396–400. doi:10.1021/jo01317a018
23. Herdeis, C.; Gebhard, R. *Arch. Pharm.* **1987,** *320,* 546–553. doi:10.1002/ardp.19873200612
24. Seebach, D. *Angew. Chem., Int. Ed. Engl.* **1979,** *18,* 239–258. doi:10.1002/anie.197902393
25. Matsumoto, M.; Harada, M.; Yamashita, Y.; Kobayashi, S. *Chem. Commun.* **2014,** *50,* 13041–13044. doi:10.1039/C4CC06156J
26. Liu, X.; Gao, A.; Ding, L.; Xu, J.; Zhao, B. *Org. Lett.* **2014,** *16,* 2118–2121. doi:10.1021/ol500522d
27. Wu, Y.; Hu, L.; Li, Z.; Deng, L. *Nature* **2015,** *523,* 445–450. doi:10.1038/nature14617

License and Terms

BEILSTEIN JOURNAL OF ORGANIC CHEMISTRY

Base metal-catalyzed benzylic oxidation of (aryl)(heteroaryl)methanes with molecular oxygen

Hans Sterckx, Johan De Houwer, Carl Mensch, Wouter Herrebout, Kourosch Abbaspour Tehrani and Bert U. W. Maes*

Full Research Paper

Open Access

Address:
Department of Chemistry, University of Antwerp, Groenenborgerlaan 171, B-2020 Antwerp, Belgium

Email:
Bert U. W. Maes* - bert.maes@uantwerpen.be

* Corresponding author

Keywords:
base metal; benzylic; catalyzed; molecular oxygen; oxygenation

Beilstein J. Org. Chem. **2016,** *12,* 144–153.
doi:10.3762/bjoc.12.16

Received: 09 October 2015
Accepted: 12 January 2016
Published: 27 January 2016

This article is part of the Thematic Series "Sustainable catalysis".

Guest Editor: N. Turner

Abstract

The methylene group of various substituted 2- and 4-benzylpyridines, benzyldiazines and benzyl(iso)quinolines was successfully oxidized to the corresponding benzylic ketones using a copper or iron catalyst and molecular oxygen as the stoichiometric oxidant. Application of the protocol in API synthesis is exemplified by the alternative synthesis of a precursor to the antimalarial drug Mefloquine. The oxidation method can also be used to prepare metabolites of APIs which is illustrated for the natural product papaverine. ICP–MS analysis of the purified reaction products revealed that the base metal impurity was well below the regulatory limit.

Introduction

Direct oxidation of C(sp^3)–H bonds is a useful and fast method to convert fairly unreactive substrates to useful functional groups for organic synthesis like alcohols, ketones, aldehydes and carboxylic acids. Classical oxidation protocols rely on the use of (super)stoichiometric quantities of oxyanions of toxic metals like Mn(VII) and Cr(VI) [1,2]. The amount of waste these oxidants produce and limitations on their use by new legislation [3] has prompted scientists to search for more sustainable oxidation methods. The use of transition metal- or organocatalysis in combination with molecular oxygen has received a great deal of attention from the scientific community [4-7]. Molecular oxygen is considered to be the greenest oxidant available and it is already widely employed by the commodity chemical industry [8]. However, when looking at the preparation of more complex molecules, typical for fine chemicals, the use of aerobic oxidations is more the exception than the norm [9]. This is partly due to the limited synthetic scope and selectivity of the available oxidation methods. Further research into selective and mild aerobic oxidations is therefore of vital importance. Of special interest are the transition metal- and organocatalyzed oxidations of activated methylenes such as in benzylic methylenes or their heteroaromatic an-

alogues. Due to the activation, the formation of the corresponding ketones and aldehydes becomes feasible under mild conditions. Oxidations of this kind using Oxone® [10,11], NaOCl [12] or especially peroxides [13-19] as the terminal oxidant are quite numerous. However, transformations using molecular oxygen are rare. Ishii showed that organocatalysts such as *N*-hydroxyphthalimide (NHPI) in combination with molecular oxygen can be used to perform benzylic oxidations [20]. The aerobic copper-catalyzed α-oxygenation of 2-arylthioacetamides was reported by Moghaddam [21]. In this transformation $CuCl_2$ and K_2CO_3 in DMF were used to produce α-ketoarylthioacetamides. The coupling of 2-arylacetaldehydes with anilines resulting in the formation of 2-aryl-α-ketoacetamides was reported by Jiao [22] and a closely related intramolecular variant leading to isatins has been published by Ilangovan [23]. A remarkable Cu-catalyzed chemoselective oxidative C–C bond cleavage of methyl ketones was reported by the group of Liu and Bi [24]. This useful transformation makes use of CuI/O_2 in DMSO to convert methyl ketones into aldehydes in a sustainable manner.

Recently our group reported a synthetic protocol for the copper- and iron-catalyzed aerobic oxidation of the methylene group of aryl(di)azinylmethanes using acetic acid as a promotor [25]. The resulting ketones are very valuable as they are intermediates in the synthesis of a variety of pharmaceuticals such as the antimalarial Mefloquine (Lariam®), the antihistamine Acrivastine, the β_2-adrenergic agonist Rimiterol and the anxiolytic Bromazepam [26]. Furthermore, they can also be used to synthesize the 1st and 2nd generation antihistamines Carbinoxamine, Bepotastine and Triprolidine through an alternative synthetic route. In addition to these synthetic examples it has been shown by Kamijo that 4-benzoylpyridines can act as efficient organocatalysts in the photoinduced oxidation of secondary alcohols [27]. Very recently the group of Zhuo and Lei disclosed an alteration to our reaction conditions to further extend the substrate scope [28]. Ethyl chloroacetate was used as the promotor instead of acetic acid, allowing the authors to additionally oxidize less reactive alkyl-substituted pyridines. Gao showed that NH_4I can also be used as an organocatalyst in combination with AcOH to facilitate the oxidation of benzylpyridines to benzoylpyridines [29]. Satoh and Miura showed that when replacing O_2 for $Na_2S_2O_8$ chemoselective methylenation occurred over oxygenation of the methylene with DMA acting as a one-carbon source [30]. An alternative method to synthesize picolinic amides from picolines and ammonium acetate or amines using a similar oxidation protocol was simultaneously proposed by the groups of Deng and Yin [31,32]. In the current work we study the expansion of the scope of our previously disclosed method and provide specific examples of applications in organic synthesis.

Results and Discussion

Substrate scope

In our communication we provided a reaction scope of phenyl-substituted 2-benzylpyridines and showed that both, electron-withdrawing and donating groups are well tolerated. The results additionally indicated that either Cu and Fe catalysts (CuI and $FeCl_2{\cdot}4H_2O$) worked equally well for this substrate class [25]. In the framework of this work a similar study was executed for the regioisomeric 4-benzylpyridines using $FeCl_2{\cdot}4H_2O$ as the catalyst. Under the standard conditions previously developed for 2-benzylpyridines these substrates smoothly oxidized giving the corresponding ketones in moderate to good yields (Table 1). Also in this case electron-donating as well as electron-withdrawing substituents on the phenyl ring are well tolerated and their electronic properties have little influence on the yield of the reaction. Even substituents that are sensitive to oxidation such as NH_2 (**2b**) and SMe (**2c**) appear to be no problem although the reaction products were isolated in slightly lower yields.

Table 1: Iron-catalyzed aerobic oxidation of phenyl-substituted 4-benzylpyridines (**1**).[a]

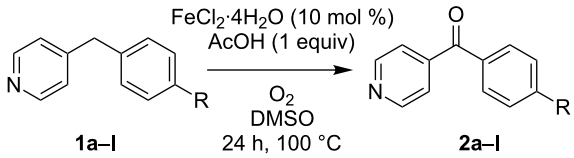

Entry	Substrate	R	Product	Yield (%)[b]
1	**1a**	H	**2a**	70
2	**1b**	NH_2	**2b**	55
3	**1c**	SMe	**2c**	56
4	**1d**	OMe	**2d**	67
5	**1e**	Me	**2e**	79
6	**1f**	I	**2f**	77
7	**1g**	Br	**2g**	85
8	**1h**	Cl	**2h**	66
9	**1i**	F	**2i**	76
10	**1j**	CO_2Et	**2j**	61
11	**1k**	CN	**2k**	79
12	**1l**	NO_2	**2l**	60

[a]Reactions were performed on a 0.5 mmol scale in 1 mL of solvent using 1 atmosphere of O_2 (balloon). [b]Isolated yields.

Next, pyridine rather than phenyl-substitution was studied. In contrast to the phenyl-substituted compounds, substitution on the pyridine ring exerted a large influence on the rate of the reaction (Table 2). This is not surprising when considering the mechanism of the reaction involving an initial acid catalyzed imine–enamine tautomerization (the calculation of the equilibrium constants can be found in Supporting Information File 1,

Table 2: Iron and copper-catalyzed aerobic oxidation of pyridine-substituted 2-benzylpyridines (**3**).[a]

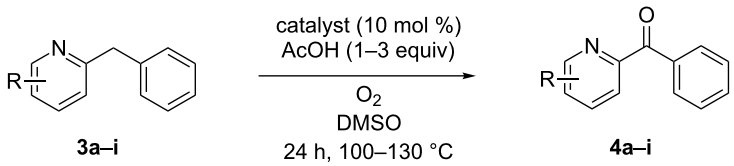

3a–i **4a–i**

Entry	Catalyst	Substrate	R	Product	Yield **3** (%)[b]	Yield **4** (%)[b]
1	$FeCl_2{\cdot}4H_2O$	**3a**	5-CN	**4a**	19	67
2	CuI	**3a**	5-CN	**4a**	18	66
3	CuI	**3a**	5-CN[c]	**4a**	0	83
4	$FeCl_2{\cdot}4H_2O$	**3b**	5-Me	**4b**	9	73
5	CuI	**3b**	5-Me	**4b**	9	82
6	CuI	**3b**	5-Me[c]	**4b**	0	72
7	$FeCl_2{\cdot}4H_2O$	**3c**	5-OMe	**4c**	65	15
8	CuI	**3c**	5-OMe	**4c**	66	15
9	CuI	**3c**	5-OMe[d,e]	**4c**	0	65
10	$FeCl_2{\cdot}4H_2O$	**3d**	5-CO_2Me	**4d**	0	69
11	CuI	**3d**	5-CO_2Me	**4d**	0	62
12	$FeCl_2{\cdot}4H_2O$	**3e**	5-NHCOMe	**4e**	0	64
13	CuI	**3e**	5-NHCOMe	**4e**	27	56
14	CuI	**3e**	5-NHCOMe[c]	**4e**	0	91
15	$FeCl_2{\cdot}4H_2O$	**3f**	4-Cl	**4f**	0	85
16	CuI	**3f**	4-Cl	**4f**	8	88
17	$FeCl_2{\cdot}4H_2O$	**3g**	3-Cl	**4g**	73	23
18	CuI	**3g**	3-Cl	**4g**	71	22
19	CuI	**3g**	3-Cl[d,e]	**4g**	0	87
20	$FeCl_2{\cdot}4H_2O$	**3h**	5-Cl	**4h**	70	20
21	CuI	**3h**	5-Cl	**4h**	69	15
22	CuI	**3h**	5-Cl[d,e]	**4h**	0	92
23	$FeCl_2{\cdot}4H_2O$	**3i**	6-Cl	**4i**	90	0
24	CuI	**3i**	6-Cl	**4i**	91	0
25	CuI	**3i**	6-Cl[e, f]	**4i**	0	59

[a]Reactions were performed on a 0.5 mmol scale in 1 mL of solvent using 1 atmosphere of O_2 (balloon). [b]Isolated yields. [c]48 h. [d]AcOH (3 equiv). [e]130 °C. [f]TFA (3 equiv).

Table S1) [33]. As the substituent is now located in the ring where the tautomerization will take place the electronic effect and the position of this substituent is expected to have a large effect on it. In general one expects the tautomerization to proceed more efficiently when the pyridine nitrogen becomes more basic and the methylene hydrogen becomes more acidic. In Table 2 the results on pyridine-substituted 2-benzylpyridines using both Fe and Cu catalysis are shown. Under the standard conditions only a small number of substrates reached full conversion after 24 hours. Based on our findings that placing substituents on the phenyl ring, both in 2- and 4-benzylpyridines and irrespective of their electronic nature, has little influence on the yield of the reaction the largest substituent effect is expected to be on the basicity of the pyridine nitrogen and not that much on the acidity of the methylene hydrogen.

While the thermodynamical equilibrium constant between the imine and enamine tautomers predicts whether or not a substrate can be oxidized (see Supporting Information File 1), it does not provide an explanation for the incomplete conversion that is seen in most cases of the pyridine-substituted 2-benzylpyridines. We attribute the low conversions to the fact that the pyridine nitrogen becomes less basic and therefore protonation by AcOH becomes unfavored. This is supported by the fact that the rate of deuterium incorporation in the benzylic position of **16** and **3h** through acid-catalyzed imine–enamine tautomerization is dependent on the strength of the acid used (Figure 1). The rate of deuterium incorporation in 2-benzylpyridine (**16**, $pK_a \approx 5.2$) is much faster when using TFA-d_1 than with AcOH-d_4 [34,35]. With the less basic 2-benzyl-5-chloropyridine (**3h**, $pK_a \approx 3.0$) the difference is even more pronounced: Almost no

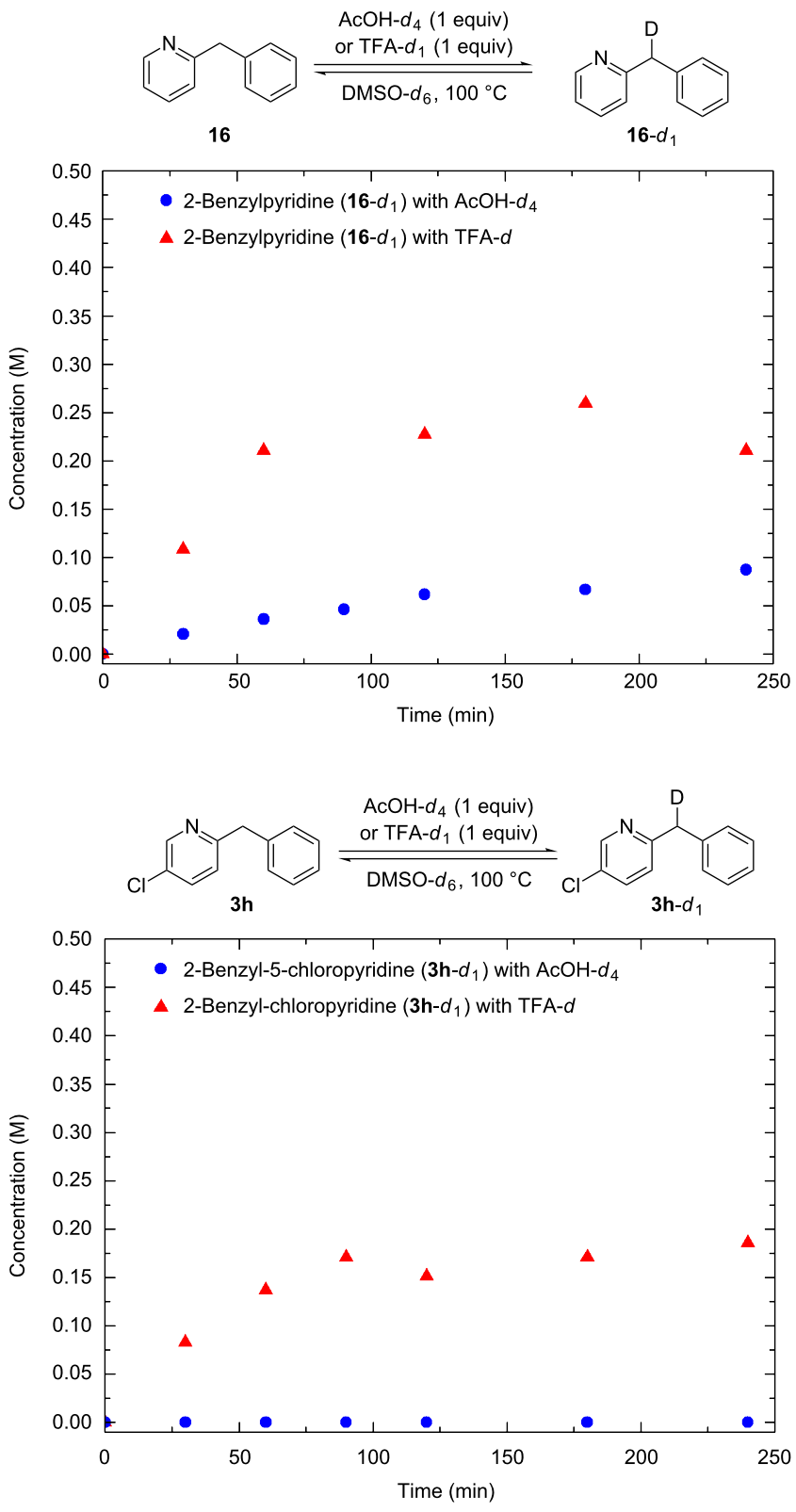

Figure 1: Hydrogen–deuterium exchange through acid-catalyzed imine–enamine tautomerization of **3h** (0.5 M) and **16** (0.5 M) using AcOH-d_4 (0.5 M) or TFA-d_1 (0.5 M). ^{1}H NMR spectroscopy was used to quantify the monodeuterated species.

deuterium incorporation could be detected using AcOH-d_4 while the reaction ran smoothly using the stronger acid TFA-d_1. From this we conclude that when the pyridine nitrogen becomes less basic and protonation by the acid thus becomes more difficult, using more equivalents of the acid or a stronger acid is needed to reach full conversion. When we compare the different pK_a values of substituted pyridines we see that 2-benzylpyridine (**16**, pK_a ≈ 5.2) is one of the most basic pyridines [34,35]. Substituents in the 5-position generally give poor conversion in accordance with their lower p*K*a values: 5-CN (pK_a ≈ 1.3, Table 2, entries 1 and 2), 5-OMe (pK_a ≈ 4.9, Table 2, entries 7 and 8) and 5-Cl (pK_a ≈ 3.0, Table 2, entries 20 and 21) with the exception of 5-CO_2Me (pK_a ≈ 3.1, Table 2, entries 10 and 11). When investigating regioisomeric substrates featuring chloro substituents in all possible positions of the pyridine ring only the 4-Cl (pK_a ≈ 3.8, Table 2, entries 15 and 16) substrate reaches full conversion under the standard conditions. The 3-Cl and 5-Cl regioisomers have a similar pK_a value (pK_a ≈ 2.98) and therefore show similar reactivity (Table 2, entries 17 and 18 and entries 20 and 21) with only limited conversion. A remarkable case is the 6-Cl-substituted substrate (pK_a ≈ 0.8, Table 2, entries 23 and 24), which did not react at all under the standard conditions. The low basicity of the pyridine nitrogen is the reason for this lack of reactivity. In addition the enamine form of this compound is also highly unfavored (see Supporting Information File 1).

To reach full conversion for all substrates we re-optimized the reaction conditions. Although similar results for Fe and Cu catalysis were obtained after 24 h, CuI was selected for this purpose. The reasoning behind this is reflected in the chemoselectivity experiments (vide infra), where it was shown that CuI is a slightly more potent catalyst than $FeCl_2{\cdot}4H_2O$. Additionally, comparison of the reaction rate for both catalysts on the standard substrate 2-benzylpyridine (**16**) further supports this ($v_{i,Cu} = 1.088 \times 10^{-3}$ M min^{-1}; $v_{i,Fe} = 1.013 \times 10^{-3}$ M min^{-1}, see Supporting Information File 1, Figure S2). For substrates that already gave reasonable conversions (>60%) using the standard conditions (Table 2, entries 3, 6 and 14) the reaction time was doubled to 48 hours which was sufficient to achieve full conversion. For substrates that are harder to oxidize (<60% conversion) due to too low pK_a a combination of a higher temperature and the addition of more (three) equivalents of acetic acid was needed (Table 2, entries 9, 19 and 22). Considering the low basicity of compound **3i**, 3 equivalents of the stronger acid TFA were used (Table 2, entry 25).

Next, the effect of benzoannulation (quinoline) and C–H for N substitution (diazines) in the pyridine ring was studied. Scheme 1 provides an overview of the results for these more challenging substrates. Interestingly, phenyl(quinolin-2-yl)methanone (**6a**) and phenyl(quinolin-4-yl)methanone (**6b**) were formed in moderate yields indicating that larger aromatic systems are compatible with the reaction conditions. In the case of 2-(4-chlorobenzyl)pyrimidine (**5c**) the standard conditions allowed smooth oxidation providing the target compound in an excellent yield. For the regioisomeric diazine, (4-chlorobenzyl)pyrazine (**5d**), no oxidation was observed after 24 h at 100 °C. To our delight, by increasing the reaction temperature to 130 °C, (4-chlorophenyl)(pyrazin-2-yl)methanone (**6d**) could

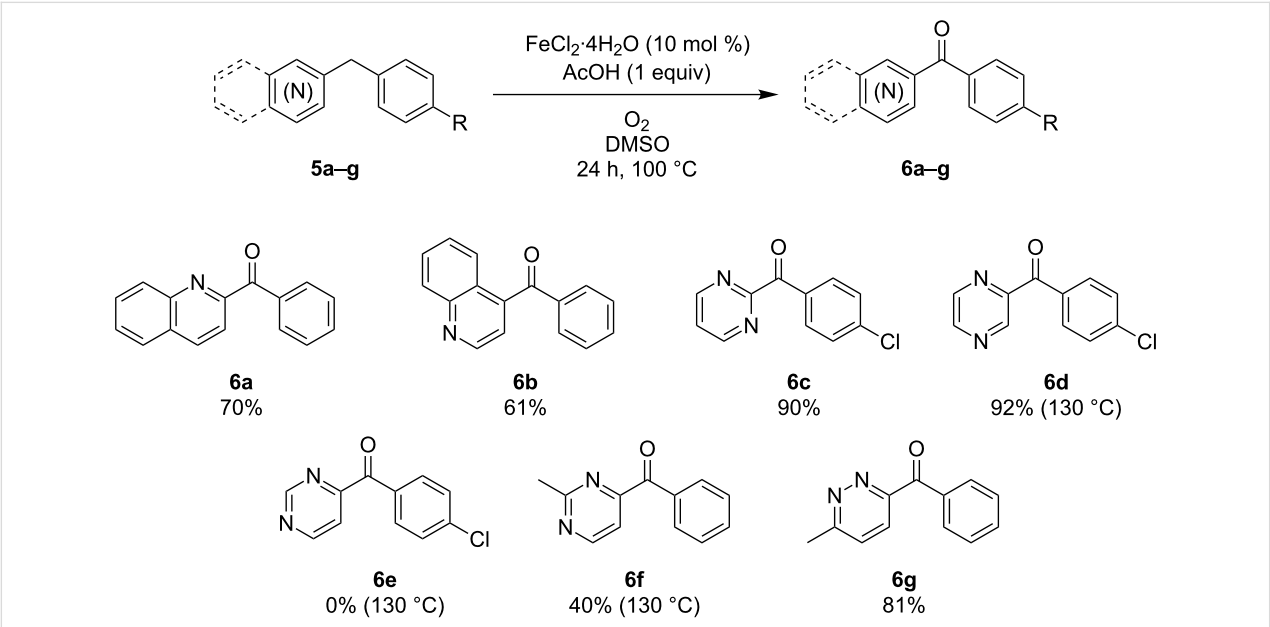

Scheme 1: Benzylic oxygenation of benzoannulated azines and diazines (**5**).

be obtained in 92% yield. In contrast to the two former cases, 4-(4-chlorobenzyl)pyrimidine (**5e**) could neither be oxidized at 100 °C nor at 130 °C. Competitive C–H activation of the 2 position is presumed to be the reason for this observation. Blocking this position by a methyl group (**5f**) delivered the corresponding ketone **6f**, albeit in a poor yield of 40%, thus supporting the metalation hypothesis. The regioisomer of diazine **5f**, 3-benzyl-6-methylpyridazine (**5g**), could be smoothly oxidized to the corresponding ketone in 81% yield. It is worth mentioning that in **5f** as well as **5g** no additional oxidation of the methyl group was seen [25].

Applications

An example of an important pharmaceutical which is industrially prepared from an azinyl benzoazinyl ketone, namely (2,8-bis(trifluoromethyl)quinolin-4-yl)(pyridin-2-yl)methanone (**10**), is the antimalarial Mefloquine (**13**) [36]. This drug is listed on the World Health Organization essential medicines list and despite numerous side effects it remains one of the most effective antimalarial drugs on the market [37,38]. Its classical synthesis (Scheme 2, top) is based on the lithiation of 4-bromo-2,8-bis(trifluoromethyl)quinoline (**7a**) and quenching with CO_2 resulting in the formation of 2,8-bis(trifluoromethyl)quinoline-4-carboxylic acid (**8**). Reaction of **8** with in situ generated 2-pyridyllithium (**9**) finally yields ketone **10** [39].

We considered a new approach based on 4-(pyridin-2-ylmethyl)-2,8-bis(trifluoromethyl)quinoline (**12**) as the substrate. This compound is structurally interesting as it is activated by both a pyridin-2-yl and a quinolin-4-yl moiety (Scheme 2, bottom). The synthesis of substrate **12** was accomplished by a cross-coupling reaction of pyridine alcohol **11** with commercial 4-chloro-2,8-bis(trifluoromethyl)quinoline (**7b**) according to a procedure published by Oshima [40]. In this way, **12** was obtained in 63% yield and its subsequent Fe-catalyzed oxidation provided **10** in 63% isolated yield. In principle substrate **7a** could also be used but the chloro analogue is cheaper. The final reduction of **10** into Mefloquine has been described earlier and can also be achieved in an enantioselective manner [41].

Human metabolism can produce metabolites of pharmaceuticals that possess completely different properties such as for instance biological activity, toxicity and clearance rates. Rapid identification and synthesis of potential drug metabolites is therefore of great importance to facilitate the drug discovery process [42]. For this purpose chemoselective oxidation protocols are a valuable tool since they can provide us with metabolites typically generated by cytochrome P450 enzymes. Bearing this in mind we attempted to oxygenate the benzylic position of the antispasmodic drug papaverine (**14**) applying our oxidation protocol (Scheme 3). The resulting compound is known as papaveraldine (**15**), a byproduct from the extraction of papaverine from *Papaver somniferum*. Papaverine is a challenging substrate as besides the methylene part it also features two oxidation sensitive veratrole units. Interestingly, a highly chemose-

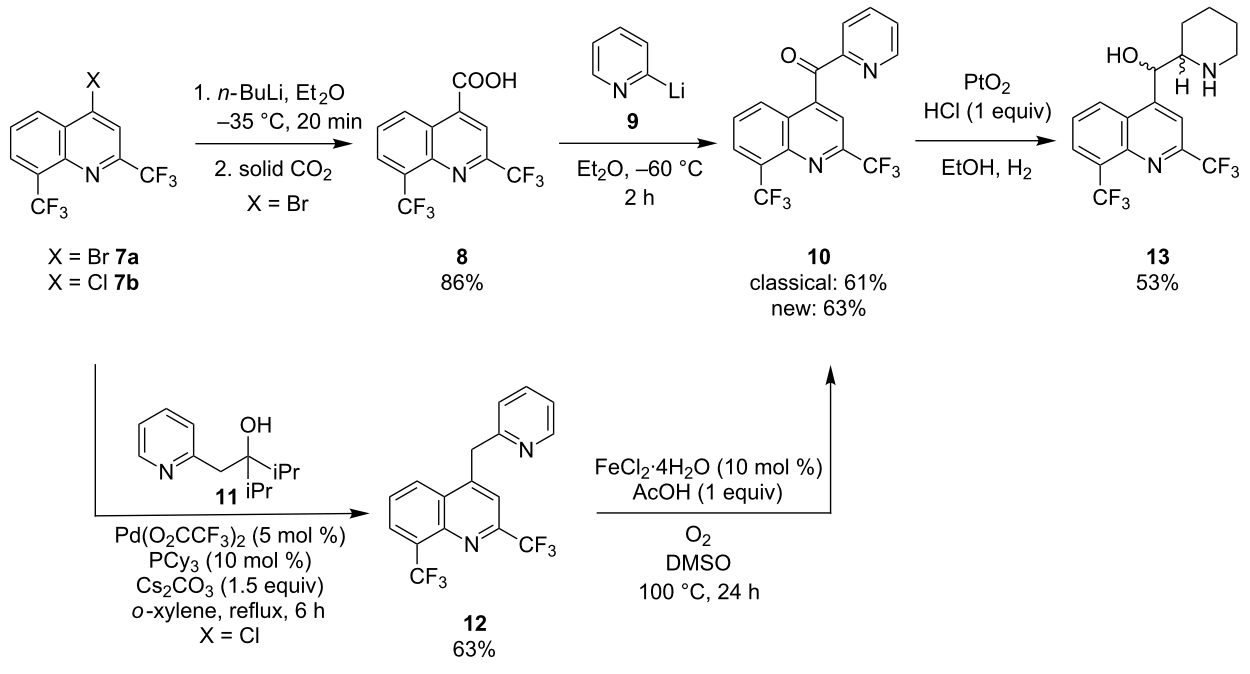

Scheme 2: Classical (top) and new formal (bottom) synthesis of Mefloquine.

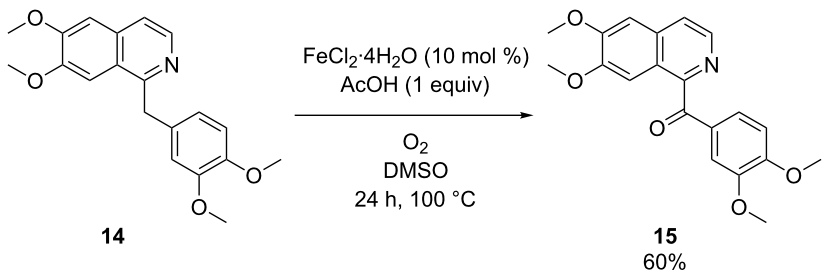

Scheme 3: Iron-catalyzed aerobic oxidation of papaverine (**15**).

lective oxidation was observed and compound **15** was isolated in 60% yield.

Trace metal analysis

When using transition metal catalysis in the synthesis of compounds designated for application (pharmaceuticals, agrochemicals, materials) it is of vital importance to control and determine any metal impurity in the reaction product. In case the selected purification methods proved insufficient to get the metal contaminations below the maximum allowed threshold value set for active ingredients (AIs), an extra treatment might be required. This is especially true if the catalysis is performed in a late stage of a synthesis thus making the method less attractive and sustainable. While class 1 metals such as Pd and Pt have oral exposure limits of 10 ppm, Cu and Fe are respectively class 2 and class 3 metals with oral exposure limits of 250 ppm and 1300 ppm [43]. The fact that Cu and Fe are more abundant, cheaper and benign makes them an interesting choice as transition metal catalysts. To determine the Cu and Fe contents present in our samples ICP–MS analysis was performed. Copper contents ranged from 5 to 21 ppm, all well below the limit of 250 ppm. Iron contents were slightly higher ranging from 29 to 57 ppm but again still well below the regulatory maximum value (see Supporting Information File 1, Figure S1). It should be noted that these values pertain to the purified compounds after column chromatography. The influence of the work-up procedure on the remaining metal impurities was investigated for one of our applications, namely the papaveraldine (**15**) synthesis (Table 3). Applying the standard purification resulted in 54 ppm of Fe remaining. Omitting the column chromatography step and solely performing the aqueous extraction provided a much higher value, namely 1097 ppm. However, if after the extraction a recrystallization step of the reaction product is performed the Fe level can be lowered further to 300 ppm which is well below the legal limit for oral exposure (see Supporting Information File 1).

Alternative solvents

A solvent screening was subsequently performed focusing mainly on greener solvents than DMSO with a boiling point above 100 °C in order to allow a direct comparison at the same reaction temperature [44,45] (Table 4). All reactions were performed in a round-bottomed flask equipped with a reflux condenser under oxygen atmosphere at a 5 mmol scale to be able to reliably quantify remaining starting material. 2-Benzylpyridine (**16**) was selected as the substrate for this study. The reaction in anisole and *n*-BuOAc gave full conversion after 24 hours with excellent yields. With 1,4-dioxane, toluene, cyclopentyl methyl ether and *n*-BuOH as the solvent some starting product was recovered, however, with a good mass balance suggesting that the reaction is just slower in these solvents than in DMSO. From this we can conclude that the reaction is compatible with a variety of other solvents. In addition to the above results, Kappe et al. successfully applied our protocol in a flow process [46]. They intensified the process by working at 200 °C which allowed them to lower the catalyst loading ($FeCl_3$) to 5 mol % and to omit acetic acid as the activator. As DMSO degraded and produced repulsive odors at these high

Table 3: The influence of the purification method on the amount of Fe impurities in papaveraldine (**15**) after oxidation.

Entry	Purification method	Fe impurity in **15** (ppm)
1	Extraction[a] + column chromatography[b]	54
2	Extraction[a]	1097
3	Extraction[a] + recrystallization[c]	300

[a]Washing subsequently with sat. aq $NaHCO_3$ and brine, extraction with dichloromethane. [b]Silica flash cartridge applying a heptane/ethyl acetate gradient. [c]Recrystallization from a 2 M HCl solution.

temperatures the authors switched to propylene carbonate as the solvent.

Table 4: An extended solvent screening for the base metal-catalyzed aerobic oxidation reaction.[a]

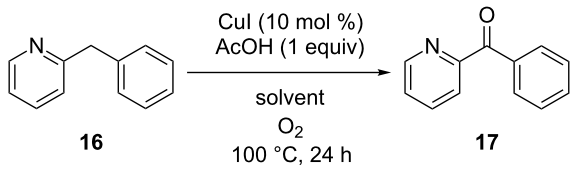

Entry	Solvent[b]	Yield **16** (%)[c]	Yield **17** (%)[c]
1	DMSO[d]	0	87
2	anisole[e]	0	85
3	*n*-BuOAc[e]	0	89
4	1,4-dioxane[f]	2	85
5	toluene[d]	18	67
6	CPME[d]	5	80
7	*n*-BuOH[e]	5	73

[a]Reactions were performed on a 5 mmol scale in 10 mL of solvent using 1 atmosphere of O_2 (balloon). [b]Classification of solvents as provided in [44]. [c]Isolated yields. [d]Problematic. [e]Recommended. [f]Hazardous.

Chemoselectivity

When multiple activated methylene motifs are present the chemoselective oxidation of one of these positions can be achieved as we previously exemplified for 2-methyl-6-(4-methylbenzyl)pyridine (**18b**, Table 5, entries 4 and 5). This interesting selectivity was further expanded on 6-(4-methylbenzyl)-2-methylpyrazine (**18a**). Pyrazine **18a** features three possible positions for methylene oxidation: a benzyl, benzhydryl and a 1,4-diazinylmethyl moiety. When **18a** was submitted to the Cu-catalyzed reaction conditions at 130 °C, only the bis-oxidation product 6-(4-methylbenzoyl)pyrazine-2-carbaldehyde (**20a**) was obtained in 61% (Table 5, entry 1). Interestingly, when switching to $FeCl_2{\cdot}4H_2O$ as the catalyst in the reaction, only mono-oxidation at the benzhydrylic methylene occurred, providing (6-methylpyrazin-2-yl)(*p*-tolyl)methanone (**19a**) in 57% yield (Table 5, entry 2). A similar chemoselectivity was observed for the oxidation of **18b** where Cu catalysis lead to bis-oxidation (**20b**, Table 5, entry 4) while Fe catalysis resulted in mono-oxidation (**19b**, Table 5, entry 5).

When the reaction with **18a** using Cu catalysis is performed in *n*-BuOAc as solvent instead of DMSO only compound **19a** was isolated after 48 hours of reaction (starting material was still present after 24 hours, Table 5, entry 3). The same trend was observed in the reaction of **18b**. Here under Cu catalysis at 130 °C in *n*-BuOAc also only benzhydrylic oxidation occurred and (6-methylpyridin-2-yl)(*p*-tolyl)methanone (**19b**) was isolated in 64% yield as the sole product. These results demonstrate that the oxidation power of the catalytic system can be tuned by careful selection of the solvent as well as the base metal.

Conclusion

This work shows that the oxidation protocol disclosed in 2012 by our group can be applied to a much broader substrate scope than originally investigated. Furthermore we have shown that when the nature of the substituents does not permit full conver-

Table 5: Chemoselectivity obtained by selection of catalyst and solvent.[a]

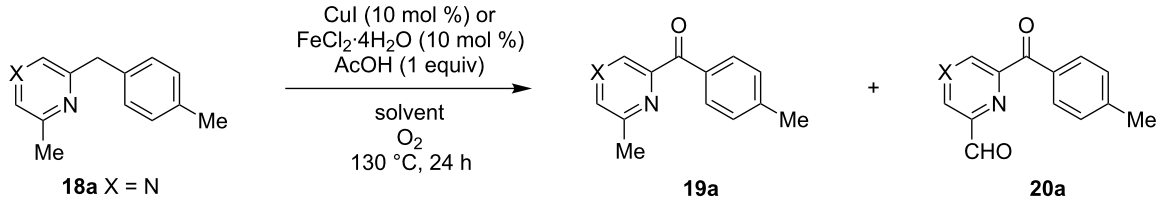

Entry	Substrate	Catalyst	Solvent	Yield **19** (%)[b]	Yield **20** (%)[b]
1	**18a**	CuI	DMSO	0	61
2	**18a**	$FeCl_2{\cdot}4H_2O$	DMSO	57	0
3	**18a**	CuI	*n*-BuOAc	78[c]	0
4	**18b**[d]	CuI	DMSO	0	62
5	**18b**[d]	$FeCl_2{\cdot}4H_2O$	DMSO	85	0
6	**18b**	CuI	*n*-BuOAc	64	0

[a]Reactions were performed on a 0.5 mmol scale in 1 mL of solvent using 1 atmosphere of O_2 (balloon). [b]Isolated yields. [c]48 h. [d]Reported in our communication, see [25].

sion after 24 hours, the standard conditions can be easily amended to increase the rate of the reaction. ICP–MS analysis was performed on a representative set of molecules from the scope disclosed to determine the Cu or Fe impurities remaining after work-up of the reaction products. This revealed that only low amounts remained, that are well below the regulatory limits. In addition, for papaveraldine a comparison between different purification procedures was performed in order to determine their influence on the amount of metal impurity remaining. While the reaction is compatible with a large number of solvents including sustainable ones, DMSO appears to give the fastest reactions. This is also reflected in the chemoselectivity studies where DMSO is the only solvent in which oxidation of a (di)azinylmethyl is possible.

Supporting Information

Supporting Information File 1

Experimental procedures, compound characterization data and copies of ^{1}H and ^{13}C NMR spectra of all new starting materials and reaction products.
[http://www.beilstein-journals.org/bjoc/content/supplementary/1860-5397-12-16-S1.pdf]

Acknowledgements

This work was supported by the Research Foundation Flanders (FWO-Flanders), the Agency for Innovation by Science and Technology (IWT-Flanders), the University of Antwerp (BOF, IOF) and the Hercules Foundation. The authors thank Philippe Franck, Heidi Seykens and Norbert Hancke for technical assistance.

References

1. Shaabani, A.; Mirzaei, P.; Naderi, S.; Lee, D. G. *Tetrahedron* **2004,** *60,* 11415–11420. doi:10.1016/j.tet.2004.09.087
2. Rathore, R.; Saxena, N.; Chandrasekaran, S. *Synth. Commun.* **1986,** *16,* 1493–1498. doi:10.1080/00397918608056400
3. European chemicals agency (ECHA) website. http://echa.europa.eu/web/guest/regulations/reach/legislation.
4. Sun, C.-L.; Li, B.-J.; Shi, Z.-J. *Chem. Rev.* **2011,** *111,* 1293–1314. doi:10.1021/cr100198w
5. Allen, S. E.; Walvoord, R. R.; Padilla-Salinas, R.; Kozlowski, M. C. *Chem. Rev.* **2013,** *113,* 6234–6458. doi:10.1021/cr300527g
6. Shi, Z.; Zhang, C.; Tang, C.; Jiao, N. *Chem. Soc. Rev.* **2012,** *41,* 3381–3430. doi:10.1039/c2cs15224j
7. Punniyamurthy, T.; Velusamy, S.; Iqbal, J. *Chem. Rev.* **2005,** *105,* 2329–2364. doi:10.1021/cr050523v
8. Campbell, A. N.; Stahl, S. S. *Acc. Chem. Res.* **2012,** *45,* 851–863. doi:10.1021/ar2002045
9. Caron, S.; Dugger, R. W.; Ruggeri, S. G.; Ragan, J. A.; Ripin, D. H. B. *Chem. Rev.* **2006,** *106,* 2943–2989. doi:10.1021/cr040679f
10. Ojha, L. R.; Kudugunti, S.; Maddukuri, P. P.; Kommareddy, A.; Gunna, M. R.; Dokuparthi, P.; Gottam, H. B.; Botha, K. K.; Parapati, D. R.; Vinod, T. K. *Synlett* **2009,** *1,* 117–121. doi:10.1055/s-0028-1087384
11. Moriyama, K.; Takemura, M.; Togo, H. *Org. Lett.* **2012,** *14,* 2414–2417. doi:10.1021/ol300853z
12. Jin, C.; Zhang, L.; Su, W. K. *Synlett* **2011,** *10,* 1435–1438. doi:10.1055/s-0030-1260760
13. Pan, J.-F.; Chen, K.-M. *J. Mol. Catal. A: Chem.* **2001,** *176,* 19–22. doi:10.1016/S1381-1169(01)00238-2
14. Velusamy, S.; Punniyamurthy, T. *Tetrahedron Lett.* **2003,** *44,* 8955–8957. doi:10.1016/j.tetlet.2003.10.016
15. Bonvin, Y.; Callens, E.; Larrosa, I.; Henderson, D. A.; Oldham, J.; Burton, A. J.; Barrett, A. G. M. *Org. Lett.* **2005,** *7,* 4549–4552. doi:10.1021/ol051765k
16. Catino, A. J.; Nichols, J. M.; Choi, H.; Gottipamula, S.; Doyle, M. P. *Org. Lett.* **2005,** *7,* 5167–5170. doi:10.1021/ol0520020
17. Pavan, C.; Legros, J.; Bolm, C. *Adv. Synth. Catal.* **2005,** *347,* 703–705. doi:10.1002/adsc.200404315
18. Nakanishi, M.; Bolm, C. *Adv. Synth. Catal.* **2007,** *349,* 861–864. doi:10.1002/adsc.200600553
19. Zhang, J. T.; Wang, Z. T.; Wang, Y.; Wan, C. F.; Zheng, X. Q.; Wang, Z. Y. *Green Chem.* **2009,** *11,* 1973–1978. doi:10.1039/b919346b
20. Ishii, Y.; Nakayama, K.; Takeno, M.; Sakaguchi, S.; Iwahama, T.; Nishiyama, Y. *J. Org. Chem.* **1995,** *60,* 3934–3935. doi:10.1021/jo00118a002
21. Moghaddam, F. M.; Mirjafary, Z.; Saeidian, H.; Javan, M. J. *Synlett* **2008,** *6,* 892–896. doi:10.1055/s-2008-1042925
22. Zhang, C.; Xu, Z.; Zhang, L.; Jiao, N. *Angew. Chem., Int. Ed.* **2011,** *50,* 11088–11092. doi:10.1002/anie.201105285
23. Ilangovan, A.; Satish, G. *Org. Lett.* **2013,** *15,* 5726–5729. doi:10.1021/ol402750r
24. Zhang, L.; Bi, X.; Guan, X.; Li, X.; Liu, Q.; Barry, B.-D.; Liao, P. *Angew. Chem., Int. Ed.* **2013,** *52,* 11303–11307. doi:10.1002/anie.201305010
25. De Houwer, J.; Abbaspour Tehrani, K.; Maes, B. U. W. *Angew. Chem., Int. Ed.* **2012,** *51,* 2745–2748. doi:10.1002/anie.201108540
26. Kleemann, A.; Engel, J.; Kutscher, B.; Reichert, D. *Pharmaceutical Substances,* 4th ed.; Georg Thieme Verlag: Stuttgart, 2001.
27. Kamijo, S.; Tao, K.; Takao, G.; Tonoda, H.; Murafuji, T. *Org. Lett.* **2015,** *17,* 3326–3329. doi:10.1021/acs.orglett.5b01550
28. Liu, J.; Zhang, X.; Yi, H.; Liu, C.; Liu, R.; Zhang, H.; Zhuo, K.; Lei, A. *Angew. Chem., Int. Ed.* **2015,** *54,* 1261–1265. doi:10.1002/anie.201409580
29. Ren, L.; Wang, L.; Lv, Y.; Li, G.; Gao, S. *Org. Lett.* **2015,** *17,* 2078–2081. doi:10.1021/acs.orglett.5b00602
30. Itoh, M.; Hirano, K.; Satoh, T.; Miura, M. *Org. Lett.* **2014,** *16,* 2050–2053. doi:10.1021/ol500655k
31. Xie, H.; Liao, Y.; Chen, S.; Chen, Y.; Deng, G.-J. *Org. Biomol. Chem.* **2015,** *13,* 6944–6948. doi:10.1039/C5OB00915D
32. Huang, Y.; Chen, T.; Li, Q.; Zhou, Y.; Yin, S.-F. *Org. Biomol. Chem.* **2015,** *13,* 7289–7293. doi:10.1039/C5OB00685F
33. Sterckx, H.; De Houwer, J.; Mensch, C.; Caretti, I.; Tehrani, K. A.; Herrebout, W. A.; Van Doorslaer, S.; Maes, B. U. W. *Chem. Sci.* **2016,** *7,* 346–357. doi:10.1039/C5SC03530A

34. The pK_a values mentioned are those of the corresponding monosubstituted pyridines since the benzyl group is the same in every pyridine and data for the compounds are not available. *Tables of Rate and Equilibrium Constants of Heterolytic Organic Reactions;* Palm, V., Ed.; VINITI: Moscow-Tartu, 1975–1985.
35. Güven, A. *Int. J. Mol. Sci.* **2005,** *6,* 257–275. doi:10.3390/i6110257
36. Adam, S. *Tetrahedron* **1989,** *45,* 1409–1414. doi:10.1016/0040-4020(89)80138-3
37. World Health Organization (WHO) website. http://www.who.int/medicines/publications/essentialmedicines/en/.
38. Schlagenhauf, P.; Adamcova, M.; Regep, L.; Schaerer, M. T.; Rhein, H.-G. *Malar. J.* **2010,** *9,* 357. doi:10.1186/1475-2875-9-357
39. Lutz, R. E.; Ohnmacht, C. J.; Patel, A. R. *J. Med. Chem.* **1971,** *14,* 926–928. doi:10.1021/jm00292a008
40. Niwa, T.; Yorimitsu, H.; Oshima, K. *Angew. Chem., Int. Ed.* **2007,** *46,* 2643–2645. doi:10.1002/anie.200604472
41. Hems, W. P.; Jackson, W. P.; Nightingale, P.; Bryant, R. *Org. Process Res. Dev.* **2012,** *16,* 461–463. doi:10.1021/op200354f
42. Genovino, J.; Lütz, S.; Sames, D.; Touré, B. B. *J. Am. Chem. Soc.* **2013,** *135,* 12346–12352. doi:10.1021/ja405471h
43. Class 1 metals include metals that are known or suspect human carcinogens or show any other significant toxicity. Class 2 metals include metals with lower toxicity to man and are typically encountered with administration of medicinal products. Class 3 metals include metals with no significant toxicity and are well tolerated up to doses far exceeding typically encountered with the administration of medicinal products. European medicines agency, committee for medicinal products for human use, see http://www.ema.europa.eu/ema/index.jsp?curl=pages/regulation/general/general_content_000356.jsp&mid=WC0b01ac0580028e8c for a detailed description.
44. Henderson, R. K.; Jiménez-González, C.; Constable, D. J. C.; Alston, S. R.; Inglis, G. G. A.; Fisher, G.; Sherwood, J.; Binks, S. P.; Curzons, A. D. *Green Chem.* **2011,** *13,* 854–862. doi:10.1039/c0gc00918k
45. Prat, D.; Wells, A.; Hayler, J.; Sneddon, H.; McElroy, C. R.; Abou-Shehada, S.; Dunn, P. J. *Green Chem.* **2016,** *18,* 288–296. doi:10.1039/C5GC01008J
46. Pieber, B.; Kappe, C. O. *Green Chem.* **2013,** *15,* 320–324. doi:10.1039/c2gc36896j

License and Terms

BEILSTEIN JOURNAL OF ORGANIC CHEMISTRY

Highly stable and reusable immobilized formate dehydrogenases: Promising biocatalysts for in situ regeneration of NADH

Barış Binay[*1,§], Dilek Alagöz[*2,¶], Deniz Yildirim[3], Ayhan Çelik[4] and S. Seyhan Tükel[5]

Full Research Paper

Open Access

Address:
[1]Istanbul AREL University, Faculty of Science and Letters, Department of Molecular Biology and Genetics, Tepekent, Büyükcekmece, Istanbul, Turkey, [2]University of Cukurova, Vocational School of Imamoglu, Adana, Turkey, [3]University of Cukurova, Vocational School of Ceyhan, Adana, Turkey, [4]Gebze Technical University, Department of Chemistry, Gebze, Kocaeli, Turkey and [5]University of Cukurova, Faculty of Arts and Sciences, Department of Chemistry, 01330, Adana, Turkey

Email:
Barış Binay[*] - binaybaris@gmail.com; Dilek Alagöz[*] - dalagoz@cu.edu.tr

* Corresponding author
§ Telephone: + 90 212 8672500/1049; Fax: +90 212 8600481
¶ Telephone: + 90 322 3386081/25; Fax: +90 322 3386070

Keywords:
biocatalysis; *Candida methylica*; formate dehydrogenase; Immobead 150; regeneration of NADH; stabilization

Beilstein J. Org. Chem. **2016,** *12,* 271–277.
doi:10.3762/bjoc.12.29

Received: 22 November 2015
Accepted: 05 February 2016
Published: 12 February 2016

This article is part of the Thematic Series "Sustainable catalysis".

Guest Editor: N. Turner

Abstract

This study aimed to prepare robust immobilized formate dehydrogenase (FDH) preparations which can be used as effective biocatalysts along with functional oxidoreductases, in which in situ regeneration of NADH is required. For this purpose, *Candida methylica* FDH was covalently immobilized onto Immobead 150 support (FDHI150), Immobead 150 support modified with ethylenediamine and then activated with glutaraldehyde (FDHIGLU), and Immobead 150 support functionalized with aldehyde groups (FDHIALD). The highest immobilization yield and activity yield were obtained as 90% and 132%, respectively when Immobead 150 functionalized with aldehyde groups was used as support. The half-life times ($t_{1/2}$) of free FDH, FDHI150, FDHIGLU and FDHIALD were calculated as 10.6, 28.9, 22.4 and 38.5 h, respectively at 35 °C. FDHI150, FDHIGLU and FDHIALD retained 69, 38 and 51% of their initial activities, respectively after 10 reuses. The results show that the FDHI150, FDHIGLU and FDHIALD offer feasible potentials for in situ regeneration of NADH.

Introduction

Dehydrogenases are one of the most promising enzymes in biocatalysis since these enzymes have a great potential in the enantioselective reduction of ketones [1,2] and/or carbon–carbon double bonds [3,4] to produce optically active compounds. However, most dehydrogenases use an expensive cofactor such as NAD(H) or NADP(H) [5]. Therefore, the regeneration of the

cofactor is required to decrease operational costs. NAD^+-dependent formate dehydrogenase (FDH, EC 1.2.1.2) catalyzes oxidation of formate to carbon dioxide (CO_2) [6]. FDH is industrially used as coenzyme for the regeneration of NADH [7,8], as sensor for the determination of formic acid [9], and as catalyst for the production of methanol or formate from CO_2 [10,11]. It was reported that FDH is a promising enzyme for the regeneration of NADH since the reaction product of FDH-catalyzed formate oxidation is CO_2 which does not interfere with the purification of the final product [12,13]. However, free FDHs have low thermal stability [14] and lack of reusability, therefore, the immobilization of FDH has been of increasing interest in the recent years. For example, Netto et al. [15] immobilized FDH from *Candida boidinii* on three different magnetic supports and the results showed that conversion rates and recycling values were changed depending on the support used for immobilization. Bolivar et al. [16] used different strategies for the immobilization of FDH from *Candida boidinii* and reported that the stabilization factors were changed depending on the immobilization protocol. Kim et al. [17] immobilized FDH from *Candida boidinii* as cross-linked enzyme aggregate (CLEA) and demonstrated that the residual activity and thermal stability of CLEA were strictly dependent on the type of cross-linker.

Epoxy group containing supports are widely used in enzyme immobilization studies to obtain highly stable enzyme preparations by using multi-point attachment strategies [18-20]. The immobilization mechanism of enzymes is based on the hydrophobic adsorption of enzymes onto the supports and then the covalent immobilization of enzymes. Besides, these supports are easily modified to generate new groups for the immobilization of enzymes with different mechanism. This allows us the preparation of biocatalysts with different properties [21-23]. Glutaraldehyde-activated supports have been extensively used in enzyme immobilization studies for many years [24]. However, the exact structure of the groups formed by glutaraldehyde is still under discussion, a Schiff base reaction between the carbonyl group of glutaraldehyde and the terminal amino functional group could be expected [25,26].

Candida methylica FDH is a dimeric enzyme [27] and it may be easily inactivated by the dissociation of its subunits depending on reaction conditions. Hence, the use of a proper immobilization technique and support could stabilize its dimeric form. In this study, NAD^+-dependent FDH from *Candida methylica* was covalently immobilized onto Immobead 150, an epoxy group containing commercial support, and Immobead 150 support modified with ethylenediamine and then activated with glutaraldehyde, and Immobead 150 support functionalized with aldehyde groups. The optimum conditions of free and immobilized FDH preparations were determined for formate oxidation. The thermal stability of free and immobilized FDH preparations was tested at 35 and 50 °C. The operational stability studies of the immobilized FDHs were performed in a batch reactor. As far as we know, this is the first report regarding the covalent immobilization of *Candida methylica* FDH.

Results and Discussion

It is well documented that one of the factors affecting the performance of an immobilized enzyme is the type of binding groups on the support which provides higher loading of enzyme and higher retention of activity [28]. Epoxy group containing supports are widely used in the immobilization of many enzymes through multi-point covalent attachments since epoxy groups can easily react with different nucleophiles highly abundant in the protein surface such as primary amine, sulfhydryl and carboxylic groups [21]. In this study, Immobead 150 was used as epoxy group containing supports for the immobilization of *C. methylica* FDH (Figure 1a). The amount of bound protein was determined as 85% of the initial loading protein per gram of Immobead 150 support and the immobilized FDH (FDHI150) showed 31% activity of the free FDH upon immobilization. Another commonly used strategy to covalently immobilize enzyme is using a bifunctional reagent glutaraldehyde. A Schiff base is formed between the carbonyl group of glutaraldehyde and the amino functional groups of the enzyme [29]. In this study, Immobead 150 support was modified with ethylenediamine and then activated with glutaraldehyde for the covalent immobilization of *C. methylica* FDH (Figure 1b). The amount of bound protein was determined as 75% of the initial loading protein per gram of the support and the immobilized FDH (FDHIGLU) showed 105% activity of the free FDH upon immobilization. In recent years, using short spacer arm containing supports has become very popular in enzyme immobilization due to enhancement of the stability of the enzyme [30]. In this study, Immobead 150 support was kept in 1 M acetic acid solution to produce vicinal diols and then the formed diols were oxidatively cleaved with $NaIO_4$ to produce aldehyde groups onto the support (Figure 1c). The amount of bound protein was determined as 90% of the initial loading protein per gram of the support and the immobilized FDH (FDHIALD) showed 132% activity of the free FDH upon immobilization. The higher retention activities of FDHIGLU and FDHIALD may be related to the prevention of subunit dissociation depending on the immobilization procedure.

The activity changes of free and immobilized FDH preparations depending on the medium pH were given in Figure 2. The free FDH showed 2% of its maximum activity at pH 4.0 whereas FDHI150, FDHIGLU and FDHIALD showed 64, 45 and 59% of their maximum activities at the same pH. The activities of both free and immobilized FDH preparations increased by in-

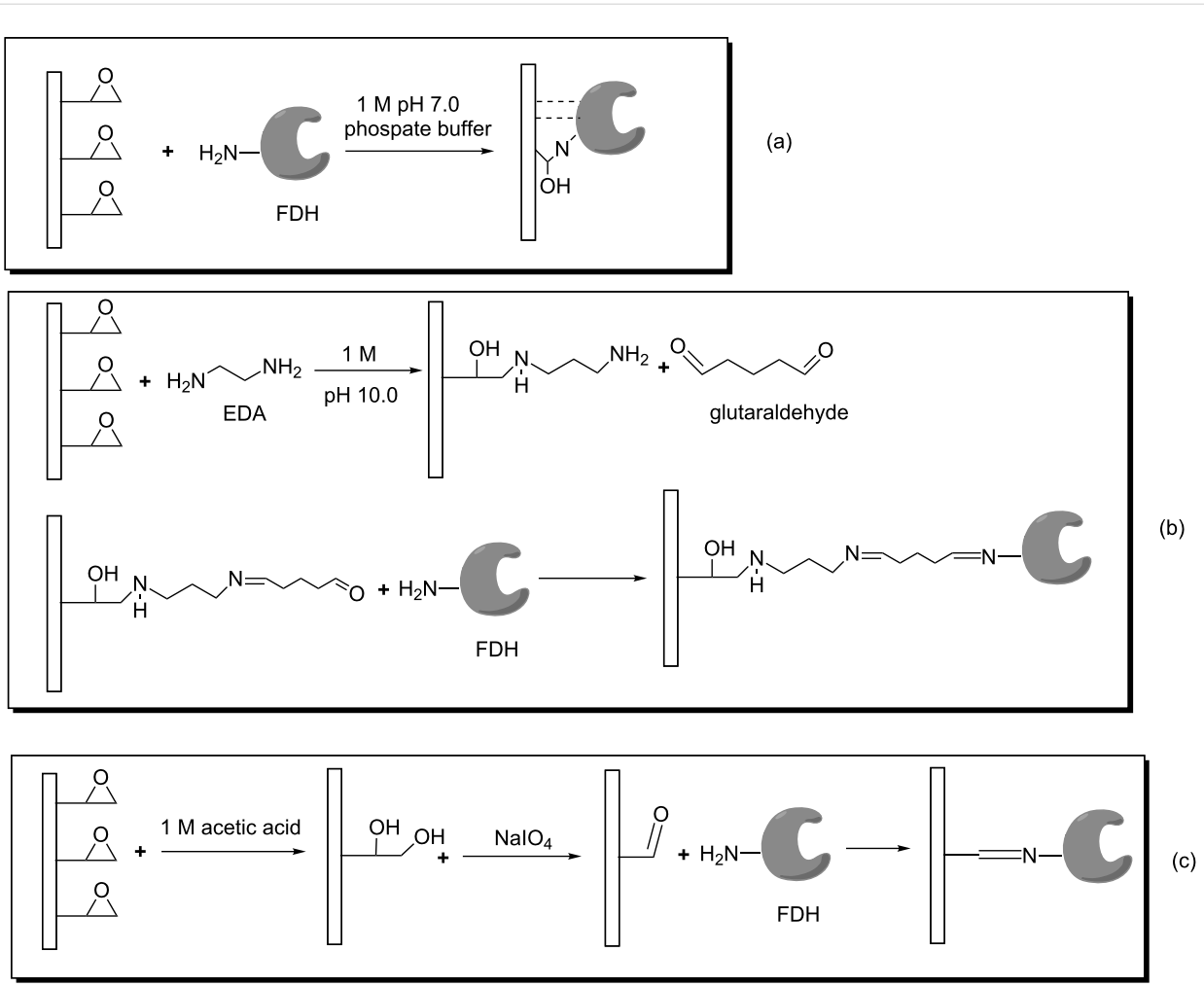

Figure 1: The immobilization scheme of FDH onto Immobead 150 and modified Immobead 150 supports.

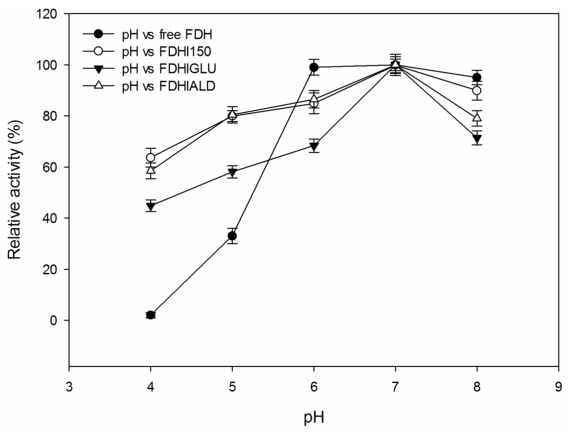

Figure 2: The effect of pH on the activities of free and immobilized FDH preparations. The FDH activity at pH 7.0 was taken as 100% for the each preparation. The experiments were run in triplicate.

creasing the pH and all the FDH preparations showed their maximum activities at pH 7.0. When the pH was further increased to 8.0, the determined activities of free FDH, FDHI150, FDHIGLU and FDHIALD were 95, 90, 71 and 79% of their maximum activities, respectively. Gao et al. [31] reported the optimal pH values were 7.0 for both free FDH and immobilized FDH onto polydopamine-coated iron oxide nanoparticles (PD-IONPs). The optimum pH values of the both free *Pseudomonas sp.* 101 FDH and its immobilized form onto glyoxylagarose were reported as 7.0 [16].

The temperature–activity profiles of free and immobilized FDH preparations were given in Figure 3. The relative activities were 67, 78, 64 and 88%, respectively for free FDH, FDHI150, FDHIGLU and FDHIALD at 25 °C. The activities of free and immobilized FDHs increased with the temperature increasing from 25 to 35 °C and all the FDH preparations showed their maximum activities at 35 °C. The activities of free and immobi-

lized FDH preparations decreased at the temperatures above 35 °C. Netto et al. [15] reported that the optimum temperature of free *Candida boidinii* FDH was 37 °C whereas the optimum temperatures of its immobilized forms were quite different depending on the used immobilization procedure. The optimum temperature of *C. boidinii* FDH immobilized onto magnetite nanoparticles silanized with (3-aminopropyl)triethoxysilane was 42 °C whereas the optimum temperature was 27 °C when this support was further coated with glyoxylagarose and then *C. boidinii* FDH was immobilized onto it.

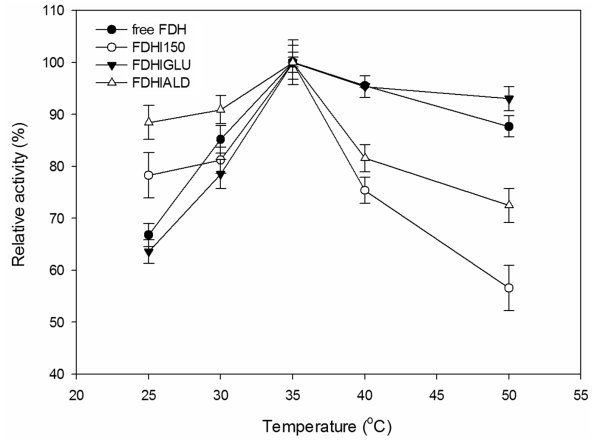

Figure 3: The effect of temperature on the activities of free and immobilized FDH preparations. The enzyme activity at 35 °C is taken as 100% for the each preparation. The experiments were run in triplicate.

It is generally expected from the covalently immobilized enzymes that they should be more durable against temperature inactivation than their free forms. As shown in Figure 4, the free FDH completely lost its initial activity at 35 °C after 24 h incubation time. However, FDHI150, FDHIGLU and FDHIALD retained 62, 48 and 69% of their initial activities, respectively at 35 °C after 24 h incubation time. At 50 °C, the free FDH completely lost its initial activity whereas FDHI150, FDHIGLU and FDHIALD retained 54, 35 and 56% of their initial activities, respectively after 24 h incubation time (Figure 5). The half-life times ($t_{1/2}$) of free FDH, FDHI150, FDHIGLU and FDHIALD were calculated as 10.6, 28.9, 22.4 and 38.5 h, respectively at 35 °C (Table 1). The corresponding $t_{1/2}$ values were 8.1, 23.1, 15.1 and 23.9 h at 50 °C. These results showed that the free FDH was stabilized 2.7, 2.1 and 3.1 fold at 35 °C and 2.8, 1.9 and 2.9 fold at 50 °C when it was immobilized onto Immobead 150, Immobead 150 via glutaraldehyde spacer arm, and Immobead 150 support functionalized with aldehyde group. These results show that a strong and stable imino bond could be formed between the aldehyde group of the modified Immobead 150 support and the terminal

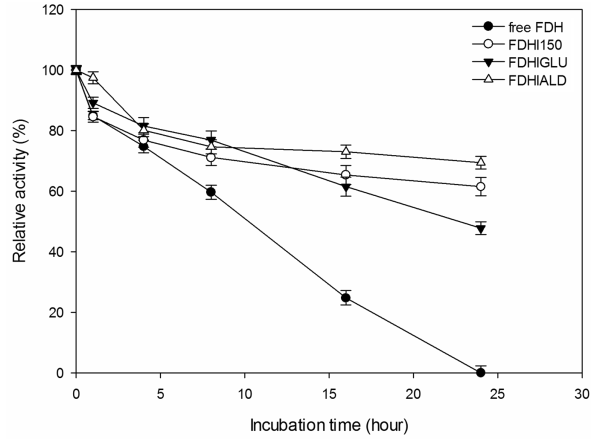

Figure 4: Thermal stability of free and immobilized FDH preparations at 35 °C.

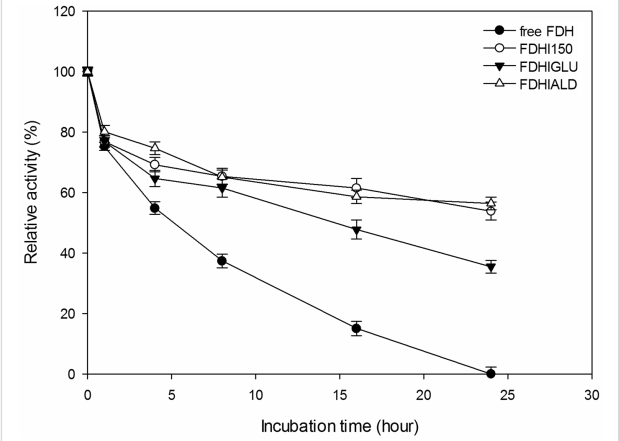

Figure 5: Thermal stability of free and immobilized FDH preparations at 50 °C.

Table 1: The results of thermal stability experiments of free and immobilized FDH at 35 and 50 °C.

Catalyst	Temperature	$t_{1/2}$ (h)	k_i (h^{-1})	Stabilization factor
Free FDH	35 °C	10.6	6.5×10^{-2}	–
	50 °C	8.1	8.5×10^{-2}	–
FDHI150	35 °C	28.9	2.4×10^{-2}	2.7
	50 °C	23.1	3.0×10^{-2}	2.8
FDHIGLU	35 °C	22.4	3.1×10^{-2}	2.1
	50 °C	15.1	4.6×10^{-2}	1.9
FDHIALD	35 °C	38.5	1.8×10^{-2}	3.6
	50 °C	23.9	2.9×10^{-2}	2.9

amino group of the enzyme at pH 6.0. Kim et al. [17] investigated the thermal stability of free *C. boidinii* FDH and immobilized FDH as cross-linked enzyme aggregates and reported that cross-linked enzyme aggregates of *C. boidinii* FDH prepared with dextrane polyaldehyde and glutaraldehyde showed 3.6 and 4.0 folds higher stability than the free FDH at 50 °C.

It is an important feature to reuse a biocatalyst for many cycles without loss of initial activity. In this study, the operational stability of immobilized FDHs was tested in the batch type reactor for 10 reuses (Figure 6). The immobilized FDHs nearly protected their initial activities after 2 reuses. The remaining activities of FDHI150, FDHIGLU and FDHIALD were 69, 38 and 51%, respectively after 10 reuses. Gao et al. [31] reported that mutant FDH immobilized onto PD-IONPs protected 60% of its initial activity after 17 cycles. Kim et al. [17] determined that *C. boidinii* FDH immobilized as cross-linked enzyme aggregates prepared with dextrane polyaldehyde and glutaraldehyde, retained 96 and 89% of their initial activities, respectively after 10 reuses.

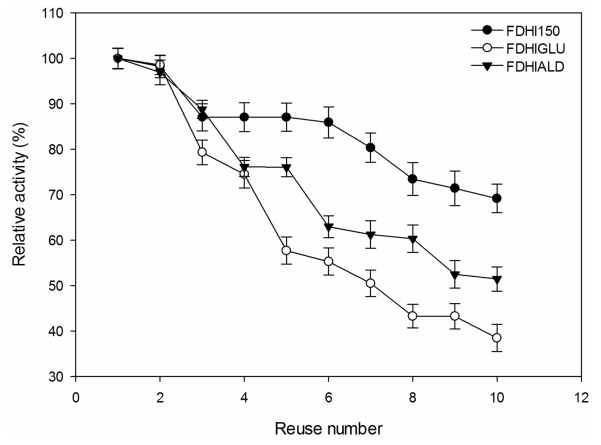

Figure 6: The reusability of immobilized FDHs.

Conclusion

In this study, the covalent immobilization of *C. methylica* FDH onto Immobead 150 support and modified Immobead 150 supports were investigated. A higher immobilization yield was obtained when tthe Immobead 150 support functionalized with aldehyde groups was used as support. Of the tested FDH preparations, FDHIALD showed highest catalytic efficiency and stability than the free FDH, FDHI150 and FDHIGLU. FDHI150, FDHIGLU and FDHIALD retained 69, 38 and 51% of their initial activities, respectively after 10 reuses. In conclusion, Immobead 150 support functionalized with aldehyde groups may be a potential candidate for the immobilization of enzymes and the immobilized FDHs, especially FDHIALD, is a robust biocatalyst and it may be used in the combination with other dehydrogenases to regenerate NADH.

Experimental

Nicotinamide adenine dinucleotide hydrate (NAD^+) was purchased from Acros Organics (New Jersey, USA). Sodium formate, Immobead 150 (Polyacrylic matrix, particle size 250 μm, oxirane content ≥200 μmol/g dry support), ethylenediamine (EDA), glutaraldehyde and sodium metaperiodate were obtained from Sigma-Aldrich (St. Louis, MO, USA). All other chemicals used in this study were of analytical grade and used without further purification.

Purification of *C. methylica* FDH

The purification of FDH was performed according to Demir et al. [32]. Briefly, 7 g of wet *E. coli* BL21 (DE3) cell paste containing the expressed FDH protein was suspended in 10 mL buffer solution (20 mM Tris–HCl, pH 7.8, 0.5 M NaCl, 5 mM imidazole) at 4 °C. Then, the cells were disrupted by sonication and the sonicated cells were harvested by centrifugation (28000 × *g*, 30 min) at 4 °C. The cell pellet was resuspended in an ice-cold buffer (20 mM NaH_2PO_4, 0.5 M NaCl, 30 mM imidazole, pH 7.4). The resuspended cells were further lysed by adding lysozyme. Then the lysate was filtered through a 0.45 μm filter. The filtered samples were loaded to a His-trap column after equilibration with 5 mL of the ice-cold buffer. Then the column was washed with 5 mL of the same buffer. FDH was eluted with a series of elution buffers: 3 mL of elution buffer (20 mM phosphate buffer, 0.5 M NaCl with 100 mM imidazole pH 7.4), 5 mL of elution buffer (20 mM phosphate buffer, 0.5 M NaCl with 0.2 M imidazole pH 7.4), and finally 3 mL of elution buffer (20 mM phosphate buffer, 0.5 M NaCl with 0.4 M imidazole pH 7.4). The collected fractions were analyzed on SDS-PAGE.

Preparation of modified supports

The modification of Immobead 150 support with EDA and glutaraldehyde was performed according to Yildirim et al. [33]. One gram of Immobead 150 support was treated with 10 mL of EDA solution (1 M in water, pH 10) for 12 h with mild stirring at room temperature. Then, the obtained supports were washed with distilled water and then dried at room temperature. One gram of EDA treated support was mixed with 25 mL phosphate buffer (50 mM, pH 7.0) containing 2.5% glutaraldehyde (w/v). After gently 2 h stirring, the supports were washed with distilled water and then dried at room temperature.

One gram of Immobead 150 support was treated with 10 mL of 1 M acetic acid solution for 12 h with mild stirring at room temperature. Then, the obtained supports were washed with distilled water and then dried at room temperature. One gram of

the support was added onto 25 mL of sodium meta periodate solution. After 2 h stirring time the supports were washed with distilled water and then dried at room temperature.

Immobilization of FDH

The covalent immobilization of FDH onto Immobead 150 support was performed according to Alagöz et al. [34]. One gram of Immobead 150 support was mixed with 9.0 mL of FDH solution containing 1.0 mg/mL protein in 1.0 M, pH 7.0 phosphate buffer. The mixture was gently shaken at 25 °C in a water bath during 24 h immobilization time. The immobilized FDH preparations were filtrated to collect them and washed with distilled water.

The covalent immobilization of FDH onto Immobead 150 via a glutaraldehyde spacer arm was performed according to Yildirim et al. [33] with slight modification. One gram of the modified support was treated with 9.0 mL of FDH solution containing 1.0 mg/mL protein in 50 mM, pH 7.0 phosphate buffer. The immobilization was allowed to continue in a water bath at 5 °C for 4 h with slow shaking. Then, the immobilized FDH preparations were filtrated to collect them and washed with distilled water.

The covalent immobilization of FDH onto Immobead 150 functionalized with aldehyde groups was carried out by adding 9.0 mL of FDH solution containing 1.0 mg/mL protein in 50 mM, pH 6.0 citrate buffer onto 1 g of the support. The immobilization was allowed to continue in a water bath at 5 °C for 4 h with slow shaking. Then, the immobilized FDH preparations were filtrated to collect them and washed with distilled water.

The protein contents of filtrates were checked by measuring their absorbance values at 280 nm and the washing procedure was continued until no absorbance were detected in the filtrates. After that, the immobilized FDH preparations were stored at 5 °C until use. The amounts of immobilized protein onto the supports were determined using a Bradford protein assay [35].

FDH assay

The FDH activity was measured spectrophotometrically at 340 nm according to Özgün et al. [36]. Five milligrams of immobilized FDH or 50 µL of free FDH (5.4 mg protein/mL), 2.6 mL of phosphate buffer (0.1 M, pH 7.0) and 0.5 mL of 0.1 M sodium formate solution (0.1 M in pH 7.0 phosphate buffer) were mixed in a test tube. The reaction was started by the addition of 0.1 mL NAD^+ solution (10 mM in water) at 25 °C in a water bath. After 10 min reaction time, an aliquot of 3 mL was taken from the reaction mixture and its absorbance was measured at 340 nm. The same procedure was applied to a blank tube containing no free or immobilized FDH sample. One unit of FDH activity was defined as the amount of enzyme produced 1.0 µmol of CO_2 from formate in the presence of NAD^+ under the assay conditions.

Characterization of FDH

The effect of pH on the activities of free and immobilized FDHs was investigated at different pHs ranging from 5.0 to 8.0 at 35 °C. The optimal temperatures of free and immobilized FDH preparations were determined in a temperature range of 25–50 °C at pH 7.0.

The thermal stability of free and immobilized FDH preparations was tested by incubating the preparations at 35 and 50 °C and measuring the activities of the samples in certain time intervals.

Operational stability of immobilized FDH

The operational stability of the immobilized FDHs was investigated in a batch type column reactor. The immobilized FDH preparation (0.1 g of each) was loaded to the reactor and 2.6 mL of phosphate buffer (0.1 M, pH 7.0) and 0.5 mL of 0.2 M sodium formate solution (0.1 M in pH 7.0 phosphate buffer) were added. The reaction was started by the addition of 0.1 mL NAD^+ solution (10 mM in water) at 25 °C in a water bath. The reaction mixture was separated from the immobilized FDH and its absorbance was measured at 340 nm. For the next cycle, the immobilized FDH was rinsed with the phosphate buffer (5 mL) and the freshly prepared reaction mixture was added onto it.

References

1. Stewart, J. D. *Curr. Opin. Chem. Biol.* **2001,** *5,* 120–129. doi:10.1016/S1367-5931(00)00180-0
2. Goldberg, K.; Schroer, K.; Lütz, S.; Liese, A. *Appl. Microbiol. Biotechnol.* **2007,** *76,* 237–248. doi:10.1007/s00253-007-1002-0
3. Stuermer, R.; Hauer, B.; Hall, M.; Faber, K. *Curr. Opin. Chem. Biol.* **2007,** *11,* 203–213. doi:10.1016/j.cbpa.2007.02.025
4. Kataoka, M.; Kotaka, A.; Hasegawa, A.; Wada, M.; Yoshizumi, A.; Nakamori, S.; Shimizu, S. *Biosci., Biotechnol., Biochem.* **2002,** *66,* 2651–2657. doi:10.1271/bbb.66.2651
5. Berenguer-Murcia, A.; Fernandez-Lafuente, R. *Curr. Org. Chem.* **2010,** *14,* 1000–1021. doi:10.2174/138527210791130514
6. Tishkov, V. I.; Popov, V. O. *Biochemistry (Moscow)* **2004,** *69,* 1252–1267. doi:10.1007/s10541-005-0071-x
7. Xu, G.; Jiang, Y.; Tao, R.; Wang, S.; Zeng, H.; Yang, S. *Biotechnol. Lett.* **2016,** *38,* 123–129. doi:10.1007/s10529-015-1957-3
8. Roche, J.; Groenen-Serrano, K.; Reynes, O.; Chauvet, F.; Tzedakis, T. *Chem. Eng. J.* **2014,** *239,* 216–225. doi:10.1016/j.cej.2013.10.096
9. Mori, H.; Ohmori, R. *J. Health Sci.* **2008,** *54,* 212–215. doi:10.1248/jhs.54.212
10. Wu, H.; Huang, S.; Jiang, Z. *Catal. Today* **2004,** *98,* 545–552. doi:10.1016/j.cattod.2004.09.018

11. Lu, Y.; Jiang, Z.-y.; Xu, S.-w .; Wu, H. *Catal. Today* **2006,** *115,* 263–268. doi:10.1016/j.cattod.2006.02.056
12. Wichmann, R.; Vasic-Racki, D. *Adv. Biochem. Eng./Biotechnol.* **2005,** *92,* 225–260. doi:10.1007/b98911
13. Weckbecker, A.; Gröger, H.; Hummel, W. *Adv. Biochem. Eng./Biotechnol.* **2010,** *120,* 195–242. doi:10.1007/10_2009_55
14. Tishkov, V. I.; Popov, V. O. *Biomol. Eng.* **2006,** *23,* 89–110. doi:10.1016/j.bioeng.2006.02.003
15. Netto, C. G. C. M.; Nakamura, M.; Andrade, L. H.; Toma, H. E. *J. Mol. Catal. B: Enzym.* **2012,** *84,* 136–143. doi:10.1016/j.molcatb.2012.03.021
16. Bolivar, J. M.; Wilson, L.; Ferrarotti, S. A.; Fernandez-Lafuente, R.; Guisan, J. M.; Mateo, C. *Enzyme Microb. Technol.* **2007,** *40,* 540–546. doi:10.1016/j.enzmictec.2006.05.009
17. Kim, M. H.; Park, S.; Kim, Y. H.; Won, K.; Lee, S. H. *J. Mol. Catal. B: Enzym.* **2013,** *97,* 209–214. doi:10.1016/j.molcatb.2013.08.020
18. Turková, J.; Bláha, K.; Malaníková, M.; Vančurová, D.; Švec, F.; Kálal, J. *Biochim. Biophys. Acta, Enzymol.* **1978,** *524,* 162–169. doi:10.1016/0005-2744(78)90114-6
19. Mateo, C.; Grazú, V.; Pessela, B. C. C.; Montes, T.; Palomo, J. M.; Torres, R.; López-Gallego, F.; Fernández-Lafuente, R.; Guisán, J. M. *Biochem. Soc. Trans.* **2007,** *35,* 1593–1601. doi:10.1042/BST0351593
20. Barbosa, O.; Torres, R.; Ortiz, C.; Berenguer-Murcia, Á.; Rodrigues, R. C.; Fernandez-Lafuente, R. *Biomacromolecules* **2013,** *14,* 2433–2462. doi:10.1021/bm400762h
21. Mateo, C.; Grazu, V.; Guisan, J. M. Immobilization of enzymes on monofunctional and heterofunctional epoxy-activated supports.. In *Immobilization of Enzymes and Cells;* Guisan, J. M., Ed.; Methods in molecular biology; Humana Press: New York, 2013; pp 43–57.
22. dos Santos, J. C. S.; Barbosa, O.; Ortiz, C.; Berenguer-Murcia, A.; Rodrigues, R. C.; Fernandez-Lafuente, R. *ChemCatChem* **2015,** *7,* 2413–2432. doi:10.1002/cctc.201500310
23. Mateo, C.; Grazu, V.; Palomo, J. M.; Lopez-Gallego, F.; Fernandez-Lafuente, R.; Guisan, J. M. *Nat. Protoc.* **2007,** *2,* 1022–1033. doi:10.1038/nprot.2007.133
24. Betancor, L.; López-Gallego, F.; Hidalgo, A.; Alonso-Morales, N.; Mateo, G. D.-O. C.; Fernández-Lafuente, R.; Guisán, J. M. *Enzyme Microb. Technol.* **2006,** *39,* 877–882. doi:10.1016/j.enzmictec.2006.01.014
25. Park, S. W.; Kim, Y. I.; Chung, K. H.; Hong, S. I.; Kim, S. W. *React. Funct. Polym.* **2002,** *51,* 79–92. doi:10.1016/S1381-5148(02)00028-7
26. Alptekin, Ö.; Tükel, S. S.; Yildirim, D.; Alagöz, D. *Enzyme Microb. Technol.* **2011,** *49,* 547–554. doi:10.1016/j.enzmictec.2011.09.002
27. Avilova, T. V.; Egorova, O. A.; Ioanesyan, L. S.; Egorov, A. M. *Eur. J. Biochem.* **1985,** *152,* 657–662. doi:10.1111/j.1432-1033.1985.tb09245.x
28. Cao, L. Covalent Enzyme Immobilization. *Carrier-bound Immobilized Enzymes;* Wiley-VCH Verlag GmbH & Co. KGaA: Weinheim, 2006; pp 169–316.
29. Alptekin, Ö.; Tükel, S. S.; Yıldırım, D.; Alagöz, D. *J. Mol. Catal. B: Enzym.* **2009,** *58,* 124–131. doi:10.1016/j.molcatb.2008.12.004
30. Lopez-Gallego, F.; Fernandez-Lorente, G.; Rocha-Martin, J.; Bolivar, J. M.; Mateo, C.; Guisan, J. M. Stabilization of enzymes by multipoint covalent immobilization on supports activated with glyoxyl groups. In *Immobilization of Enzymes and Cells;* Guisan, J. M., Ed.; Methods in molecular biology; Humana Press: New York, 2013; pp 59–71.
31. Gao, X.; Ni, K.; Zhao, C.; Ren, Y.; Wei, D. *J. Biotechnol.* **2014,** *188,* 36–41. doi:10.1016/j.jbiotec.2014.07.443
32. Demir, A. S.; Talpur, F. N.; Sopaci, S. B.; Kohring, G.-W.; Celik, A. *J. Biotechnol.* **2011,** *152,* 176–183. doi:10.1016/j.jbiotec.2011.03.002
33. Yildirim, D.; Tükel, S. S.; Alagöz, D.; Alptekin, Ö. *Enzyme Microb. Technol.* **2011,** *49,* 555–559. doi:10.1016/j.enzmictec.2011.08.003
34. Alagöz, D.; Tükel, S. S.; Yildirim, D. *J. Mol. Catal. B: Enzym.* **2014,** *101,* 40–46. doi:10.1016/j.molcatb.2013.12.019
35. Bradford, M. M. *Anal. Biochem.* **1976,** *72,* 248–254. doi:10.1016/0003-2697(76)90527-3
36. Özgün, G.; Karagüler, N. G.; Turunen, O.; Turner, N. J.; Binay, B. *J. Mol. Catal. B: Enzym.* **2015,** *122,* 212–217. doi:10.1016/j.molcatb.2015.09.014

License and Terms